40100

National Library of Canada
Bibliothèque nationale du Canada

CANADIAN THESES ON MICROFICHE

THÈSES CANADIENNES SUR MICROFICHE

NAME OF AUTHOR/*NOM DE L'AUTEUR* ROBERT D BURKE

TITLE OF THESIS/*TITRE DE LA THÈSE* DEVELOPMENT OF THE LARVAL DIGESTIVE TRACT OF ECHINOIDS

UNIVERSITY/*UNIVERSITÉ* U of ALBERTA

DEGREE FOR WHICH THESIS WAS PRESENTED/ *GRADE POUR LEQUEL CETTE THÈSE FUT PRÉSENTÉE* Ph.D.

YEAR THIS DEGREE CONFERRED/*ANNÉE D'OBTENTION DE CE GRADE* 1978

NAME OF SUPERVISOR/*NOM DU DIRECTEUR DE THÈSE* F.S. CHIA

Permission is hereby granted to the NATIONAL LIBRARY OF CANADA to microfilm this thesis and to lend or sell copies of the film.

The author reserves other publication rights, and neither the thesis nor extensive extracts from it may be printed or otherwise reproduced without the author's written permission.

L'autorisation est, par la présente, accordée à la BIBLIOTHÈQUE NATIONALE DU CANADA de microfilmer cette thèse et de prêter ou de vendre des exemplaires du film.

L'auteur se réserve les autres droits de publication; ni la thèse ni de longs extraits de celle-ci ne doivent être imprimés ou autrement reproduits sans l'autorisation écrite de l'auteur.

DATED/*DATÉ* 17 Oct. SIGNED/*SIGNÉ* Robert D. Burke

PERMANENT ADDRESS/*RÉSIDENCE FIXÉ*
R.R. #1
MILL BAY, BRITISH COLUMBIA
V0R 2P0

NL-91 (3-74)

National Library of Canada

Cataloguing Branch
Canadian Theses Division

Ottawa, Canada
K1A 0N4

NOTICE

The quality of this microfiche is heavily dependent upon the quality of the original thesis submitted for microfilming. Every effort has been made to ensure the highest quality of reproduction possible.

If pages are missing, contact the university which granted the degree.

Some pages may have indistinct print especially if the original pages were typed with a poor typewriter ribbon or if the university sent us a poor photocopy.

Previously copyrighted materials (journal articles, published tests, etc.) are not filmed.

Reproduction in full or in part of this film is governed by the Canadian Copyright Act, R.S.C. 1970, c. C-30. Please read the authorization forms which accompany this thesis.

THIS DISSERTATION
HAS BEEN MICROFILMED
EXACTLY AS RECEIVED

Bibliothèque nationale du Canada

Direction du catalogage
Division des thèses canadiennes

AVIS

La qualité de cette microfiche dépend grandement de la qualité de la thèse soumise au microfilmage. Nous avons tout fait pour assurer une qualité supérieure de reproduction.

S'il manque des pages, veuillez communiquer avec l'université qui a conféré le grade.

La qualité d'impression de certaines pages peut laisser à désirer, surtout si les pages originales ont été dactylographiées à l'aide d'un ruban usé ou si l'université nous a fait parvenir une photocopie de mauvaise qualité.

Les documents qui font déjà l'objet d'un droit d'auteur (articles de revue, examens publiés, etc.) ne sont pas microfilmés.

La reproduction, même partielle, de ce microfilm est soumise à la Loi canadienne sur le droit d'auteur, SRC 1970, c. C-30. Veuillez prendre connaissance des formules d'autorisation qui accompagnent cette thèse.

LA THÈSE A ÉTÉ
MICROFILMÉE TELLE QUE
NOUS L'AVONS REÇUE

NL-339 (3/77)

THE UNIVERSITY OF ALBERTA

DEVELOPMENT OF THE LARVAL DIGESTIVE TRACT OF ECHINOIDS

by

© ROBERT DOUGLAS BURKE

A THESIS

SUBMITTED TO THE FACULTY OF GRADUATE STUDIES AND RESEARCH
IN PARTIAL FULFILMENT OF THE REQUIREMENTS FOR THE DEGREE
OF DOCTOR OF PHILOSOPHY

DEPARTMENT OF ZOOLOGY

EDMONTON, ALBERTA
FALL, 1978

THE UNIVERSITY OF ALBERTA

FACULTY OF GRADUATE STUDIES AND RESEARCH

The undersigned certify that they have read, and recommend to the Faculty of Graduate Studies and Research, for acceptance, a thesis entitled "Development of the Larval Digestive Tract of Echinoids," submitted by Robert Douglas Burke in partial fulfilment of the requirements for the degree of Doctor of Philosophy.

....
Supervisor

....

A. D. Spencer
....

B. S. Heming
....

Sara E. Zalik
....

....

Woollacott
....
External Examiner

Date. 28 Sept. 1978........

ABSTRACT

A functional digestive tract (esophagus, stomach, and intestine) is formed from the archenteron in *Strongylocentrotus purpuratus* embryos in 44 hours (15°C). Morphogenetic events forming the larval gut include: sphincter formation, coelom formation, shaping and bending of the gut.

The cardiac and pyloric sphincters first appear as constrictions in the archenteron. The sphincter cells change from cubes to wedges during constriction. The apical ends of the sphincter cells contain an electron-dense region in which microfilaments can be discerned. Constriction of the archenteron was reversibly inhibited with cytochalasin B. However, cytochalasin B had no effect once the constrictions had fully formed. Neither the electron-dense region nor the microfilaments were observed after cytochalasin B treatment.

The coeloms form from two diverticula that emerge from the tip of the archenteron. During coelom formation, filopodia extend from the coelomic cells; their contraction appears to facilitate the egression of the coeloms. The filopodia contain arrays of microfilaments and coelom formation was reversibly inhibited with cytochalasin B.

The number of cells in the developing larval digestive tract increases linearly from 0 to 100 during gastrulation, and sigmoidally to 425 cells in the larval gut. Allometric cell proliferation was eliminated as a morphogenetic mechanism shaping the stomach by inhibiting cytokinesis with colchicine; treated embryos formed normal guts comprised of 150 cells. Autoradiographs of embryos exposed to H^3thymidine during shaping of the stomach indicated no regions of enhanced thymidine incorporation.

The bending of the larval gut into a 'J' shape is apparently produced by the length of the gut doubling between two fixed points, the mouth and the anus.

The sequence of morphogenetic events that forms the larval gut was inhibited by treatment throughout gastrulation with actinomycin D. Treatment after gastrulation did not affect gut morphogenesis. Autoradiographs of embryos treated with H^3actinomycin D during or after gastrulation indicated that both stages are equally permeable to actinomycin D. Puromycin arrested development almost immediately.

The archenterons of gastrulae and prisms of *Dendraster excentricus* are comprised of one ultrastructural type of relatively unspecialized cell. Throughout formation of the gut the amount of rough endoplasmic reticulum increases and the number of yolk vesicles decreases. At the time the early pluteus begins to secrete digestive enzymes there is a marked increase in the number of one type of vesicle. In the four-armed pluteus the cells of the esophagus, stomach, and intestine are somewhat specialized, although cell functions are more apparent in the eight-armed pluteus.

The esophagus of the eight-armed pluteus is divided into two regions; the upper esophagus is comprised of ciliated cells, and the lower esophagus consists of cells that evidently secrete mucus. The esophageal muscles form a network around the esophagus; muscle fibers are oriented circumferentially around the upper esophagus and longitudinally about the lower esophagus. The esophageal muscles contain myofibrils that have a combination of smooth and striated characteristics. Axons, with putative synapses, are associated with ciliated cells and muscles in the upper esophagus. The cardiac sphincter is a ring of cross-striated myoepithelial cells separating the stomach and esophagus. The stomach epithelium contains two cell types: one type evidently secretes digestive enzymes and absorbs and stores nutrients, the other type apparently phagocytizes whole algal cells. The pyloric and anal sphincters are comprised of myoepithelium; both are simpler than the cardiac sphincter. The intestine consists of unspecialized cells and probably functions as a conductive tube for undigested material.

At metamorphosis, the digestive tract and larval epidermis of *D. excentricus* undergo histolysis. The gut cells dedifferentiate while the epidermal cells become necrotic. After metamorphosis, the gut cells phagocytize and digest the epidermal cell debris. Seven days after metamorphosis, when the juvenile begins to feed, gut cells have re-associated and histogenesis of the adult gut has begun.

PREFACE

This dissertation examines various aspects of the development of a single organ system in two species of echinoids. The investigation has dealt primarily with the structure of the larval digestive tract, through the embryonic development of form and function, to the transformation of the larval gut into the adult gut.

The relevance of investigating the digestive tract, rather than any other larval structure, lies in the striking nature of its development, which occurs with speed and simplicity, and the obvious importance the digestive tract has to a larva that is essentially a feeding stage.

There is a considerable amount of information available on many aspects of the early development of echinoids (see recent reviews by: Horstadius, 1973; Giudice, 1973; Stearns, 1974; Czihak, 1975). It has been the intention of this research to examine later aspects of echinoid development, trusting that applicability may be found in providing a better understanding of the nature of the pluteus larva.

ACKNOWLEDGEMENTS

I am grateful to Dr. A. O. D. Willows and Dr. R. R. Strathmann for making available to me the research facilities of the University of Washington Friday Harbor Laboratories. Dr. S. K. Malhotra graciously provided use of the electron microscope facilities of the Biological Sciences Electron Microscope Laboratory at the University of Alberta. I also thank the Department of Zoology of the University of Alberta for providing the innumerable amenities that I have enjoyed during the past four years.

Dr. Fu Shiang Chia, Louise Bickell, Elizabeth Grant, Helen Amerongen, and Kay Baert provided advice and assistance during the final preparation of this dissertation. I thank my examination committee: Dr. D. M. Ross, Dr. B. S. Heming, Dr. S. K. Malhotra, Dr. A. N. Spencer, and Dr. S. E. Zalik of the University of Alberta, and Dr. R. M. Woollacott of Harvard University, for critically reading this manuscript.

My supervisor, Fu Shiang Chia, has been throughout our association both a mentor and a tormentor; without him this thesis would never have been undertaken.

My family has been a continuous source of encouragement and unquestioning and steadfast support. I also heartily thank my friends who have contributed to this endeavour in many ways, and to whom I shall always be grateful.

The research presented in this thesis was generously supported by a National Research Council of Canada (NRC) operating grant to Dr. F. S. Chia and an NRC Post-graduate Scholarship to the author.

TABLE OF CONTENTS

	Page
Abstract	iv
Preface	vii
Acknowledgements	viii
List of Figures	xiii
List of Tables	xix

Chapter

I. MATERIALS AND METHODS 1
  A. Culture Methods 1
  B. Light Microscopy 2
  C. Transmission Electron Microscopy 2
  D. Scanning Electron Microscopy (SEM) 4
  E. Cytochalasin B Experiments 4
  F. Cell Counting Procedure 5
  G. Colchicine Experiments 6
  H. Actinomycin D Experiments 6
  I. Puromycin Experiments 7
  J. Autoradiography Experiments 7
  K. Induction of Metamorphosis 9

II. MORPHOGENESIS OF THE LARVAL DIGESTIVE TRACT 10
  Introduction 10
  A. Morphogenetic Mechanisms in Animals 10
    i) Changes in the form of cell sheets 11
    ii) Fusions, detachments, and migrations . . 13

Chapter Page

II. iii) Enhanced cell proliferation 14
iv) Cell death 14
v) Cell rearrangement 15
B. Morphogenesis in Sea Urchins 16
i) Cleavage 17
ii) Blastula formation 18
iii) Ingression of the primary mesenchyme . . 18
iv) Gastrulation 20
C. Gene Activity and Morphogenesis 22
D. Objectives 23
Results 23
A. General Observations 23
B. Sphincter Formation 27
i) TEM 27
ii) Cytochalasin B 28
C. Coelom Formation 30
D. Shaping of the Larval Stomach 32
i) Number of cells 32
ii) Colchicine 32
iii) Autoradiography 34
iv) Stomach epithelium thickness 34
v) Length of the gut 35
Discussion 37
A. Morphogenetic Mechanisms 39
i) Sphincter formation 39

Chapter | Page

II. ii) Coelom formation 42

iii) Shaping of the larval stomach 43

iv) Bending of the larval digestive tract . 47

B. Genetic Control of Morphogenesis 47

Summary 52

III. HISTOGENESIS AND FUNCTIONAL ANATOMY OF THE LARVAL DIGESTIVE TRACT 54

Introduction 54

Results 56

A. Late Gastrula 56

B. Prism 57

C. Early Pluteus 58

D. Four-armed Pluteus 60

E. Eight-armed Pluteus 65

Discussion 73

A. Histogenesis 73

B. Feeding Behavior 76

C. Esophagus 78

D. Stomach 85

E. Intestine 86

Summary 87

Chapter Page

IV. METAMORPHOSIS AND THE FATE OF THE LARVAL DIGESTIVE TRACT 89
Introduction 89
Results 90
A. Metamorphosis 90
B. Changes in Larval Structures at Metamorphosis 94
Discussion 97
Summary 100

LITERATURE CITED 226

LIST OF FIGURES

Figure Page

1. Nomarski differential interference contrast (DIC) images of gastrulae of *Strongylocentrotus purpuratus* 44 hours after fertilization before and after treatment to dissociate ectoderm 103

2. Nomarski DIC images of *S. purpuratus* embryos 105

3. Nomarski DIC images of an *S. purpuratus* embryo 72 hours after fertilization 107

4. Nomarski DIC images of an *S. purpuratus* pluteus larva 88 hours after fertilization 107

5. Nomarski DIC images of *Dendraster excentricus* embryos 109

6. Ventral view of a 72 hour embryo of *S. purpuratus* and a lateral view of a 66 hour *S. purpuratus* embryo . 111

7. Nomarski DIC image of surface of the esophagus of a 90 hour pluteus of *S. purpuratus* 111

8. Scale drawings made from fixed *S. purpuratus* embryos depicting the morphogenesis of the larval digestive tract 113

9. A time-line showing the sequence and duration of morphogenetic events observed in the development of the larval digestive tract in *S. purpuratus* embryos 115

10. A series of micrographs demonstrating the constriction of the archenteron that results in the formation of the cardiac sphincter in *S. purpuratus* 117

11. Transmission electron micrographs (TEM) of cells in the presumptive sphincter region of the archenteron of a *S. purpuratus* embryo 119

12. TEM of a section cut obliquely through the forming cardiac sphincter of a 60 hour *S. purpuratus* embryo 121

Figure Page

13. TEM of a cell sectioned parallel to the long axis of the archenteron of an *S. purpuratus* embryo that was fixed during the formation of the sphincter 121

14. The luminal region of a sphincter-forming cell sectioned at right angles to the long axis of the archenteron 121

15. The luminal region of a sphincter-forming cell cut in cross-section 121

16. *S. purpuratus* embryos between 58 and 60 hours of development used in an experiment to test the effects of cytochalasin B (CCB) on sphincter formation 123

17. *S. purpuratus* embryos that were used in an experiment to test the effects of CCB on sphincter formation 125

18. Experiment testing the effects of CCB on the constriction in the archenteron after it had formed 125

19. A graphical summary of the experiments performed to examine the effects of CCB on sphincter formation in *S. purpuratus* embryos 127

20. *S. purpuratus* embryos between 48 and 62 hours after fertilization summarizing the morphogenesis of the coeloms 129

21. Nomarski DIC images of coeloms, during their formation, showing the filopodia extending from the surfaces of the cells 129

22. TEM of cells in the region of the presumptive sphincter of embryos that were treated with 5 μg/ml CCB for two hours prior to fixation, and the juxtaluminal region of a presumptive sphincter cell of an embryo that was treated with 5 μg/ml CCB 131

23. TEM of filopodia that extend from the blastocoelar surface of coelomic cells during the formation of the coeloms 131

Figure Page

24. *S. purpuratus* embryos used in an experiment to examine the effects of CCB on coelom formation 133

25. TEM of a filopodium located on the blastocoelar surface of a coelomic cell of an embryo treated for two hours with 5 μg/ml CCB prior to fixation . . . 133

26. The number of cells in the developing larval digestive tract 135

27. Embryos summarizing the experiments that tested the ability of the larval gut to form independently of cell division 137

28. Autoradiographs of *S. purpuratus* embryos used to analyse patterns of H^3thymidine incorporation 139

29. Thickness of stomach epithelium during development of *S. purpuratus* embryo 141

30. *S. purpuratus* embryos 88 and 56 hours after fertilization 143

31. Experiments testing the effects of actinomycin D on morphogenesis of the larval digestive tract 145

32. A graphical summary of the effects of actinomycin D on morphogenesis of the larval gut when treated at various times during development 147

33. Autoradiographs of cross-sectioned archenterons from embryos cultured at different stages in MFSW containing H^3actinomycin D 149

34. Experiments testing the effects of puromycin on morphogenesis of the larval digestive tract 151

35. A graphical summary of the effects of puromycin on the morphogenesis of the larval gut when introduced at various times during development 153

36. A graphical representation of the changes in cell shape that were observed during the constriction of the archenteron 155

37. A graphical representation of the model hypothesized to account for the changes in shape of the cells forming sphincters in the larval gut of *S. purpuratus* 157

Figure Page

38. Light micrographs of 1 μm sections of *Dendraster excentricus* 159

39. TEM of archenteron cells of gastrulae of *D. excentricus* 161

40. TEM of archenteron cells of gastrulae of *D. excentricus* 163

41. TEM of archenteron cells of prisms of *D. excentricus* 165

42. TEM of the presumptive larval stomach of an early pluteus 167

43. Filopodial extensions of mesenchyme cells that will form the esophageal muscles 167

44. TEM of the esophageal epithelium of a four-armed pluteus of *D. excentricus* 169

45. TEM of the myoepithelium that comprises the cardiac sphincter in a four-armed pluteus of *D. excentricus* 171

46. Epithelium of the stomach of a four-armed pluteus of *D. excentricus* 173

47. Epithelium of the stomach of a four-armed pluteus of *D. excentricus* 175

48. Epithelium of the intestine of a four-armed pluteus of *D. excentricus* 177

49. Scale drawings of four-, six- and eight-armed plutei of *D. excentricus* 179

50. SEM of eight-armed plutei of *D. excentricus* 181

51. Light micrographs of mid-frontal and mid-sagital sections of eight-armed plutei of *D. excentricus* 183

52. SEM and light micrographs of the esophagus of the four- and eight-armed plutei of *D. excentricus* 185

53. TEM of a cross-section of the upper and lower esophageal epithelium 187

Figure Page

54. TEM of esophageal muscles of eight-armed *D. excentricus* plutei 189

55. Cells of the lower esophageal epithelium and a septate junction between two cells of the upper esophageal epithelium of an eight-armed pluteus 191

56. Nervous tissues associated with the upper esophageal epithelium and the esophageal muscles of an eight-armed pluteus of *D. excentricus* 191

57. TEM of the lower esophageal epithelium, light micrograph of a cross-section through the cardiac sphincter, and TEM of the myoepithelium that forms the cardiac sphincter in an eight-armed pluteus 193

58. TEM of myoepithelial cells in the cardiac sphincter of an eight-armed *D. excentricus* pluteus 195

59. Type I stomach cells of eight-armed *D. excentricus* plutei 197

60. Type I stomach cells of an eight-armed pluteus of *D. excentricus* 199

61. Type II stomach cell of an eight-armed *D. excentricus* pluteus 201

62. Intestinal epithelium of an eight-armed *D. excentricus* pluteus 203

63. A graphical representation of peristalsis in the esophagus of pluteus larvae of *D. excentricus* 205

64. Competent *D. excentricus* larvae 207

65. The sequence of metamorphosis of *D. excentricus* 209

66. The sequence of metamorphosis of *D. excentricus* 211

67. Juvenile *D. excentricus* six days after metamorphosis 213

Figure Page

68. Juvenile *S. purpuratus* six days after metamorphosis 215

69. Light micrographs of a *D. excentricus* larva fixed during metamorphosis 217

70. TEM of a *D. excentricus* larva fixed during metamorphosis 219

71. Light micrographs of a juvenile *D. excentricus* which was fixed 49 hours after metamorphosis 221

72. A juvenile *D. excentricus* which was fixed 7 days after metamorphosis 221

73. TEM of stomach cells from a juvenile *D. excentricus* which was fixed 48 hours after metamorphosis 223

74. TEM of the primary loop of the gut of a juvenile *D. excentricus* which was fixed 7 days after metamorphosis 225

LIST OF TABLES

Table Page

1. The proportion of cells in each part of the larval gut, expressed as a percentage of the total number of cells in the gut at each stage 33

MATERIALS AND METHODS

A. Culture Methods

All embryos and plutei were reared from fertilized eggs using the standard procedures outlined by Hinegardner (1969), Strathmann R. (1971), and Strathmann M. (1968). Adult *Strongylocentrotus purpuratus* were collected intertidally from San Juan Island, Washington, or Clallam Bay, Washington. Adult urchins were also obtained from Pacific Biomarine Supply, Venice, California. Adult *Dendraster excentricus* were collected intertidally from Orcas Island, Washington.

Spawning was induced by intracoelomic injection of 0.55 M KCl. Embryos developed normally in either Millipore filtered sea-water (MFSW) or artificial sea-water made from synthetic sea-salts (Instant Ocean Inc.). Embryonic cultures were maintained at sea table temperatures at Friday Harbor Laboratories (10° to 15°C) or in a controlled environment chamber (15°C).

Cultures with a high degree of synchrony, for experimental purposes, were started using a modified insemination procedure. About 1 ml of a dense suspension of freshly spawned eggs was put into 50 ml of MFSW. 0.1 ml of freshly spawned sperm was diluted in 10 ml of MFSW to obtain a concentration of about 4×10^6 cells/ml. 0.1 ml of the diluted sperm solution was added to the egg suspension, which was swirled for 10 seconds to facilitate rapid mixing. The gametes were left at this concentration for 45 seconds and then diluted with 500 ml of MFSW. Sea-water was immediately aspirated from the culture through a 35 μm Nitex mesh. The concentrated suspension of fertilized eggs was then divided into two beakers and 500 ml of MFSW added to each. When the embryos hatched from their fertilization membranes and began to swim (ca. 30 hours), the first embryos to rise to the surface were subcultured and used for experimentation.

Larval and juvenile stages were cultured in natural sea-water (SW) at a concentration of about 1 larva/ml. Cultures were agitated with paddles attached to a 2 RPM electric motor. Larvae were fed *ad libitum* a mixed diet of *Phaeodactylum tricornutum* and *Dunaliella salina* or plankton collected from Friday Harbor which had been passed through a 53 μm Nitex mesh.

B. Light Microscopy

Nomarski differential interference contrast micrographs of live, unstained specimens were made using the techniques outlined by Allen et al. (1969). Specimens were immobilized either by entrapment beneath a footed coverslip or by treatment for 5 minutes with SW containing nicotine leached from a cigarette filter (Strathmann, 1968).

Micrographs of sectioned material were made from specimens fixed and embedded as stated below for transmission electron microscopy. One micrometer sections were cut with glass knives and stained with methylene blue and azure II (Richardson et al., 1960).

The events of metamorphosis were photographed on a Zeiss compound microscope fitted for epi-illumination. Larvae were induced to metamorphose in an excavated slide and photographed without any form of immobilization.

C. Transmission Electron Microscopy (TEM)

Several fixation techniques were tried throughout the course of this study. Good results were repeatably obtained by initially fixing the tissues for 1 to 2 hours, at room temperature, in a solution containing 2.5% monomeric glutaraldehyde, 0.2 M phosphate buffer (Millonig, 1961), and 0.14 M sodium chloride (Cloney and Florey, 1968). Specimens were then rinsed in a solution of 0.2 M phosphate buffer and 0.34 M sodium chloride (Cloney and Florey, 1968). Tissues were post-fixed for 1 to 2 hours, at room temperature, in a solution containing 2% osmium tetroxide and either 1.25% sodium bicarbonate (Cloney and Florey, 1968) or 0.2 M phosphate buffer (Millonig, 1961).

An alternative technique, which gave equally good results, began with an initial fixation for 15 minutes, at room temperature, in a 6% glutaraldehyde solution buffered with 0.2 M cacodylate (pH 7.4) (Fankboner, 1978). The glutaraldehyde solution was diluted from a stock solution of 25% glutaraldehyde containing 3% calcium carbonate. After a brief rinse in distilled water, the tissues were post-fixed for 30 minutes, at room temperature, in 2% osmium tetroxide buffered with Dorey's solution B (Dorey, 1965). 3.5% potassium chloride was substituted for the sucrose originally prescribed in the Dorey formula (Fankboner, 1978).

After fixation, the specimens were rinsed in distilled water and dehydrated in increasing concentrations of ethanol. The tissues were then transferred through two changes of propylene oxide and infiltrated and embedded in Epon according to the method of Luft (1961). The specimens were flat embedded in a thin layer of Epon in disposable metal weighing pans. Individual specimens could be cut from the resulting disc under a dissecting microscope and mounted with precise orientation on a stub for sectioning.

Sections were cut on a Porter-Blum MT II ultramicrotome with a diamond knife. Ribbons of sections, with silver-grey interference colours were mounted on parlodion-coated copper grids. Sections were stained in 50% ethanol saturated with uranyl acetate (Watson, 1958), and lead hydroxide chelated with sodium citrate (Reynolds, 1963). Sections were observed and photographed on either a Philips EM 201 or EM 300.

D. Scanning Electron Microscopy (SEM)

Specimens were initially fixed as for TEM and post-fixed for 2 hours, at room temperature, in a solution containing 4% osmium tetroxide and 2.5% sodium bicarbonate. They were then rinsed in distilled water and dehydrated with ethanol. Specimens were transferred through increasing concentrations of iso-amyl acetate and critical point dried. Individual larvae were mounted on metal stubs and some specimens were fractured to reveal internal detail. The specimens were sputter-coated with gold and viewed on a Cambridge Stereoscan SEM.

E. Cytochalasin B Experiments

Embryos were cultured in MFSW containing cytochalasin B (CCB) during sphincter formation or coelomic pouch formation. Eggs were inseminated using the procedure for enhanced synchrony outlined above. Measured volumes of MFSW and embryos were subcultured in five 60 mm × 15 mm glass petri dishes. A stock solution of 1 mg/ml CCB (Aldrich Biochemicals) in dimethyl sulfoxide (DMSO) was prepared, and appropriate volumes of it were added to three of the petri dishes to obtain final concentrations of 1 μg/ml CCB in 0.1% DMSO, 5 μg/ml CCB in 0.5% DMSO, and 10 μg/ml in 1% DMSO. Control cultures containing 1% DMSO and MFSW were similarly prepared. Individual embryos were isolated from these experimental cultures and put into depression slide wet chambers for repeated observations. All of the experimental cultures, including the wet chambers, were kept at sea-water temperatures.

Embryos were returned to MFSW by being hand centrifuged, then rinsed in MFSW, and resuspended in MFSW. Embryos from wet chambers were removed with a pipet and put into a watch glass containing 10 to 15 ml of MFSW.

Observations were made at frequent intervals and the experimental and control embryos were sketched and photographed using the techniques already described. Embryos to be prepared for TEM were hand centrifuged, resuspended in primary fixative, and processed as outlined above.

F. Cell Counting Procedures

The cells of the developing archenteron and gut were counted after the dissociation of the ectodermal cells. A modification of the dissociation technique reported by McClay et al. (1977) was used. Embryos, from cultures of enhanced synchrony, were hand centrifuged and suspended, for 5 minutes, in 1 M glycine with 2 mM EDTA (ethylenediaminetetraacetic acid). The embryos were then concentrated and suspended in calcium- and magnesium-free MFSW. To aid in dissociation of the cells, the embryos were gently squirted out of a pasteur pipet against the bottom of the centrifuge tube. After hand centrifugation and rinsing in calcium- and magnesium-free MFSW, a small drop was placed on a glass slide and covered with an un-footed cover slip.

The cells of the ectodermal epithelium were removed leaving the blastocoelar basal lamina containing the primary mesenchyme cells and the archenteron (Fig. 1). The gut formed a flattened tube of cells which could be counted, with consistent repeatability, under a 100X (n.a. = 1.25) planachromatic objective, and Nomarski differential interference contrast optics.

Averages ($\overline{Y}$) and standard deviations (s) were calculated from data obtained from at least 10 specimens of two cultures.

G. Colchicine Experiments

Embryos that had completed gastrulation were cultured in MFSW containing colchicine throughout the formation of the larval digestive tract.

Measured volumes of MFSW and embryos, from cultures of enhanced synchrony, were put into four 60 mm × 15 mm glass petri dishes. A stock solution of 40 mg/ml colchicine (Sigma Chemical) in MFSW was prepared, and appropriate volumes of it were added to three of the petri dishes to obtain final concentrations of 5×10^{-5} M, 5×10^{-4} M, 5×10^{-3} M colchicine. The control culture contained only MFSW. Individual embryos were put into depression slide wet chambers for repeated observations. All of the experimental cultures were kept at sea table temperatures.

The embryos were sketched and photographed at the beginning and end of each experiment, and observations were made at frequent intervals.

Cell counts, as outlined above, were made on 10 embryos from each petri dish.

H. Actinomycin D Experiments

Embryos, at various stages throughout the development of the larval digestive tract, were put into MFSW containing actinomycin D.

A measured volume of MFSW and embryos were removed from cultures of enhanced synchrony and put into two 60 mm × 15 mm glass petri dishes. A stock solution of 5 mg/ml actinomycin D (Sigma Chemical) was prepared, and an appropriate volume of it added to one of the dishes to obtain a final concentration of 25 μg/ml. Individual embryos were isolated in depression slide wet chambers for repeated observations. All of the experimental cultures were kept at sea table temperature (10° to 15°C). Embryos were returned to MFSW after being hand centrifuged and rinsed.

Experimental cultures were prepared with embryos that ranged in their state of development from the initiation of gastrulation to the completion of sphincter formation. The experimental embryos were all kept until the control cultures had reached a feeding stage.

Observations were made at frequent intervals. The experimental and control embryos were sketched and photographed, using the techniques already described.

I. Puromycin Experiments

Embryos, at various stages throughout the development of the larval digestive tract, were put into MFSW containing puromycin. A stock solution of 4 mg/ml puromycin (Sigma Chemical) was used to prepare a final concentration of 20 μg/ml; otherwise, all the procedures for these experiments were the same as those for the actinomycin D experiments described above.

J. Autoradiography Experiments

The incorporation of a radioactively-labelled nucleotide during the shaping of the larval digestive tract was analysed autoradiographically. Embryos, of enhanced synchrony, that were beginning the formation of coelomic pouches (48 hours at 15°C) were put into three 60 mm × 15 mm glass petri dishes. The dishes contained:

1) MFSW, with 250 μg/ml Streptomycin Sulfate (Sigma Chemical),
2) MFSW, with 250 μg/ml Streptomycin Sulfate and 10 μci/ml H^3thymidine, specific activity 6.7 ci/mmole (New England Nuclear), and
3) MFSW, with 250 μg/ml Streptomycin Sulfate and 20 μci/ml H^3thymidine, specific activity 6.7 ci/mmole (New England Nuclear).

The embryos were cultured throughout the shaping of the gut (until 72 hours old) and then fixed and processed for TEM.

Serial sections, 1.0 μm thick, were cut with a glass knife and mounted on gelatin subbed, glass slides (Rogers, 1969). The slides were dipped in nuclear track emulsion (Kodak NTB 2), dried, and kept at 4°C for a 10-day exposure period. The emulsion was developed in Kodak Dektol developer, fixed in 30% sodium thiosulfate, and the slides were washed in distilled water. The sections were stained with 0.25% toluidine blue in 0.5% sodium borate (Stell and Lightfoot, 1975). The slides were photographed on a Zeiss Universal microscope fitted for Koehler critical illumination.

Embryos cultured without labelled nucleotide (dish 1) served as chemographic controls. A single slide bearing sections of a labelled embryo was exposed to white light as a control for latent image fading.

The permeability of embryos to actinomycin D both before and after gastrulation was also examined autoradiographically. Mid-gastrulae (36 hours) and post-gastrulae (48 hours) were cultured in media containing 12.5 µci/ml H^3actinomycin D, specific activity 7.9 ci/mmole (Amersham). After 1 and 4 hours embryos were removed from the radioactive culture media and fixed as for TEM.

Subsequent processing was as is described above except the slides were dipped in Kodak NTB 3 nuclear track emulsion and exposed (4°C) for 65 days. Chemography and latent image fading were controlled with unlabelled embryos and fogged slides.

K. Induction of Metamorphosis

Larvae that had the morphological characteristics of competency were removed from stock cultures and put into 60 × 15 mm glass petri dishes that contained MFSW and the materials to be tested as inducers. One dish contained only MFSW and served as a control for handling procedures. Observations were made at frequent intervals with a dissecting microscope, and experiments lasted from 24 hours to several days.

MORPHOGENESIS OF THE LARVAL DIGESTIVE TRACT

INTRODUCTION

Morphogenesis is, quite simply, the development of form. In an embryological context it refers to the fertilized egg assuming the form of the adult. Practically, the study of morphogenesis deals with descriptions of the changes in structure that occur during the development of an organism.

Morphogenetic mechanisms are the physiological processes that are directly responsible for changes in structure. In embryos these processes produce changes in form principally by movements of cells and tissues.

Morphogenesis of the larval digestive tract in echinoids is the transformation of a tube into a functional, tripartite gut. This aspect of sea urchin development is examined with reference to morphogenetic mechanisms that have been previously identified in animals, and to what is known of morphogenesis in sea urchins.

A. Morphogenetic Mechanisms in Animals

Systematic analysis of development in terms of morphogenetic mechanisms began at the end of the last century when His (1874), Roux (1895), and Rhumbler (1902) stressed the importance of *Entwichlungsmechanik*. Since that time a variety of morphogenetic mechanisms have been hypothesized and investigated. These are reviewed by Morgan (1927), Trinkaus (1965, 1967), and Gustafson and Wolpert (1963a, 1967).

Morphogenetic mechanisms can be broadly classified into five groups: i) changes in the form of cell sheets; ii) fusions, detachments, and migrations; iii) enhanced cell proliferation; iv) cell death, and v) cell rearrangements. The first two mechanisms discussed are responsible for the majority of morphogenetic events and each has multifarious applications. The remaining three mechanisms, although they occur in a variety of animals, have more restricted use.

i) Changes in the Form of Cell Sheets

Folding, evagination, invagination, pallisading, and epiboly are all morphogenetic processes that are changes in the form of simple epithelial layers. All involve alterations in the thickness and curvature of cell sheets. These processes have been implicated in a plethora of morphogenetic events.

For example, the initial stages of gastrulation in many animals is an infolding or invagination. The formation of diverticula exemplifies outfolding and evagination. The thickening and thinning of epithelia is a phenomenon common to the development of many animals; the formation of lens placodes and the thinning and overgrowth (epiboly) of blastodermal epithelium in amphibians are two examples.

These processes are unified by the idea that a cell sheet can be made to thicken, thin, fold, or pocket, by altering the shape of the cells which form the sheet. This idea was originally suggested by Rhumbler (1902). The mechanism is reviewed by Morgan (1927), Moore (1930) and Trinkaus (1965, 1967).

A flat sheet of cuboidal cells can be made thicker by the cells becoming columnar in shape; their cross-sectional area and their volume need not change. Conversely, the sheet may be enlarged by the cells becoming squamous. Curvature can be produced in the sheet by making the

6

cells trapezoidal in outline. Concave and convex curves can be alternatively produced, depending upon which end of each cell narrows or broadens. Compound curves (inpocketings and outpocketings) result from changing the dimensions of the cells along two axes.

A variety of mechanisms that would cause cells to change their shape have been hypothesized. Rhumbler (1902) and Glaser (1914) suggested changes in cell surface tension. Bütschli (1915) proposed differential swelling on the two sides of the cell layer. Gillette (1944) and Lewis (1947) hypothesized differential contraction of the cell surfaces or superficial layers. Moore (1930) implicated alterations of cell connections. Gustafson and Wolpert (1963a) envisioned changes in adhesion between the cells, and between cells and supporting structures, integrated with changes in tension in the cell membrane, as producing the forces that cause cells to change their shape.

There is a body of evidence that suggests alteration in cell shape in many animals may be mediated by microtubules and microfilaments. Cytoplasmic microtubules have been found to be associated with cells that are extending processes or elongating (Gibbins et al., 1969; Byers and Porter, 1964; Granholm and Baker, 1970). Microfilaments have been found to be associated with a variety of contractile events in cells (Inoué and Stephens, 1975; Goldman et al., 1976). Both of these organelles have been observed in cells within epithelia that are undergoing changes in form (Cloney, 1966; Baker and Schroeder, 1967; Granholm and Baker, 1970; Perry and Waddington, 1966). The precise nature by which microtubules and microfilaments produce and direct forces remains essentially unknown.

ii) Fusions, Detachments, and Migrations

The development of form in most animal embryos involves one or more of these processes: a) detachment of tissues from tissues; b) detachment of cells from tissues; c) fusion of tissues with other tissues; d) fusion of cells into tissues, and e) the migration of free cells. These processes are allied in that they all involve the predetermined making or breaking of specific cellular contacts.

There are numerous examples of these phenomena from a variety of animals. The release of presumptive mesoderm, in the form of mesenchyme, is common to most eumetazoan phyla (cf. Kumé and Dan, 1968). The fusion of tissue layers occurs in the development of most organisms during the formation of the digestive tract. The endoderm and ectoderm reunite to form the mouth in deuterostomes and the anus in protostomes. In vertebrates the migration and fusion of mesenchyme to form tissues such as kidney tubules and dermal papillae are examples of directed migrations of cells (Balinsky, 1975).

All of the factors responsible for the making and breaking of cellular contacts are not known. Alterations in both protein and carbohydrate moieties on the surface of the cells are apparently involved (Kemp et al., 1973). Similarly, the factors responsible for the direction and specificity of cell migrations are obscure. The observation that the direction of cell movement can be altered by the substrate over which it is moving has formed the basis of current theory (Weiss and Garber, 1952).

The mechanisms of cell locomotion are reviewed by Trinkaus (1973) and Wessells et al. (1973). There are apparently relationships between the extension and retraction of cytoplasmic processes that occur during locomotion, and microtubules and microfilaments found within migrating cells.

iii) Enhanced Cell Proliferation

Regions in which cells are replicating at a higher rate than adjacent regions have a proportionally faster rate of growth; this allometry can contribute to the development of the body form.

This phenomenon is best known during morphogenesis associated with regeneration. Hay (1962) describes an enhanced mitotic index in the newly formed blastema in amphibians, and similar situations exist during regeneration in annelids, nemerteans, and platyhelminthes (Berrill, 1961). Localized proliferations have also been described during stolon elongation and bud formation in coelenterates (Berrill, 1961).

Regions of enhanced proliferation have been hypothesized for embryonic morphogenesis, but convincing evidence of their existence, in most instances, is lacking. The accumulation of mesenchyme during the formation of dermal papillae in vertebrates was attributed, in part, to regions of rapid cell division. Counting mitoses (Balinski, 1950) and tritiated thymidine incorporation (Wessells and Roessner, 1965) failed to indicate the presence of such regions. In some situations, morphogenesis can be accounted for by other mechanisms; the apparent 'growth' of epiboly occurs independently of cell division (Richards and Porter, 1935).

iv) Cell Death

Cell death plays a role opposite to that of growth; it eliminates tissue. Saunders (1966) and Saunders and Fallon (1967) review in detail cell death during development in vertebrates. The best known example of necrosis contributing to the development of form is described by Saunders et al. (1962). Intensive cell degeneration occurs during chick development in the shaping of the wing and in the removal of tissues between the digits. It has been determined that necrosis is a morphogenetic event controlled by the immediate cellular and humoral environment (Saunders, 1966).

v) Cell Rearrangement

Fristrom (1976) found that the dramatic changes in shape that occur during the eversion of imaginal discs in *Drosophila melanogaster* is, in part, due to cellular rearrangement. The essence of the idea is that an epithelial sheet can change its dimensions by cells moving to new positions. For example, a flat sheet of cells, 4 cells by 4 cells, can double its length by becoming 8 cells by 2 cells. The cells of one row need only intercalate between the cells of an adjacent row.

Fristrom (1976) observed that after eversion of the leg discs, there is an increase in length and a decrease in diameter of the simple epithelial tubes. These changes are accompanied by a decrease in the number of cells around the circumference, as a model of rearrangement would predict. Cell division and cell shape changes were eliminated as possible mechanisms (Fristrom and Fristrom, 1975). Observations of somatic mosaics, where clonally related cells can be identified in patches, further supported her hypothesis of rearrangement (Fristrom, 1976).

B. Morphogenesis in Sea Urchins

The sequence of morphogenetic events proceeding from the fertilized egg to the feeding pluteus have been described for numerous species of sea urchin. The first descriptions published are those of Krohn (1849, cited by MacBride, 1903). Agassiz (1872, 1874) amplified Krohn's and Müller's (1846-1854) observations, providing a complete sequence of major morphogenetic events in the formation of the pluteus and its subsequent metamorphosis.

Gustafson and Wolpert with various co-workers have provided descriptions, in detail, of nearly every aspect of urchin development to pluteus (see Gustafson and Wolpert, 1963a, 1967, for review). Their descriptions are aimed at elucidating the morphogenetic mechanisms responsible for the formation of the pluteus. Their observations indicate that two morphogenetic mechanisms can account for all aspects of development that they have described: 1) alterations in the form of cell sheets, and 2) directed migrations involving detachments and fusions of cells.

Gustafson and Wolpert (1963a, 1967) have further hypothesized that the forces responsible for the alterations in the shape of cell sheets in echinoid embryos are produced by changes in the adhesion between adjacent cells and supporting layers and variations in the tension within cell membranes. Their hypothesis predicts that increases in the area of adhesion between cells and a corresponding loss of adhesion between the cells and a supporting layer results in a more columnar arrangement of the epithelium. Conversely, squamous epithelia could be produced by reducing the adhesion between cells and increasing the adhesion to the supporting layer. Curvature in cell sheets can be produced by increasing intercellular adhesion and maintaining cell-supporting layer adhesion. Increasing the tension within the membranes of cells in an epithelium causes a decrease in the amount of contact between adjacent cells. At a maximum the tension will produce round cells with only point contacts with adjacent cells. These authors also suggest that the integration of these two processes facilitates the change in form of cell sheets in echinoids.

Gustafson and Wolpert (1963a, 1967) hypothesized that the migration of cells and the release of cells from tissues was facilitated by the extension and subsequent contraction of filopodia. They observed cells to move in the direction of shortening filopodia. Variations in cell adhesion and the relative strengths of cell-filopodia attachments were hypothesized to be factors determining the direction of cell migration.

The aspects of sea urchin morphogenesis that have received the most attention are: i) cleavage of the fertilized egg, ii) formation of the blastula, iii) ingression of the primary mesenchyme cells, and iv) gastrulation.

i) Cleavage

The fertilized egg divides meridionally to form two blastomeres. The division is characterized by a furrow that constricts the egg into two equal parts.

Rappaport (1967) and Hiramoto (1975) have measured tensile forces of 10^{-3} to 10^{-2} dynes within the cleavage furrow. Schroeder (1969) described a band of microfilaments that are circumferentially oriented beneath the plasmalemma of the furrow for the duration of the constriction phase of cleavage. The filaments are sensitive to cytochalasin B (Schroeder, 1972), hydrostatic pressure (Tilney and Marsland, 1969), and under specific conditions are able to bind heavy meromyosin (Schroeder, 1973). The temporal and geometric association of the microfilaments with the cleavage furrow, the disintegration of the band upon application of inhibitors to furrow formation, and the alliance of the microfilaments with actin, a contractile protein, support the hypothesis that they are responsible for generating the forces of cleavage constriction (Schroeder, 1976).

ii) Blastula Formation

The egg continues to divide and by the seventh synchronous division the resulting mass of cells begins to form a hollow ball, the blastula.

A sphere will result from an equilibrium between a uniform expansive force applied centrifugally and a uniform tension within a surface resisting it (Sears and Zamanski, 1960). Gustafson and Wolpert (1963a) suggest that the tension within the cell sheet, the blastoderm, could be generated by the resiliency of the blastomere membranes, the intercellular connections, the hyalin layer, or a combination of any or all of these. The expansive force applied normal to the cell sheet could be generated by a pressure differential between the interior and the exterior of the blastocoel (Monné and Hardé, 1951) or by a centrifugal force due to the adherence of the blastomeres to the hyalin layer (Dan, 1960).

iii) Ingression of the Primary Mesenchyme

The blastula anticipates the ingression of the primary mesenchyme by becoming flattened in the vegetal region. The mesenchyme cells migrate from this vegetal plate into the blastocoel where they form a syncytium and secrete the larval skeleton (see Gustafson and Wolpert, 1963a, 1967; Dan, 1960; Okazaki, 1975, for reviews).

Gustafson and Kinnander (1965) report that the primary mesenchyme cells, prior to entering the blastocoel, begin to pulsate and extend lobes and filopodia from their blastocoelar surface. Subsequently, the cells dissociate from the vegetal plate and form a clump of rounded cells on the vegetal pole of the blastocoel.

Gustafson and Wolpert (1967) analyse the initial stages of this behavior as a variation in cellular adhesion and an increase in membrane tension. This frees the cells from the blastoderm and gives them a rounded profile.

Gibbins et al. (1969) report that the distribution of microtubules in the primary mesenchyme cells changes from an orderly apical array focusing on the basal body of the cilium, to a random distribution extending into the pulsatory lobes. They further report that in the primary mesenchyme cells within the blastocoel, a centriole is located near the center of the now spherical cells and an array of microtubules radiates from it. They concluded that the microtubules play a role in the development of cell shape.

Deuterium stabilizes microtubular structure (Marsland and Zimmerman, 1963, 1965). Colchicine and hydrostatic pressure disassemble microtubules and prevent their reassembly (Zimmerman and Marsland, 1964). Application of colchicine and hydrostatic pressure halted the development of the primary mesenchyme and tended to spherulate the cells that had moved into the blastocoel (Tilney and Gibbins, 1969a). Exposure to deuterium similarly halted further development, but cell asymmetries persisted.

Once the primary mesenchyme cells have entered the blastocoel, they send out numerous filopodia (Gustafson and Wolpert, 1961). The filopodia extend from the surface of the primary mesenchyme cells and make random explorations of the blastocoel wall. The attachment and contraction of the filopodia disperses the cells. The initial displacement of the cells appears to be random as the cells become scattered throughout the vegetal half of the blastula. The primary mesenchyme cells soon form a syncytial chain that circles the vegetal plate with two anteriorly oriented branches on the ventral wall. The larval skeleton is secreted into an organic matrix within a membrane-limited vacuole in the cytoplasm of the syncytium (Gibbins et al., 1969).

Wolpert and Gustafson (1961) attribute the motive force of this directed migration to the contraction of the filopodia. Gibbins et al. (1969) have demonstrated that the filopodia contain microtubules and microfilaments, an observation supporting the idea that the contractile force is localized within the filopodia.

Gustafson and Wolpert (1963a) suggest that the direction of movement of the cells is determined by the yielding of filopodia that have made weak attachments to filopodia that have made firmer attachments.

iv) Gastrulation

Gastrulation is a process of displacement of presumptive organ rudiments from the blastoderm to the interior of the embryo. A blind tube, the archenteron, invaginates from the vegetal plate and extends across the blastocoel to fuse with the presumptive stomodeum.

Gustafson and Kinnander (1956) and Dan and Okazaki (1956) simultaneously observed the process of gastrulation to take place in two distinct phases. By plotting the length of the invaginating archenteron against time, Gustafson and Kinnander found that invagination proceeded at a uniform rate until the archenteron had travelled one third of the way across the blastocoel. Filopodia then extended from the secondary mesenchyme cells at the tip of the archenteron and stretched to the presumptive stomodeum. As this occurred the rate of lengthening of the archenteron increased, making a distinct inflexion point on the time-length plot. Gustafson and Kinnander (1956) have hypothesized that the filopodia are contractile and supply the motive force for the second phase of gastrulation.

Moore and Burt (1935) have demonstrated that the forces necessary for the first phase of gastrulation are localized in the vegetal plate. They were able to observe the initial invagination in excised vegetal plates. Gustafson and Wolpert (1963a) attribute the invagination to alterations in cell adhesion leading to a deformation of the cell sheet.

As the archenteron extends to the limits of the autonomous phase, filopodia begin to appear at the tip. Tilney and Gibbins (1969b) observed 5 nm filaments to be a dominant organelle in the filopodia. Microtubules were present at the bases of these cytoplasmic extensions but were rarely observed in the filopodia themselves. They concluded that both microtubules and microfilaments are involved in filopodial movements. They suggest that the microtubules are instrumental in the formation and elongation of the filopodia and that the microfilaments are implicated in their contractility.

C. Gene Activity and Morphogenesis

It is an unquestioned paradigm of biology today that the structure and function of an organism are determined by the genetic character of the organism. The cells and tissues of an animal owe their structural and functional attributes to the nature of their constituent proteins, which result from the expression of the information encoded in the genes of the cells. The details of the relationship between developmental phenomena and this central dogma remain enigmatic. However, considerable research has been directed towards understanding mechanisms of the flow of genetic information during the initial stages of development in sea urchin embryos.

Upon fertilization of the egg, there is an immediate increase in the rate of protein synthesis (Epel, 1967). Experiments with inter-species hybrids, enucleated eggs, and actinomycin D indicate that the initial events of embryogenesis, which are presumably directed by these newly synthesized proteins, are not under the direction of the embryonic genome (reviewed by Davidson, 1968 and Stearns, 1974). The development of the fertilized egg to gastrulation is instead determined, almost wholly, by the translation of messenger RNA allotted to the egg during oogenesis. Accordingly, development after gastrulation is controlled by proteins that are encoded in the embryonic genome.

Barros et al. (1966) and Giudice et al. (1968) analysed the temporal relationships between gene activity and morphogenesis in echinoderms. Pulse treatments of actinomycin D throughout pregastrular development indicate there is a brief period (5 to 6 hours) during which interfering with the synthesis of RNA blocks gastrulation. The transcription of proteins vital to gastrulation evidently occurs during a finite period of development some 15 to 18 hours before gastrulation.

D. Objectives

It is clear that a great deal is known about morphogenesis in sea urchin embryos, though interest has been predominantly with early development, and hypothesized morphogenetic mechanisms have not all been tested experimentally. The formation of the larval digestive tract is an aspect of the development of the pluteus that has received only cursory attention from investigators.

The objectives of this portion of my research are:

1) to describe and document the morphogenesis of the larval digestive tract,

2) to investigate the mechanisms responsible for specific morphogenetic events during the development of the larval gut, and

3) to investigate temporal aspects of the genetic control of morphogenetic events contributing to the formation of the larval digestive tract.

RESULTS

A. General Observations

Eggs of *S. purpuratus* begin their first cleavage three hours after fertilization (15°C). The subsequent divisions occur more rapidly, and by 24 hours a morula has formed. The ensuing mesenchyme-blastula stage hatches from the protective fertilization membrane at about 30 hours. The initial invagination of gastrulation begins at 38 hours (Fig. 2a).

The second phase of gastrulation, which is directed by the contraction of filopodia, begins at about 40 hours, and gastrulation is completed by 44 hours (Fig. 2b).

The embryo, at the completion of gastrulation, is roughly ovoid in shape, although the ventral surface is somewhat flattened. The archenteron is a blind tube that lies along the anterior-posterior axis; the tip is flexed slightly toward the ventral surface and apposed to the ectodermal epithelium.

The epithelium in regions of the archenteron where the cardiac and pyloric sphincter are to form has begun to thicken by 54 hours. The single layer of cells is about 3 μm thick at the completion of gastrulation and becomes 5 to 7 μm thick prior to the formation of the sphincters. The cardiac sphincter forms first; it appears initially as a constriction of the tube 20 to 25 μm from the anterior end. The constriction takes about two hours to form beginning at 58 hours (Fig. 9). The pyloric sphincter forms in about the same amount of time beginning shortly after the cardiac sphincter (Figs. 2, 9).

The regions of the archenteron that will form the larval esophagus, stomach, and intestine are distinct by about 64 hours (Figs. 3, 8). The stomach is spindle-shaped at this stage; between 64 and 72 hours it bulges to become more spherical (Figs. 8, 9). By 76 hours the stomach has expanded in diameter from 20 to 50 μm. The esophagus increases to 40 μm at its widest part, while the intestine becomes 30 μm at its greatest width (Figs. 4, 8).

Between 64 and 76 hours the digestive tract, which began as a straight tube, bends to form a 'J'; the intestine points anteriorly from the pyloric sphincter (Figs. 8, 9). The stomodeum forms between 60 and 72 hours (Fig. 9). The tip of the archenteron fuses with the ectodermal epithelium and a small opening appears (Figs. 3, 4). It gradually enlarges to become 15 μm in diameter and the larva becomes capable of feeding about 88 hours after fertilization (Figs. 4, 8, 9).

The coeloms form at the tip of the archenteron beginning at about 48 hours (Figs. 2, 3, 4, 8, 9). After the completion of gastrulation there is an apparent proliferation of the mesodermal cells that will become the coeloms. A single mass of cells emerges from the dorsal surface of the tip of the archenteron. By 52 hours the cells have separated into two clumps at the sides of the archenteron. The two lateral masses soon become hollow pouches; their lumina remain continuous with the lumen of the archenteron (Fig. 2c). By 56 hours the coeloms have extended further from the archenteron and become triangular in outline (Fig. 2d).

The coeloms by 60 hours are paired ear-like sacs attached to the sides of the presumptive esophagus (Fig. 3). The connections between the lumina of the coeloms and the lumen of the esophagus become occluded by about 64 hours. The coeloms continue to grow posteriorly, becoming flattened and apposed to the sides of the esophagus in the feeding pluteus (Figs. 4, 6).

In the 64 hour embryo, cells extend from the posterior tips of the coelomic pouches and attach to the ventral transverse rods of the larval skeleton (Fig. 6a). These strands will form the ventral dilator muscles of the larval mouth. Another extension from the dorsal surface of the left coelom to the epidermis forms the hydroporic canal (Fig. 6b).

Extensions of the coelomic cells that will form the esophageal muscles begin to wrap around the esophagus at 68 hours (Figs. 7, 9). The coeloms at this stage are comprised of two groups of cells: one group occupies the blastocoelar surface and the other group forms the surface of the pouches apposed to the developing esophagus. The cells in the first group are each 10 to 12 μm in diameter and the cells of the second group are each 5 to 7 μm. The group of smaller cells produces the filopodia that form the esophageal muscles. The filopodia extend from the sides toward the midline of the esophagus. By 84 hours they are capable of the sequential contractions that produce the peristaltic movements of the esophagus.

The sequence of morphogenetic events leading to the formation of the larval digestive tract in *D. excentricus* is essentially the same as the sequence in *S. purpuratus*. However, it is compressed into a much shorter period of time (Fig. 5). While gut formation (gastrulation to feeding) takes about 44 hours in *S. purpuratus*, it is accomplished in 24 hours in *D. excentricus* (15°C). As well, the tissues of the archenteron-gut in *D. excentricus* differ notably in thickness from those of *S. purpuratus* (Figs. 2, 3, 5). The endodermal cells in *D. excentricus* are 10 to 12 μm tall while the endodermal cells in *S. purpuratus* are 4 to 7 μm tall.

In *D. excentricus* gastrulation is completed 36 hours after fertilization (15°C) (Fig. 5b). The constrictions of the archenteron that become the sphincters occur at about 40 hours (Fig. 5c). The stomach expands from a spindle shape to become a sphere between 42 and 48 hours (Fig. 5d). The formation of the coeloms takes about 10 hours beginning at the completion of gastrulation. The larval mouth breaks open at 46 hours and the larva is capable of ingesting and digesting food by 60 hours (Fig. 5d).

B. Sphincter Formation

i) TEM

The archenteron, prior to formation of the sphincters, is comprised of simple cuboidal epithelium. The cells are nearly square in outline, 4 µm by 4 µm (Fig. 11). Near the luminal surface, the cells are attached with maculate septate junctions, and a thin basal lamina lines the blastocoelar surface. Each cell contains a centrally located nucleus, 2 µm in diameter. Yolk vesicles, 0.5 µm in diameter, and clear vacuoles are scattered throughout the cytoplasm. There appear to be two classes of yolk vesicles; one contains a homogeneous substance of medium electron-density, and the other has granular contents and is less electron-dense (Figs. 11, 13). The cytoplasm also includes cisternae of rough endoplasmic reticulum, clumps of ribosomes, and mitochondria. Each cell bears a single cilium on its luminal surface, and the plasmalemma around the base of the cilium is elaborated into a collar of 8 to 10 microvilli.

Between 54 and 58 hours, the cells in the region of the presumptive sphincter increase to 7 µm in height (Fig. 10). The cells are rectangular in outline and the polarity of the cytoplasm becomes apparent as the nuclei are located in the basal regions.

During the constriction of the archenteron, the cells that participate in the formation of the sphincter change in outline from rectangular to triangular (Figs. 10, 11). The cells immediately above and below the wedge-shaped sphincter cells change in outline from rectangles to parallelograms.

Specimens fixed during the constriction of the archenteron were observed to contain an electron-dense region, 0.1 μm thick, immediately beneath the plasmalemma on the luminal surface of the wedge-shaped sphincter cells (Figs. 12, 13). The electron-dense region is comprised of a fine granular matrix; in some specimens microfilaments, 7 nm in diameter, can be discerned (Figs. 14, 15). The microfilaments appear to be aligned circumferentially. In some sections the microfilaments are sparse and short, 0.1 μm long, in others the microfilaments are more dense and occur in lengths up to 0.7 μm (Figs. 14, 15). The apical surface of the wedge-shaped cells also appears to bear a greater density of 0.5 μm long microvilli than adjacent cells (Figs. 11, 12, 13).

The sphincter cells in embryos fixed after the formation of the sphincters are also wedge-shaped (Fig. 11). No electron-dense region adjacent to the plasmalemma of the luminal surface was observed. The cytoplasmic constituents of the cells appear unchanged from their condition prior to sphincter formation (Fig. 11).

ii) Cytochalasin B

The first set of experiments was performed on embryos in which the epithelium of the presumptive sphincters had thickened (Figs. 16a, 19a). After one hour the control embryos (MFSW and DMSO) had formed recognizable constrictions in the archenteron. Embryos treated with 1 μg/ml CCB maintained the thickened epithelium in the presumptive sphincter region, and some individuals showed further constriction. Embryos treated with either 5 μg/ml or 10 μg/ml CCB had no apparent constrictions in the archenteron.

After two hours the control embryos had completed the constriction of the tube (Fig. 16c). The embryos treated with 1 μg/ml CCB were retarded with respect to the control embryos; the sphincters were at a stage comparable to the control embryos after one hour. In embryos treated with 5 μg/ml CCB there was no evidence of constriction of the archenteron; the endodermal cells appeared somewhat rounded and the thickened regions had disappeared. The ectodermal epithelium was pulled away from the hyalin layer, though the cells remained attached to it where the cilia projected through (Fig. 16b). Embryos treated with 10 μg/ml CCB were similar to those treated with 5 μg/ml in not having formed any semblance of a sphincter, however, they displayed dissociation of the ectoderm and rounding of the cells to a greater extent.

When the experimental embryos were rinsed and returned to MFSW the effects of the treatments abated. Those previously treated with 1 μg/ml CCB responded quickly (within one hour) and completed the formation of the sphincter. The embryos that had been treated with 5 μg/ml CCB showed re-annealment of the ectoderm to the hyalin layer and recognizable sphincters within 2 hours (Figs. 16d, 19a). The 10 μg/ml treatment was not as readily reversed; the dissociation of the ectoderm and rounding of endodermal cells in most cases remained even after 6 to 8 hours in MFSW.

The second set of experiments involved treating embryos in which the constriction in the archenteron had begun to form (Fig. 19b). Treatment with 5 μg/ml or 10 μg/ml CCB removed the constrictions within one hour (Fig. 17). The 1 μg/ml CCB treatment did not obviously affect the constriction process. Embryos in both of the control cultures remained unaffected.

Removal of the embryos from the 5 μg/ml CCB treatment after one hour returned the sphincters to a state comparable to the control cultures. The 10 μg/ml CCB treatment was also reversible, however, embryos that had undergone extensive dissociation of the ectoderm or endoderm were unable to return to their previous condition.

In the third set of experiments embryos were treated with CCB after the constrictions in the archenteron had fully formed (Fig. 19c). The sphincters were unaffected by all of the concentrations of CCB, even when treated for up to 4 hours (Fig. 18). The 10 μg/ml CCB treatment caused extensive dissociation of the ectoderm from the hyalin layer, yet the sphincters remained essentially unaffected.

Ultrastructurally, the cells of the presumptive sphincter in embryos treated with 5 μg/ml CCB were unlike the sphincter cells in the control embryos. The cells remained columnar, though somewhat rounded, and there were no apparent elaborations of the luminal surface (Fig. 22). The electron-dense region adjacent to the apical membrane was not observed (Fig. 22b). All other ultrastructural characteristics of the CCB-treated embryos were essentially the same as in the control embryos.

C. Coelom Formation

Throughout the formation of the coeloms numerous 0.2 μm diameter filopodia extend from the coelomic cells (Figs. 20, 21). Initially the filopodia radiate from the tip of the archenteron and attach to the ectodermal epithelium. During the expansion of the coeloms, and as they come to lie against the archenteron, the filopodia are oriented in the same direction as the coelom. There is a marked decrease in the number of filopodia upon completion of coelom formation.

The coeloms are comprised of simple cuboidal epithelium that is ultrastructurally indistinguishable from the other parts of the archenteron, except for the filopodia. The filopodia protrude from the blastocoelar surface of all of the coelomic cells. The cytoplasm of the filopodia contain numerous ribosomes, a few 0.1 µm diameter vesicles, and a moderately electron-dense ground substance (Fig. 23). As well, parallel arrays of microfilaments, 5 to 7 nm thick, are oriented along the major axis of the filopodium. The attachments of the filopodia to the ectoderm appear as regions of closely apposed membranes.

Treatment of embryos during the formation of the coeloms with 5 µg/ml CCB and 10 µg/ml CCB inhibits the expansion of the coeloms as compared to the control cultures (MFSW and DMSO) (Fig. 24). Treatment with 1 µg/ml showed no marked effect on coelom formation. Returning the embryos to MFSW from 5 µg/ml CCB resulted in continued development of the coeloms. After treatment for four hours in 10 µg/ml CCB, dissociation of the cells frequently prevented further development of the embryo when it was returned to MFSW.

Filopodia were present after four hours in 5 µg/ml CCB, however, they were less numerous than in the control cultures. The filopodia of the experimental embryos were essentially the same ultrastructurally as those of the control embryos, except for the notable absence of the arrays of microfilaments (Fig. 25).

D. Shaping of the Larval Stomach

i) Number of Cells

Figure 26 summarizes the data collected on the number of cells in the developing larval digestive tract. During gastrulation there is a linear increase in the number of cells from 0 to 100 ($\bar{Y} = 98.7$, $s = 10.9$). There is a subsequent sigmoidal increase throughout the formation of the gut, resulting in about 425 cells ($\bar{Y} = 427.8$, $s = 25.5$) in the feeding pluteus. These numbers represent all of the cells in the intestine, stomach, esophagus, and coeloms; no attempt was made to include the secondary mesenchyme cells that migrate from the archenteron during the initial stages of gut development.

Table 1 summarizes the proportions of the cells in each region of the digestive tract. The cells of the mouth, coeloms, and esophagus are indistinguishable and therefore are presented together. There is an apparent increase in the proportion of cells in the anterior region of the digestive tract as compared to the stomach and intestine.

ii) Colchicine

Embryos that had just begun coelom formation when cultured in MFSW containing 5×10^{-5} M, 5×10^{-4} M, or 5×10^{-3} M colchicine, for 24 to 36 hours, were able to form tripartite digestive tracts similar to the digestive tracts of embryos cultured for the same period in MFSW (Fig. 27). There was an apparent dosage response to the colchicine; embryos treated with 5×10^{-5} M colchicine were more like control embryos than those cultured in 5×10^{-3} M colchicine. The development of embryos that received the heavier dose appeared retarded; the stomach remained spherical and the epithelium 7 to 10 μm thick, a condition similar to

TABLE 1. The proportion of cells in each part of the larval gut, expressed as a percentage of the total number of cells in the gut at each stage.

Hours of Development: Organ:	68	80	92
Intestine	24%	21%	16%
Stomach	43%	34%	33%
Esophagus	33%	45%	51%

embryos at an earlier stage. The stomachs of embryos treated with 5×10^{-5} M colchicine were heart-shaped and the epithelium 3 to 5 μm thick.

None of the experimentally treated embryos formed a typical pluteus shape; all remained as prisms. There was a notable inhibition of growth of the larval skeleton in all colchicine treated embryos.

Immediately prior to the experiment a sampling of the embryos to be used had a mean of 146.3 (s = 8.4) cells in the archenteron. After 24 hours there was a mean of 364.3 (s = 12.1) cells in the gut of embryos cultured in MFSW. Embryos cultured in 5×10^{-5} M colchicine had a mean of 213.5 (s = 16.3) cells and embryos cultured in 5×10^{-3} M colchicine had 152.1 (s = 18.2) cells.

iii) Autoradiography

Autoradiographs of embryos that were exposed to H^3thymidine during the initial phases of the shaping of the larval digestive tract showed grain deposition over the entire gut (Fig. 28). There appeared to be two densities of silver grains deposited. Regions of heavy grain deposits were over nuclei and appeared randomly scattered throughout the stomach. The esophagus and intestine contained more regions of heavy deposition than the stomach. About one half of the cells in the stomach were covered with light deposits. Some of the regions with light deposits were over parts of the section in which a nucleus was not included, other areas with light deposits were over nuclei.

iv) Stomach Epithelium Thickness

There is an apparent thinning of the stomach epithelium between 72 and 88 hours of development. Figure 29 summarizes the measurements of the stomach epithelium of embryos fixed at various stages. The epithelium of the larval intestine and esophagus undergo marked reductions in height as well (Fig. 30).

v) Length of the Gut

The archenteron at the completion of gastrulation (48 hours) averages 75 μm in length. The length of the digestive tract of feeding plutei (96 hours) averages 145 μm; this represents the sum of the average lengths of the esophagus, stomach, and intestine (61 μm, 48 μm, 36 μm) measured along their major axes.

The average linear distance between the presumptive stomodeum and the blastopore in 48 hour gastrulae is 78 μm. The average linear distance between the center of the mouth and the anus in 96 hour feeding plutei is 86 μm.

E. Genetic Control of Morphogenetic Events

i) Actinomycin D

Embryos that had developed to a stage prior to the completion of gastrulation and were then transferred to MFSW containing 25 μg/ml actinomycin D failed to undergo morphogenesis of the larval digestive tract (Figs. 31, 32). Embryos that had completed the initial ingression phase of gastrulation would complete gastrulation but develop no further. There was neither proliferation nor release of secondary mesenchyme cells from the tip of the archenteron in embryos treated in this manner.

Embryos that had completed gastrulation prior to being exposed to actinomycin D were capable of morphogenesis of the larval digestive tract (Figs. 31, 32). Coelom formation, sphincter formation, shaping and bending of the gut occurred in all post-gastrular embryos treated with actinomycin D.

Embryos that were exposed to actinomycin D for prolonged periods (up to 60 hours) were unable to swim, developed a large number of small rounded cells in the blastocoel, and failed to form ciliary bands and esophageal muscles. These abnormalities occurred in all of the experimental groups irrespective of the stage at which the embryo was exposed to actinomycin D.

ii) Autoradiography

In autoradiographs of embryos that were treated with H^3actinomycin D for one hour prior to completing gastrulation, silver grains were deposited over archenteron cells at higher than background densities (Fig. 33a). Autoradiographs of embryos treated with H^3actinomycin D for four hours prior to the completion of gastrulation showed silver grain deposition that was about two times denser than that observed for embryos treated for one hour (Fig. 33c). The silver grains were, in most instances, close to or over nuclei, though some were over regions of cytoplasm.

Autoradiographs of embryos that had completed gastrulation and were treated with H^3actinomycin D for either one or four hours showed silver grain deposition over most of the archenteron cells (Fig. 33b, d). The silver grains were deposited over both the cytoplasm and the nuclei of endodermal cells. There was no readily apparent difference in the grain densities observed over embryos that had been exposed to H^3actinomycin D for either one or four hours.

iii) Puromycin

Embryos that were cultured in MFSW containing 20 μg/ml puromycin halted development at the stage at which they were introduced to the experimental conditions (Figs. 34, 35). Embryos that had not completed gastrulation prior to puromycin treatment developed no further. Development was also halted prior to and during coelom formation. Embryos that had begun the thickening of the endodermal epithelium preparatory to sphincter formation were, in some instances, able to form a constriction in the archenteron.

Some of the embryos that were returned to MFSW after development had been halted by puromycin were able to form a normal pluteus.

DISCUSSION

The description of formation of the larval digestive tract in *S. purpuratus* and *D. excentricus* agrees with the descriptions of gut development reported for many other species (see review by Hyman, 1955; Kumé and Dan, 1968; Czihak, 1971). Although most of the published reports deal with the formation of the gut incidentally, the overall pattern of development appears consistent amongst all the echinoid orders. Gustafson and Wolpert (1963a,b, 1967) described aspects of gut formation in *Psammechinus miliaris* and *Echinocardium cordatum* in detail. The account given here is in accord with the observations of those authors.

The most remarkable difference in the development of the digestive tract in the two species examined here is the rate at which the gut forms. The relationship between egg size and the rate of development, for a variety of species, was reported by Steele (1977) as correlating positively, and by Underwood (1974) as being without correlation. The data presented here for *S. purpuratus* and *D. excentricus* contradict the contention of Steele (1977). *D. excentricus* develops to a feeding stage from a 115 μm egg in 60 hours and *S. purpuratus* develops from a smaller egg (75 μm) to a feeding pluteus in a relatively longer time (88 hours).

The significance of the relationship between egg size and time of development lies in the models of Vance (1973) which relate the energetic efficiency of reproduction to egg size. He was attempting to reconcile the observations of Thorsen (1946) that the reproductive strategies of marine benthic invertebrates fall into three classes. In doing so Vance (1973) based his models on the assumption that there was a positive correlation between egg size and the length of time the larva was lecithotrophic (pre-feeding). He suggested that an increase in egg size is, in general, associated with a lengthening of the pre-feeding period, a shortening of the period of larval feeding, and a shortening overall in the duration of larval life (to metamorphosis). Strathmann (1977) points out that larval size and variability of larval stages are factors that complicate the relationship between egg size and the duration of feeding and pre-feeding stages.

Although the reproductive strategies of *S. purpuratus* and *D. excentricus* are very similar and the two class-related species share a similar larval environment, no simple relationship is supported by the observation that the rate of development to an independently feeding pluteus is achieved more quickly in the species with the larger egg. Egg size in this situation does not appear to be determined solely by the selective pressures exerted on the rate of development.

The development of form in the larval digestive tract is a predictable sequence of events. The entire sequence is a continuum in which stages may be recognized. As a matter of convenience, the morphogenetic events have been treated as distinct entities; the extent to which one event relies upon another is unknown. It must be remembered that the process of gut formation is an integration of all the morphogenetic events; it should be considered as a *gestalt*.

A. Morphogenetic Mechanisms

Four events of morphogenesis of the larval digestive tract have been investigated in detail: i) sphincter formation, ii) coelom formation, iii) shaping of the stomach, and iv) bending of the gut into a 'J' shape.

i) Sphincter Formation

It is hypothesized that the formation of both the cardiac and pyloric sphincters is initially accomplished by an active contraction of the apical ends of the sphincter cells, altering their shape and resulting in the apparent constriction of the archenteron (Figs. 36, 37). It is suggested that the force is produced by the contraction of microfilaments.

The sphincters first appear as thickenings and then constrictions of the archenteron. Intuitively, this change in form can most easily be accomplished by a contractile force arranged circumferentially. Moore (1927) noted that sphincters form in the archenterons of exogastrulae and gastrulae from which the animal hemisphere had been removed. He concluded that the formation of the tripartite gut (sphincter formation) was an autonomous process; it can occur without the influence of other tissues. The contractile force is apparently localized within the archenteron.

Microfilaments were not observed in the apical ends of cells of embryos that were fixed prior to or after sphincter formation. This transient presence of the microfilaments allies them with the constriction of the tube. The location and orientation of the microfilaments also provide circumstantial evidence for their participation in this event.

The appearance of microvilli on the luminal surface, coincidental with sphincter formation, can be interpreted as resulting from contraction of the apical cytoplasm of the sphincter cells. Presumably the contraction of the cytoplasm immediately beneath the plasmalemma would result in the plication of the membrane. Cloney (1966) and Baker and Schroeder (1967) noted similar folding of membranes associated with contraction of cell surfaces.

Numerous non-muscle cells have been demonstrated to contain the contractile proteins actin and myosin (Pollard and Weihing, 1973; Inoué and Stephens, 1975; Goldman et al., 1976). Filaments, 5 to 7 nm thick, have been shown to be associated, both temporally and geometrically, with contractile events in many of these cells. Microfilaments have the ultrastructural characteristics of actin and, under specific conditions, have been demonstrated to bind heavy meromyosin, as does actin (Ishikawa et al., 1969). Although the nature of the conversion of chemical energy to mechanical energy is not understood in non-muscle cells, microfilaments (actin) have been hypothesized to be tension-bearing elements in sliding-filament models (Schroeder, 1975).

The formation of the sphincters was reversibly inhibited with CCB, and neither the electron-dense region nor microfilaments were observed in sphincter cells of embryos treated with CCB. CCB is known to inhibit numerous contractile processes in non-muscle cells and disrupt microfilaments associated with contraction (Wessells et al., 1971). Little is known of the means whereby it interferes with either the filaments or the cellular contractility. CCB has been demonstrated to bind to proteins on the cytoplasmic surface of cell membranes (Tannenbaum et al., 1977) and to interfere with hexose transport (Kletzien et al., 1972). However, the significance of these observations in relation to cellular contractility is not known. Wessells et al. (1971) have concluded that the drug may be used as a diagnostic tool for contractile activity, in spite of our ignorance of the inhibitory mechanism of CCB.

CCB is unable to alter sphincter constrictions that are fully formed. Presumably there are factors that stabilize the newly formed sphincter which are refractory to CCB. Examination of changes in cell junctions, glucosaminoglycans, and collagen may provide further evidence of stabilizing factors.

Gustafson and Wolpert (1963a) hypothesized a general rule for the changes in form of cell sheets in echinoid embryos. They postulated that alterations were accomplished by localized increases and decreases in the extent of lateral adhesion between adjacent cells. These changes in adhesion facilitated changes in the shape of the cells. Wolpert and Gustafson (1963a) state that sphincters form in this manner. The evidence presented here indicates that the changes in cell shape precede the alterations in lateral apposition; the change in apposition is an effect rather than a cause of the constriction.

Baker and Schroeder (1967) proposed that the contraction of microfilaments in the apical ends of cells in the neural plate of amphibian embryos was the cause of the change in shape of the cells that facilitated the formation of the neural groove and tube. Gustafson and Wolpert (1967) state that this morphogenetic process is fundamentally different from the morphogenetic processes they described in echinoid embryos. Apparently what they describe as "changes in membrane tension" does not correspond directly with cytoplasmic contractility.

The hypothesis suggested here for the formation of sphincters is based upon a series of coincidental associations. The occurrence of microfilaments is coincidental with the constriction of the tube; it is not known if, indeed, the microfilaments are contractile proteins. Sensitivity to CCB is coincident with the constriction of the tube and the occurrence of microfilaments. Regardless of the somewhat premature contention of Wessells et al. (1971) that cytochalasin B can be used as a diagnostic tool for contractile activity, until the precise nature of its interference with cellular contractility is better understood its effects must be interpreted advisedly.

ii) Coelom Formation

Gustafson and Wolpert (1963b) describe, in detail, the formation of the coeloms in *Psammechinus miliaris*. The observations reported here for *S. purpuratus* agree in essence with their account. They hypothesized that the motive force for the egression of the cells that will form the coeloms and the expansion of the coeloms is provided by the contraction of filopodia. The basis of this postulation is the coincidence of formation of the filopodia with the release of the coelomic cells from the archenteron and the location and orientation of the filopodia during expansion of the coeloms.

The presence of parallel arrays of microfilaments, oriented along the major axes of the filopodia, and the reversible sensitivity of coelom formation to CCB lends further support to Gustafson and Wolpert's hypothesis. The force responsible for the expansion of the coeloms is apparently localized within the filopodia.

Tilney and Gibbins (1969b) report similar arrays of microfilaments in the filopodia that extend from the secondary mesenchyme cells during the second phase of gastrulation in both *Arbacia punctulata* and *Echinarachnius parma*. Dan and Okazaki (1956) and Gustafson and Kinnander (1956) had previously suggested that these filopodia were responsible for the lengthening of the archenteron. Analogous observations of microfilaments have been reported by Gibbins et al. (1969) and Tilney and Gibbins (1969a) for the filopodia associated with the ingression and migration of primary mesenchyme cells. Crawford and Chia (1978) found coelom formation in asteroid embryos to be similarly mediated by the contraction of filopodia, which they noted to contain microfilaments.

The reservations expressed for the involvement of microfilaments in sphincter formation and their sensitivity to CCB pertain as well to these observations regarding the contraction of filopodia.

iii) Shaping of the Larval Stomach

There is an increase in size and a change in the shape of the larval stomach between 60 and 72 hours after fertilization. The middle segment of the archenteron changes from a straight-walled cylinder, to a spindle-shaped cylinder, to an obtuse cone, and doubles its original diameter. It was initially hypothesized that this change in form could be accomplished by regions of enhanced growth in the stomach epithelium.

Growth, by definition, is an increase in the mass of living matter (Balinski, 1975). It is difficult to determine the mass of the tissues of the developing digestive tract. However, there is no significant change in the size of the cells throughout the development of the gut, so the increase in cell number provides a reasonable approximation of growth.

The number of cells in the archenteron increases linearly throughout gastrulation. There is a subsequent fourfold, sigmoidal increase during the formation of the gut. The exponential nature of the curve is typical of an increase by geometrical progression. The asymptotic nature of the cessation of cell division implies there is some factor (or factors) limiting further cell replication.

The proportion of the cells present in each region of the gut changes throughout development. The proportion of cells in the esophagus, mouth, and coeloms increases, while the proportion in the stomach and intestine decreases slightly. These changes may be, at least in part, attributed to the growth of the coeloms and the incorporation of oral ectoderm into the mouth; it is impossible to distinguish the origins of the cells in counting preparations. These changes in proportion do not reflect the increase in size of the regions of the gut and probably do not indicate allometry.

Treatment with colchicine effectively stopped cell division, as was indicated by the cell numbers in the experimental embryos. Yet, the shaping of the larval gut occurred in embryos with only the complement of cells normally possessed in gastrulae. The morphogenesis of the larval gut proceeds independently of cell division. Thus, regional enhancement of cell replication is probably not a mechanism contributing to the shaping of the larval stomach.

Regions of enhanced cell replication would be expected to display enhanced incorporation of H^3thymidine and consequently greater deposition of silver grains in autoradiographs. The random distribution of heavy grain deposits observed supports the results of the colchicine experiments; allometric cell replication does not contribute to the shaping of the larval stomach.

It must be noted that using labelled thymidine incorporation as an assay for cell replication can give spurious results. The regions of dense silver grains in the autoradiographs should be interpreted only as corresponding to cells that have incorporated the labelled DNA precursor; it does not necessarily indicate that the cell is newly divided.

There were two distinct densities of silver deposition observed. The heaviest regions, which were associated with nuclei, probably correspond to newly divided cells or cells that have incorporated the label replicating their nuclear DNA. The regions of moderate density, which did not correspond with any specific region of the cytoplasm, may represent label taken into the cytoplasmic pool of nucleotides, or label incorporated into replicated mitochondrial DNA and nuclear DNA through a repair pathway.

Some sections contained nuclei that incorporated little or no H^3thymidine. One possible interpretation of this observation is that there is an asychrony of cell cycles; in the 24 hour labelling period some cells replicated and others did not. The total number of cells in the archenteron-gut increases fourfold in 48 hours; if all of the cells of the archenteron participate in this increase each would go through two complete cell cycles. The period would be about 24 hours.

It is not possible to state, with any certainty, the mechanisms responsible for the shaping of the larval gut. However, the mechanisms that participate in the formation of the sphincters may also function in bulging the sides of the stomach and esophagus. Subtle changes in cell shape could introduce the curvature into the gut epithelium. Microfilaments were never observed in the cells of either the stomach or the esophagus and the bulging is not obviously inhibited by cytochalasin B. Gustafson and Wolpert (1963a, 1967) have attributed the bulging of the stomach to curvature of the cell sheet induced by changes in the extent of lateral apposition between the cells.

It is possible that cell rearrangement, as described by Fristrom (1976), is responsible for the shaping of the gut. If cells near both sphincters of the stomach shifted towards the mid-region, bulging would result. It is necessary to control both cell division and cell shape changes to be certain that one is observing cell rearrangement; owing to this, the shaping of the larval gut is not amenable to investigation of this morphogenetic mechanism.

Measurements of the thickness of the stomach epithelium indicate there is a significant decrease in cell height between 72 and 88 hours of development. The thinning serves to expand the larval stomach, increasing its volume. It is also partly through this change that the obtuse cone-shape of the stomach is achieved. These functional interpretations are speculative and the thinning of the stomach epithelium may also serve a purpose not related to the development of form in the larval gut.

iv) Bending of the Larval Digestive Tract

The bending of the digestive tract is a gradual process occurring between 64 and 76 hours. The esophagus and stomach remain anteriorly-posteriorly aligned, while the intestine becomes directed anteriorly from the pyloric sphincter, on the ventral side of the stomach.

The length of the digestive tract almost doubles during its development, while the blastopore (anus) and stomodeum (mouth) remain in the same positions, relative to one another. It is suggested that the bending of the digestive tract is a passive process, resulting from the lengthening of the gut between two fixed points. The factors responsible for the increase in size of the larval stomach are probably the cause of the lengthening as well.

The formation of straight tripartite guts in exogastrulae lends support to this argument. The figures of Hinegardner (1975) and Horstadius (1973) indicate that when one end of a developing gut remains unconstrained in exogastrulae, the digestive tract fails to bend.

B. Genetic Control of Morphogenesis

Treatment with actinomycin D prior to the completion of gastrulation (40 hours at 15°C) inhibits coelom formation, sphincter formation, and the initial stages of shaping of the larval gut. Embryos that were exposed to actinomycin D at any stage after the completion of gastrulation were able to proceed with these initial morphogenetic events of gut formation.

Actinomycin D is an antibiotic thought to bind directly to DNA molecules and thus prevent transcription (Kersten et al., 1960). Thus, it inhibits RNA synthesis and interrupts the flow of genetic information directing the synthesis of new proteins. Presumably, morphogenetic events are directed by proteins that are transcribed and translated at some time prior to the occurrence of the event. Accepting these premises, the experiments with actinomycin D may be interpreted as indicating that the transcription of the embryonic genome during gastrulation produces RNA that is vital to the morphogenesis of the larval gut. The inability of actinomycin D to block gut formation after the completion of gastrulation indicates that the transcription of the genes responsible for gut formation is completed 20 hours before the beginning of gut morphogenesis.

These experiments are similar to those performed by Barros et al. (1966) and Giudice et al. (1968). Their experiments investigated the temporal relationships between transcription and gastrulation. Barros et al. (1966) found that the transcription vital to gastrulation occurs between 4 and 9 hours prior to the initial stages of gastrulation in the starfish *Asterias forbesii*. Treatment with actinomycin D either prior to or after that period did not affect gastrulation. Giudice et al. (1968) report that transcription essential to gastrular morphogenesis in the urchin *Paracentrotus lividus* begins 12 hours before the initiation of gastrulation.

Actinomycin D has been used in a variety of experiments in sea urchin embryos and consequently a circumspect attitude has been taken towards the nature of its effects. Gross et al. (1964) and Greenhouse et al. (1971) reported that RNA synthesis was inhibited by more than 90% in embryos treated with actinomycin D. Thaler et al. (1969) suggested that the differential effects of actinomycin D on gastrulation were, in part, accounted for by changes in permeability to the antibiotic after the elevation of the fertilization membrane. Summers (1970) was able to obtain the same differential susceptibility to actinomycin D as other workers, using embryos from which the jelly coats and fertilization membranes had been removed. Greenhouse et al. (1971) demonstrated autoradiographically that embryos are permeable to H^3actinomycin D from cleavage through to blastula. DeVincentiis and Lancieri (1970) investigated the toxic side effects of the antibiotic using desaminoactinomycin C_3, an analogue that does not form complexes with DNA and thereby prevent transcription. Eggs cultured in desaminoactinomycin C_3 from fertilization formed feeding plutei in which the only apparent abnormalities were somewhat shorter larval arms.

Wolsky and Wolsky (1969) found that actinomycin D may cause delay of cleavage and some chromosomal aberrations. Kiefer et al. (1969) reported additional mitotic abnormalities; they suggested that these were the result of the actinomycin D interfering with the transcription of RNA coding for histone proteins. The deficiencies in histones cause aberrations in the formation of chromatin and subsequently the chromosomes.

Although there are undoubtedly a multitude of side effects that result from the use of actinomycin D for relatively long periods of time, as a chemical enucleant it is widely accepted that the primary effects are owing to its direct inhibition of transcription (Stearns, 1974; Davidson, 1968).

The results of the autoradiographic experiments with H^3actinomycin D indicate that the cells are permeable to actinomycin D both before and after gastrulation. Within a one-hour period, either before or after gastrulation, detectable label was incorporated into nuclei of archenteron cells. These results agree with the results of Greenhouse et al. (1971) who examined permeability during cleavage. The drug affects embryos treated for long periods, indicating that actinomycin D will eventually inhibit development regardless of the stage at which it was administered.

Puromycin, an antibiotic regarded as a specific inhibitor of protein synthesis, blocks morphogenesis of the larval digestive tract almost immediately upon application. Although morphogenesis is apparently dependent upon continued protein synthesis, it cannot be assumed that the proteins being synthesized at the time of inhibition are all proteins involved directly in a morphogenetic event. Undoubtedly, embryos at this stage are producing a variety of proteins for various functions (cf. Spiegel et al., 1965). Interference with any anabolic or catabolic pathway upon which a morphogenetic event is in some way dependent could produce the results observed equally as well. The immediacy of translation to a morphogenetic event cannot be determined unequivocally with inhibition experiments.

A number of morphogenetic events in sea urchin embryos appear to be directed by relatively long-lived informational RNA and reliant upon proteins being synthesized throughout the duration of the event. The initial cleavages of the fertilized egg are thought to be programmed by RNA that was transcribed from the maternal genome during oogenesis (Gross et al., 1964). Gastrulation is dependent upon transcription events which occur some time before the invagination of the archenteron (Giudice et al., 1968). Both cleavage and gastrulation are dependent upon continuous protein synthesis (Hultin, 1961). The morphogenesis of the larval digestive tract appears to fit a similar pattern of genetic control.

Davidson (1968) recognized three classes of gene products that are classified according to their longevity: a) gene products that are very long-lived, b) gene products that are moderately long-lived, and c) gene products that decay immediately after synthesis. He cites as an example of a long-lived RNA the maternal messages transcribed during oogenesis which remain unused until they are translated sometime after fertilization. Examples of moderately long-lived RNA's include hemoglobin template RNA in autonomously enucleated mammalian reticulocytes (Kruh and Borsook, 1956) and the gene products directing the differentiation of notochord, somites, and anterior neural structures in the chick (Klein and Pierro, 1963). α-aminolevulinic acid synthetase, an enzyme that is induced by the presence of enzyme substrate in rat liver, is apparently translated from RNA with a half-life of 40 to 70 minutes and is cited by Davidson (1968) as an example of short-lived messenger RNA (Tschudy et al., 1965).

Davidson et al. (1963) coined the term "immediacy of gene activity" and suggest the rate at which the genome is expressed in proteins is a subtle mechanism for regulation of cellular function. Davidson (1968) notes that patterns of high immediacy of control (short-lived RNA) are not apparent until the onset of differentiation when cells are required to respond in their program of differentiation to their environment. The production of very long-lived RNA's associated with oocytes and plant seeds (Dure and Watters, 1965) is a strategy of obvious advantage in ensuring a rapid and coordinated start to life for progeny. The use of moderately long-lived gene products by cells that have lost their nuclei is clearly a strategy to maintain the function of cells that have a programmed death. The full implications of the different strategies of genetic control on cellular function and development are yet to be realized.

SUMMARY

Morphogenesis of the larval digestive tract in *D. excentricus* and *S. purpuratus* is described.

Constrictions in the archenteron, which form the cardiac and pyloric sphincters, are accompanied by a change in the sphincter cells from cuboidal to wedge-shaped. The apical ends of sphincter cells from embryos fixed during the constriction of the archenteron contained an electron-dense region in which microfilaments could be discerned. The constriction of the archenteron could be reversibly inhibited with CCB if treated during sphincter formation, but treatment after the constriction has fully formed had no effect. CCB treatment caused the disappearance of the electron-dense region and the microfilaments.

The formation of the coeloms involves the emergence of two diverticula from the anterior end of the archenteron. Coelomic cells extend numerous filopodia to the ectoderm and contain arrays of microfilaments oriented along the major axes of the filopodia. Coelom formation was reversibly inhibited with CCB.

The number of cells in the developing larval digestive tract increases linearly from 0 to 100 during gastrulation, and sigmoidally to about 425 cells during gut formation. Embryos in which cytokinesis

had been inhibited with colchicine were able to form a digestive tract comprised of only 150 cells. Autoradiographs of embryos that had been exposed to H^3thymidine during the initial stages of shaping of the gut indicated no regions of enhanced thymidine incorporation.

Bending of the larval gut is apparently facilitated by a doubling in the length of the digestive tract between two fixed points, the mouth and the anus.

The sequence of morphogenetic events was inhibited with actinomycin D up to a point in development just prior to the completion of gastrulation, while puromycin was found to arrest development at the stage at which it was introduced. Autoradiographs of embryos treated with H^3actinomycin D prior to or after the completion of gastrulation indicated that the archenteron cells are permeable to actinomycin D at both stages of development.

HISTOGENESIS AND FUNCTIONAL ANATOMY OF THE LARVAL DIGESTIVE TRACT

INTRODUCTION

The anatomy of an echinopluteus was first described and discussed by Müller in his seven volume memoir (1846-1854). Müller traced the morphological transformation of the different parts of the four-armed larva into the eight-armed larva and described the main features of metamorphosis. Müller worked almost exclusively from larvae obtained from plankton; as a consequence he was unable, in most cases, to state to which species the larvae belonged. Mortensen (1920, 1921, 1931, 1937, 1938) provided comprehensive descriptions and illustrations of over 50 species of echinoid larvae, grown from fertilized eggs. Mortensen's intention was to document the diversity of larval forms and investigate the implications these had upon classification of adults, however, his treatise also examines many aspects of larval anatomy.

Bury (1896), MacBride (1903) and von Ubisch (1913) were the first to examine echinoplutei that were fixed, sectioned, and stained. They were primarily interested in the details of development of the adult rudiment and metamorphosis. Observations of whole larvae were difficult owing to their opacity. Histological preparation provided the opportunity to examine larval structure with greater resolution. The intricate and exhaustive details presented by these authors are, with few exceptions, the only complete accounts of larval development of echinoids.

Balinsky (1959) and Endo and Uno (1960) described ultrastructural aspects of the cell attachments and supporting layers in echinoid blastulae and gastrulae. Wolpert and Mercer (1963), Okazaki and Niijima (1964), Gilula (1972, 1973) and Lundgren (1974a,b) have examined cell junctions and attachments in stages up to early pluteus. Bacon and Julier (1963) and Immers and Lundgren (1972) reported ultrastructural aspects of cilia and adjacent structures in early plutei. Ryberg and Lundgren (1975) described ultrastructural and histochemical features of secretory cells in the esophagus of four-armed plutei. Ryberg (1977) described the organization of the network of "neuron-like" cells within the blastocoel of early plutei and Burke (1978) described the structure of the larval nervous system of four- and eight-armed plutei.

The behavior of planktotrophic echinoderm larvae has been described by Gemmill (1914, 1916), Runnstrom (1918), Tattersall and Sheppard (1934), Strathmann (1971, 1974, 1975), and Strathmann et al. (1972). The repertoire of larval behavior for echinoplutei is based upon feeding; it includes forward swimming, particle capture, rejection of particles, and changing the direction of swimming (Strathmann, 1971).

The larvae of most species of echinoids develop rapidly from egg to a phase of slow growth and development leading to metamorphosis (Mortensen, 1920-1938). The length of time the embryo takes to develop from an egg to the commencement of feeding determines, in part, the amount of metabolic reserve allocated to each egg by the parent (Strathmann, 1977). Therefore it is of some adaptive significance that the embryo rapidly develop the ability to feed.

The objectives of this portion of my research are: a) to document and analyse the histogenesis of the larval digestive tract, and b) to present a functional interpretation of the structure of the larval gut.

RESULTS

A. Late Gastrula

Thirty-four hours after fertilization *D. excentricus* embryos have nearly completed gastrulation. The embryo at this time is ovoid in shape, 125 by 150 μm, though the presumptive ventral surface is flattened. The archenteron has advanced four-fifths of the way across the blastocoel and the tip is attached to the presumptive stomodeum by secondary mesenchyme cells (Fig. 38a).

The archenteron is comprised of simple, columnar epithelium 12 to 15 μm thick (Fig. 38a). The archenteron is 95 μm in diameter at the base and tapers to 50 μm in diameter at the tip. The ectoderm is simple, cuboidal epithelium, 8 to 10 μm thick, and the blastocoel contains numerous mesenchyme cells scattered throughout.

The cells of the archenteron are, at this stage of development, ultrastructurally indistinguishable. Each cell is trapezoidal in outline, 12 to 15 μm in height, 8 μm wide basally, and 5 μm wide apically (Fig. 39). The cytoplasm contains numerous yolk vesicles which are 1 to 2 μm in diameter and contain granules, each of which is about 30 nm in diameter. Some yolk vesicles appear homogeneous while others have a coarse granular appearance owing to the density to which the yolk granules are packed (Fig. 39). Yolk granules are also dispersed throughout the cytoplasm; frequently they appear aggregated into clumps (Figs. 39, 40).

Each of the archenteron cells contains a basally situated nucleus which is 5 to 6 μm in diameter. The nucleoplasm includes numerous electron-dense patches and one or more nucleoli, each 1 μm in diameter

(Fig. 39). The nucleus is usually surrounded by a layer of rough endoplasmic reticulum, which constitutes most of the rough endoplasmic reticulum in the archenteron cells (Fig. 39), although clumps of ribosomes are dispersed through the cytoplasm (Fig. 40).

Each cell contains one or more prominent Golgi bodies, usually centrally situated (Fig. 40). Each Golgi body is surrounded by numerous vesicles, 100 to 200 nm in diameter, which contain fine, granular material of medium electron-density. Mitochondria are distributed throughout the cells. Vacuoles that contain flocculent material are restricted to the apical cytoplasm (Figs. 39, 40).

A single cilium projects into the lumen of the archenteron from the surface of each cell (Fig. 40). The basal body of the cilium is formed from paired centrioles oriented at right angles to each other. The centrioles give rise to a striated rootlet which extends up to 2 µm into the cytoplasm of the cells and is surrounded by smooth endoplasmic reticulum. An array of moderately dense strands appears to project from the basal body of the cilium into the cell (Fig. 40).

Archenteron cells are attached near their luminal surface by small zonulae adhaerentes; no basal lamina was observed at this stage of development.

B. Prism

After 40 hours of development the embryos have become early prisms. The entire embryo is tetrahedral in shape, about 190 µm long and 110 µm wide. The archenteron has contacted the ectoderm in the region of the presumptive stomodeum, however, the mouth is yet to form (Fig. 38b). The ectoderm that circumscribes the oral field has begun to thicken, anticipatory to the formation of the ciliary band. The larval skeleton has developed to the extent that arm-buds of the anterolateral and post-oral arms are discernible.

Constrictions in the archenteron that will form the cardiac and pyloric sphincters are evident at this stage of development. The endoderm remains as simple columnar epithelium, 15 µm thick, except in the constricted regions which have become 17 to 19 µm thick (Fig. 38b). The ectoderm is simple cuboidal epithelium except in regions of the presumptive ciliary band, which tend to be columnar. The primary mesenchyme cells have formed a syncytium which has become the skeletogenic epithelium associated with the larval skeleton. Numerous secondary mesenchyme cells remain scattered throughout the blastocoel.

The cells of the archenteron, in the prism, are essentially unchanged in ultrastructural characteristics from the cells of the archenteron in the late gastrula (Fig. 41).

C. Early Pluteus

After 50 hours of development *D. excentricus* is an early pluteus. The paired anterolateral and post-oral arms are distinct, as is the ciliary band which outlines the oral field. The embryo no longer swims forward spinning about a longitudinal axis, but has, with the development of the ciliary band, begun to swim as a pluteus, the oral field foremost, with no rotation. The early pluteus is 210 µm long and 110 µm at its greatest width.

The sequence of morphogenetic events that lead to the formation of the larval gut is nearly completed at this stage of development, although the embryo is still unable to feed. The stomach, esophagus, and intestine are anatomical entities, and the stomodeum has opened (Fig. 38c). The coeloms have become flattened sacs apposed to the sides of the esophagus and the esophageal muscles have begun to form.

The gut remains as simple columnar epithelium, however, it is thinner than previous stages. It is now 11 to 13 μm thick. Similarly, the ectodermal epithelium, with the exception of the ciliary band, has thinned to between 5 and 7 μm (Fig. 38c).

Although the stomach, esophagus, and intestine have formed, there are few qualitative ultrastructural differences amongst the cells that comprise these organs. Notwithstanding this lack of disparity, there are notable changes in all the gut cells from the previous stages described.

There are fewer yolk vesicles per cell at this stage of development than in gastrulae or prisms. The numbers of yolk vesicles counted in thin sections of cells of comparable size ranged from 10 to 19 in gastrulae, 10 to 17 in prisms, and from 3 to 8 in early plutei (Figs. 39, 41, 42). The yolk vesicles remain the same size as the yolk vesicles in gastrulae, about 1 μm in diameter (Fig. 42).

There are numerous cisternae of rough endoplasmic reticulum dispersed throughout the cytoplasm of gut cells in early plutei, whereas the rough endoplasmic reticulum in archenteron cells of gastrulae was restricted to a single cisterna enclosing the nucleus (Figs. 39, 42). As well, there is an apparent increase in the amount of clumped ribosomal material, which has become a major cytoplasmic constituent in early pluteus cells (Fig. 42).

There were no observed changes in the ultrastructural characteristics of organelles such as: nuclei, Golgi bodies, cilia, vacuoles, and cell attachments (Fig. 42).

The esophageal muscles have begun to form in the early pluteus. The cells that will comprise the esophageal muscles are derived from secondary mesenchyme cells which extend filopodia around the esophagus. The filopodia will form a meshwork that circumscribes the esophagus and is responsible for the peristaltic movements of the esophagus.

The filopodia are uniaxial extensions, 100 nm in diameter and up to several micrometers in length (Fig. 43). Small swellings, 200 to 250 nm in diameter, occur throughout their length. The cytoplasm of the filopodia is electron-dense in comparison to the major portion of the cell, and contains numerous aligned filaments about 7 nm in diameter (Fig. 43). The cytoplasm of the swellings contains ribosomal particles in a granular and amorphous matrix of moderate electron-density.

D. Four-armed Pluteus

Seventy-two hours after fertilization, *D. excentricus* is a fully formed pluteus, capable of collecting, ingesting, digesting, and egesting unicellular algae, which are the larval fare. The larval body is an inverted cone with the arms extending from the perimeter of the base of the cone (Fig. 49). The larval mouth is situated between the anterolateral arms which are joined throughout most of their length. The shape of the pluteus, at this stage, indeed resembles an inverted artist's easel as Müller (1846) suggested in naming it.

The ciliary band of the four-armed pluteus is a thickened region of densely ciliated epidermis that outlines the oral field and traces the edges of the larval arms. The ciliary band functions throughout larval life as both a locomotory and feeding organ (Strathmann, 1971). A second region of dense ciliation, the adoral ciliary band, outlines the larval mouth. The remaining areas of larval epidermis are all sparsely ciliated.

The esophagus of the four-armed pluteus is a tube that connects the mouth and the stomach (Fig. 38d). The mouth is a triangular opening, 40 by 70 μm, outlined by the adoral ciliary band. Two palp-like prominences form the lower lip. The stomach is large, elliptical in shape, and occupies most of the larval body (Fig. 38d). The intestine is sausage-shaped and extends anteriorly to the anus from the pyloric sphincter. The anus is located midventrally, immediately posterior to the ventral, transverse portion of the ciliary band.

The upper 60 μm of the esophagus in the four-armed pluteus is a straight walled tube, 30 μm in diameter, comprised of columnar epithelium 10 to 12 μm thick (Fig. 38d). The lower 40 μm of the esophagus is flared to 50 μm in diameter and comprised of simple, cuboidal epithelium, 5 to 7 μm thick. All of the cells of the esophagus appear to be of one ultrastructural type (Fig. 44).

Each cell has a basal nucleus which contains numerous dense, granular patches and a single electron-opaque nucleolus. The perinuclear cytoplasm contains a lamella of rough endoplasmic reticulum which encloses the nucleus (Fig. 44).

The apical cytoplasm contains a few scattered yolk vesicles, mitochondria, and vesicles, 275 μm in diameter, which contain a homogeneous substance of medium electron-density that stains blue-green with methylene blue. In the juxtaluminal cytoplasm there are vacuoles that contain membranous and amorphous material. The ground substance is predominantly ribosomes and clumps of yolk granules (Fig. 44).

Each cell bears a single cilium arising from a depression in the apical surface of the cell and surrounded at its base by a collar of 10 microvilli up to 1 μm in length. The basal body consists of a pair of centrioles at right angles to each other and a striated rootlet which extends up to 4.5 μm into the cell. The striated rootlet has associated with it stacked lamellae and tubules of smooth endoplasmic reticulum (Fig. 44).

The cells are attached near the luminal surface by zonulae adhaerentes and the entire epithelium is supported by a basal lamina which consists of fine, filamentous material compressed into a single sheet 45 nm thick.

The junction between the esophagus and the stomach is formed by the cardiac sphincter, a constriction consisting of columnar myoepithelial cells (Fig. 45). In the four-armed pluteus, the sphincter cells are spatulate in outline, 13 μm long, 7 μm wide apically, and 3 μm wide basally. The base of each cell appears to be folded and interdigitated with adjacent cells (Fig. 45).

The apical cytoplasm contains numerous clear vesicles about 600 nm in diameter, scattered clumps of ribosomes and, occasionally, yolk vesicles (Fig. 45). The nucleus is located in the basal half of the cells and contains granular patches of electron-dense material and one or more nucleoli. The cytoplasm around the nucleus typically contains rough endoplasmic reticulum and a number of Golgi bodies.

Apposed to the basal plasmalemma there are thick and thin filaments organized into striated bands. The myofibrils are oriented circumferentially and the sarcomere length is about 750 nm (Fig. 45). The basal cytoplasm also contains numerous cisternae of rough endoplasmic reticulum, mitochondria, and microtubules which appear to extend the length of the cell. Myofibrils also appear infrequently in the apical half of the cell (Fig. 45).

The stomach in the four-armed pluteus consists of a single layer of ciliated, cuboidal epithelium, 7 μm thick (Fig. 46). Ultrastructurally, the tissue is composed of a single type of cell (Figs. 46, 47). The nucleus of each cell has at least one electron-opaque nucleolus, 0.5 μm in diameter. The cytoplasm contains vesicles that can be classified, on a basis of size and contents, into three types. The most common, type A, range in size from 100 to 500 nm and contain fine, granular material of medium electron-density (Fig. 47). These small, gray vesicles are often associated with Golgi bodies. Type B vesicles are 500 to 650 nm in diameter and variably contain flocculent and membranous material (Fig. 47). The third and least common type are yolk vesicles, which remain as previously described.

Associated with the nucleus and the peripheral regions of the stomach cells are numerous, and often extensive, cisternae of rough endoplasmic reticulum. Bundles of rough endoplasmic reticulum that appear concentrically wound around a core of mitochondria and free ribosomes were infrequently observed (Fig. 47). The cytoplasm also includes numerous aggregates of ribosomes and clumps of yolk granules. The cilium borne by each cell is similar in description to cilia of the archenteron cells previously described.

The stomach cells attach near their luminal surface by zonulae adhaerentes and remain apposed closely to adjacent cells throughout their length. The epithelium is supported by a basal lamina which appears to be a continuation of the basal lamina of the esophagus.

The intestine of the four-armed pluteus is comprised of simple, squamous epithelium, 5 µm thick, which is ultrastructurally homogeneous in cell type (Fig. 48).

Each intestinal cell contains a centrally located nucleus, about 3 µm in diameter. The nucleus is surrounded with rough endoplasmic reticulum and the basal portion of each cell contains numerous cisternae of rough endoplasmic reticulum. Intestinal cells each contain a Golgi body that has associated with it numerous vesicles, 100 to 200 nm in diameter, which themselves contain fine granular material of moderate electron-density. A few yolk vesicles remain and clumps of yolk granules are scattered throughout the cells. A few vacuoles with a variety of amorphous contents are usually located in the apical cytoplasm (Fig. 48).

The intestinal cells all have a single cilium on their luminal surface (Fig. 48). The basal body is a pair of centrioles, each of which gives rise to a striated rootlet. The striated rootlets extend into the cytoplasm oriented at right angles and are surrounded by stacked lamellae of smooth endoplasmic reticulum (Fig. 48). The basal body serves as a focus for an array of microtubules which extend through the cell.

The cells are attached by apical zonulae adhaerentes and supported by a basal lamina (Fig. 48). Fibers that have the axial periodicity of collagen are located near the basal lamina in areas where mesenchymal cells are associated with the blastocoelar surface of the intestine.

E. Eight-armed Pluteus

Four weeks after fertilization *D. excentricus* has become an eight-armed pluteus (Fig. 49). During the second week of larval life the posterodorsal arms grow from between the post-oral and and anterolateral arms (Figs. 49, 50). The pre-oral arms are added to the oral hood during the third week after fertilization.

The eight-armed pluteus is 475 μm long and 250 μm wide. At this stage of development the post-oral and posterodorsal arms are 275 μm long and the anterolateral and pre-oral arms are 180 μm long. The ciliary band in the eight-armed pluteus is organized in a similar manner to that of the four-armed pluteus; it traces the edges of the larval arms and circumscribes the mouth (Fig. 50). As well, six ciliated lobes grow from between the arms to become specialized locomotory organs (Fig. 50).

The esophagus in the eight-armed pluteus is divided into two distinct regions; the upper esophagus is narrow and densely ciliated, while the lower esophagus is bulbous and only sparsely ciliated (Fig. 51).

The upper esophagus, a tube 50 μm in length, has an elliptical cross-section 30 by 20 μm in diameter (Fig. 52). It is comprised of a single layer of ciliated epithelium, the thickness of which varies from 2 to 15 μm. The cells, arranged in three tracts of columnar cells, extend the length of the upper esophagus (Fig. 52). The two tracts forming the ventral surface of the esophagus are extensions of the palp-like prominences which are the lower lip. The esophageal muscles are arranged circumferentially in bands which surround the entire esophagus (Fig. 52). A pair of laterally disposed bundles of axons run throughout the length of the upper esophagus within the esophageal epithelium.

The cells of the upper esophageal epithelium appear to be of one ultrastructural type (Fig. 53). On its apical surface each cell bears a single cilium which arises from a pit and is surrounded, at its base, by a collar of 8 to 10 microvilli. The cilia are of the metazoan type II (Pitelka, 1974), the basal plate being elevated above the surface of the cell. Paired centrioles, oriented at right angles to each other, and a striated rootlet up to 5 µm in length, occur in the apical cytoplasm beneath each cilium.

A single elliptical nucleus, containing scattered electron-dense patches, occupies the central portion of each cell (Fig. 53). A layer of rough endoplasmic reticulum surrounds the nucleus. Golgi bodies and scattered cisternae of rough endoplasmic reticulum are frequently observed in the perinuclear cytoplasm. Mitochondria and vacuoles containing flocculent material are scattered throughout the cytoplasm. Numerous free ribosomes and a fine, granular ground substance give the cells a moderate electron-density.

The cells are attached near their apical surface by zonulae adhaerentes and the entire epithelium is supported by a basal lamina, 30 nm thick, which separates it from the esophageal muscles.

The esophageal muscles in an eight-armed pluteus form a network of 1 to 2 µm diameter fibers that may be up to 75 µm in length (Fig. 52). The muscle fibers are predominantly aligned around the upper esophagus, although short, orthogonally-directed branches connect adjacent bands (Fig. 52).

Muscle cells contain a filamentous region, 0.5 to 1 µm wide, which runs throughout the length of the cell apposed to the sarcolemma adjacent to the esophageal epithelium (Figs. 53, 54). The thick and thin filaments are organized in a manner similar to smooth muscle, although dense bodies are aligned across the width of the filamentous region, giving the muscle something of a striated appearance (Fig. 54). In cross-section the thick filaments (28 nm in diameter) are surrounded by a region of intermediate electron-density, 55 to 60 nm in diameter, around the perimeter of which the thin filaments (9 nm in diameter) are arrayed. The filaments appear to attach to the sarcolemma on electron-dense plaques. The sarcolemma adjacent to the esophagus is crenulated and frequently extends to the basal lamina (Fig. 54).

Numerous mitochondria occur in the sarcoplasm juxtaposed to the filamentous regions. Microtubules, oriented along the major axis of the cell, lipid droplets, and an elliptical nucleus comprise the balance of the organelles observed in the muscle cells of the eight-armed pluteus.

On both sides of the esophagus, at the base of the thin epithelium where the dorsal tract of columnar cells meets the two ventral tracts, there is a bundle of 6 to 10 axons which extend throughout the length of the upper esophagus (Fig. 56). The axons are 50 to 270 nm in diameter and contain numerous vesicles, 50 to 80 nm in diameter. The vesicles contain a flocculent material of moderate electron density, as well, some appear to contain a dense core. Mitochondria and microtubules are also contained within the axons.

Verrucosities, with vesicles apposed to the membranes, periodically occur along the length of the axons. Some of these swellings, which may be terminal regions of the axons, are apposed to the basal lamina of the esophageal epithelium.

The lower esophagus is bulbous, measuring 25 μm in length and 45 μm in diameter (Fig. 51). It is comprised of cuboidal epithelium, 3 to 5 μm thick. The transition from upper to lower esophagus is also marked by a change in the orientation of the esophageal muscles; the muscle bands of the lower esophagus are predominantly directed parallel to the central axis (Fig. 52). Axons have not been observed in the lower portion of the esophagus.

The cells of the lower esophagus are ultrastructurally distinct from the cells of the upper esophagus (Figs. 53, 55). The nucleus of each cell is elliptical, measuring 3 by 6 μm, and contains coarse granular chromatin predominantly condensed around the perimeter. The perinuclear cytoplasm contains rough endoplasmic reticulum and a large Golgi body.

Clear vacuoles, ranging in size from 0.2 to 0.6 μm, are distributed throughout the apical cytoplasm. Some of these vacuoles contain flocculent material. The ground substance of these cells is more electron-lucent than that of the upper esophageal epithelium; as well, there are notably fewer ribosomes. The cells are attached near their apical surface by zonulae adhaerentes and the epithelium is supported by a basal lamina separating it from the esophageal muscles (Fig. 55).

The lower esophagus is less densely ciliated than the upper esophagus. This may be owing to the cuboidal cells of the lower esophagus being less densely packed than the columnar cells of the upper esophagus, or the cells of the lower esophagus may not all bear a cilium. Those cells that do, have a cilium of similar description to the cilia of the upper esophagus.

The cardiac sphincter connects the stomach and the esophagus and acts as a valve that allows the entry of food from the esophagus to the stomach yet maintains a separation between the internal environments of both organs.

The cardiac sphincter consists of an 'hourglass-like' constriction which is formed from simple, striated myoepithelium, 10 to 13 μm thick (Fig. 51). When the sphincter is closed, the cells are spatulate in outline (Fig. 57). The sphincter cells are about 10 μm wide apically and have a plicated base, the dimensions of which are difficult to ascertain reliably (Fig. 57).

The basal regions of the myoepithelial cells contain striated myofibrils, about 1 μm in diameter, oriented around the perimeter of the sphincter (Fig. 58). The sarcomere length averages 0.9 μm and neither M-lines nor H-bands were observed. Thin filaments, 7 to 9 nm in diameter, insert into dense bodies which constitute an indistinct Z-line (Fig. 58). The average length of the thick filaments (25 nm in diameter), and correspondingly the A-band, is 0.6 μm. The average I-band length is 0.3 μm. The thin filaments appear to insert into electron-dense plaques subjacent to the plasmalemma. The cytoplasm adjacent to the filament bands contains mitochondria, smooth endoplasmic reticulum, microtubules, and β-glycogen granules. The smooth endoplasmic reticulum consists of small clusters of vesicles and elongate tubules. No evidence of transverse tubules nor diads was found.

An elliptical nucleus, 6 by 3 μm, occupies a central position in the myoepithelial cells. The perinuclear cytoplasm contains a Golgi body and cisternae of rough endoplasmic reticulum. In some instances the entire nucleus is enveloped in a single layer of rough endoplasmic reticulum (Fig. 57).

The apical two-thirds of the sphincter cells contains an electron-lucent cytoplasm which includes numerous vesicles (Figs. 57, 58). The vesicles contain a small quantity of flocculent material and range in size from 0.1 to 1.0 μm. Circumferentially oriented myofibrils occur irregularly in the apical regions (Fig. 58). The cells are joined near the luminal surface of zonulae adhaerentes and supported basally by a continuation of the basal lamina of the esophageal epithelium.

The esophageal muscles insert onto the basal lamina at the point of narrowest constriction of the sphincter (Fig. 57). There do not appear to be any circumferentially oriented esophageal muscle bands in the sphincter region.

The larval stomach is comprised of simple columnar epithelium which includes at least two ultrastructurally distinct cell types (Figs. 51, 59, 61). Type I stomach cells form the major component of the epithelium and are distributed throughout the organ. Type II stomach cells form only a small fraction of the epithelium and are restricted to anterior regions of the stomach, particularly to areas adjacent to the cardiac sphincter.

Type I stomach cells are trapezoidal in outline, 13 to 15 μm in height, about 15 μm wide at the base, and 6 μm wide at the apical end (Fig. 59). The luminal surface of each cell is elaborated into numerous irregular microvilli, 2 to 3 μm in length (Figs. 52, 59). Each cell has a single cilium which extends from a slight depression in the cell surface. A pair of centrioles, oriented at right angles to each other, occurs in the cytoplasm beneath the cilium. Each centriole gives rise to a short striated rootlet. The basal body of the cilium is also the focus of an array of microtubules that extends throughout the cell.

The apical cytoplasm contains two types of vesicles. Type A vesicles are 0.2 to 0.4 µm in diameter and contain a fine granular substance of medium electron density; type B vesicles are 0.8 to 1.0 µm in diameter and contain a variety of material, including coarse granules, myelin bodies, and multivesicular bodies (Fig. 60). Golgi bodies occur in the apical cytoplasm and are usually surrounded by numerous type A vesicles (Fig. 60).

A round nucleus, 5 µm in diameter, occupies a central position in type I stomach cells. Each nucleus contains peripherally condensed chromatin and one or more nucleoli, and is itself contained within a single cisterna of rough endoplasmic reticulum (Fig. 59). Rough endoplasmic reticulum also forms cisternae which are disposed throughout the basal two-thirds of each cell subjacent to the lateral plasmalemma.

Mitochondria and a third type of vesicle (C), 0.3 to 3 µm in diameter, dominate the basal regions of the type I stomach cells. The type C vesicles are osmophilic and stain blue-green with methylene blue (Fig. 59).

The stomach cells are attached apically by zonulae adhaerentes and rest upon a basal lamina. A diffuse layer of fibers that have an axial periodicity typical of collagen separates the stomach epithelium and the squamous epithelium of the somatocoels.

Type II stomach cells are spindle-shaped, up to 20 µm in length and 10 to 12 µm at their greatest width. The cells typically contain within their cytoplasm what appear to be remnants of whole algal cells in various stages of digestion (Fig. 61). The algal cell remnants are not contained within any membrane-limited structure but appear as electron-lucent regions in the stomach cell cytoplasm. Algal cell nuclei are recognizable as bodies with electron-dense material condensed around the periphery, a form similar to the digested algal cell nuclei contained within the lumen of the stomach.

The cytoplasm of the type II stomach cell is dominated by extensive rough endoplasmic reticulum (Fig. 61). The rough endoplasmic reticulum occurs in all regions of the cell except the areas that were formerly algal cell cytoplasm. Mitochondria and microtubules are similarly dispersed throughout the stomach cells.

A nucleus, which is circular in outline and about 6 μm in diameter, is located in the basal regions of the type II stomach cell. Nuclei contain one or more prominent nucleoli 2 μm in diameter. The nucleoli consist of a cortex of electron-dense material surrounding a granular core of medium density (Fig. 61).

The apical surface of the type II stomach cells is elaborated into microvilli in a manner similar to type I stomach cells. The type II cells are attached to adjacent cells near their luminal surface with zonulae adhaerentes. Type II cells have never been observed to bear cilia.

The pyloric sphincter separates the stomach and intestine (Fig. 62). It consists of a constrictable opening at the posterior end of the stomach made up of a ring of type I stomach cells that have in their basal regions a single band of circumferentially oriented thick and thin myofilaments. The myofibril is 0.25 μm thick and does not appear to be striated.

The intestine is comprised of simple squamous epithelium,3 to 5 μm thick (Fig. 62). The cytoplasm of the intestinal cells contains numerous vesicles, 0.25 to 0.5 μm in diameter. The vesicles contain granular and flocculent material, and in some instances a second membrane-limited vesicle is contained within the first. Similar vesicles occur in the lumen of the intestine (Fig. 62).

The single cilium borne by each cell is its only apparent surface specialization. The basal body of the cilium consists of two orthogonally-directed centrioles, each of which gives rise to a short striated rootlet (Fig. 62).

An elliptical nucleus containing scattered patches of electron-dense material is centrally located in each cell (Fig. 62). Mitochondria and clumps of free ribosomes are dispersed throughout the cytoplasm. The cells are attached near their apical ends with zonulae adhaerentes and the epithelium is attached to a basal lamina.

The anus is a thickened ring of intestinal epithelium that forms a junction with the epidermis. The cells that form the anus have in their basal regions thick and thin filaments arranged in a manner similar to that described for the pyloric sphincter.

DISCUSSION

A. Histogenesis

The archenteron of the *D. excentricus* gastrula is comprised of cells which are uniform ultrastructurally and relatively unspecialized. During the transformation of the archenteron into the larval digestive tract the cells remain as a homogeneous population, although there is a gradual loss of embryonic characters amongst them. The cells that form the esophagus, cardiac sphincter, stomach, and intestine have assumed specialized structural characteristics by the time the larva begins to feed. The tissues of the larval gut continue to undergo structural specialization throughout the span of larval life.

Vacquier (1971a) and Vacquier et al. (1971) found that there is an appearance and gradual linear increase in α-amylase and β-1,3-glucanohydrase activity in the guts of *D. excentricus* embryos, beginning as the stomodeum forms. The two enzymes are capable of digesting the polysaccharides that form the algal cell walls (Bull and Chester, 1966). Vacquier (1971b) reports that the β-1,3-glucanohydrase is concentrated in the tissues of the larval gut. Vacquier (1971a) suggests that the two proteins are synthesized *de novo* as digestive enzymes and are markers for the differentiation of the larval gut.

Vacquier (1971a) reported that the increase in β-1,3-glucanohydrase activity is sensitive to treatment with cycloheximide (a known inhibitor of protein synthesis), an observation that suggests the synthesis of new proteins is required for the increase in β-1,3-glucanohydrase activity. The appearance of increased amounts of rough endoplasmic reticulum and ribosomes in the cells of the larval stomach at the early pluteus stage (the stage at which the enzyme activity increases) supports Vacquier's hypothesis that tissue-specific protein synthesis occurs at that time.

Vacquier (1971a) found that treatment of the centrifuged crude extract with sodium dodecyl sulfate was required to release the β-1,3-glucanohydrase into the supernatant. He concluded that the enzyme is membrane-bound or occurs in association with a sedimenting particle. It is not unlikely that the enzyme is stored, after synthesis, in cytoplasmic vesicles, and that these correspond to the sodium dodecyl sulfate soluble particles.

In the early and four-armed plutei, there is a marked increase from previous stages in the number and size of type A vesicles. Type A vesicles range in size from 100 to 500 nm, contain fine granular material of medium electron density, and are associated with both Golgi bodies and the apical cytoplasm of the cells of the larval stomach. These circumstantial data suggest that during the early pluteus stage the cells of the larval stomach begin synthesizing digestive enzymes contained in cytoplasmic vesicles which are subsequently released from the apical surface of the cells for extracellular digestion.

The stomach cells of the four-armed and eight-armed plutei differ considerably in their ultrastructural appearance, although they are probably performing identical functions. The type I stomach cells in the eight-armed pluteus display a definite apical-basal polarity and the allocation of organelles to specific regions of the cytoplasm is uniform throughout the tissue. The polarity of the stomach cells in the four-armed pluteus is less apparent and the disposition of organelles appears to occur with greater latitude than in the type I stomach cells.

The differences in the morphology of the two stages may be owing to subtle differences in function; the larva, with age, may acquire different dietary requirements and hence the digestive and absorbative processes would change. Alternatively, the ultrastructural specializations of the cell are realized less quickly than the functional specializations. The biochemical differentiation of the cell may occur independently of, and precede, the morphological differentiation of the cell.

It is without question that the organization of a cell and its function are directly related, but whether the structure is achieved by genetically controlled active mechanisms, or is 'worn in' passively, remains moot. The cells of the larval gut may perform the same functions throughout the span of larval life and it is the continual repetition of these tasks which determines the state of organization of the cells.

Throughout development there is a gradual decrease in the number of yolk vesicles in the cells of the embryo. The assimilation of these stored reserves, allocated during the formation of the egg, is essentially complete in the four-armed pluteus, as there are only a few scattered yolk vesicles remaining in the gut cells at this stage. The yolk vesicles decrease in number and not in size; their average diameter remains about 1 μm throughout the development of the gut. Apparently the yolk granules are released into the cytoplasm by the lysis of the vesicular membranes. The scattered clumps of yolk granules that were observed in the cytoplasm are consistent with this mechanism.

B. Feeding Behavior

Plutei, when feeding in still water, swim with the arms directed towards the surface of the water. The cilia of the ciliary band beat posteriorly, producing currents of water that pass between the larval arms (Strathmann, 1971). Food particles are retained on the upstream side of the ciliary band, apparently by a localized reversal of the ciliary beat (Strathmann et al., 1972). The food particles are passed to the larval mouth by a combination of oral field cilia and water currents (Strathmann, 1971).

The food particles, upon entering the mouth, are transported down the esophagus by ciliary beating and peristaltic contractions of the upper esophagus (Fig. 63). The algal cells are collected and formed into a bolus in the lower esophagus prior to passage to the stomach. When a peristaltic wave, which has passed down the upper esophagus, has completely constricted the lower end of the upper esophagus, the sides of the lower esophagus contract toward the upper esophagus and the cardiac sphincter is opened, everting the bolus into the stomach (Gustafson et al., 1972a). The sphincter closes rapidly and the esophagus is returned to its rest position.

The cilia of the stomach agitate the bolus, break it up, and circulate the food particles around the stomach. Strathmann (1971) reports that ingested particles are sorted in the stomach; undigested material collects in the pyloric end of the stomach and is passed to the intestine when the pyloric sphincter is opened. Particles are carried to the end of the intestine by cilia and are defecated when the anus opens (Strathmann, 1971).

Larvae can reject particles that are in too high a concentration or too large to be completely ingested (Strathmann, 1971, and others listed therein). Particles can be rejected from the buccal cavity or upper esophagus by reversing the direction of the effective stroke of the cilia (i.e., the cilia beat toward the mouth). Particles can also be rejected from the esophagus by reversing the direction of peristalsis; the offending particles are regurgitated by a wave of peristaltic contraction beginning at the lower end of the esophagus.

C. Esophagus

The cells of the upper esophageal epithelium produce the ciliary currents that assist in the transport of food particles to the lower esophagus. Ultrastructurally, the cells are relatively unspecialized in form. However, the elongate striated rootlets are distinctive characteristics of these cells. Pitelka (1974) stated that one of the obvious functions of basal bodies and root structures of cilia was to keep the active motor organelle firmly rooted in the cytoplasm so that it may exert force on its surroundings. The length of the striated rootlets of the upper esophageal epithelium may indicate an enhancement of this function.

The upper esophageal epithelium is formed into ridges that can be seen in cross-section to interdigitate when the esophageal muscles are contracted. The construction of the tube in this manner allows the lumen to become fully occluded during peristalsis. The full occlusion acts as a one-way valve that forces material to be moved exclusively in the direction of the peristaltic wave.

The epithelium of the lower esophagus is comprised of cells that are characterized by prominent Golgi bodies and numerous vesicles in the apical cytoplasm. The lower esophageal cells are similar ultrastructurally to the cells of the esophagus of *Psammechinus miliaris* that were described by Ryberg and Lundgren (1975) as being secretory. Histochemical techniques revealed that the secretory cells contain mucopolysaccharide and that the esophagus is lined with similar substances (Ryberg and Lundgren, 1975). Strathmann (1971) noted similar secretory cells to occur in the buccal cavity and esophagus of plutei of *Strongylocentrotus droebachiensis*. Apparently the lower esophagus in *D. excentricus* is not only a bulbous region for the collection of food particles, but the epithelium also secretes mucous substances which probably assist in the formation of the food bolus.

The spatulate shape and the plicated base of the sphincter cells probably contribute to the ability of the epithelium to distend, allowing the passage of food and yet maintaining the separation of the stomach and esophagus when the sphincter is closed. Being broad apically and folded basally, the cells are not required to change shape excessively when the sphincter opens and increases the diameter of the lumen.

The vacuolated appearance of the apical portions of the sphincter cells suggests that they may perform a secretory function similar to that of the lower esophageal epithelium. A coating of mucus may assist in blocking the lumen of the sphincter while the sphincter is closed.

The orientation of the esophageal muscles correlates well with the swallowing activity of the larva (Fig. 63). The bands are predominantly circumferential in the upper esophagus where the sequential contraction of the fibers produces the peristaltic waves. The muscle fibers of the lower esophagus originate around the base of the upper esophagus and insert around the sphincter. Contraction of these longitudinal bands opens the sphincter and pushes the contents of the lower esophagus into the stomach. The myoepithelium of the cardiac sphincter acts antagonistically to the lower esophageal muscles; contraction of the circumferentially oriented myofibrils closes the sphincter.

The esophageal muscles differ considerably in ultrastructure from muscles that have been previously described in adult echinoids as they possess a combination of smooth and striated characters. They are thus termed pseudostriated.

The musculature of adult echinoids is predominantly smooth (Hyman, 1955). There are ultrastructural descriptions of echinoid smooth muscle in: tube feet (Kawaguti, 1964; Coleman, 1969; Florey and Cahill, 1977), pedicellariae (Cobb, 1968), and lantern retractor muscles (Cobb and Laverack, 1966). Echinoid smooth muscle is comprised of independent fibers containing thick and thin filaments that are usually oriented parallel to the long axis of the cell. The thick filaments are about 35 to 40 nm in diameter and the thin filaments are reported to range from 5 to 10 nm in diameter (Cobb, 1968; Florey and Cahill, 1977). The ratio of thin to thick filaments is very high (Cobb and Laverack, 1966; Florey and Cahill, 1977). Florey and Cahill (1977) report the junctions between the cells to be dense regions of the sarcolemma and that Z-bodies (dense bodies) are common.

Striated fibers have been reported to occur only in pedicellariae adductors (Cobb, 1968) and the muscles controlling the specialized rotating periproct spines of *Centrostephanus longispinus* (Hyman, 1955). Cobb (1968) described the ultrastructure of the striated fibers of the pedicellariae of *Echinus esculentus*. The sarcomere length is reported to be about 0.85 μm and M-lines and H-bands do not occur. The thick filaments are about 15 nm in diameter and the thin filaments, 5 nm. A well developed T-system forms a tubular framework along the length of the fibers but there is no regular sarcoplasmic reticulum and therefore no diad nor triad system.

The arrangement of the thick and thin filaments in pseudostriated muscle in the *D. excentricus* eight-armed pluteus is sufficiently random that the fibers appear smooth. There are no recognizable A- and I-bands. There is, however, a periodic arrangement of dense bodies that results in indistinct Z-lines.

The dimensions of the thick filaments of the pseudostriated muscles are intermediate to those of striated and smooth muscles of echinoids; the thick filaments of striated muscle are 15 nm (Cobb, 1968); pseudostriated muscle, 28 nm, and smooth muscle, 35 to 40 nm (Florey and Cahill, 1977). The thin filaments of all three muscle types range from 5 to 10 nm.

In echinoid smooth muscle the thick filaments are typically surrounded by numerous thin filaments that do not appear to have any consistent geometric relationship with the thick filaments (cf. Cobb and Laverack, 1966; Florey and Cahill, 1977). In pseudostriated muscles the thick filaments each appear to be surrounded by an array of 6 to 8 thin filaments that remain about 20 nm from the thick filament. Regularly arrayed thin filaments and a low thin to thick filament ratio are characteristic of striated muscle (Smith, 1972).

The striated myofibrils located in the base of the myoepithelial cells that form the cardiac sphincter are ultrastructurally similar to the myofibrils of echinoid striated muscle (cf. Cobb, 1968). The sarcomere length of the larval striated myofibrils is 0.9 μm and that of the adult muscle is 0.85 μm. The A- and I-bands comprise similar proportions of the sarcomere in both cases and neither muscle has M-lines nor H-bands. The thin filaments of each type are of comparable diameter but the thick filaments differ; the larval thick filaments average 25 nm and the adult thick filaments are reported to be 15 nm in diameter. Mitochondria are associated with both types of myofibril but smooth endoplasmic reticulum occurs only with the larval type.

In vertebrates, two morphological muscle types, smooth and striated, correlate with distinctive physiological properties; in general, striated muscle undergoes phasic contraction and smooth muscle contracts tonically (Smith, 1972). The situation in invertebrates is not nearly so clear; the diversity of morphological types of muscle is greater (Rosenbluth, 1972) and the physiological responses of certain muscle types depends upon complicated neuromuscular interactions (Lang and Atwood, 1973).

Peristaltic contractions of the esophagus are distinctive in that they occur rapidly and irregularly. During peristalsis, the contractions of the individual muscle fibers last for only a brief period of time, and the muscle relaxes immediately afterwards. It is this phasic activity that causes the peristaltic wave to pass the length of the esophagus rapidly. The waves of peristalsis are not regular undulations but appear to occur at infrequent intervals and in response to various sorts of stimulation (Strathmann, 1971; Gustafson et al., 1972a). The combination of smooth and striated characteristics in the esophageal muscles may reflect their adaptation to the role the rapid peristalsis of the esophagus plays in the collection and transport of larval food.

The closing of the cardiac sphincter is rapid. Gustafson et al. (1972a) recorded the activity cinematographically and termed it "super-contraction". They also noted the contraction of the sphincter is followed by relaxation; presumably the myoepithelium acts to close the sphincter and it remains closed owing to the form of the tissue.

The resemblance of the sphincter myofibrils to those of the pedicellariae adductor muscles, and the limited occurrence of striated muscles in echinoids, suggests that these two muscles are functionally similar. It is likely that the striated arrangement of myofibrils provides rapid, phasic responses.

The cardiac sphincter functions to separate the internal environments of the esophagus and the stomach. The necessity for this is not readily apparent, but is suggested to be important by the rapid closure of the cardiac sphincter. If the separation were not critical, one would not expect the transfer of food from the esophagus to the stomach to occur with the alacrity with which it does. Vacquier (1971a) noted the pH optimum of the larval digestive enzyme, β-1,3-glucanohydrase, to be about 6, while the pH of sea-water is about 8. This observation indicates the environment of the larval stomach may differ from that of the esophagus, necessitating the separation provided by the cardiac sphincter.

The nerve fibers located in the upper esophagus are presumed to control the activity of the ciliated epithelium and the esophageal muscles. There is physiological evidence that the ciliated cells and the muscle cells are, at least in part, under nervous control. Gustafson and his colleagues (1972a,b) have demonstrated that serotonin and acetylcholine stimulate contractile activity in the esophageal muscles. Mackie et al. (1969) were able to record monophasic potentials from regions of the ciliary band during reversal of ciliary beat. The potentials and reversal behavior were blocked with magnesium chloride, a substance known to suppress nervous activity in vertebrates. Strathmann (1971) reported that the reversal of beat of esophageal cilia can be similarly inhibited.

The verrucosities of the axons apposed to both ciliated and muscle cells may be synapses, even though regions of pre- and post-synaptic membrane specialization are lacking. Cobb and Pentreath (1977) investigated the ultrastructure of nerve terminals in the radial nerve cords of adult starfish and found no specialization of synaptic membranes. They have urged caution in the identification of synapses, suggesting that the sites of neurotransmitter release in echinoderms are not as morphologically distinctive as in vertebrates. Whether the verrucosities described here are functional contacts between the axons and the effector cells cannot be concluded without defined morphological characteristics for synapses in echinoderms.

Nervous tissues were not observed in the lower esophagus, nor associated with the cardiac sphincter. Yet the muscles of the lower esophagus and the myoepithelium of the cardiac sphincter act in a coordinated manner. It is possible that impulses, stimulating contractions, are transmitted either within the epithelium of the esophagus or the meshwork of the esophageal muscles.

D. Stomach

Strathmann (1971) reported that several species of diatom and green algae underwent rapid disintegration after entering the stomach of echinoplutei. The coincidence of appearance of the type A vesicles with the beginning of production of digestive enzymes, and the association of the enzymes with particles (Vacquier, 1971a), suggests that type I stomach cells secrete digestive enzymes into the stomach.

Type B vesicles have various contents and are usually restricted to the apical half of the cell. Interpretations of their function are equivocal; they may represent phagocytic vesicles bringing material from the lumen into the cells, or they may contain material being transported out of the cells. Immers and Lundgren (1972) observed a gradient of vesicles with similar contents in the stomach cells of *P. miliaris* larvae. They suggested that the stomach cells ingest food phagocytically.

The accumulation of type C vesicles in the basal regions of the type I stomach cells suggests that the stomach also functions as a storage organ. The contents of the type C vesicles have the characteristics of lipid. Adult echinoids have been demonstrated to accumulate reserves of both polysaccharides and lipids in the epithelium of the stomach (Lawrence et al., 1966).

Evidently the type I cells secrete enzymes that digest the algal cells. The digestion products are then absorbed, either across the cell membrane or from phagocytized food vacuoles. Nutrients in excess of the larval demands are probably anabolized into lipids for storage.

Type II stomach cells are apparently able to ingest complete algal cells and digest them intracellularly. The type II cells are restricted in distribution and make up only a small proportion of the stomach epithelium; their contribution to the digestive physiology of the pluteus is not clear.

E. Intestine

The lumen of the intestine and the cells of the intestinal epithelium contain numerous vesicles of a single morphological class. The vesicles in the cells may represent material being absorbed from the digest passed on from the stomach. However, the absence of microvilli, lipid storage vesicles, and anabolic organelles such as rough endoplasmic reticulum and Golgi bodies suggests that the intestine functions primarily as a conductive tube for the elimination of undigested food materials.

The simple nature of the pyloric sphincter, in comparison with the cardiac sphincter, suggests that the separation required between the stomach and intestine is less than is required between the esophagus and stomach.

Strathmann (1971) noted that the movement of material from the stomach to the intestine and out of the intestine is mediated by ciliary activity. The opening and closing of the pyloric and anal sphincters is probably brought about, quite simply, by the relaxation and contraction of the sphincter myoepithelium.

Gustafson et al. (1972a) reported that the filling of the larval intestine was brought about by coordination between the pyloric and anal sphincters. When the pyloric sphincter is open and the anal sphincter is closed, the intestine fills; the opening of the anus and closing of the pyloric sphincter empties the intestine. No nervous tissues were observed associated with the intestinal sphincters in *D. excentricus* larvae, yet the intestine shows the coordination of the sphincters reported by Gustafson et al. (1972a) for *P. miliaris* larvae. The stimulus for the contraction or relaxation of the myoepithelial cells apparently arises or is transmitted within the epithelium itself.

SUMMARY

The structure of the archenteron and larval gut of gastrulae, prisms, and early, four-armed, and eight-armed plutei of *D. excentricus* are described.

The archenterons of gastrulae and prisms are comprised of a population of cells that are uniform ultrastructurally and relatively unspecialized.

Throughout the formation of the esophagus, stomach, and intestine, the cells remain ultrastructurally indistinguishable, however, there are fewer yolk vesicles and more rough endoplasmic reticulum and ribosomes by the time the early pluteus stage has been reached.

The cells of the esophagus, stomach, and intestine show some specialization in the four-armed feeding pluteus, however, the functions of gut cells in the eight-armed pluteus are more readily apparent.

The esophagus is divided into two distinct regions. The upper esophagus contains predominantly ciliated cells, and the lower esophagus, cells that evidently secrete mucus. The esophageal muscles form a network around the esophagus and contain myofibrils that have a combination of smooth and striated characters. The muscle fibers are oriented circumferentially in the upper esophagus, where they produce peristaltic

contractions, and longitudinally in the lower esophagus where their contraction opens the cardiac sphincter and forces the bolus of food into the stomach. Axons, with putative synapses, are associated with the ciliated cells and the muscles of the upper esophagus.

The cardiac sphincter is a ring of myoepithelium with cross-striated myofibrils oriented around the base of the cells which function in closing the sphincter. The apical half of the sphincter cells may perform a secretory function.

The stomach epithelium contains two cell types: type I cells predominate and evidently secrete digestive emzymes, and absorb and store nutrients; type II cells apparently phagocytize and intracellularly digest whole algal cells.

The pyloric and anal sphincters are comprised of myoepithelium. They are, however, much simpler in nature than the cardiac sphincter. The intestine is comprised of relatively unspecialized cells and probably functions as a conductive tube for the elimination of undigested material.

METAMORPHOSIS AND THE FATE OF THE LARVAL DIGESTIVE TRACT

INTRODUCTION

Metamorphosis in echinoids is a rapid and radical change in form and habit. To comprehend the fate of the larval digestive tract it is necessary to consider metamorphosis itself. Accordingly, the transformation of the larval digestive tract is investigated in the context of the metamorphic processes that occur in conjunction with it.

Early in larval development an invagination of epidermis on the left side of the pluteus forms a vestibule that comes to lie against the left hydrocoel. The floor of this sac is comprised of two tissue layers, ectodermal and mesodermal in origin, which develop throughout larval life into the oral half of the adult form (see review by Hyman, 1955). At metamorphosis, the adult rudiment is rapidly everted from the vestibule and most of the larval form is resorbed into the juvenile.

The adult digestive tract in echinoids consists of a mouth, an esophagus, a primary and recurrent loop of the gut, and an anus. The tissues that form the adult gut are derived from the larval gut and are thus endodermal in origin (Bury, 1896; MacBride, 1903). MacBride (1903) found that the larval esophagus and mouth of *Echinus esculentus* degenerate at metamorphosis and that the larval stomach and part of the larval intestine form the primary loop of the adult gut. The end of the larval intestine grows to form the recurrent loop which contacts the aboral pole to form the adult anus. von Ubisch (1913) found the primary loop in *Psammechinus miliaris* to be formed from the larval stomach and the recurrent loop to be derived from the larval intestine.

Bury (1896) and MacBride (1903, 1918) described histolysis of the larval gut during metamorphosis. The accounts of those authors state that the stomach collapses into numerous folds which nearly fill the lumen. Large numbers of stomach cells round up, undergo rapid division, and migrate into a surrounding jelly layer. The remaining cells, which MacBride (1918) referred to as "isolated pockets of embryonic cells," become reconstituted into the adult digestive tract. von Ubisch (1913) reported that cells, proliferated from the visceral layer of the somatocoel, replace the larval gut cells to form the adult digestive tract.

von Ubisch (1913) and MacBride (1903) reported that the larval epidermis is histolysized during metamorphosis and is subsequently phagocytized by pigment-bearing cells. Cameron (1975) observed autophagocytosis in histolysized gut tissues during metamorphosis of *Lytechinus pictus*.

Bury (1896) and Seeliger (1892) thought the dissociation of larval tissues they observed during metamorphosis was an artifact and considered it to be pathological.

The objectives of this portion of my research are: 1) to describe the external aspects of metamorphosis of *D. excentricus* and *S. purpuratus*, and 2) to trace the fate of the larval digestive tract at metamorphosis in *D. excentricus*. Part of the results reported here have been published elsewhere (Chia and Burke, 1978).

RESULTS

A. Metamorphosis

The period of larval development in *D. excentricus* and *S. purpuratus* varies considerably depending largely upon the temperature and the quality and quantity of food. *D. excentricus* larvae kept at 15° to 17°C and fed *ad libitum* became competent to metamorphose five to seven weeks after fertilization. *S. purpuratus* larvae, kept on a similar regime, were capable of metamorphosis after seven to ten weeks of development.

A competent larva of both species may be recognized by the bulk of the adult rudiment, which dominates the left side of the larva (Fig. 64). The increased mass of the larva frequently causes it to sink to the bottom of the culture dish.

The adult rudiment, in competent plutei, is a discoid which is contained within a vestibule of larval epidermis, and represents the future oral half of the adult. The presumptive adult mouth is at the center and adult spines and tube feet are arrayed around the perimeter (Fig. 64). The spines, which are 70 to 80 μm in length and fenestrated, lie oriented toward the center of the rudiment. Ossicles, which are to be the plates that will form the adult test, also rim the rudiment. Five triangular-shaped teeth lie beneath the peristomal epithelium and converge on the incipient mouth.

Other than the distention of the left side of the larva, owing to the bulk of the rudiment, all the structures of the competent larva remain as they were during earlier larval life. However, individuals that have been competent for several weeks begin to resorb the skeletal rods of the larval arms, causing the arms to shorten. The stomach epithelium of competent larvae is opaque, yellow, and contains many small droplets of oil (Fig. 64).

Competent larvae of *D. excentricus* may be stimulated to metamorphose with a few grains of sand that has been conditioned by the presence of an adult sand dollar (Highsmith, 1977). In one experiment, ten competent larvae were put into a dish containing conditioned sand and another ten were treated with sand that had not been conditioned. Only those treated with conditioned sand metamorphosed. One had metamorphosed within an hour, five more had metamorphosed after four hours, and a total of nine metamorphosed within 24 hours. Larvae that were treated with unconditioned sand were exposed to conditioned sand after the termination of the experiment; eight of the ten metamorphosed after 24 hours.

In another experiment, five competent larvae metamorphosed within 24 hours after being placed into dishes with conditioned sand for two hours, and then being removed, rinsed, and put into MFSW. Larvae similarly treated with unconditioned sand failed to metamorphose in MFSW.

Competent *S. purpuratus* larvae were found to be refractory to all forms of stimulation that were attempted. The stimulants tried were: sand, rocks (both those found associated with adults and those not), adult spines, tube feet, feces, whole adults, glassware coated with an unidentified algal film, and pieces of the blade of *Nereocystis leutkeana*. Three *S. purpuratus* larvae metamorphosed in unfiltered sea-water, without any apparent stimulation.

The initial reaction of competent larvae of *D. excentricus*, when stimulated, was a sustained reversal of the direction of ciliary beating and a notable increase in the movements of the spines and tube feet within the vestibule. The ciliary reversal kept the larva on the bottom of the culture dish. Frequently the opening of the vestibule dilated slightly and the larva was able to attach itself to the sand grains or the dish with its tube feet.

The first phase of metamorphosis is the eversion of the adult rudiment (Figs. 65, 66). The left post-oral and posterodorsal arms spread apart and swing posteriorly around to the right side of the larva. The vestibule opening dilates and the adult rudiment everts. Prior to metamorphosis, the rudiment is slightly concave and the spines are oriented radially towards the adult mouth. During eversion, the center of the rudiment is forced out and the oral surface becomes convex with the spines directed away from the adult mouth. The extrusion of the rudiment is similar to the reversal of concavity observable at the fingertip of a rubber glove. This process in *D. excentricus* can be completed in 3 to 5 minutes and is accompanied by violent vibrating and shuddering of the larva.

Following the eversion of the rudiment, the epidermis at the tips of the larval arms becomes opaque white and is pierced by the skeletal rods (Figs. 65, 66). The larval epidermis is then gradually drawn toward the rudiment, collapsing the larval form into a mass on the aboral surface of the juvenile. The collapse of the larval form in *D. excentricus* takes from 15 to 30 mintues, though the skeletal rods remain protruding for several hours before they are discarded (Figs. 65, 66). A transparent membranous substance is also abandoned with the larval skeleton (Fig. 66). In one instance, a larva was observed to discard a large portion of its epidermis which remained attached to the skeletal rods.

Metamorphosis was observed in a single specimen of *S. purpuratus* and appeared to proceed in a manner identical to that described for *D. excentricus*, although it required 7 hours to complete.

The newly formed juvenile is hemispherical and from 250 to 300 µm in diameter, exclusive of the spines (Figs. 67, 68). The adult test, spines, and tube feet form a ring around the base of the young sand dollar or sea urchin. The body wall becomes calcified aborally and more external appendages are added during the next two weeks of development. A thin epithelial layer covers the oral surface until the juvenile begins to feed, about seven days after metamorphosis. The spines and tube feet remain active throughout metamorphosis and immediately afterwards the juvenile uses these to move. Newly metamorphosed juveniles are able to attach themselves tenaciously to a surface with their tube feet and right themselves if inverted.

The external aspects of metamorphosis are, at this stage, complete. However, the transformation of larval tissues into adult tissues requires several days to be accomplished.

B. Changes in Larval Structures at Metamorphosis

The epidermis of competent larvae of *D. excentricus* consists of simple, squamous epithelium except in regions of the ciliary band which are comprised of columnar, ciliated cells and nervous tissues.

The squamous epidermal cells are from 0.5 to 3 µm thick and 5 or 6 µm in diameter. Each cell has an elliptical nucleus which contains relatively homogeneous chromatin and scattered electron-dense regions. All of the cells bear on their external surface a single cilium. The cytoplasm contains mitochondria, clumps of ribosomes, a cisterna of rough endoplasmic reticulum surrounding the nucleus, paired centrioles, and a short striated rootlet associated with the cilium. The cells are attached with septate junctions and rest upon a thin basal lamina.

The ciliary band is a thickening of the epidermis that outlines the oral field and traces the edges of the larval arms. The ciliary band is comprised of spindle-shaped ciliated cells which span the thickness of the band and taper at their apical and basal ends. Nerve cells are located along the edges of the band. In a central position at the base of the ciliated cells a tract of axons runs throughout the length of the band. The structure of the larval nervous system has been described by Burke (1978).

During the phase of metamorphosis in which the larval form collapses, the epidermis in *D. excentricus* undergoes a series of degenerative changes. All of the epidermis, except the regions that formed the vestibule, dissociates into clumps of rounded cells (Fig. 69). The cells lose their surface elaborations and their apical-basal polarity. Most of the cells retract their cilia into the cytoplasm (Fig. 70). Some cells undergo cytolysis and all the epidermal cell nuclei become pyknotic and fragmented (Fig. 70).

The tissues that comprise the digestive tract of competent larvae are as they were described previously for the eight-armed pluteus. During metamorphosis, the cells of the esophageal, stomach, and intestinal epithelia detach from each other and round up (Fig. 69). The gut cells, like the epidermal cells, lose their surface elaborations and their apical-basal polarity. Cilia can be seen to be drawn into the cytoplasm (Fig. 70). The nuclei of the gut cells remain as they were prior to metamorphosis, each containing scattered clumps of granular electron-dense chromatin.

Forty-eight hours after metamorphosis, the gut cells are loosely organized into a tube which convolutes through the young sand dollar (Fig. 71). The gut is still limited by the squamous epithelium of the somatocoels. The gut cells do not form a proper tissue layer as there are no cell junctions and the cells lack polarity. The gut cells contain within their cytoplasm cellular debris from the larval epidermis (Fig. 73). The degenerated epidermal cells are enclosed within vacuoles, up to 3.5 μm in diameter, frequently two or more cells will be contained within the same vacuole and each gut cell may contain two or more vacuoles (Fig. 73). The vacuoles appear to be undergoing a sequence of condensation to an electron-opaque lysosome.

Seven days after metamorphosis, juvenile *D. excentricus* have a fully formed and functional gut (Fig. 72). The gut ascends from the mouth, loops around the periphery of the sand dollar, and then turns back upon itself leading to the anus. There is a bifurcation in the initial loop where the siphon has formed. The densely staining lipid vesicles from the larval gut are restricted to the initial loop of the juvenile gut. The entire gut remains enclosed by the squamous epithelium of the somatocoels.

The gut cells have reassociated to form a simple columnar epithelium, 10 μm thick (Fig. 74). Except for the disposition of the lipid vesicles, there do not appear to be any regional specializations of the gut cells at this stage of development.

The cells are each about 5 μm wide and contain a basally situated nucleus, 3.5 μm in diameter (Fig. 74). Cisternae of rough endoplasmic reticulum and mitochondria are numerous in the basal regions of the cells. Vacuoles, 0.5 to 0.75 μm in diameter, containing myelin figures and moderately dense, granular material commonly occur in the apical half of the cells (Fig. 74). There is also a second class of vesicles dispersed through the apical portion of the cells; these are 200 to 250 nm in diameter and contain flocculent material. The only elaboration of the apical surface of the cells observed was a single cilium which had associated with it orthogonally oriented centrioles and a short striated rootlet. The cells are attached apically with zonulae adhaerentes and supported on a thin basal lamina.

DISCUSSION

The sequence of events reported here for the external aspects of metamorphosis of *D. excentricus* and *S. purpuratus* are the same as those reported for other species of regular and irregular echinoids (MacBride, 1914; Hyman, 1955; Hinegardner, 1969).

Czihak (1971) reported that metamorphosis of *Psammechinus miliaris* took several days, and Huxley (1928) refers to slow and incomplete metamorphosis in *Echinus miliaris*. These and the prolonged metamorphosis observed in *S. purpuratus* are probably owing to the absence of appropriate stimuli. The demonstration of chemical and tactile cues for the metamorphosis of three species of echinoids (Cameron and Hinegardner, 1974; Highsmith, 1977), and the large number of benthic marine invertebrates that require a cue for settlement (Chia and Rice, 1978) suggests that the general case for metamorphosis in echinoids is one in which an environmental factor serves to initiate metamorphosis.

The larval epidermis and the larval gut of *D. excentricus* were observed to undergo histolysis during metamorphosis. The cytolysis, pyknosis, and karyrrhexis observed in epidermal cells indicates that the larval epidermis probably becomes necrotic during its collapse into the aboral surface of the juvenile. Necrosis has been demonstrated to accompany metamorphosis in a wide variety of animals and is considered a programmed morphogenetic event (Saunders, 1966).

At metamorphosis, the cells of the gut apparently dedifferentiate from their larval state and become phagocytic. During the next four or five days the gut cells apparently reassociate and begin histogenesis and differentiation of the adult gut.

Bury (1896), MacBride (1903, 1918), and von Ubisch (1913) all noted the histolysis of larval tissues during metamorphosis. However, the interpretations made here of the reorganization of larval structures differ from the interpretations presented by those workers. MacBride (1903, 1918) and von Ubisch (1913) reported a rapid proliferation of cells following the histolysis of larval tissues. Their interpretation is based upon the observation of a large number of rounded cells containing more than one nucleus. Ultrastructurally, these can be seen in *D. excentricus* to be the epidermal cells containing fragmented nuclei and the gut cells containing phagosomes. MacBride (1903) suggested the phagocytes were originally larval pigment cells and von Ubisch (1913) thought they originated from the somatocoel epithelium. It is possible now to recognize ultrastructural characteristics of the phagocytic cells, such as lipid vesicles, which indicate the cells are from the larval gut. MacBride (1918) reported the adult gut was derived from pockets of embryonic cells. However, the remnant lysosomal vesicles observed in the differentiating adult gut indicate the cells probably originated from the larval gut cells. Ultrastructural observations of "autolysis" in *Lytechinus pictus* larvae suggest that a similar sequence of events occurs in the reorganization of the gut in that species (Cameron, 1975).

The esophagus, esophageal muscles, stomach, and intestine of *D. excentricus* larvae were all observed to histolysize during metamorphosis. However, unlike the stomach cells, the cells of the other parts of the larval gut preserved no characteristic organelles that allow their identification after they had dissociated and dedifferentiated. It is surmised that they all participated in the phagocytosis-redifferentiation sequence as remnant lysosomes were observed in all regions of the juvenile gut. The restriction in the distribution of the lipid vesicles to the primary loop of the juvenile gut indicates that, as MacBride (1903) and von Ubisch (1913) reported, the larval stomach forms the adult primary loop while the larval intestine probably forms the recurrent loop. The exact fate of the cells that formed the larval esophagus is difficult to ascertain, although, based on propinquity, they probably form the adult esophagus.

Structures not readily incorporated into the juvenile, such as the larval skeleton, are abandoned, while larval tissues that are specialized for the planktonic habit, such as the larval epidermis and ciliary bands, are incorporated into tissues that are transformed into adult tissues. Thus, the phagocytized cells may be made available as resources for the development of the juvenile. Saunders (1966), in discussing the disposition of the products of cell death, suggested that without direct evidence it is "gratuitous" to imply that necrotic cells are actually contributing to the remaining tissues.

It is a widely accepted idea that one of the advantages to an organism of a life cycle that has a larval stage that differs in form and habit from the adult, is that for a time the organism is able to utilize the resources of an environment that are not available to the adult. The accumulation of lipid in the stomach cells of the larva, and the subsequent transformation of the larval gut into the adult gut, enable the benthic juvenile to grow and develop on metabolic resources sequestered from a planktonic environment. The cells of the larval epidermis and ciliary bands may be similarly viewed as being derived, at least partly, from planktonic feeding.

The pleuropotency of the gut cells and the apparent programmed death of the larval epidermal cells suggests metamorphosis involves the expression of previously unused regions of the genome. The larval tissues respond, in an apparently coordinated manner, to a stimulus that in a very brief period of time induces radical changes in the cell's state of differentiation. The nature of the receptors, mechanisms of conduction, and the means of eliciting the cell's response remain the most enigmatic questions of echinoid metamorphosis.

SUMMARY

External aspects of metamorphosis of *S. purpuratus* and *D. excentricus* are described and the reorganization of the larval gut into the adult gut is examined histologically and ultrastructurally in *D. excentricus*.

Metamorphosis begins with the dilation of the opening of the vestibule containing the adult rudiment. The left post-oral and posterodorsal larval arms are swung to the right side and the adult rudiment is everted. The epidermis at the tips of the larval arms is pierced by the larval skeleton and the larval epidermis is withdrawn into the aboral surface of the juvenile. The larval skeleton is discarded. Metamorphosis is accomplished in *D. excentricus* in less than one hour.

The digestive tract and larval epidermis undergo histolysis during metamorphosis. The gut cells dedifferentiate and the epidermal cells appear to become necrotic. After metamorphosis the gut cells phagocytize and intracelluarly digest the epidermal cell debris. Seven days after metamorphosis, when the juvenile begins to feed, the gut cells have reassociated and the histogenesis of the adult gut has begun.

Figure 1. Nomarski differential interference contrast (DIC) images of gastrulae of *Strongylocentrotus purpuratus* 44 hours after fertilization; a) before treatment to dissociate the ectoderm (ec) (see text), and b) after treatment. The archenteron (ar) and the primary mesenchyme (pm) remain within the blastocoel (bl) and with a 100X objective cells can be readily counted. Bar = 20 μm.

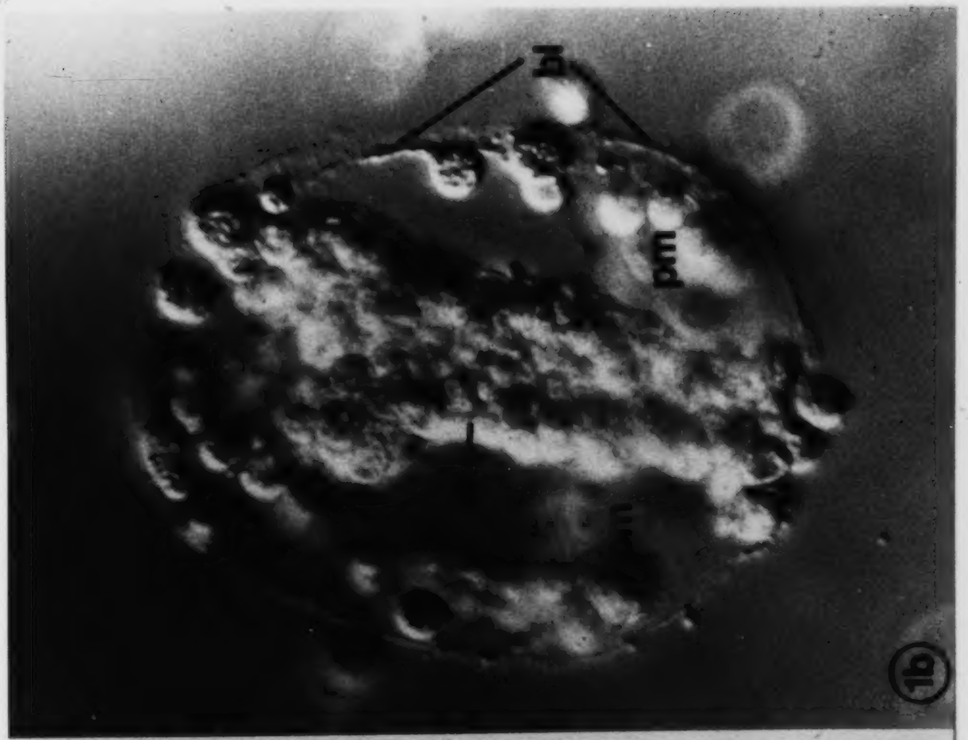
1b
bl
pm
pm

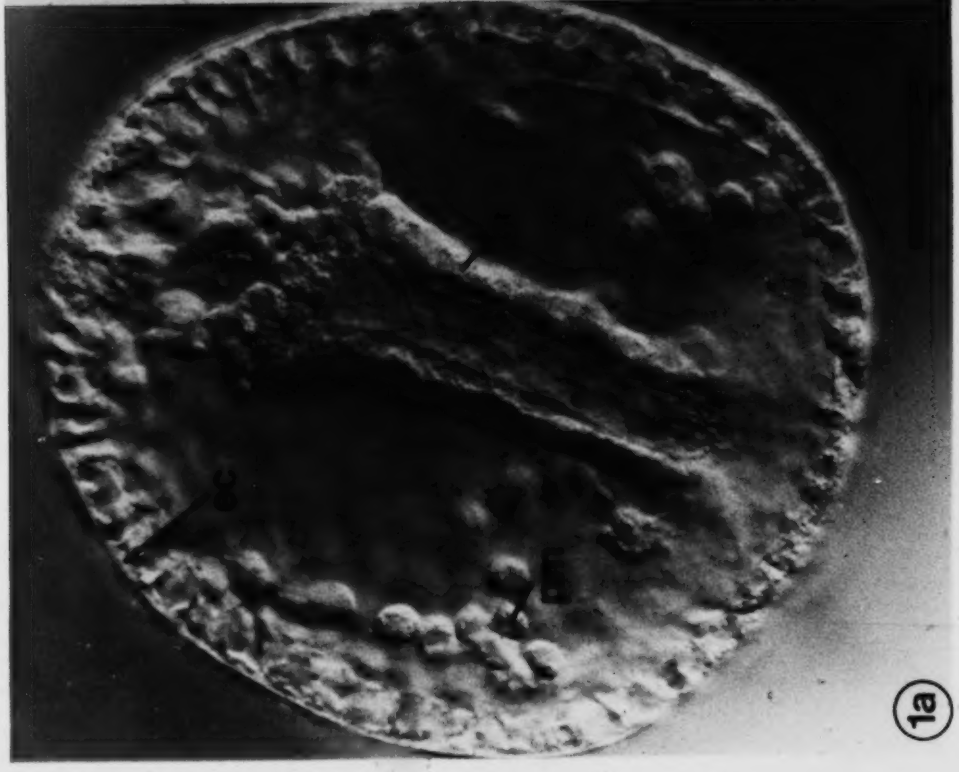
1a
ec
pm

Figure 2. Nomarski DIC images of *S. purpuratus* embryos; a) 38 hours after fertilization, during the first phase of gastrulation; b) 40 hours after fertilization, during the second phase of gastrulation; c) 59 hours after fertilization, during the formation of the coeloms (ce); and d) 61 hours after fertilization, during the formation of the cardiac sphincter (cs). ar - archenteron; pm - primary mesenchyme; sm - secondary mesenchyme. Bar = 20 μm.

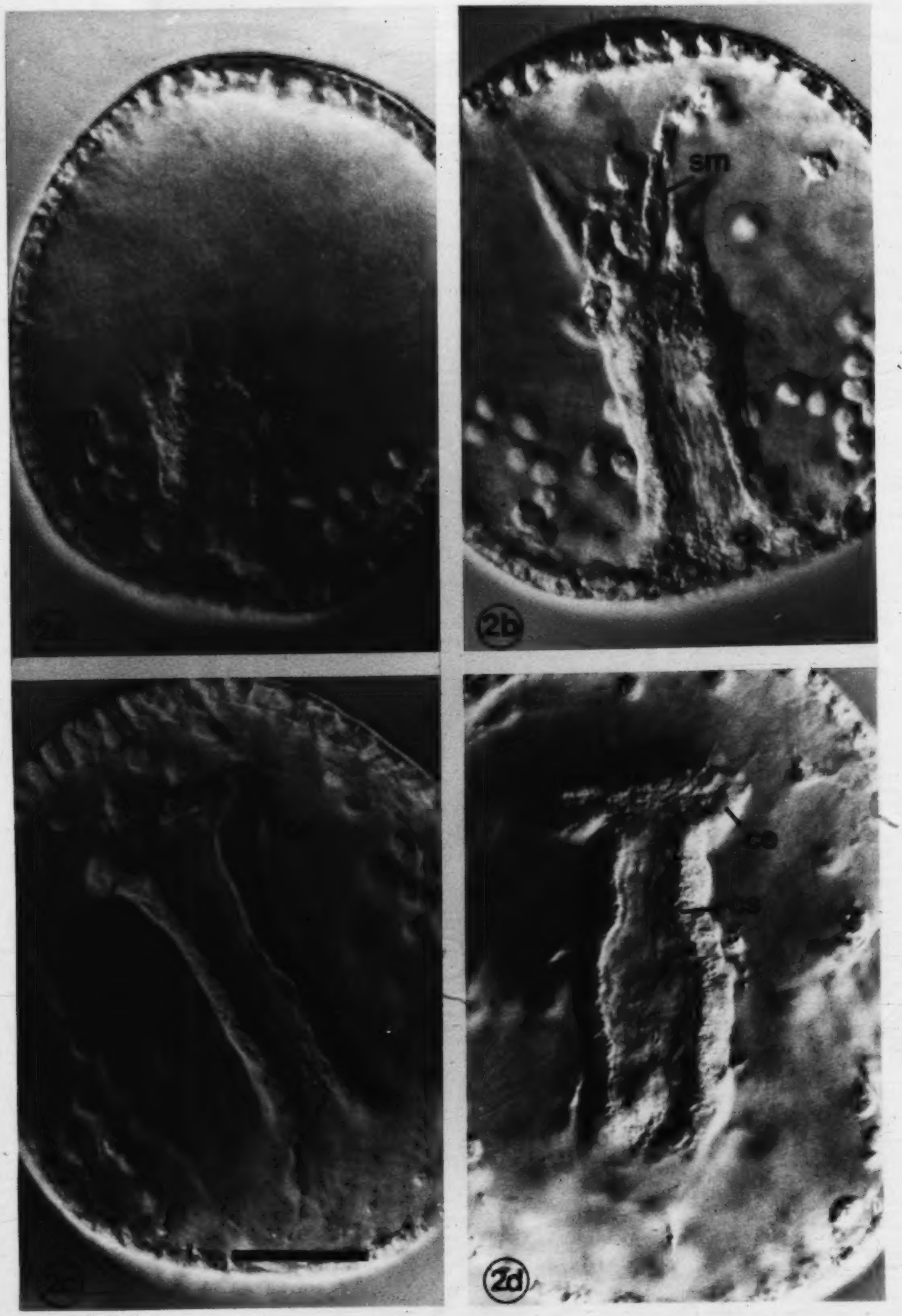
2a
sm
2b
ce
cs
2d

Figure 3. Nomarski DIC images of an *S. purpuratus* embryo 72 hours after fertilization, a) ventral view, and b) lateral view. ce - coeloms; cs - cardiac sphincter; es - esophagus; in - intestine; ps - pyloric sphincter; sk - skeletal rod; st - stomach. Bar = 20 µm.

Figure 4. Nomarski DIC images of an *S. purpuratus* larva 88 hours after fertilization, a) ventral view, and b) lateral view. Note the material in the stomach (st) indicating the larva has begun to feed. cb - ciliary band; m - mouth. Bar = 20 µm.

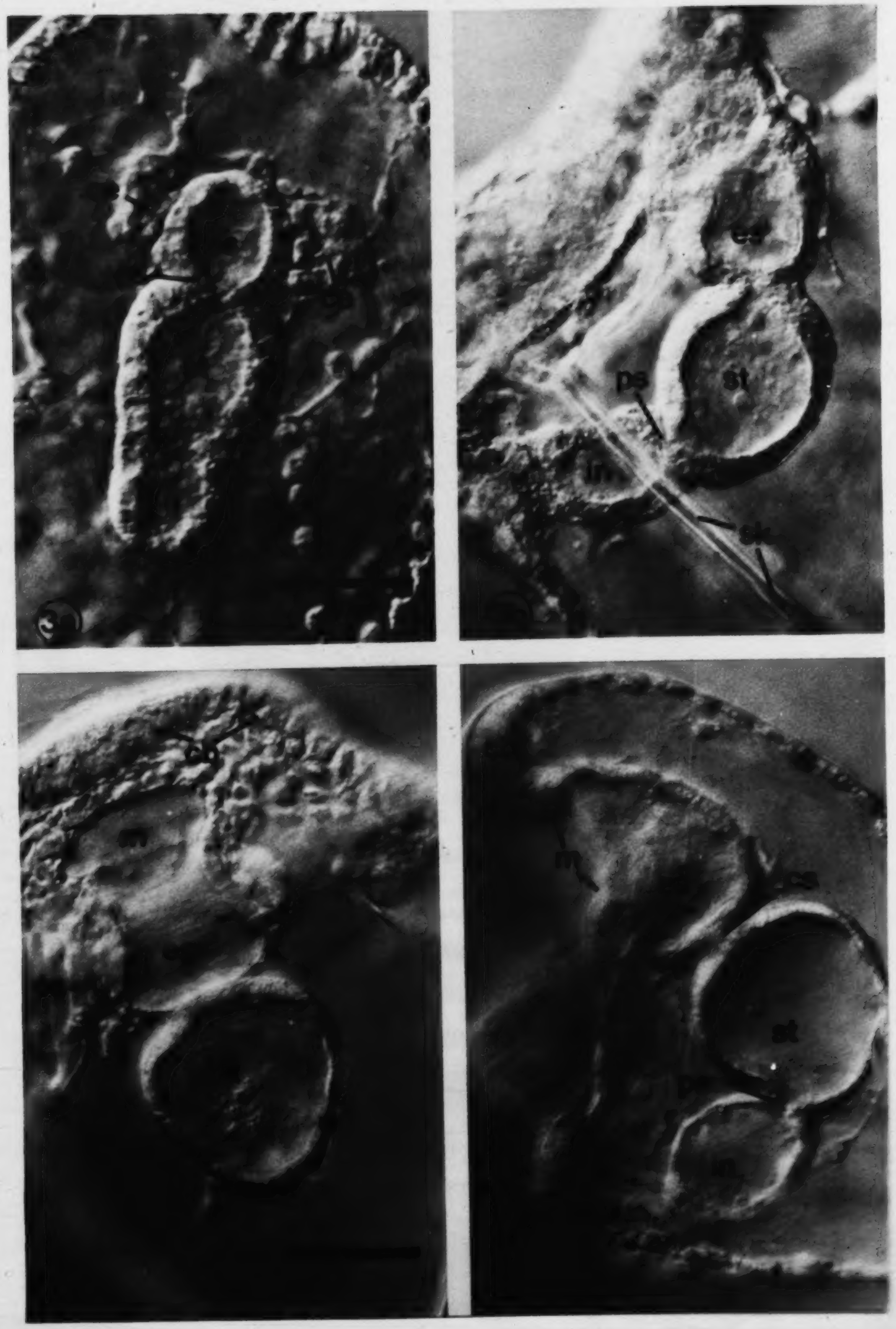
es
ps
st
in
sk
cs
st

Figure 5. Nomarski DIC images of *Dendraster excentricus* embryos: a) 26 hours after fertilization, b) 33 hours, c) 42 hours, d) 50 hours. ar - archenteron; cb - ciliary band; ce - coeloms; cs - cardiac sphincter; es - esophagus; m - mouth; sk - skeleton; sm - secondary mesenchyme; st - stomach; pm - primary mesenchyme. Bar = 20 μm.

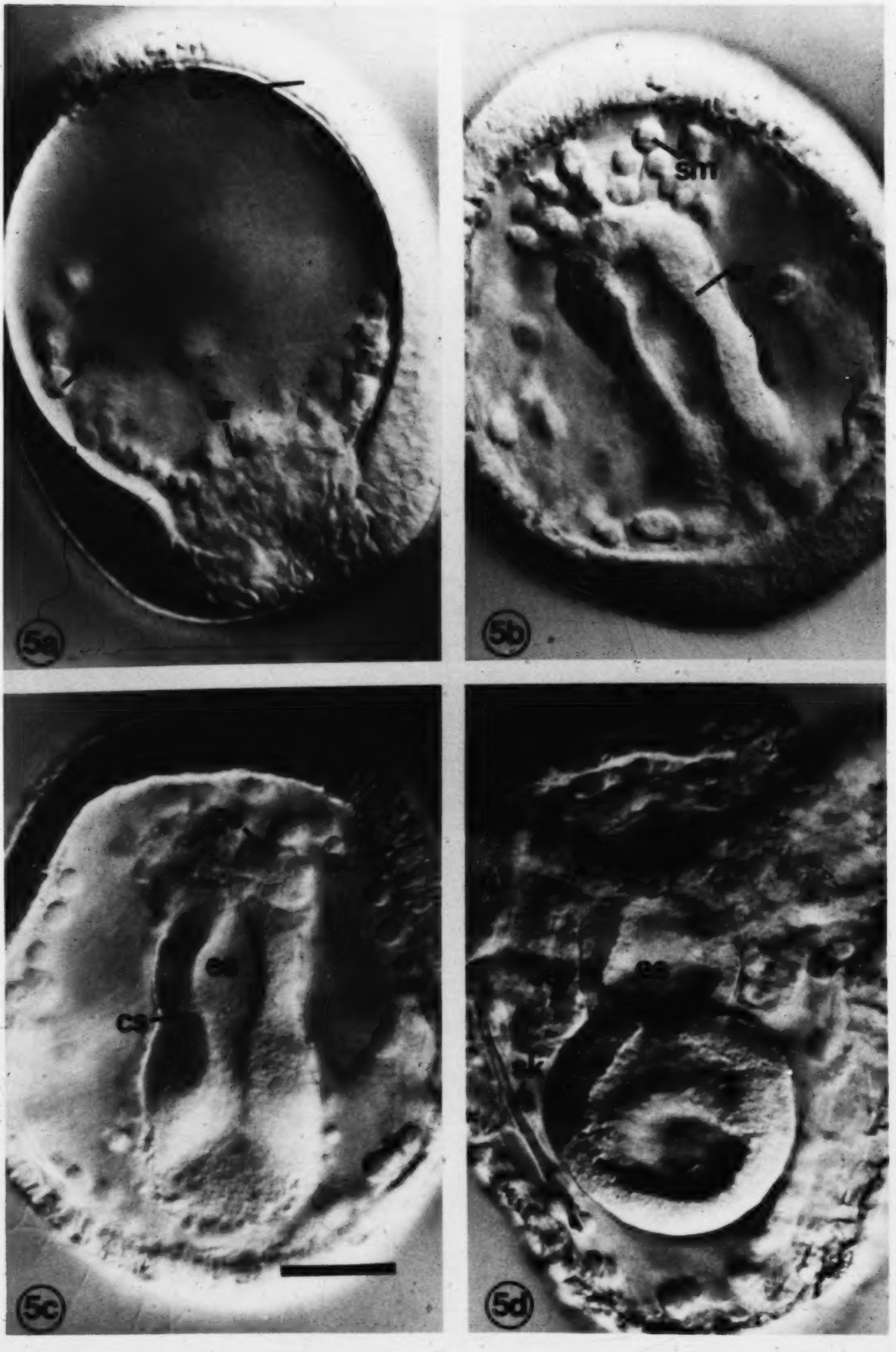
sm
5a
5b
es
cs
5c
es
5d

Figure 6. a) Ventral view of a 72 hour embryo of *S. purpuratus* showing cells that will form the ventral dilator muscles (dm) extending from the coeloms (ce). b) Lateral view of a 66 hour *S. purpuratus* embryo showing the hydroporic canal (hc) extending from the left coelom.

es - esophagus; sk - skeleton; st - stomach. Bar = 20 µm.

Figure 7. The plane of focus of this Nomarski DIC image is at the surface of the esophagus of a 90 hour pluteus of *S. purpuratus*. The esophageal muscles (esm), which arise from cells at the edge of the coelom, can be seen circumscribing the esophagus. Bar = 20 µm.

6

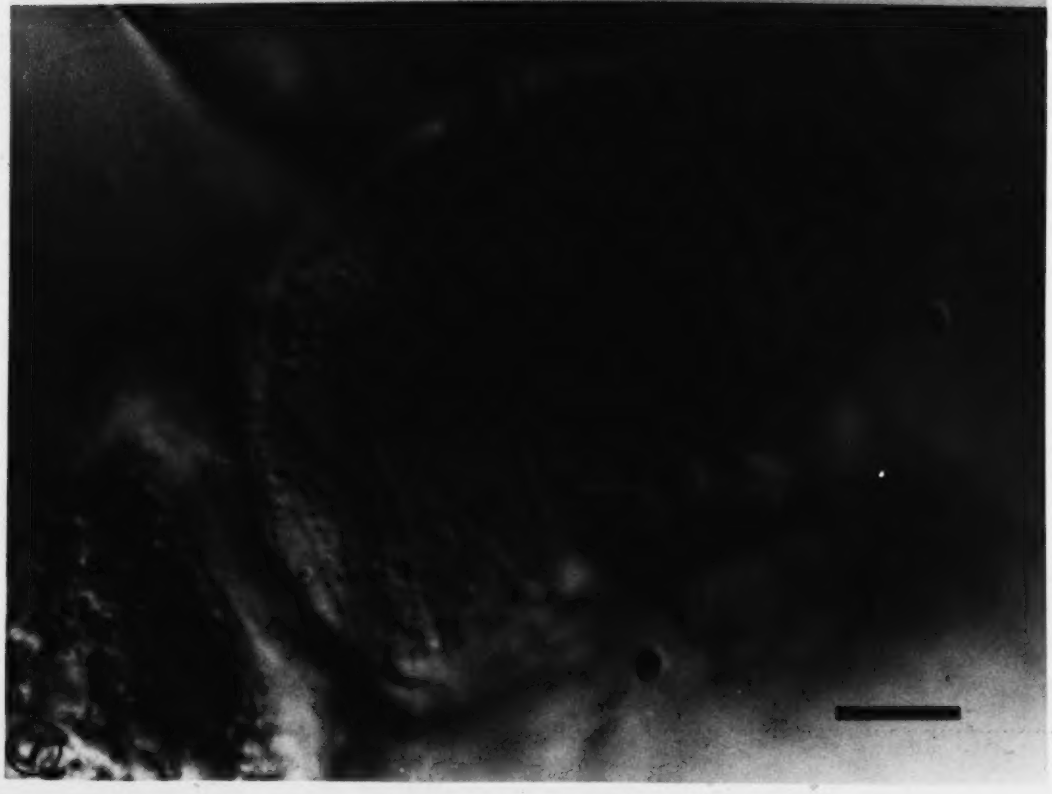

Figure 8. (a, b, c, d, e). Scale drawings made from fixed *S. purpuratus* embryos, depicting the morphogenesis of the larval digestive tract. Bar = 50 µm.

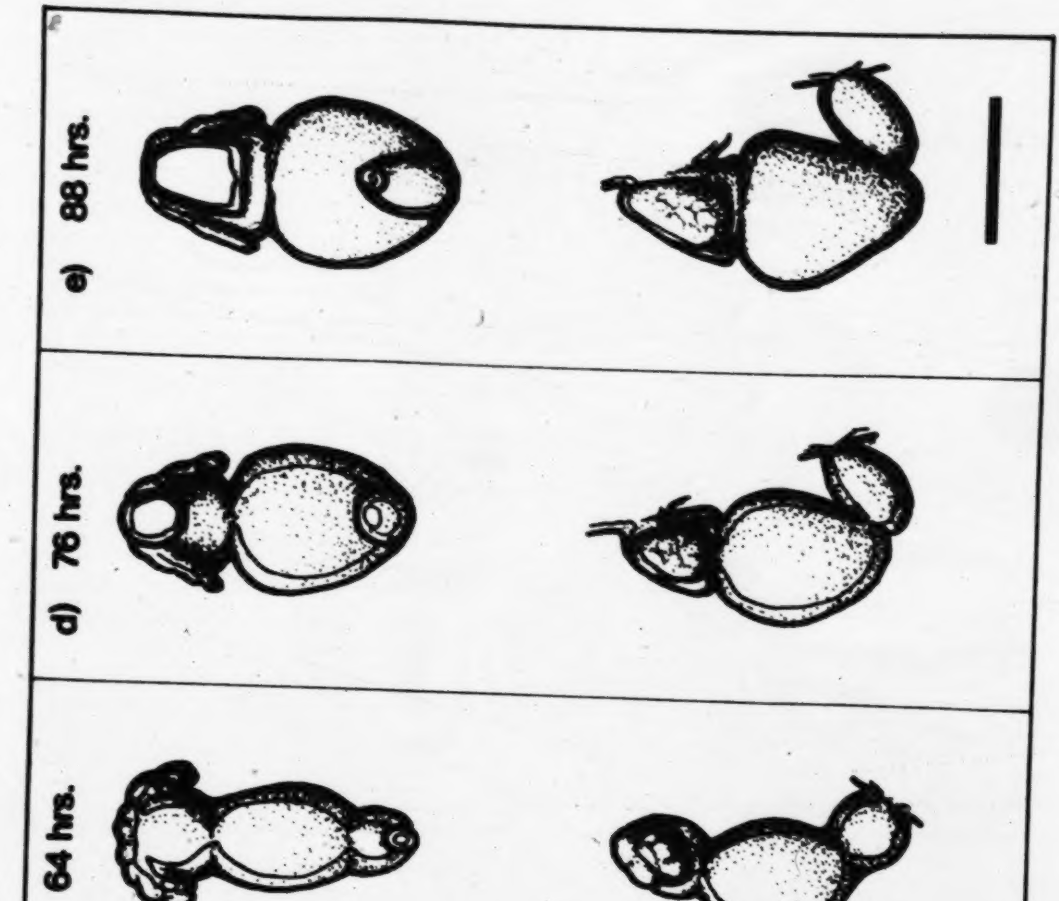
a) 40 hrs.
b) 52 hrs.
c) 64 hrs.
d) 76 hrs.
e) 88 hrs.
Ventral
Lateral

⑧

Figure 9. A time-line showing the sequence and duration of morphogenetic events observed in the development of the larval digestive tract in *S. purpuratus* embryos.

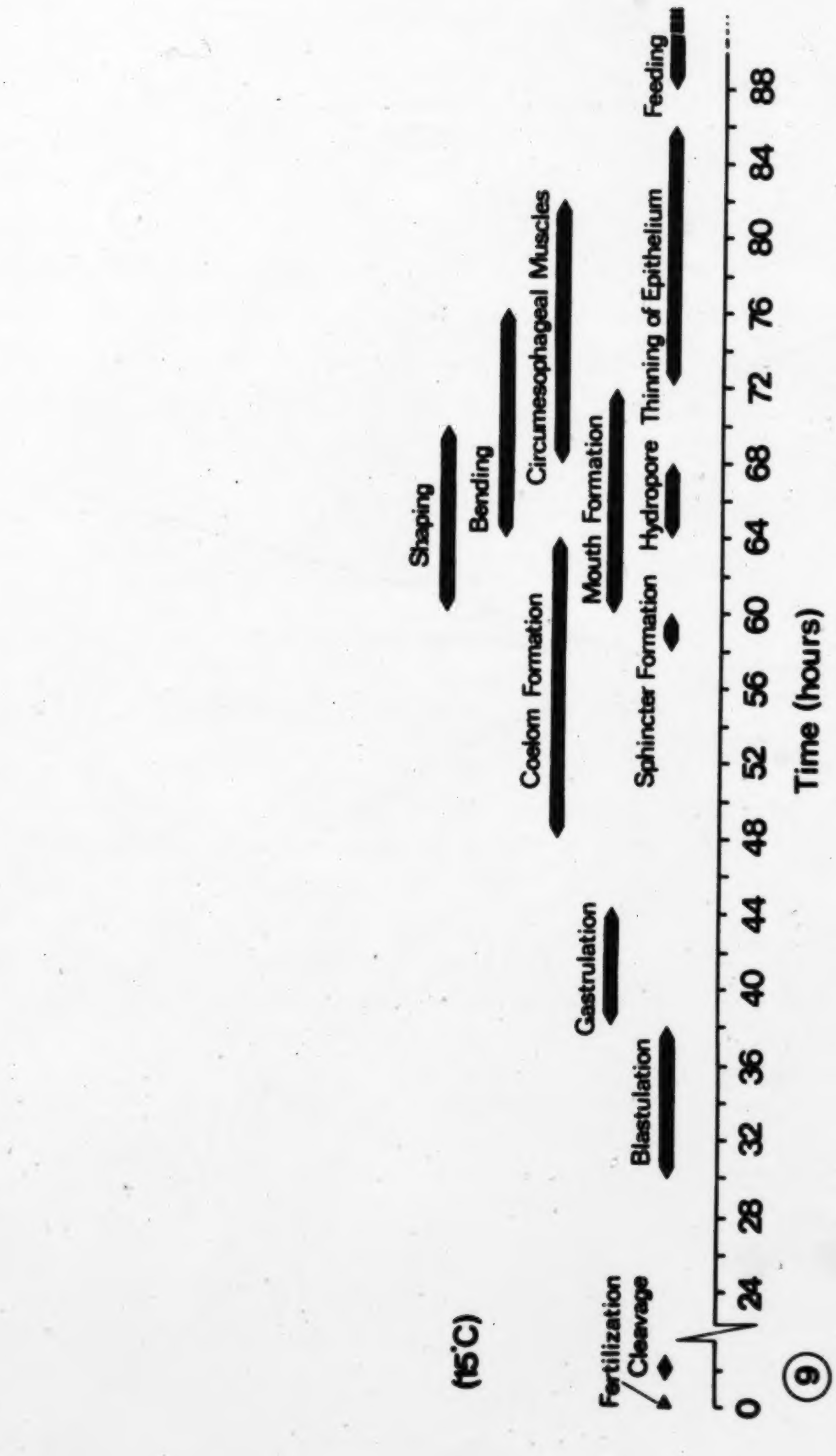

⑨

(15°C)
Fertilization
Cleavage
Blastulation
Gastrulation
Coelom Formation
Sphincter Formation
Mouth Formation
Shaping
Hydropore
Bending
Circumesophageal Muscles
Thinning of Epithelium
Feeding
0
24
28
32
36
40
44
48
52
56
60
64
68
72
76
80
84
88
Time (hours)

Figure 10. (a, b, c, d, e). A series of micrographs demonstrating the constriction of the archenteron that results in the formation of the cardiac sphincter in *S. purpuratus* embryos. Bar = 10 μm.

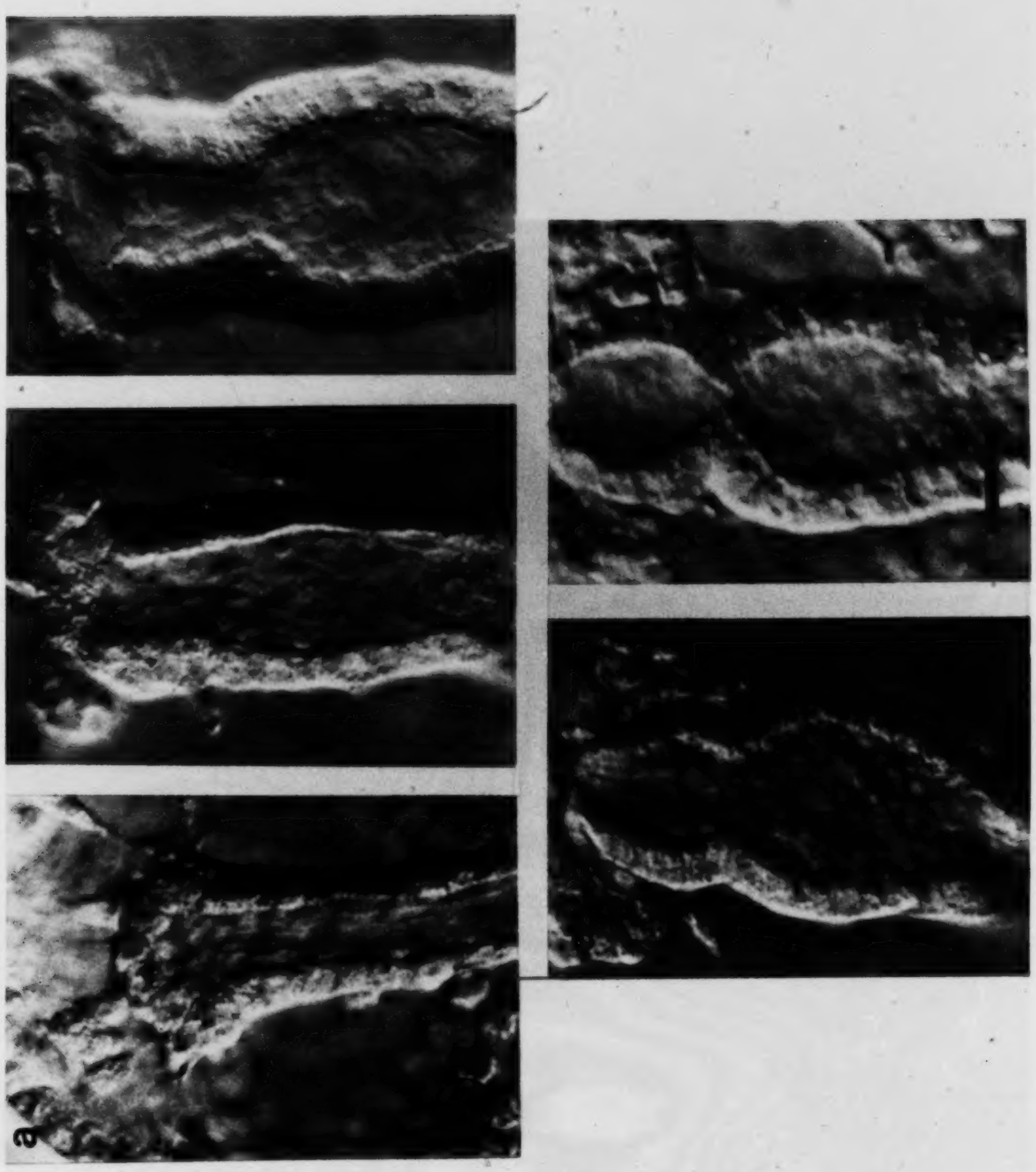
a

Figure 11. a) Transmission electron microscopy (TEM) of cells in the presumptive sphincter region of the archenteron of a *S. purpuratus* embryo prior to the formation of the constriction. b) Cells of the presumptive sphincter region of a *S. purpuratus* embryo fixed during the constriction of the archenteron. c) Presumptive sphincter cells of a *S. purpuratus* embryo fixed after the constriction of the archenteron had been completed. lu - lumen. Bars = 1 μm.

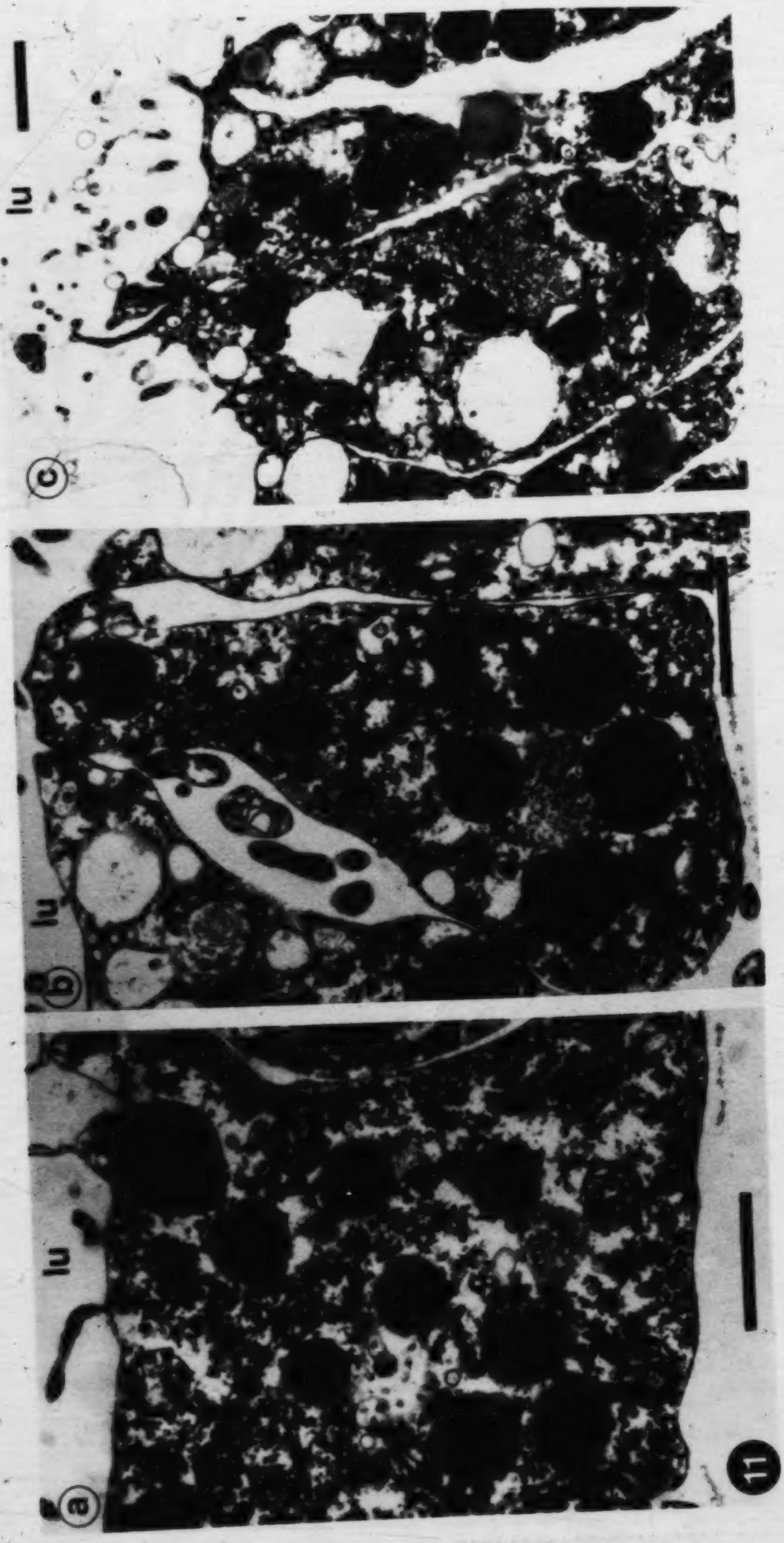
11
a
lu
b
lu
c
lu

Figure 12. TEM of a section cut obliquely through the forming cardiac sphincter of a 60 hour *S. purpuratus* embryo. The arrows indicate a juxtaluminal electron-dense region. lu - lumen of the archenteron. Bar = 1 μm.

Figure 13. TEM of a cell sectioned parallel to the long axis of the archenteron of a *S. purpuratus* embryo that was fixed during the formation of the sphincter. The electron micrograph details the apical region of a sphincter-forming cell and the arrow indicates an electron-dense region subjacent to the lumen of the archenteron (lu). Bar = 1 μm.

Figure 14. The luminal region of a sphincter-forming cell sectioned at right angles to the long axis of the archenteron. The arrows indicate the filamentous nature of the electron-dense region. Bar = 0.25 μm.

Figure 15. The luminal region of a sphincter-forming cell cut in cross-section. The arrows point out filamentous material associated with the apical plasmalemma. Bar = 0.5 μm.

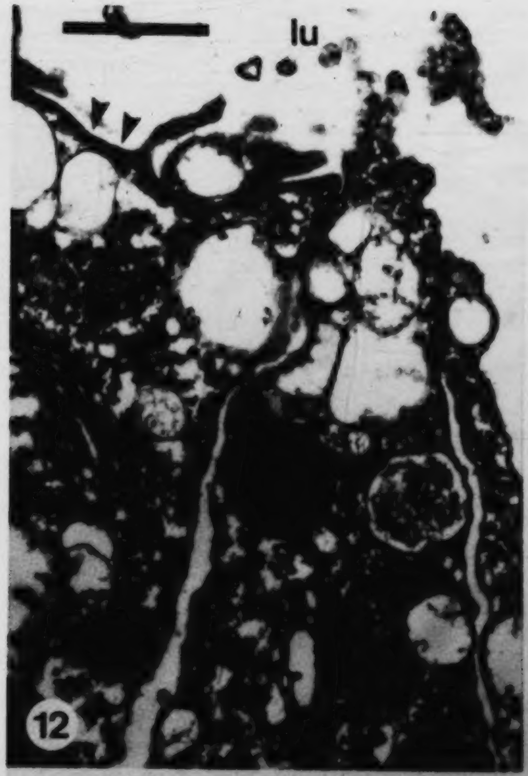
⑫

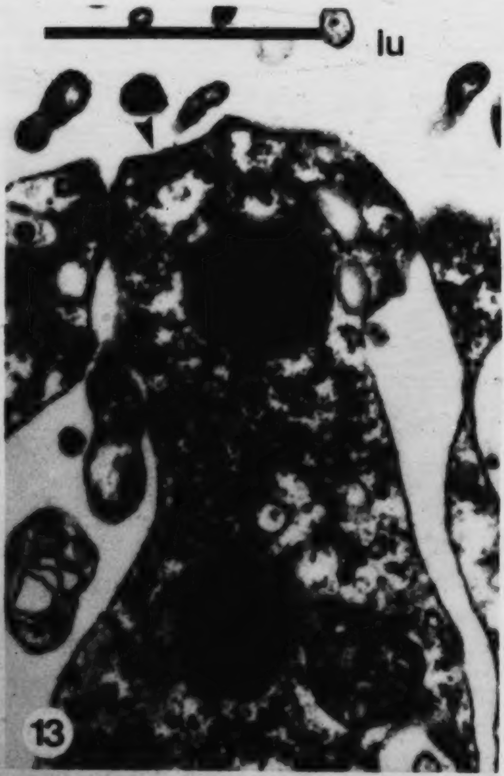
⑬

⑭

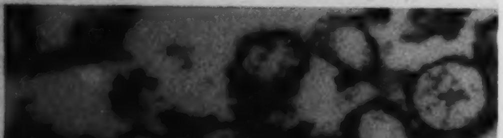
⑮

Figure 16. *S. purpuratus* embryos between 59 and 60 hours of development used in an experiment to test the effects of cytochalasin B (CCB) on sphincter formation: a) a 58 hour embryo prior to formation of the sphincter, representative of embryos at the beginning of the experiment; b) an embryo after 2 hours of treatment with 5 μg/ml CCB, the arrows indicating the region where the sphincter was to have formed; c) a control embryo after 2 hours in Millipore filtered sea-water (MFSW); and d) an embryo that was treated with 5 μg/ml CCB for 2 hours and then put into MFSW for 2 hours, the arrows indicating a slight constriction in the archenteron. Bar = 20 μm.

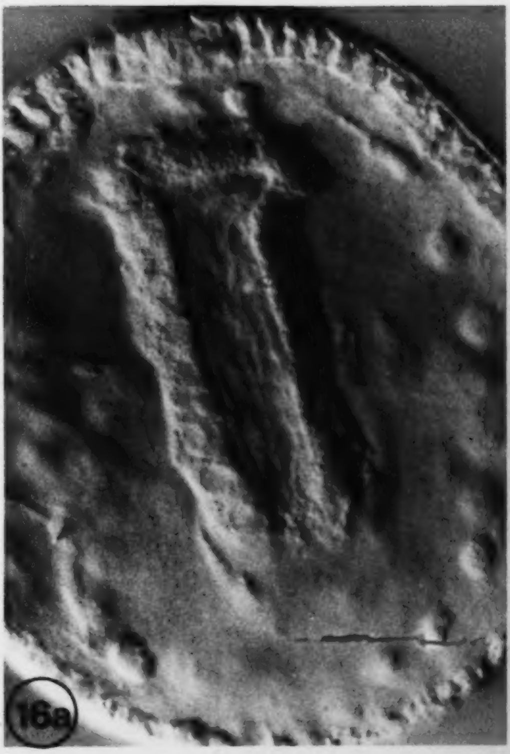

16a

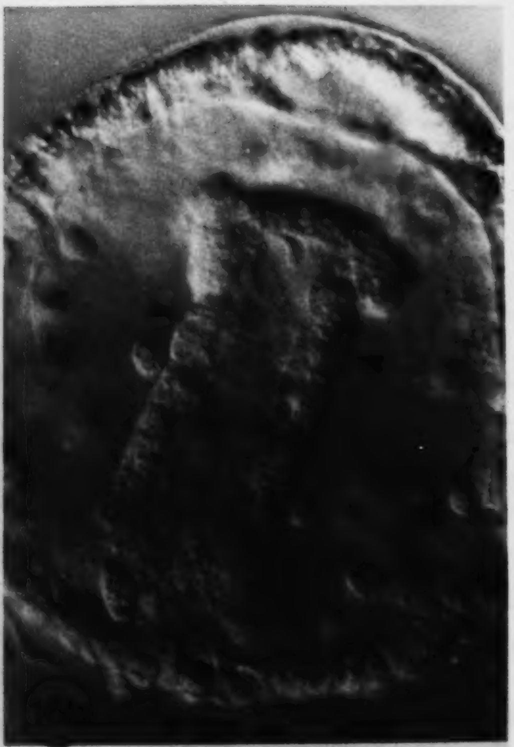

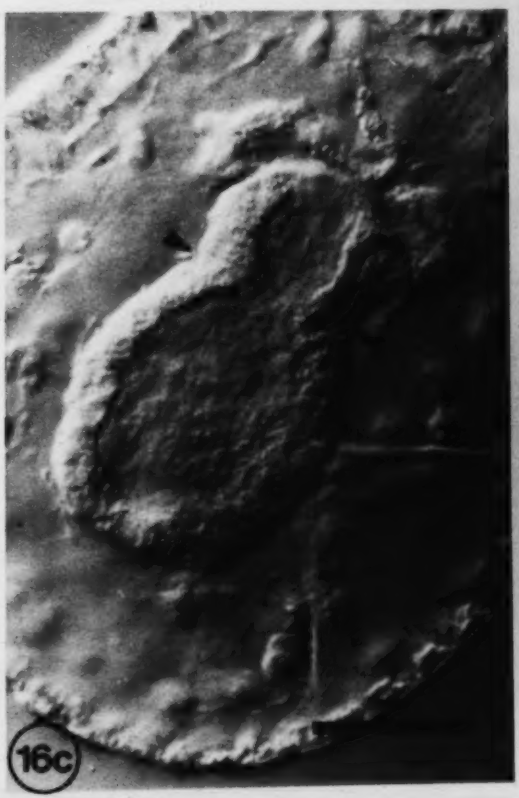

16c

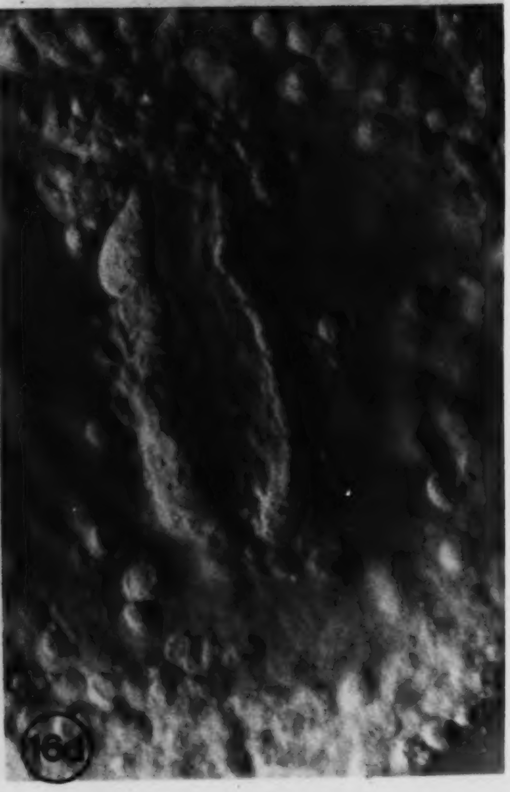

16d

Figure 17. *S. purpuratus* embryos that were used in an experiment to test the effects of CCB on sphincter formation: a) a 59 hour embryo in the midst of sphincter formation representing embryos at the beginning of the experiment; b) an embryo that was treated with 5 µg/ml CCB for 1 hour. Note that the constriction that was apparent at the beginning of the experiment has been relaxed. Bar = 20 µm.

Figure 18. This experiment tested the effects of CCB on the constriction in the archenteron after it had formed: a) an embryo 62 hours after fertilization with a fully formed sphincter constriction, typical of embryos at the beginning of the experiment; b) an embryo that had been treated with 5 µg/ml CCB for 4 hours. Note that the constriction in the archenteron remains. Bar = 20 µm.

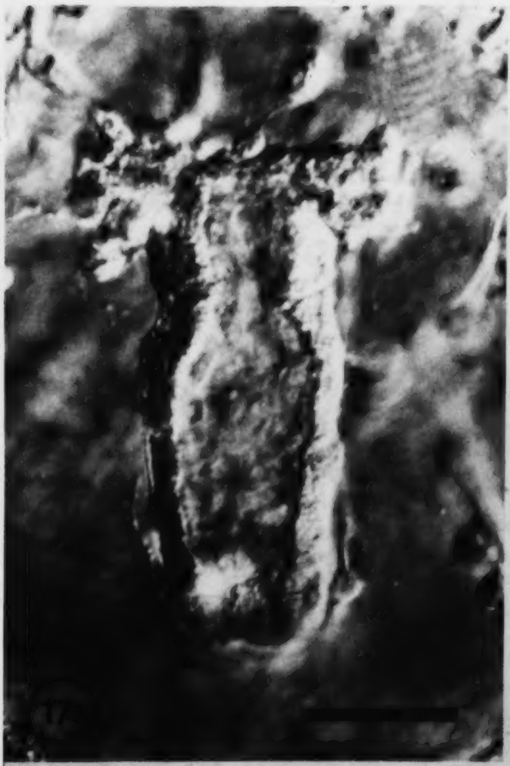

17

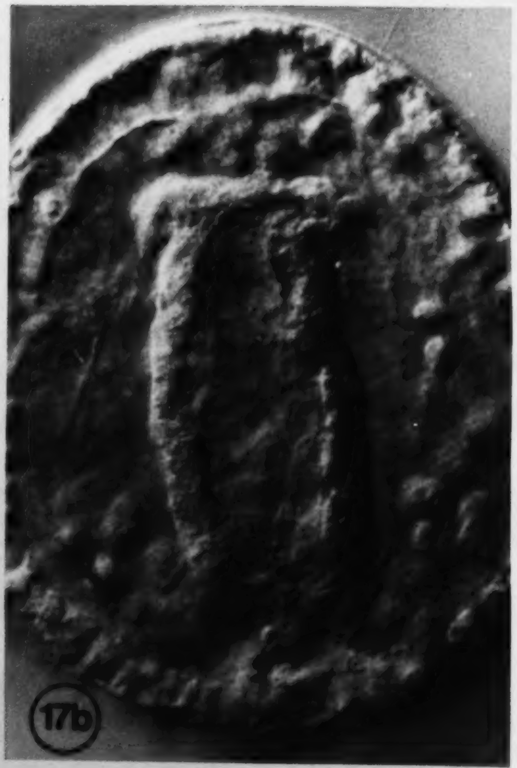

17b

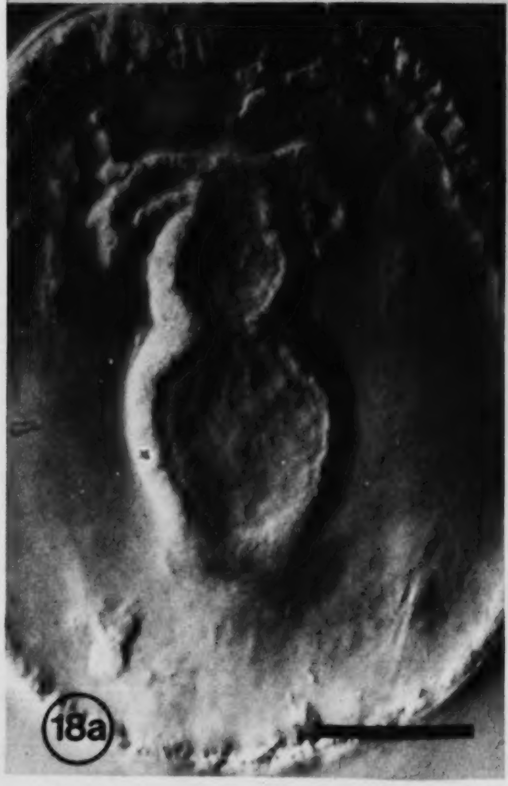

18a

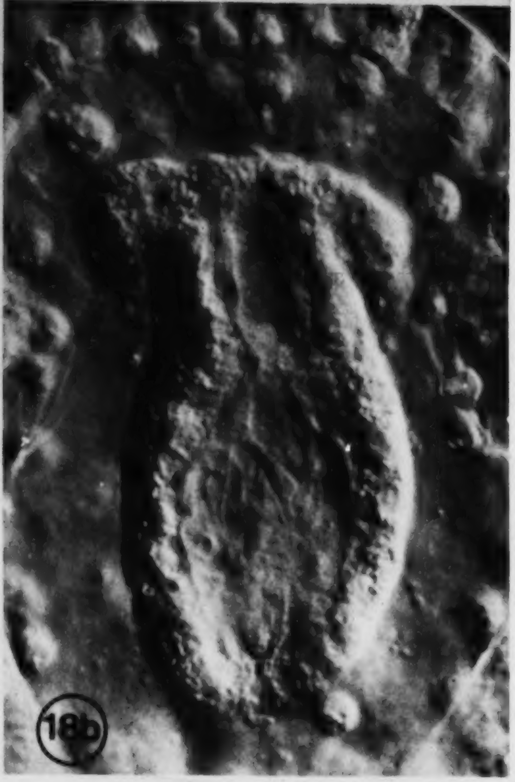

18b

Figure 19. A graphical summary of the experiments performed to examine the effects of CCB on sphincter formation in *S. purpuratus* embryos: a) treatment throughout formation of the constriction; b) treatment during formation; c) treatment after formation.

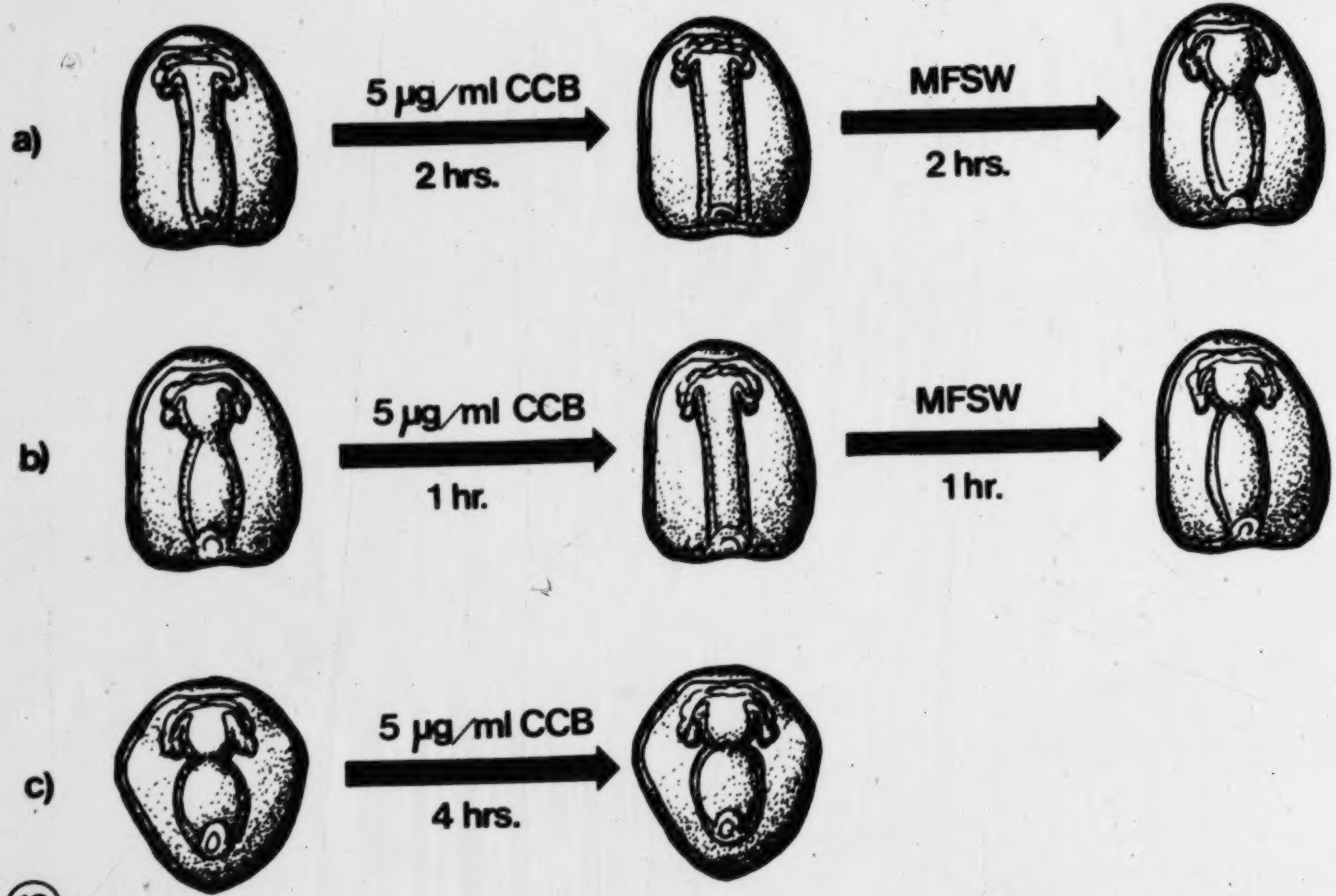
a)
5 µg/ml CCB
2 hrs.
MFSW
2 hrs.
b)
5 µg/ml CCB
1 hr.
MFSW
1 hr.
c)
5 µg/ml CCB
4 hrs.

⑲

Figure 20. *S. purpuratus* embryos between 48 and 62 hours after fertilization summarizing the morphogenesis of the coeloms: (a, b, c) the formation of the two pouches; d) expansion of the coeloms; (e, f) the coeloms extending down the sides of the esophagus. Bar = 20 μm.

Figure 21. (a, b) Nomarski DIC images of coeloms, during their formation, showing the filopodia extending from the surfaces of the cells (arrows). Bar = 10 μm.

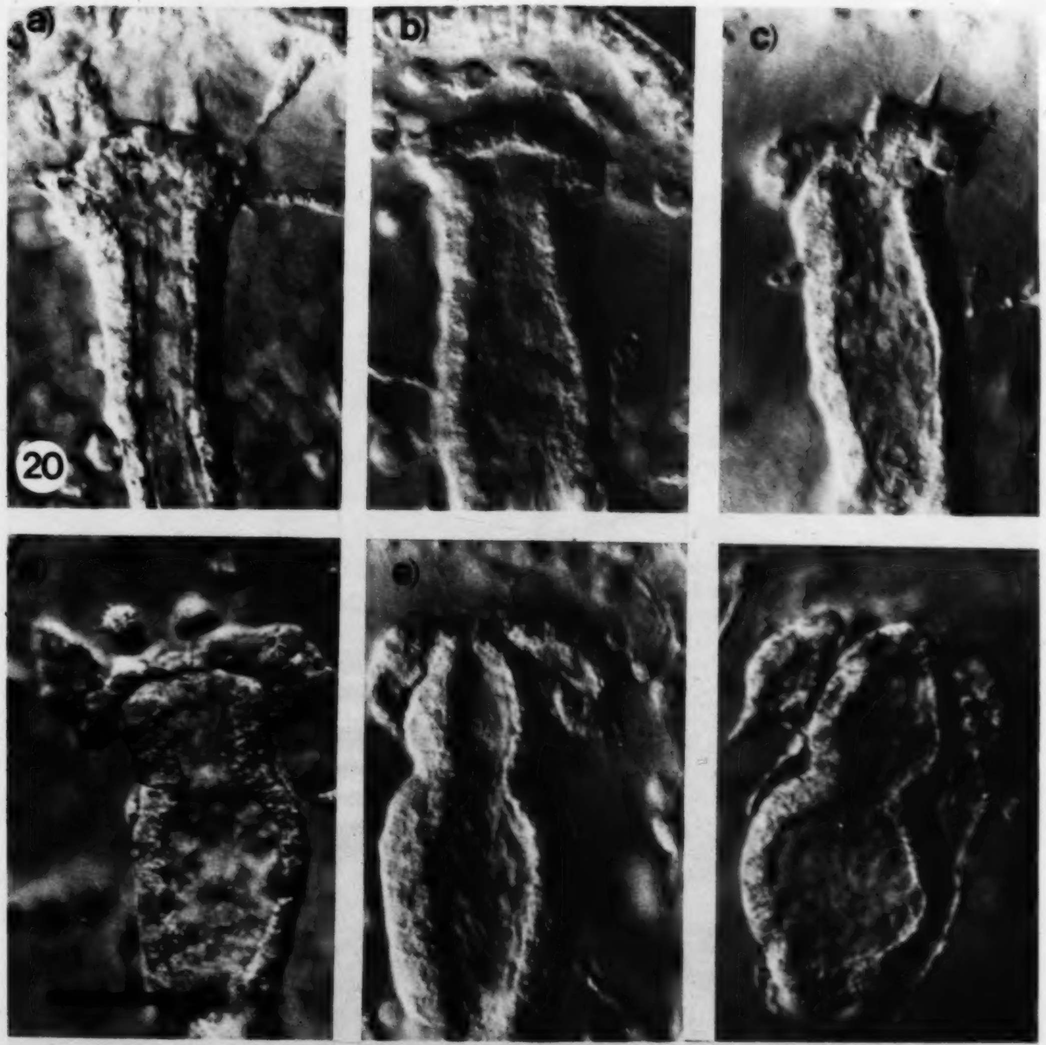

20

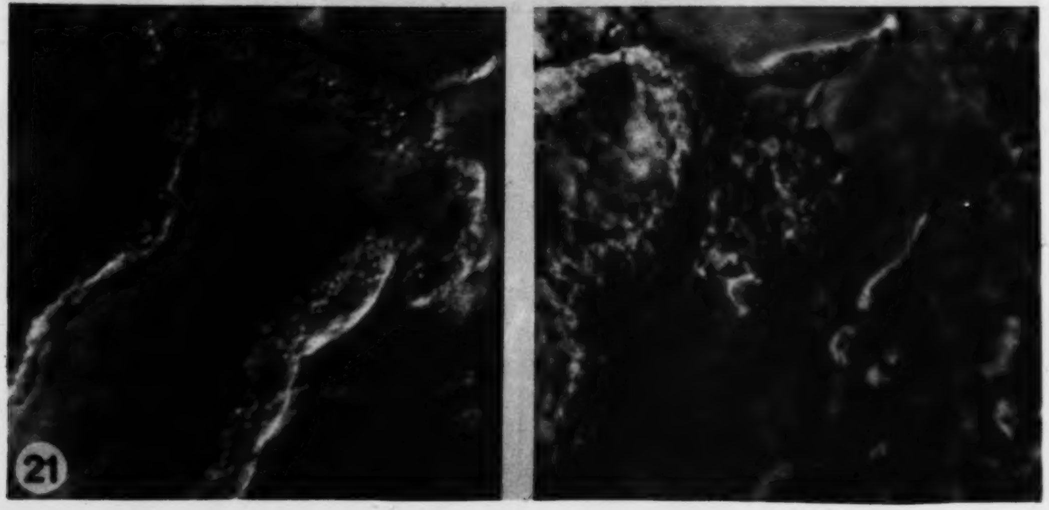

21

Figure 22. a) TEM of cells in the region of the presumptive sphincter of embryos that were treated with 5 μg/ml CCB for 2 hours prior to fixation. Bar = 1 μm. b) The juxtaluminal region of a presumptive sphincter cell of an embryo that was treated with 5 μg/ml CCB. Bar = 0.25 μm.

Figure 23. TEM of filopodia that extend from the blastocoelar surface of coelomic cells during the formation of the coeloms. Arrows indicate filamentous regions. a) Bar = 0.25 μm. b) Bar = 0.1 μm.

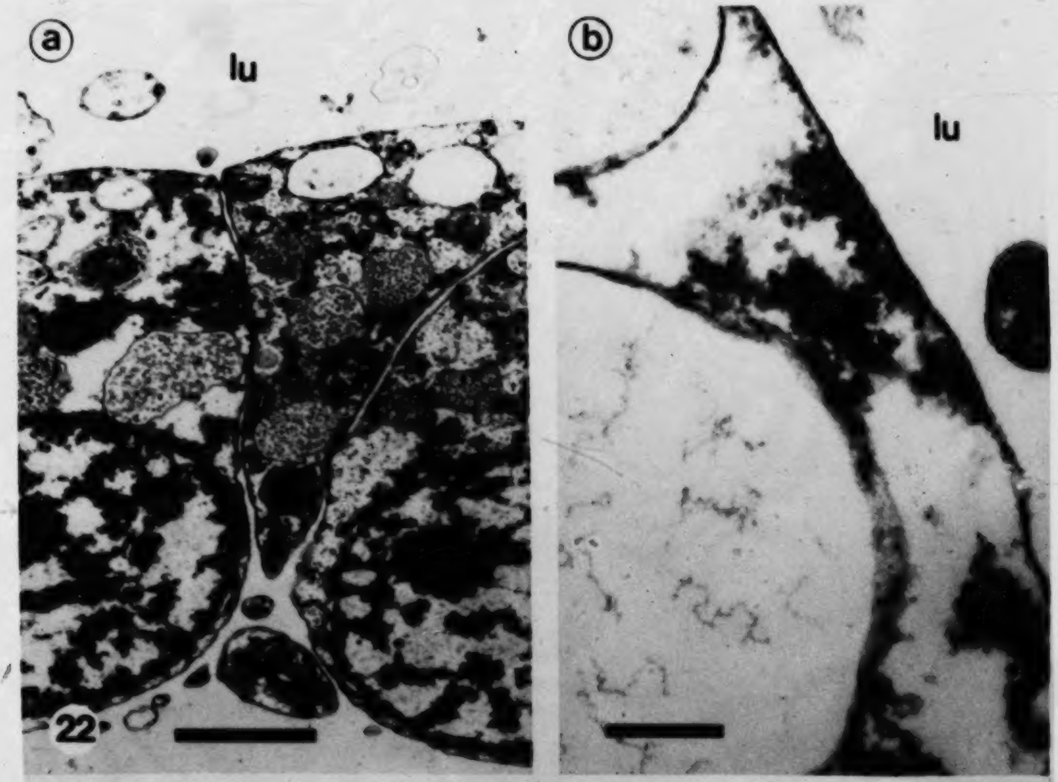
a
lu
22
b
lu

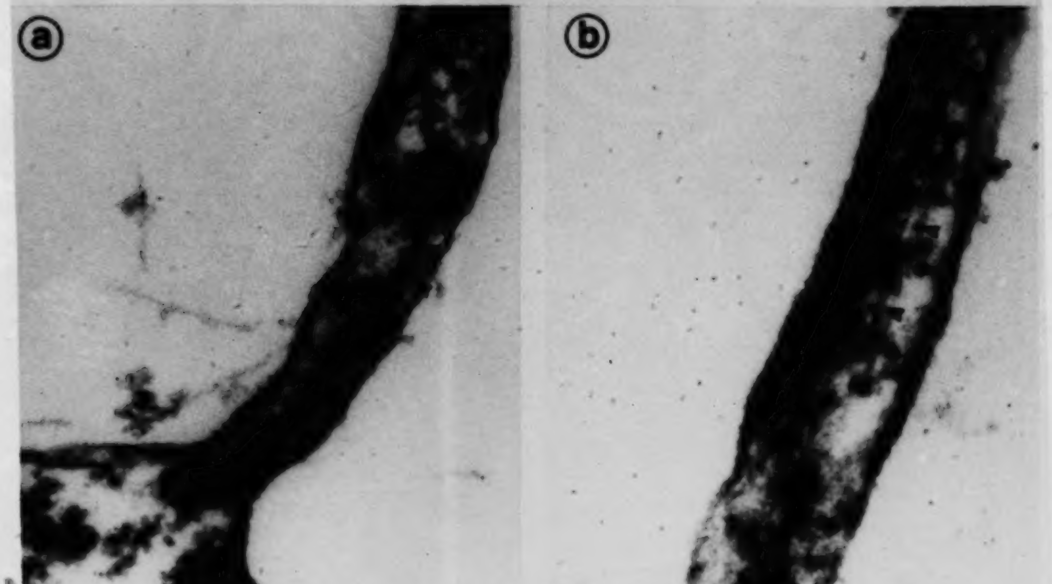
a
23
b

Figure 24. *S. purpuratus* embryos used in an experiment to examine the effects of CCB on coelom formation: a) 60 hour embryo prior to the beginning of the experiment; b) an embryo treated with 5 μg/ml CCB for 2 hours. Note that the coeloms have failed to advance down the sides of the esophagus as compared to a control embryo (c) that was treated with MFSW. Bar = 20 μm.

Figure 25. TEM of a filopodium located on the blastocoelar surface of a coelomic cell of an embryo treated for 2 hours with 5 μg/ml CCB prior to fixation. Bar = 0.1 μm.

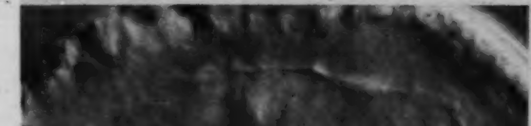

24c

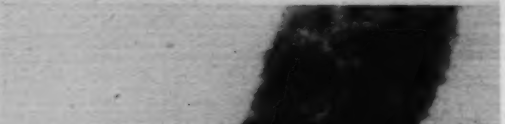

25

Figure 26. The number of cells in the developing larval digestive tract. Each vertical bar represents 1 standard deviation.

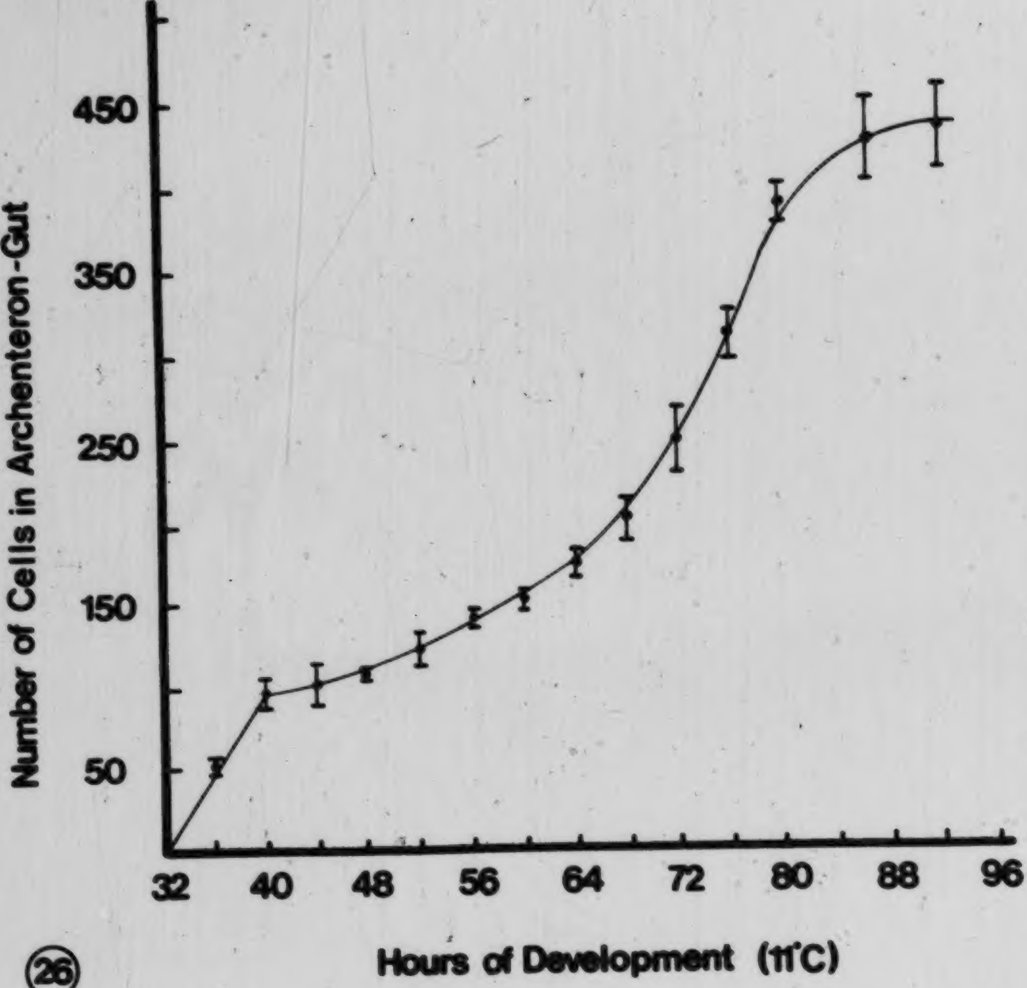
Number of Cells in Archenteron-Gut
450
350
250
150
50
32
40
48
56
64
72
80
88
96
Hours of Development (11°C)

㉖

Figure 27. These embryos summarize the experiments that tested the ability of the larval gut to form independently of cell division: a) this embryo was treated with 5×10^{-4} M colchicine for 24 hours; b) this is a control embryo the same age as the experimental; c) is representative of the form of the embryos at the beginning of the experiment. Bar = 20 µm.

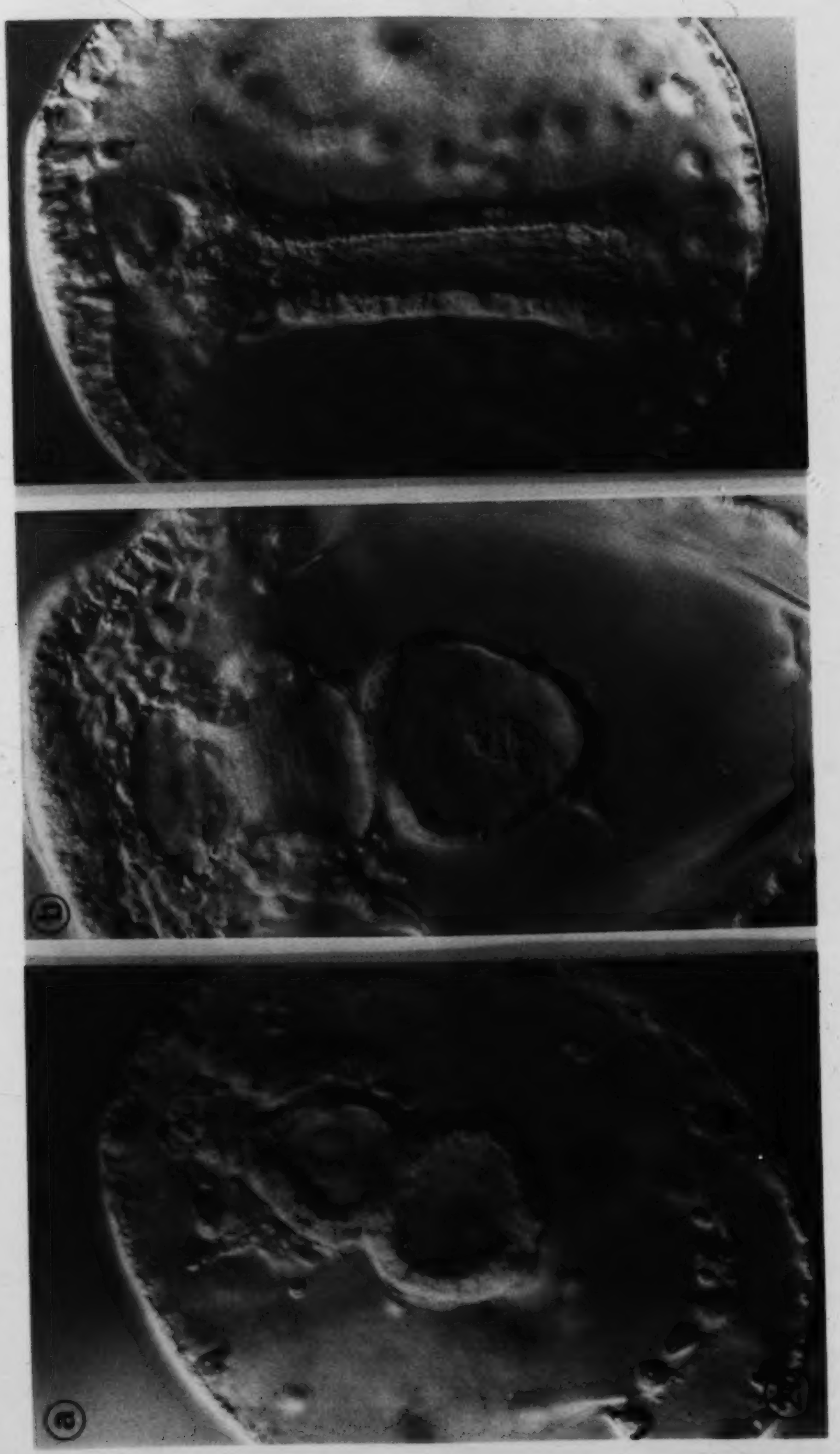
b
a

Figure 28. Autoradiographs of *S. purpuratus* embryos used to analyse patterns of H^3thymidine incorporation: a) control embryo not exposed to H^3thymidine but otherwise processed like the experimentals; the deeply staining granules in the gut wall are yolk vesicles. (b, c) Embryos exposed to H^3thymidine during the initial phases of shaping of the larval gut. The large arrows indicate regions of heavy silver deposits over nuclei, the small arrows point out regions of sparse deposition over portions of the section not including a nucleus, and the open arrows indicate nuclei that do not have heavy grain deposits associated with them. ce - coelom; es - esophagus; in - intestine; st - stomach. Bar = 20 μm.

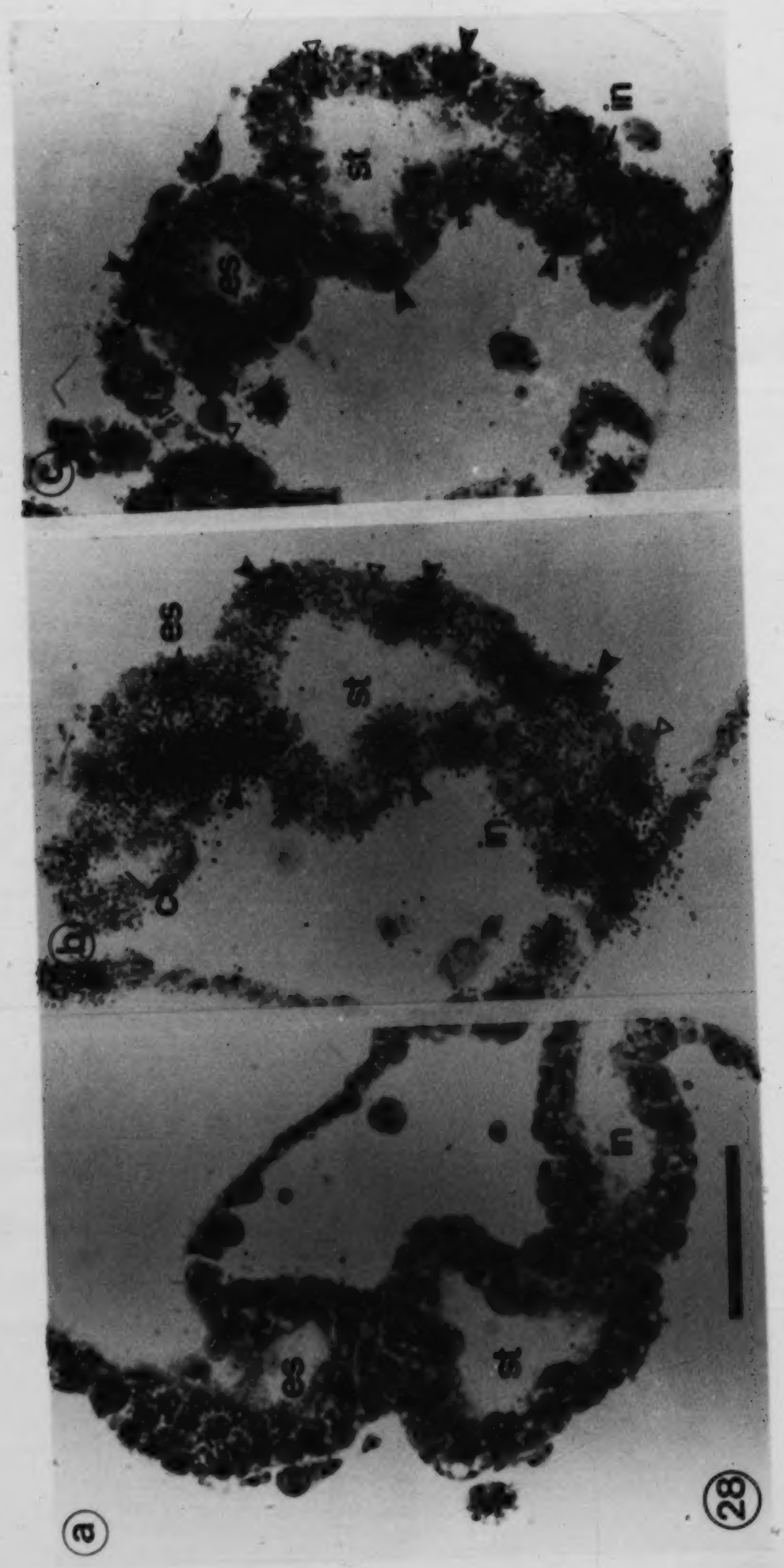

㉘

Figure 29. Thickness of stomach epithelium during development of *S. purpuratus* embryo. Each vertical bar represents the range of the measurements taken.

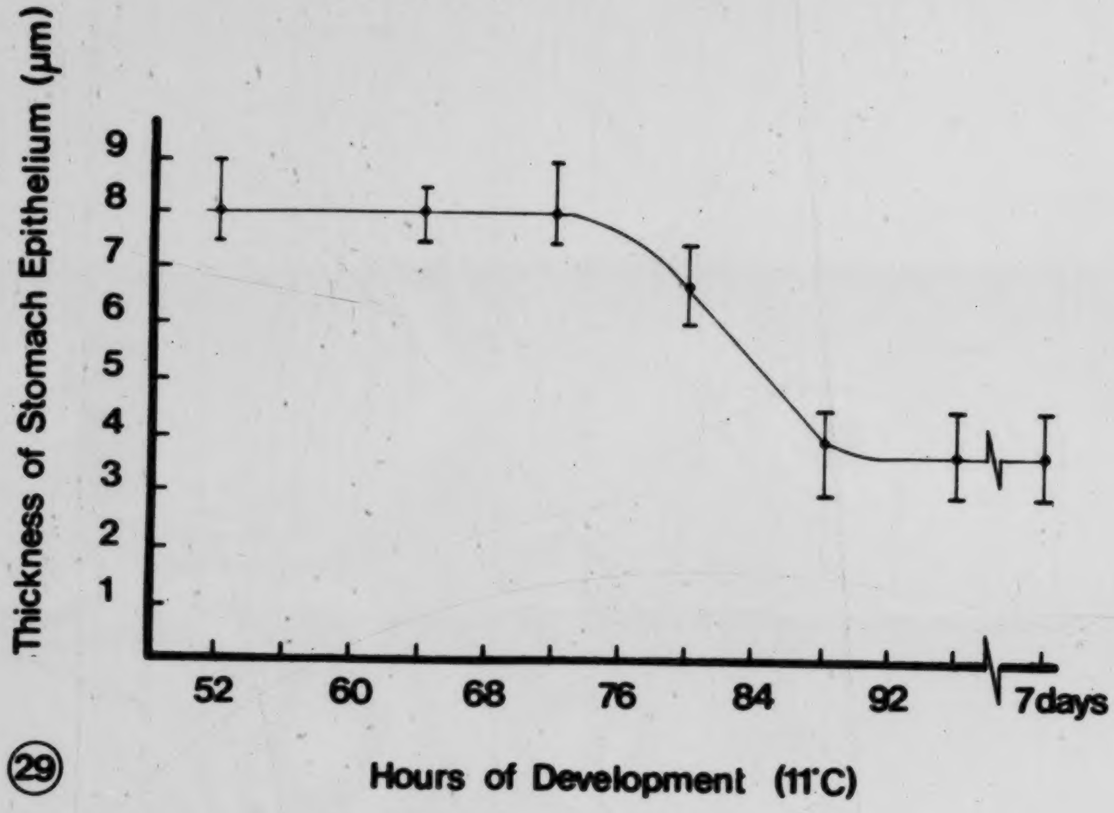
Thickness of Stomach Epithelium (µm)
9
8
7
6
5
4
3
2
1
52
60
68
76
84
92
7days
Hours of Development (11°C)

㉙

Figure 30. *S. purpuratus* embryos: a) 88 hours, and b) 56 hours after fertilization. Note the thickness of the stomach epithelium. Bar = 20 µm.

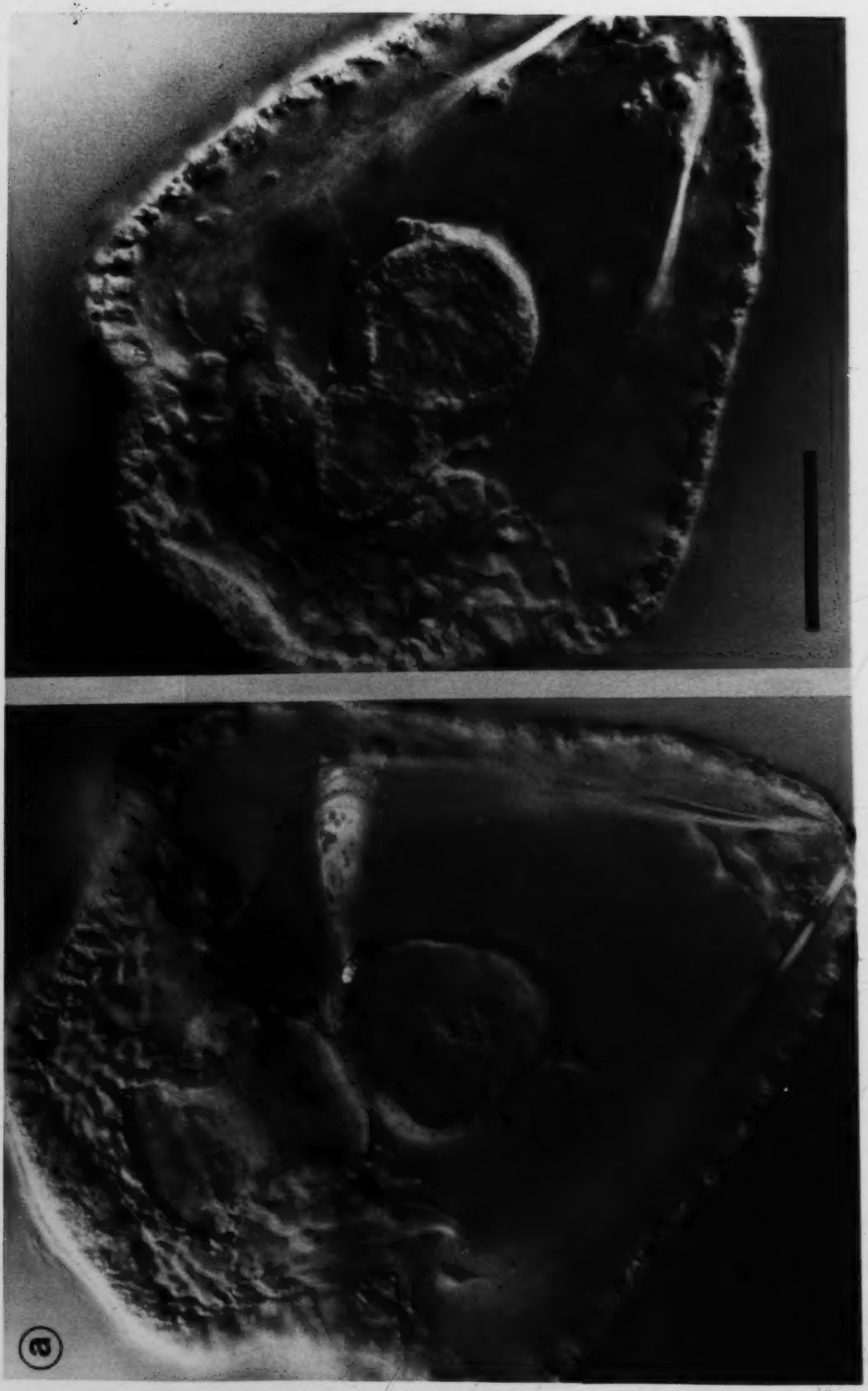
a

Figure 31. Experiments testing the effects of actinomycin D on morphogenesis of the larval digestive tract. Embryos were exposed to 25 µg/ml actinomycin D at: a) 36 hours, c) 40 hours, e) 48 hours. The extent of morphogenesis of the gut was determined at 60 hours: (b, d, f). Bar = 20 µm.

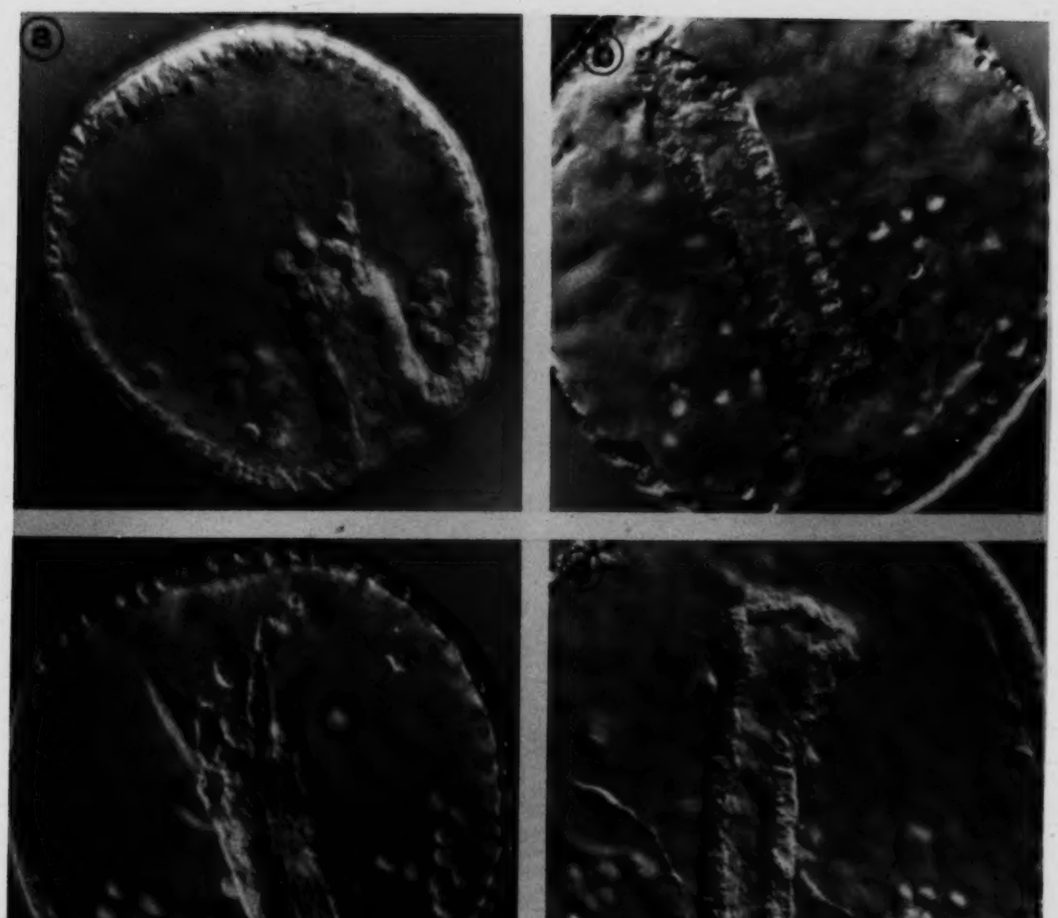

31

Figure 32. A graphical summary of the effects of actinomycin D on morphogenesis of the larval gut when treated at various times during development.

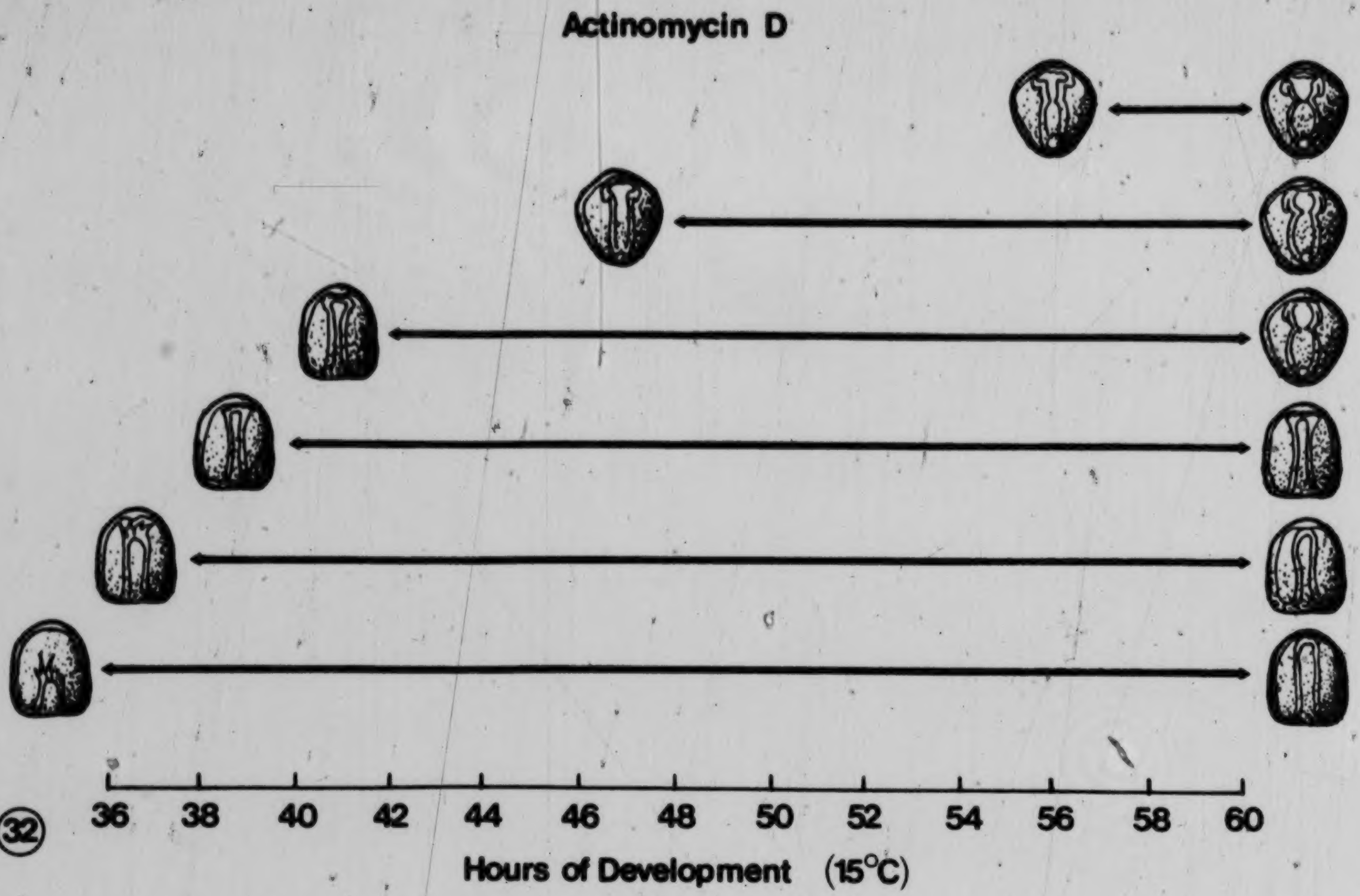

Actinomycin D

㉜

Figure 33. Autoradiographs of cross-sectioned archenterons from embryos cultured at different stages in MFSW containing H^3actinomycin D: a) 36 hour embryo treated for 1 hour with H^3actinomycin D; b) 48 hour embryo treated for 1 hour; c) 36 hour embryo treated for 4 hours; d) 48 hour embryo treated for 4 hours. The arrows indicate silver grains. Bar = 3 µm.

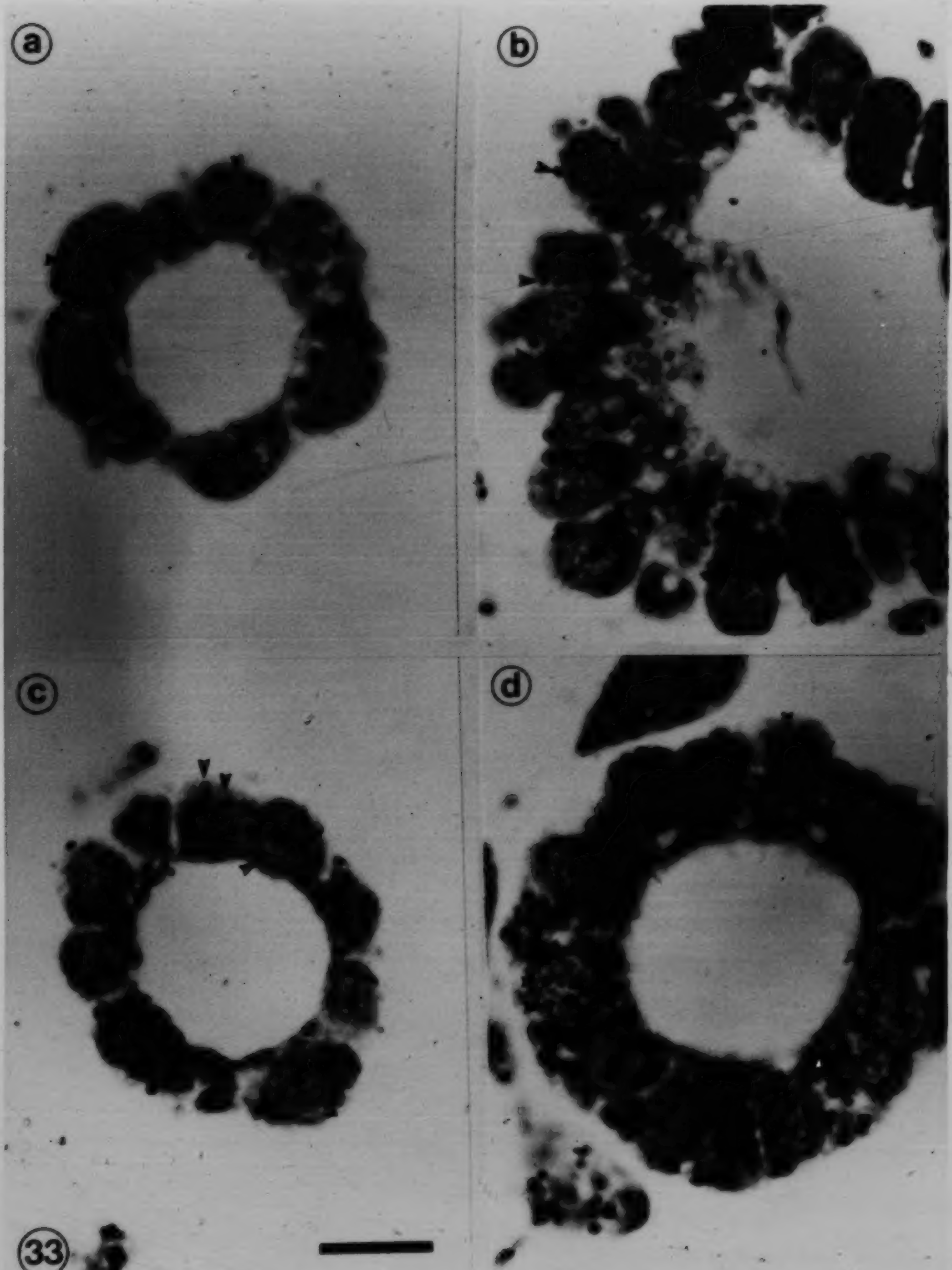
a
b
c
d
33

Figure 34. Experiments testing the effects of puromycin on morphogenesis of the larval digestive tract. Embryos were exposed to 20 µg/ml puromycin at: a) 48 hours, c) 52 hours. The extent of morphogenesis was determined at 60 hours (b, d). Bar = 20 µm.

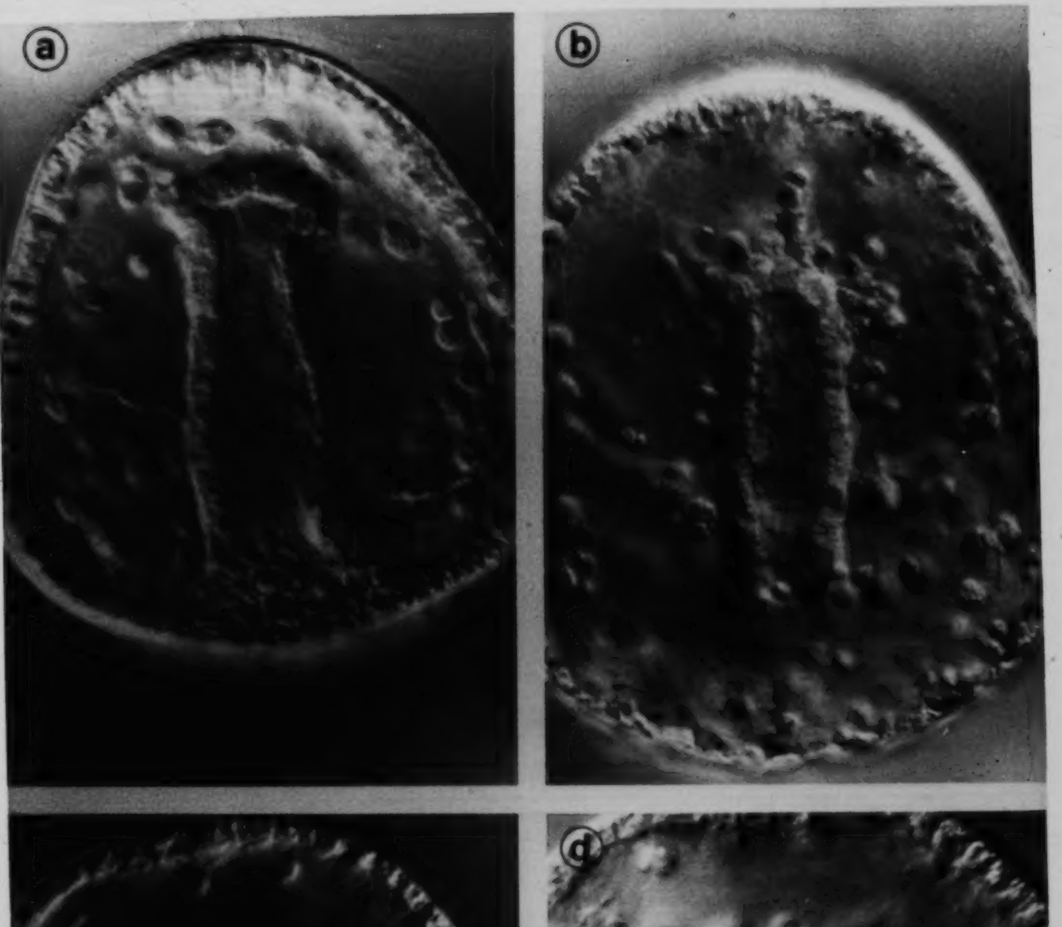
a
b
d
34

Figure 35. A graphical summary of the effects of puromycin on the morphogenesis of the larval gut when introduced at various times during development.

Puromycin

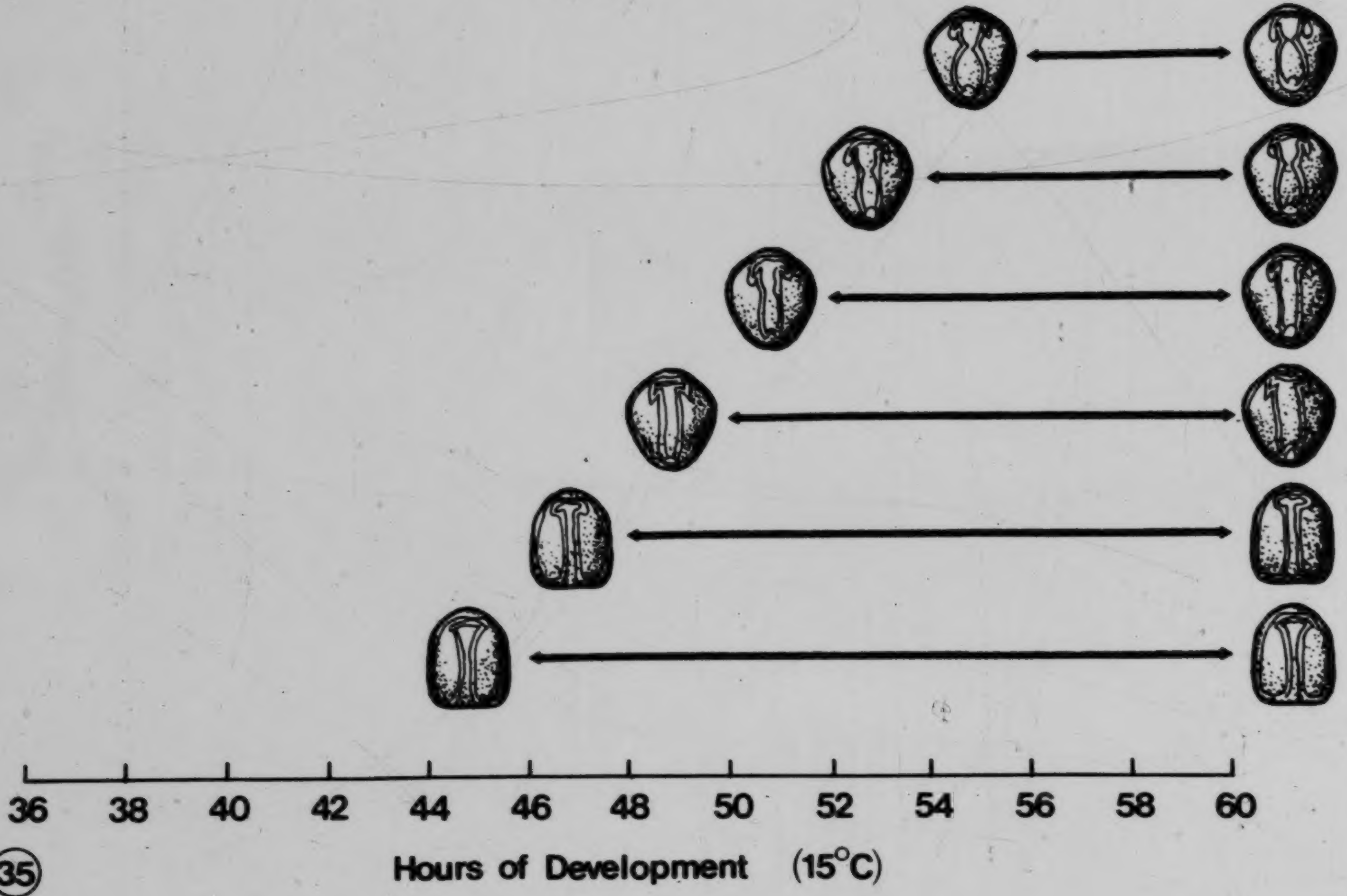
36
38
40
42
44
46
48
50
52
54
56
58
60
Hours of Development (15°C)

㉟

Figure 36. A graphical representation of the changes in cell shape that were observed during the constriction of the archenteron.

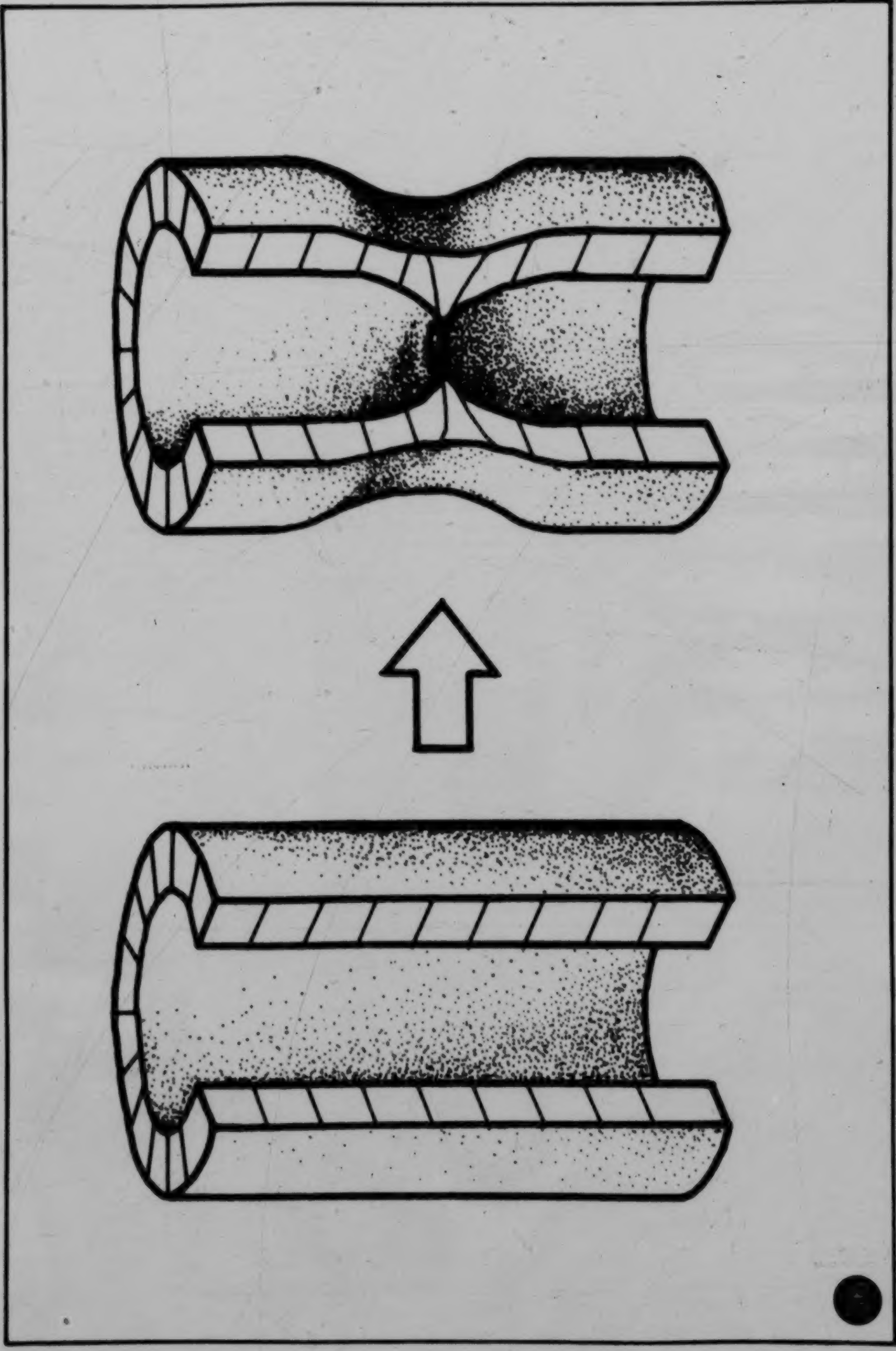

Figure 37. A graphical representation of the model hypothesized to account for the changes in shape of the cells forming sphincters in the larval gut of *S. purpuratus*. Contractile forces in the apical ends of the cells cause the cells to change in outline from square to trapezoidal.

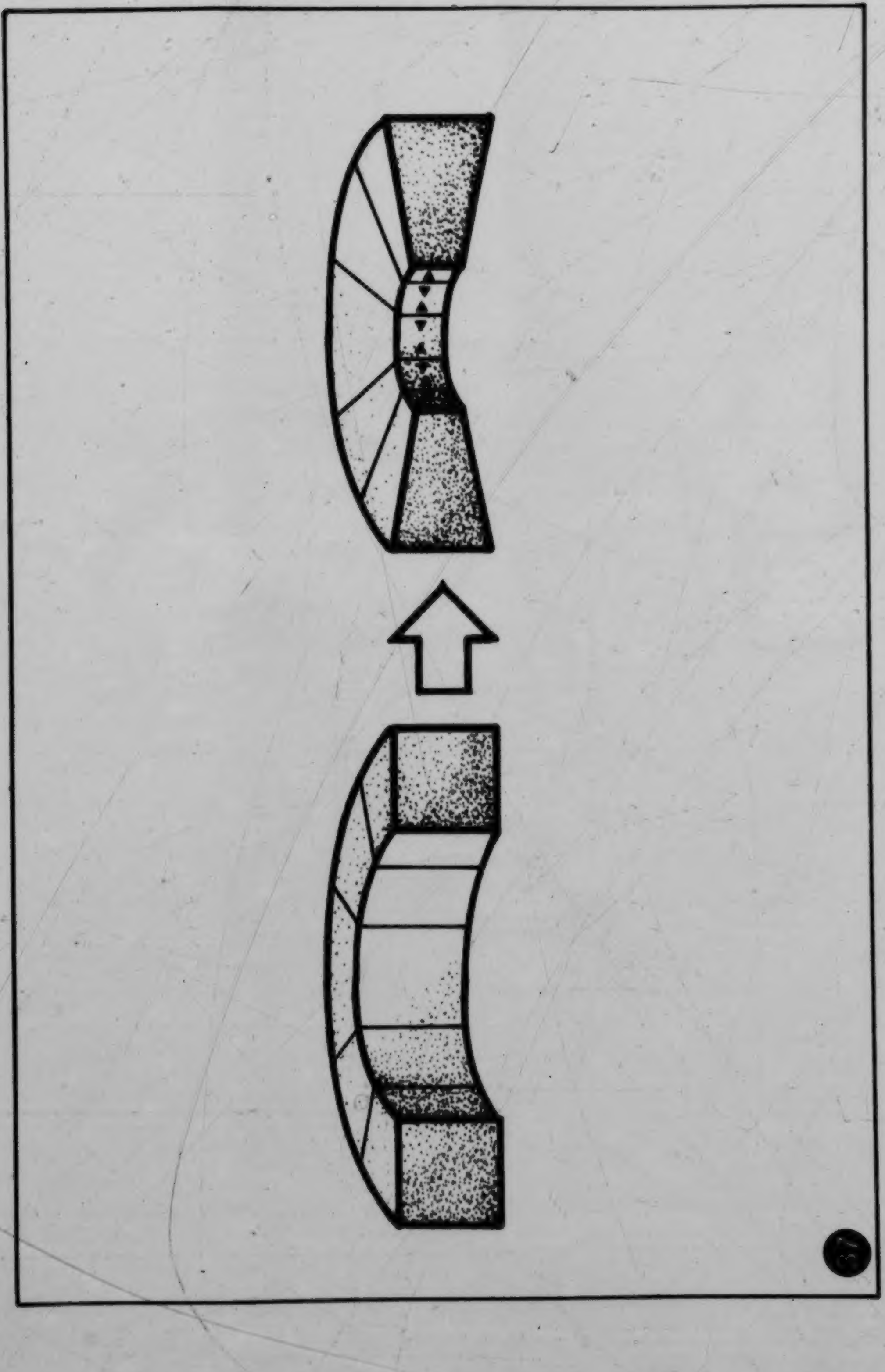

Figure 38. Light micrographs of 1 μm sections of *D. excentricus*: a) late gastrula, b) prism, c) early pluteus, d) four-armed pluteus. a - anus; ac - algal cells; ar - archenteron; bp - blastopore; cs - cardiac sphincter; ec - ectoderm; es - esophagus; in - intestine; pm - primary mesenchyme; ps - presumptive stomodeum; sm - secondary mesenchyme; so - stomodeum; st - stomach. Bar = 20 μm.

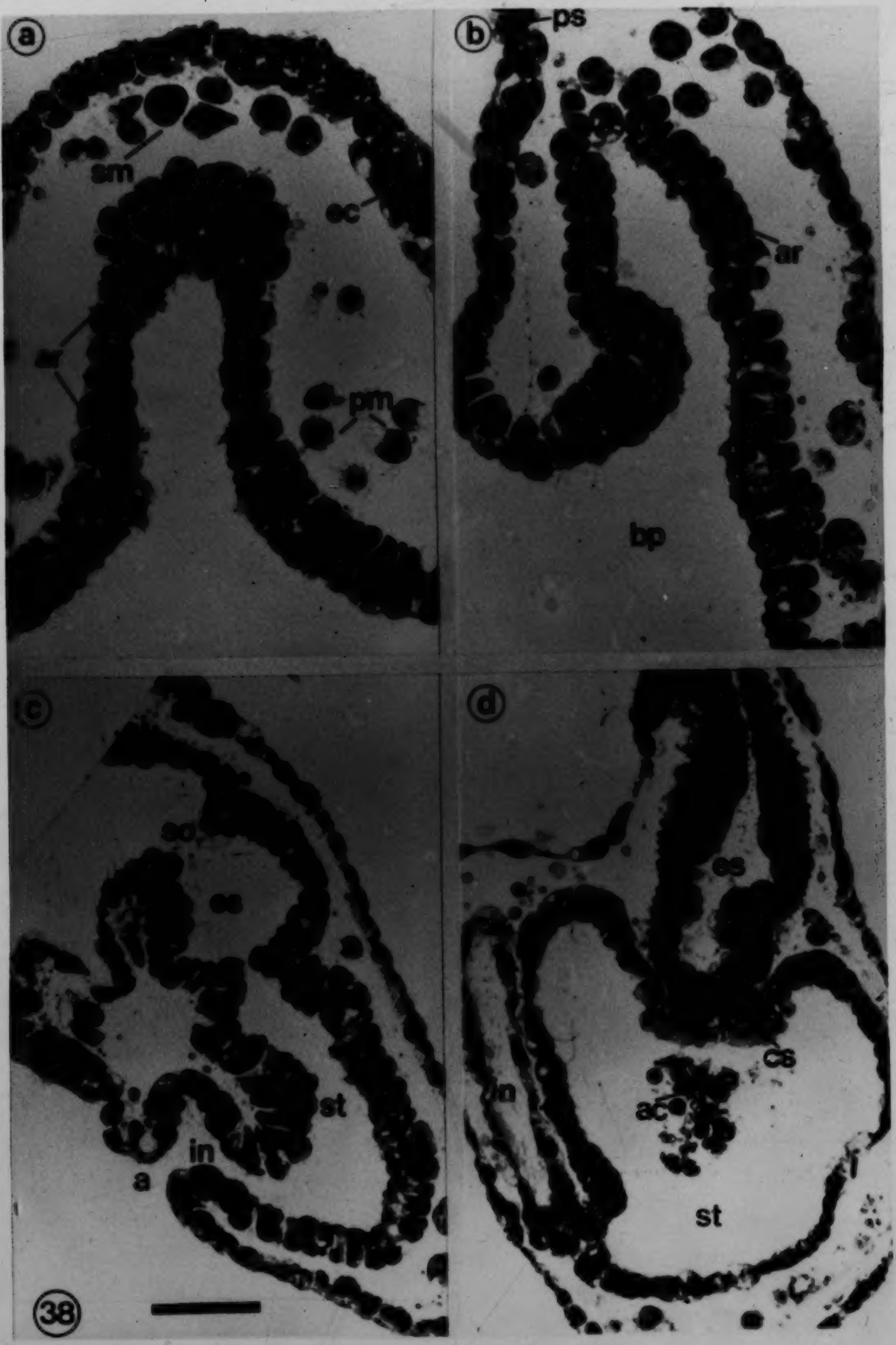

38

a
sm
ec
ar
pm
b
ps
ar
bp
c
sc
es
st
in
a
d
es
cs
ac
in
st
l

Figure 39. (a, b, c, d). TEM of archenteron cells of gastrulae of *D. excentricus*. bc - blastocoel; lu - lumen; mi - mitochondria; n - nucleus; ne - nucleolus; rer - rough endoplasmic reticulum; vo - vacuoles; yg - yolk granules; yv - yolk vesicles. Bars = 2 μm.

a
lu
b
ne
c
n
d
lu
n
39

Figure 40. (a, b, c, d). TEM of archenteron cells of gastrulae of *D. excentricus*. c - cilium; gb - Golgi body; lu - lumen; sr - striated rootlet; ve - vesicle; yg - yolk granule; yv - yolk vesicle. Bars = 0.5 μm.

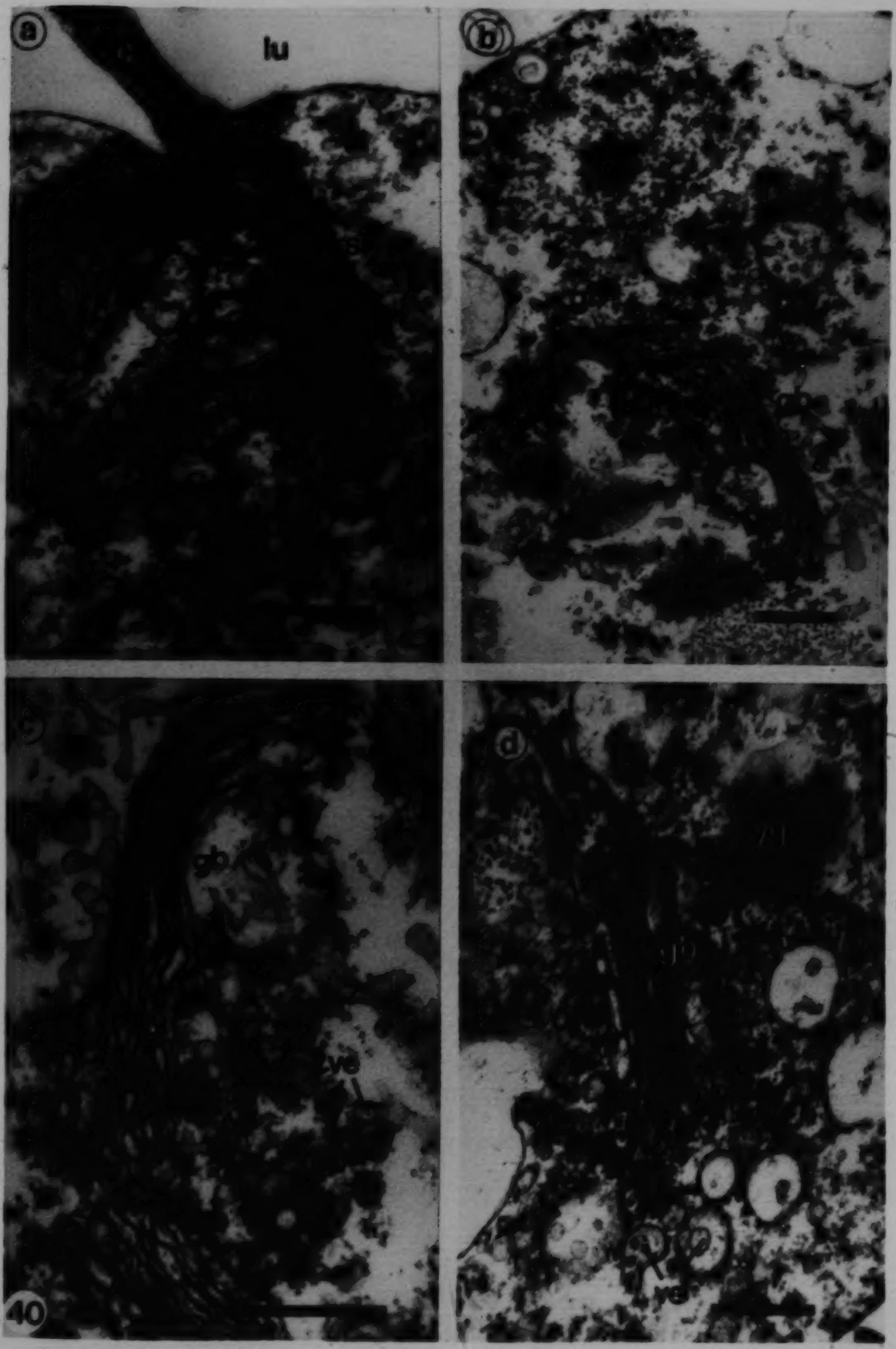
a
lu
b
c
gb
ve
d
ve
40

Figure 41. (a, b, c, d). TEM of archenteron cells of prisms of *D. excentricus*. gb - Golgi body; lu - lumen; mi - mitochondria; n - nucleus; rer - rough endoplasmic reticulum; ve - vesicle; yg - yolk granules; yv - yolk vesicles. Bars = 1 µm.

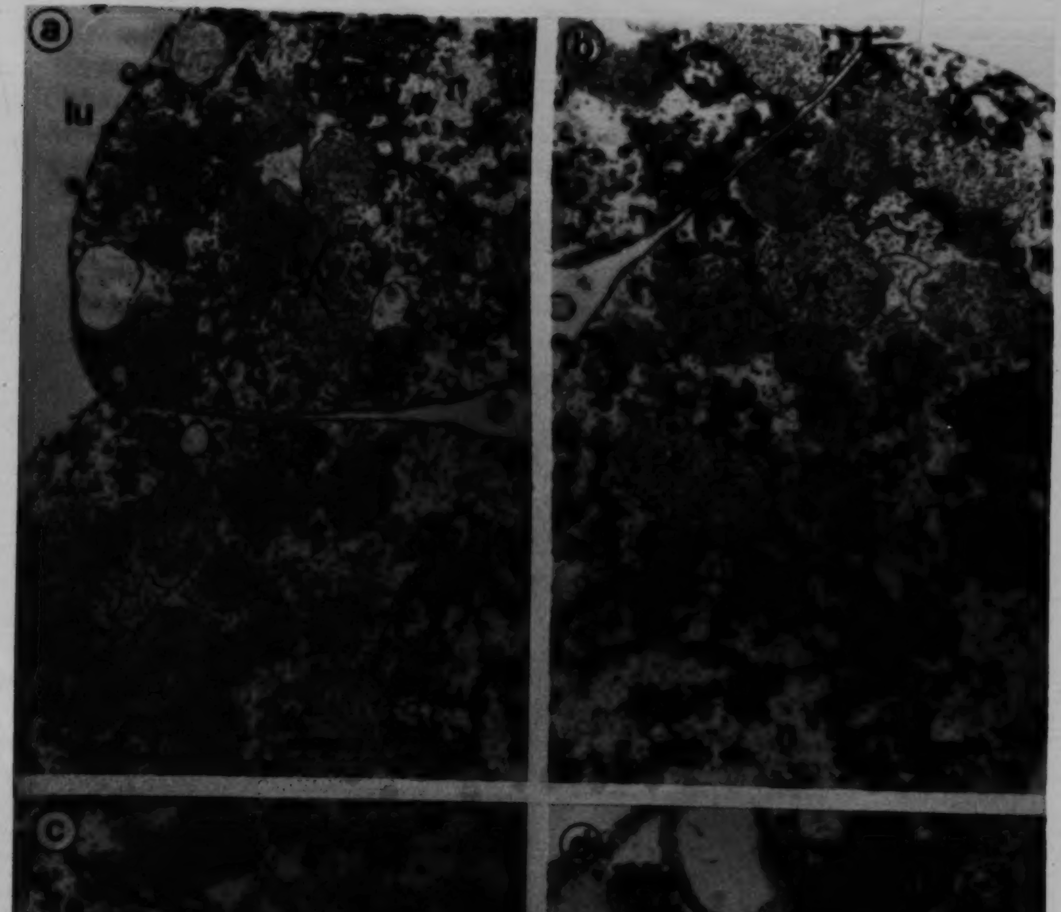
a
lu
b
c
m
d
v
gb
41

Figure 42. (a, b). TEM of the presumptive larval stomach of an early pluteus; c) cells of the presumptive esophageal epithelium. lu - lumen; mi - mitochondria; n - nucleus; ne - nucleolus; ri - ribosomes; rer - rough endoplasmic reticulum; ve - vesicles; vo - vacuoles; yv - yolk vesicles. In a) and c) bars = 2 µm; in b) bar = 1 µm.

Figure 43. (a, b). Filopodial extensions of mesenchyme cells that will form the esophageal muscles. Arrows indicate filamentous regions. Bars = 0.25 µm.

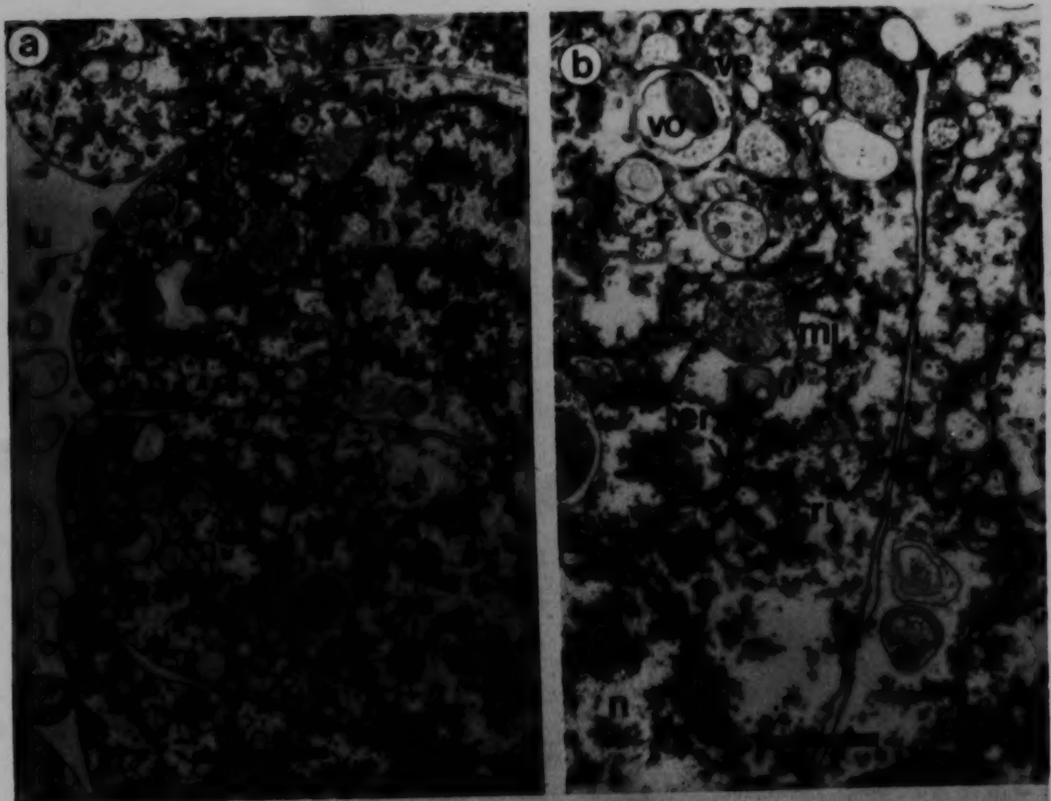
a
b
ve
vo
mi
er
r
n

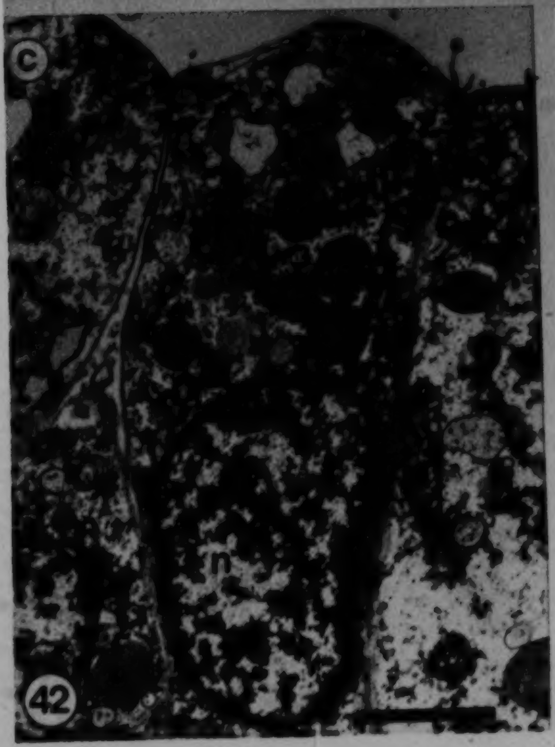
c
n
42

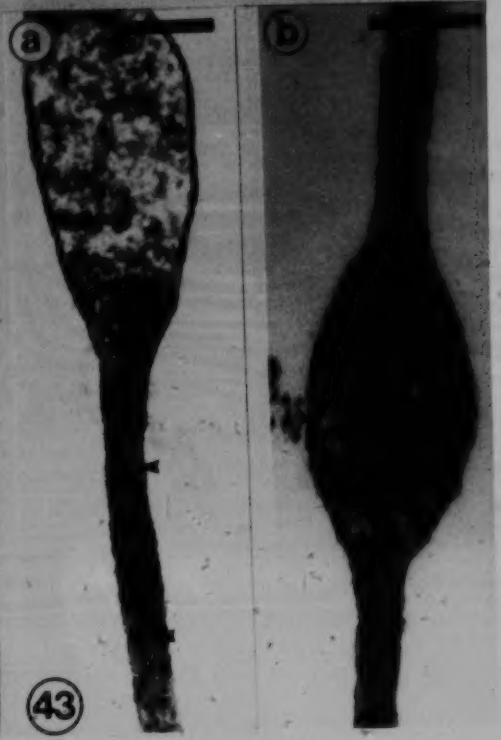
a
b
43

Figure 44. (a, b, c). TEM of the esophageal epithelium of a four-armed pluteus of *D. excentricus*. c - cilium; esm - esophageal muscles; li - lipid; lu - lumen; mi - mitochondria; n - nucleus; ne - nucleolus; ser - smooth endoplasmic reticulum; sr - striated rootlet; yg - yolk granules; yv - yolk vesicles. Bar = 1 μm.

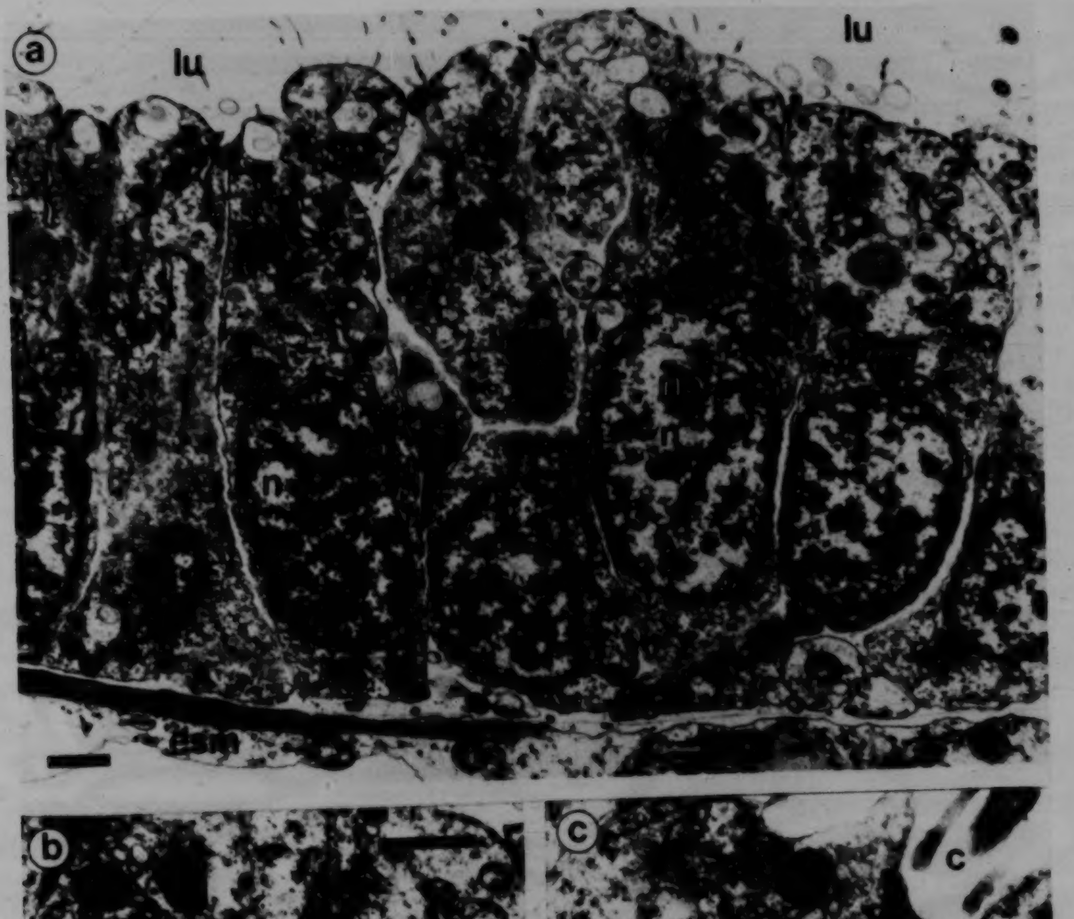
a
lu
lu
n
bsm
b
n
44
c
c
n

Figure 45. (a, b, c, d). TEM of the myoepithelium that comprises the cardiac sphincter in a four-armed pluteus of *D. excentricus*. bc - blastocoel; bl - basal lamina; lu - lumen; mf - myofibrils; mi - mitochondria; mt - microtubules; n - nucleus; ve - vesicles. In a) bar = 2 μm, and in b), c) and d), bars = 1 μm.

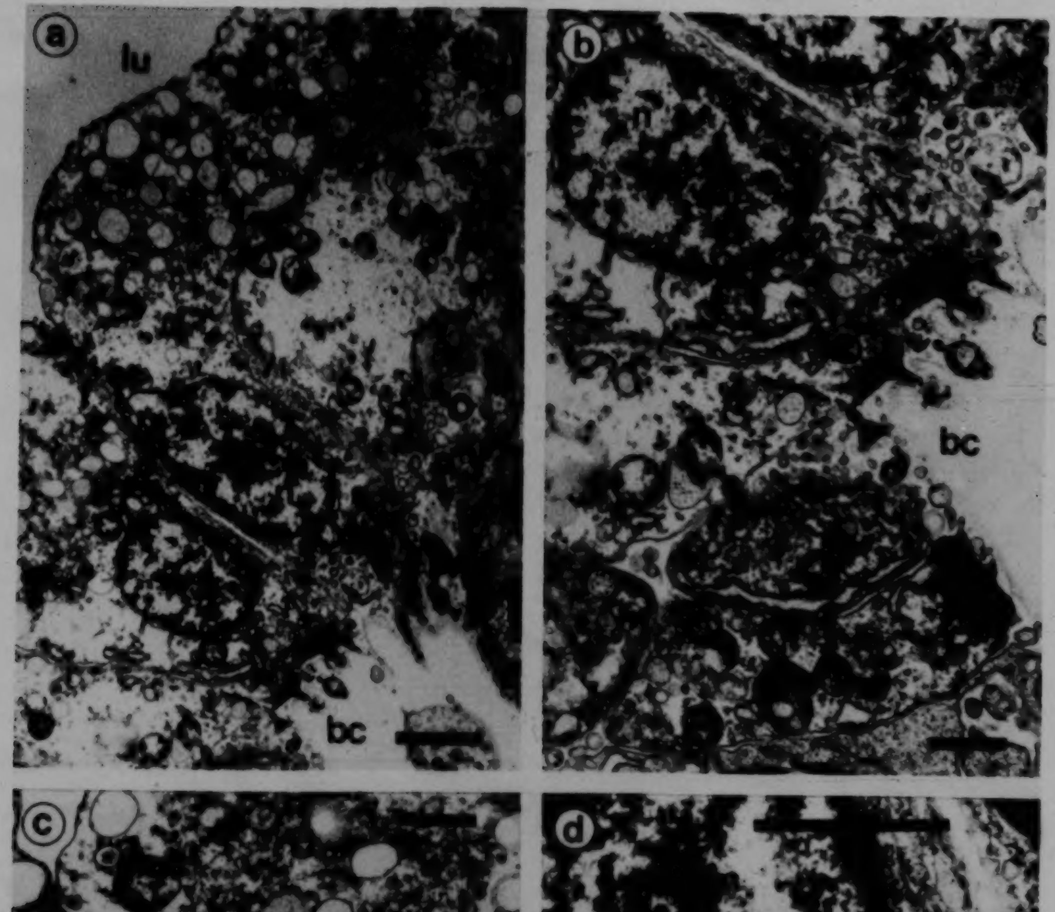
a
lu
bc
b
n
bc
c
mi
45
d
n
mi
mi
mi
bl

Figure 46. (a, b, c, d). Epithelium of the stomach of a four-armed pluteus of *D. excentricus*. bl - basal lamina; gb - Golgi body; lu - lumen; n - nucleus; ne - nucleolus; ri - ribosomes; rer - rough endoplasmic reticulum; ve_A - type A vesicles; ve_B - type B vesicles; yv - yolk vesicles. In a) and b), bars = 2 µm; in c) and d), bars = 1 µm.

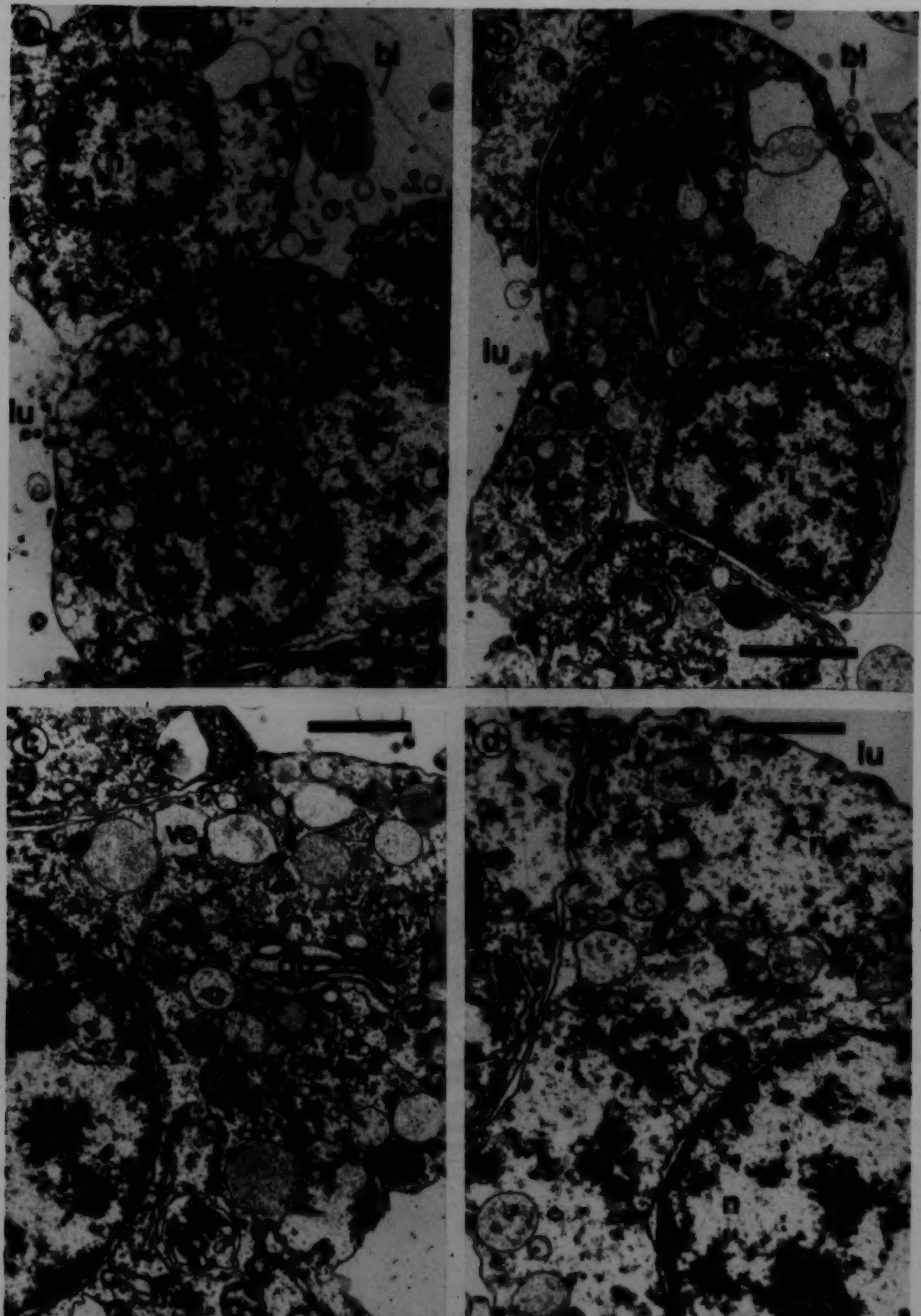
a
bl
n
lu
b
bl
lu
c
ve
46
d
lu
n

Figure 47. (a, b, c, d). Epithelium of the stomach of a four-armed pluteus of *D. excentricus*. bl - basal lamina; gb - Golgi body; mi - mitochondria; n - nucleus; ne - nucleolus; ri - ribosomes; rer - rough endoplasmic reticulum; ve_A - type A vesicles; ve_B - type B vesicles; yg - yolk granules. Bars = 1 μm.

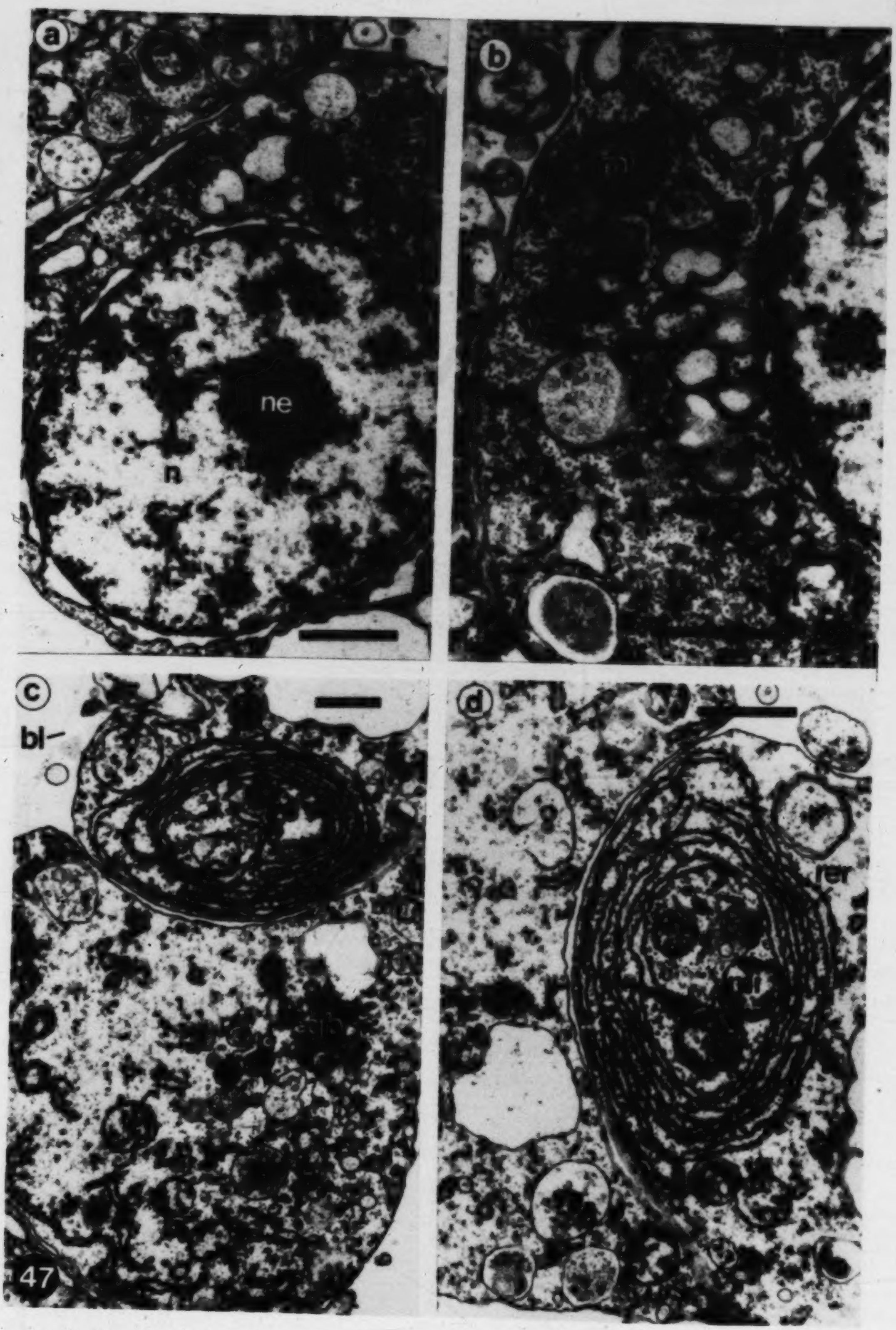
a
ne
n
b
m
c
bl
d
rer
m
47

Figure 48. (a, b, c, d). Epithelium of the intestine of a four-armed pluteus of *D. excentricus*. bl - basal lamina; cr - centriole; lu - lumen; mt - microtubule; n - nucleus; rer - rough endoplasmic reticulum; ser, smooth endoplasmic reticulum; sr - striated rootlet; ve - vesicle; yv - yolk vesicle. In a), b), and d), bars = 1 µm; in c), bar = 0.5 µm.

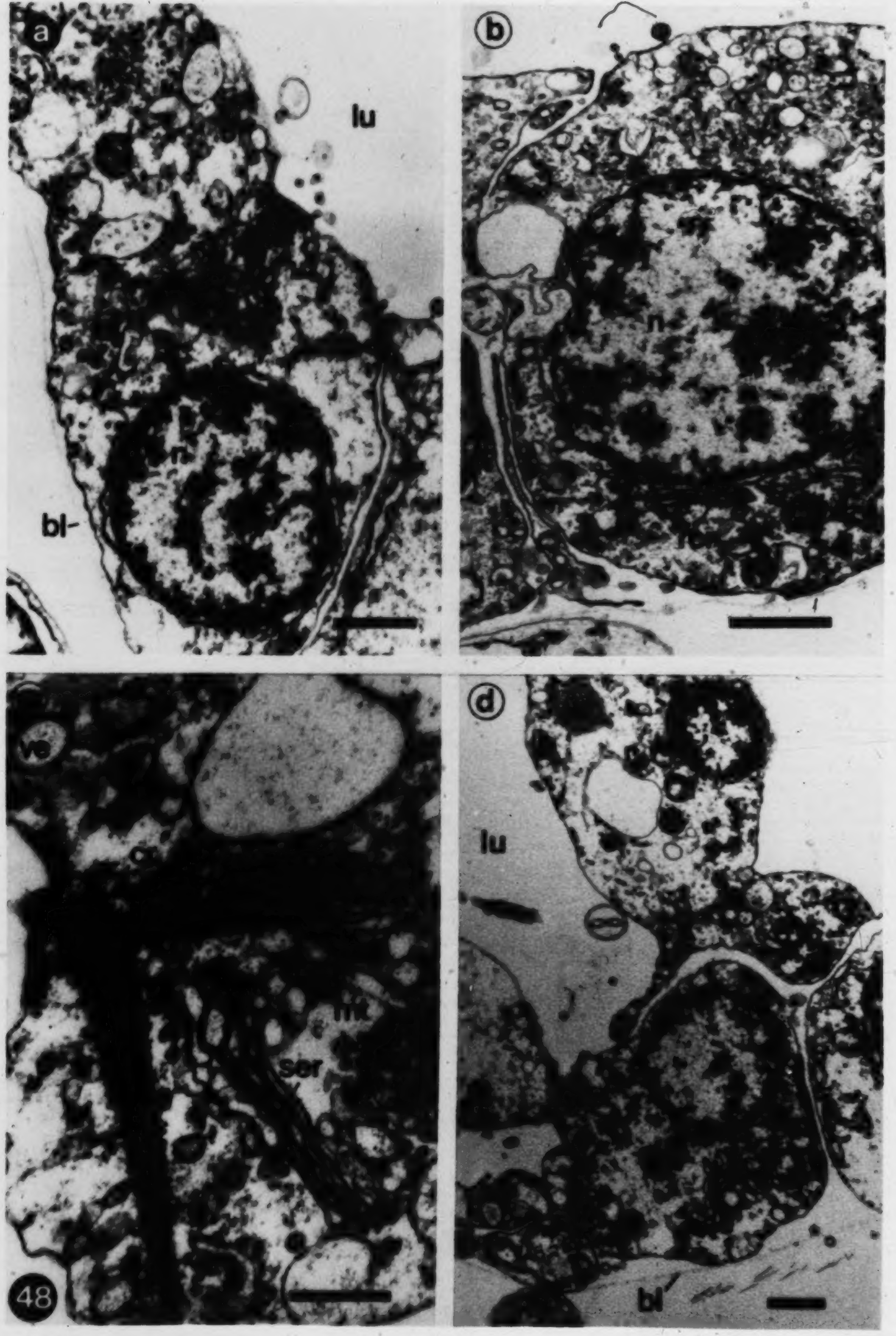
a
lu
n
bl
b
n
ve
mt
ser
48
d
lu
bl

Figure 49. Scale drawings of: a) four-armed, b) six-armed, and c) eight-armed plutei of *D. excentricus*.

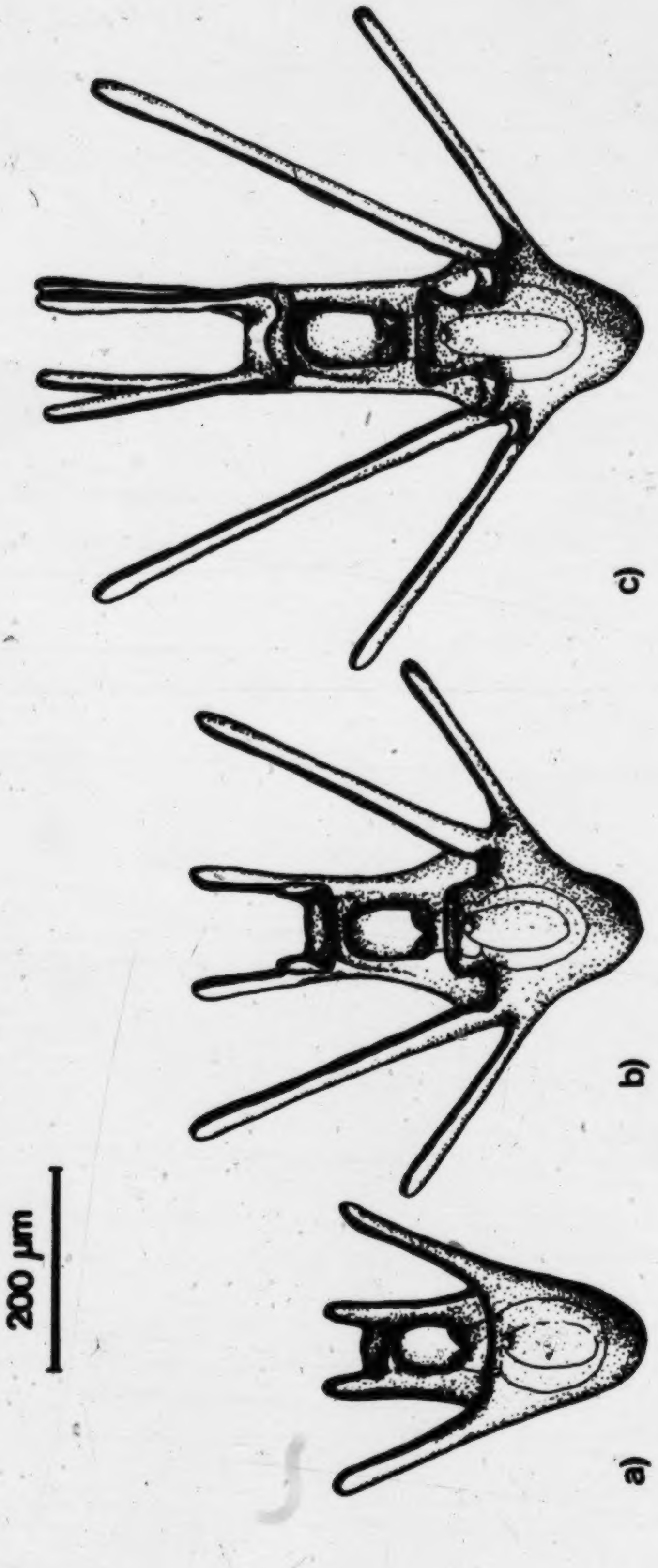

㊾

Figure 50. (a and b) Scanning electron micrographs (SEM) of eight-armed plutei of *D. excentricus*, with details of: c) the mouth, and d) the anus. a - anus; acb - adoral ciliary band; al - anterolateral arms; cb - ciliary band; fm - fecal material; m - mouth; pd - posterodorsal arms; po - post-oral arms; pr - pre-oral arms. In a) and b), bars = 50 µm; in c) and d), bars = 10 µm.

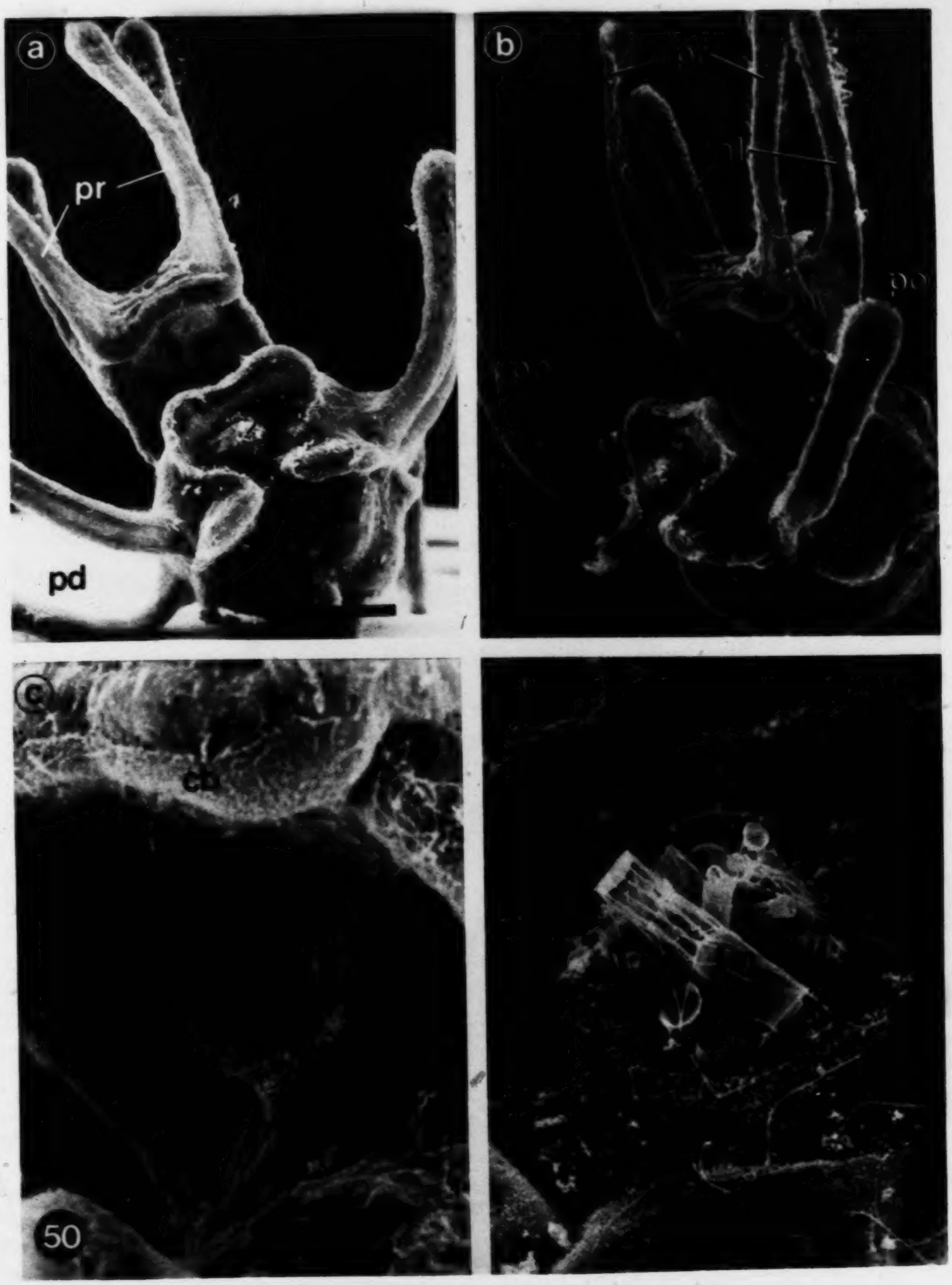
a
pr
pr
pd
b
pr
po
c
cb
50

Figure 51. Light micrographs of: a) mid-frontal, and b) mid-sagital sections of eight-armed plutei of *D. excentricus*. ad - adult rudiment; cb - ciliary band; cs - cardiac sphincter; dm - ventral dilator muscle; ep - epidermis; in - intestine; les - lower esophagus; m - mouth; ps - pyloric sphincter; sc - somatocoel; st - stomach; ues - upper esophagus. Bar = 25 μm.

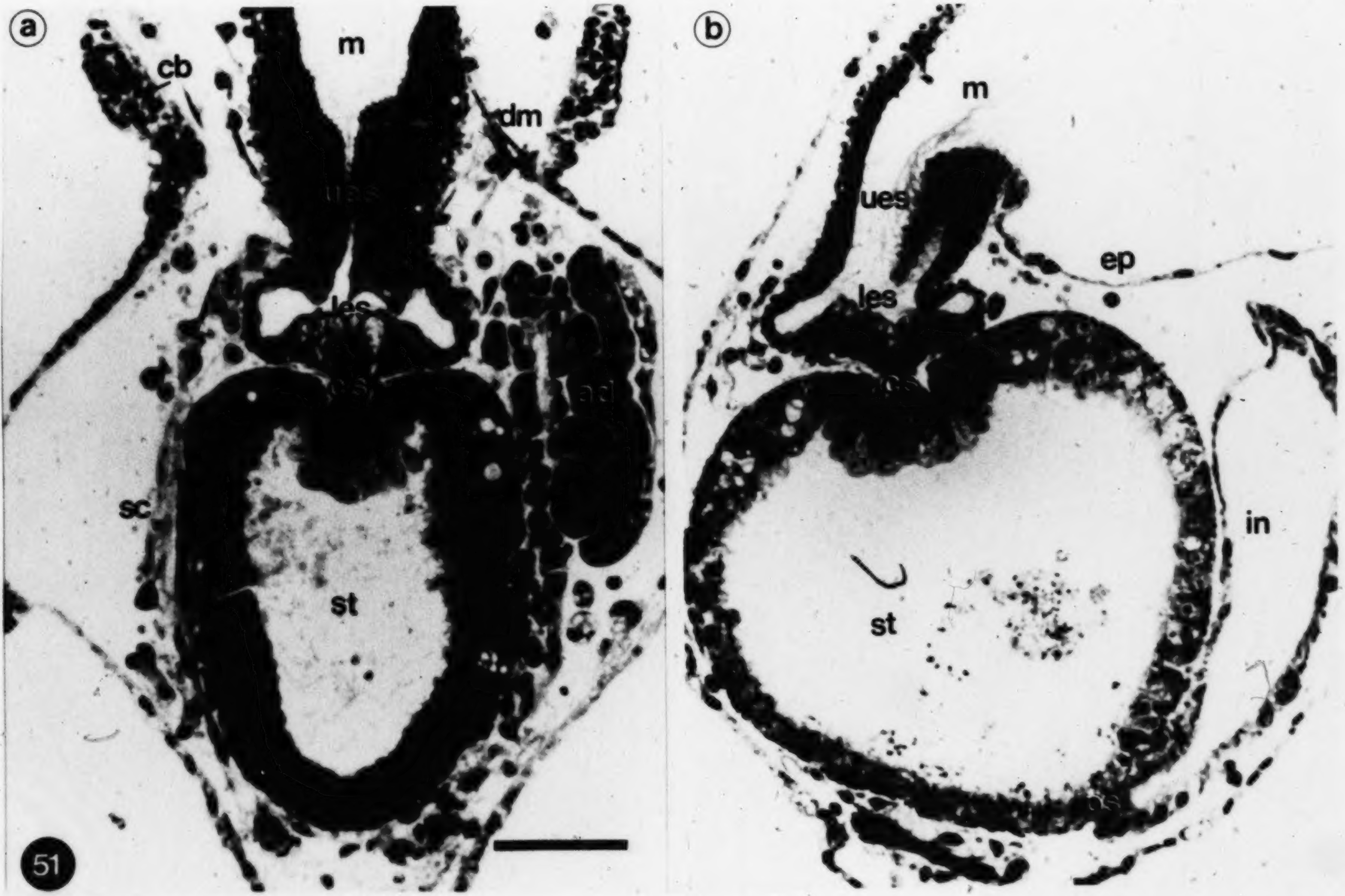
a
cb
m
dm
ues
les
oe
ad
sc
st
51
b
m
ues
ep
les
oe
in
st

Figure 52. a) SEM of the esophagus of a four-armed pluteus of *D. excentricus* from which the epidermis has been removed to expose internal structures. Bar = 2 µm.

b) Light micrograph of a cross-section of the upper esophagus of an eight-armed pluteus of *D. excentricus*. Bar = 5 µm.

c) SEM of the esophageal muscles of an eight-armed pluteus of *D. excentricus*. Bar = 1 µm.

ce - coelom; dct - dorsal ciliated tract; esm - esophageal muscles; les - lower esophagus; lu - lumen; mv - microvilli; ues - upper esophagus; vct - ventral ciliated tract.

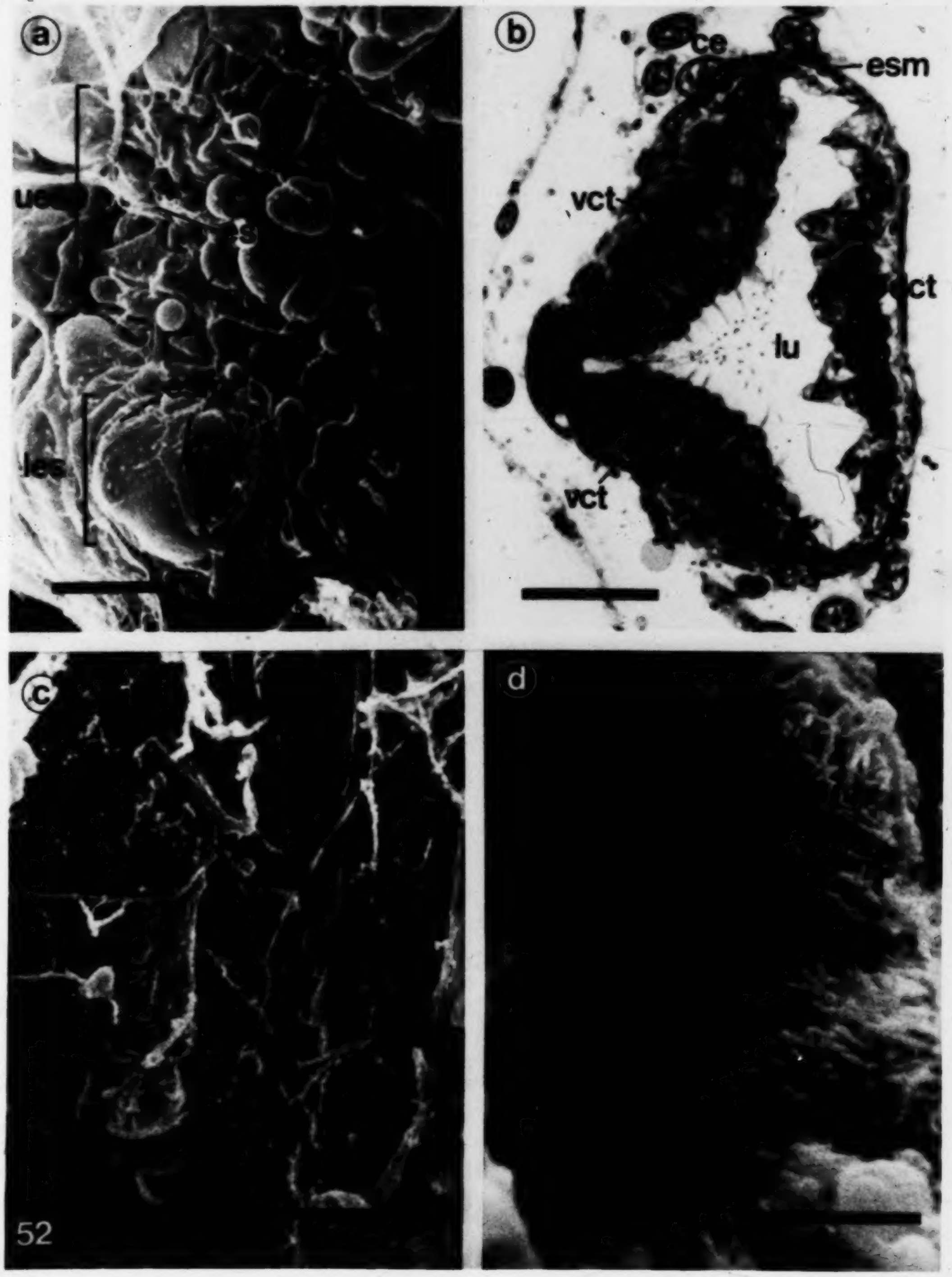
a
ues
es
les
b
ce
esm
vct
ct
lu
vct
c
d
52

Figure 53. a) TEM of a cross-section of the upper esophageal epithelium, b) TEM of a cross-section of the lower esophageal epithelium. esm - esophageal muscles; lu - lumen; n - nucleus. Bars = 2 µm.

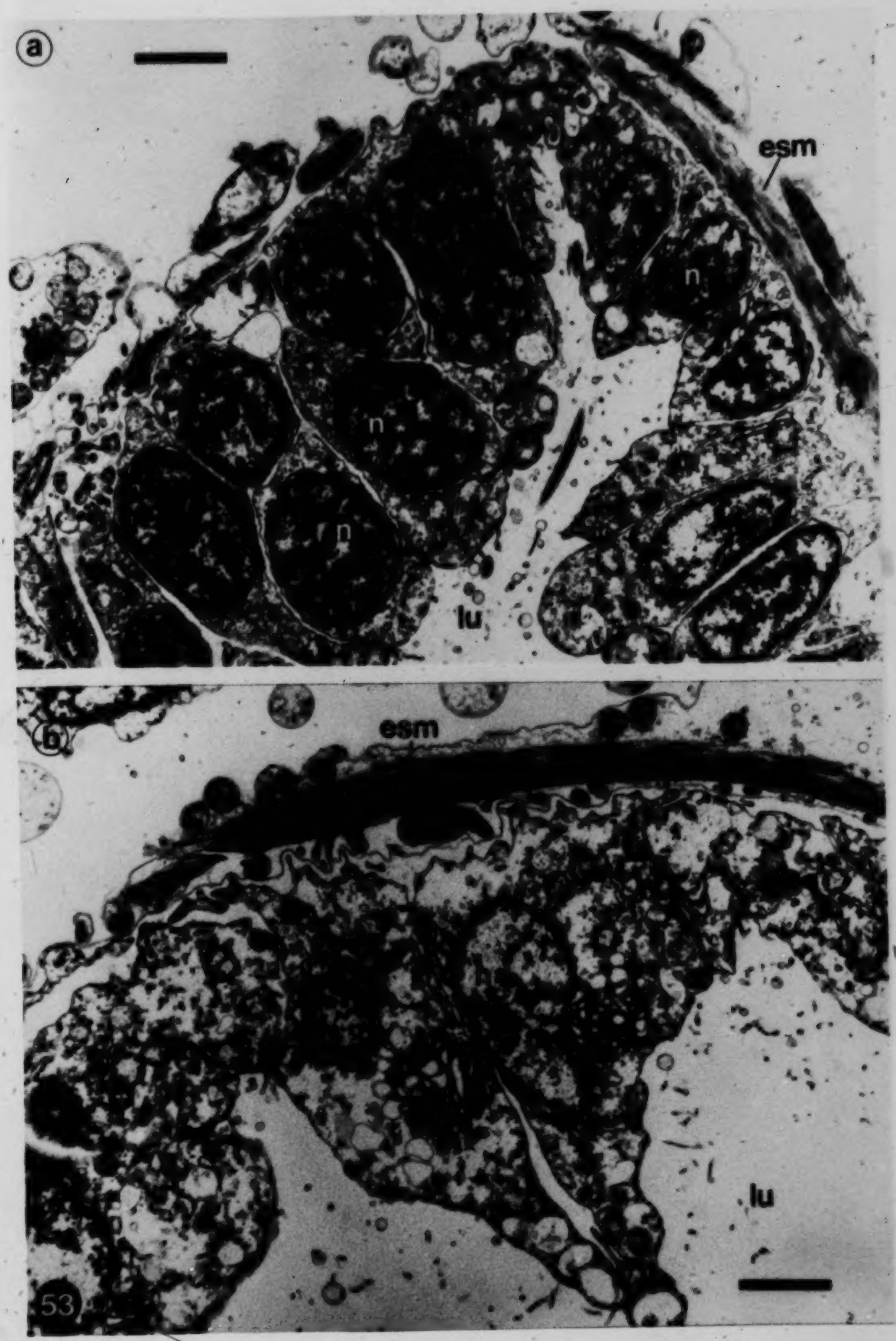
a
esm
n
n
n
n
lu
b
esm
lu
53

Figure 54. (a, b, c, d). TEM of esophageal muscles of eight-armed *D. excentricus* plutei. The arrows in a) indicate the alignment of dense bodies into indistinct Z-lines. bl - basal lamina; db - dense bodies; es - esophageal epithelium; li - lipid; mi - mitochondria; mt - microtubules. In a), bar = 1 µm; in b) and c), bars = 0.5 µm; in d) bar = 0.25 µm.

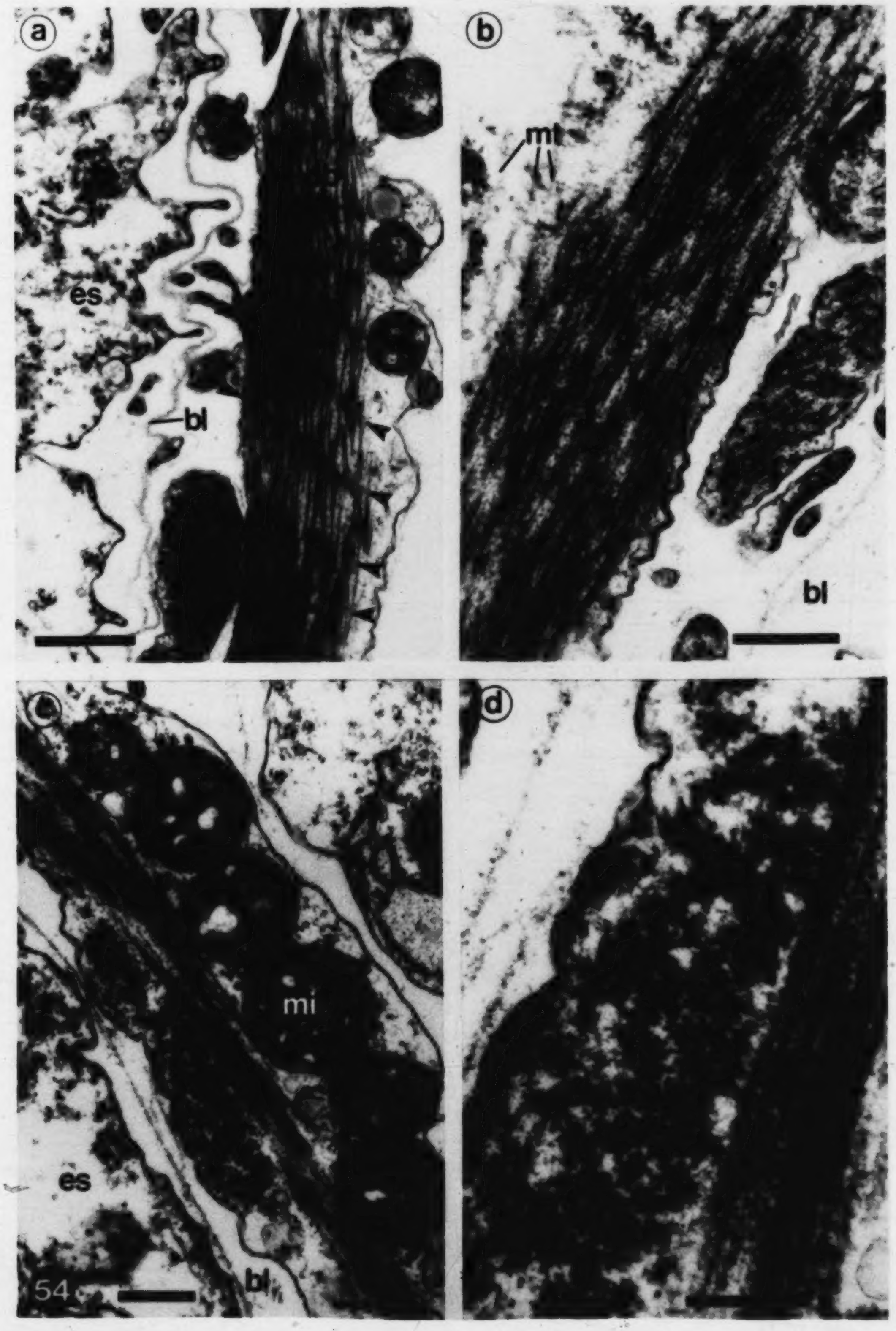
a
es
bl
b
mt
bl
c
mi
es
bl
54
d

Figure 55. a) Cells of the lower esophageal epithelium of an eight-armed pluteus of *D. excentricus*. Bar = 1 μm. b) A zonulae adhaerentes between two cells of the upper esophageal epithelium of an eight-armed pluteus. Bar = 0.25 μm.

Figure 56. (a and b) Nervous tissues associated with the upper esophageal epithelium and the esophageal muscles of an eight-armed pluteus of *D. excentricus*. Bars = 0.5 μm. ax - axon; bl - basal lamina; esm - esophageal muscles; gb - Golgi body; lu - lumen; mt - microtubules; n - nucleus; rer - rough endoplasmic reticulum; sv - synaptic vesicles; sd - septate junction (zonulae adhaerentes); vo - vacuole.

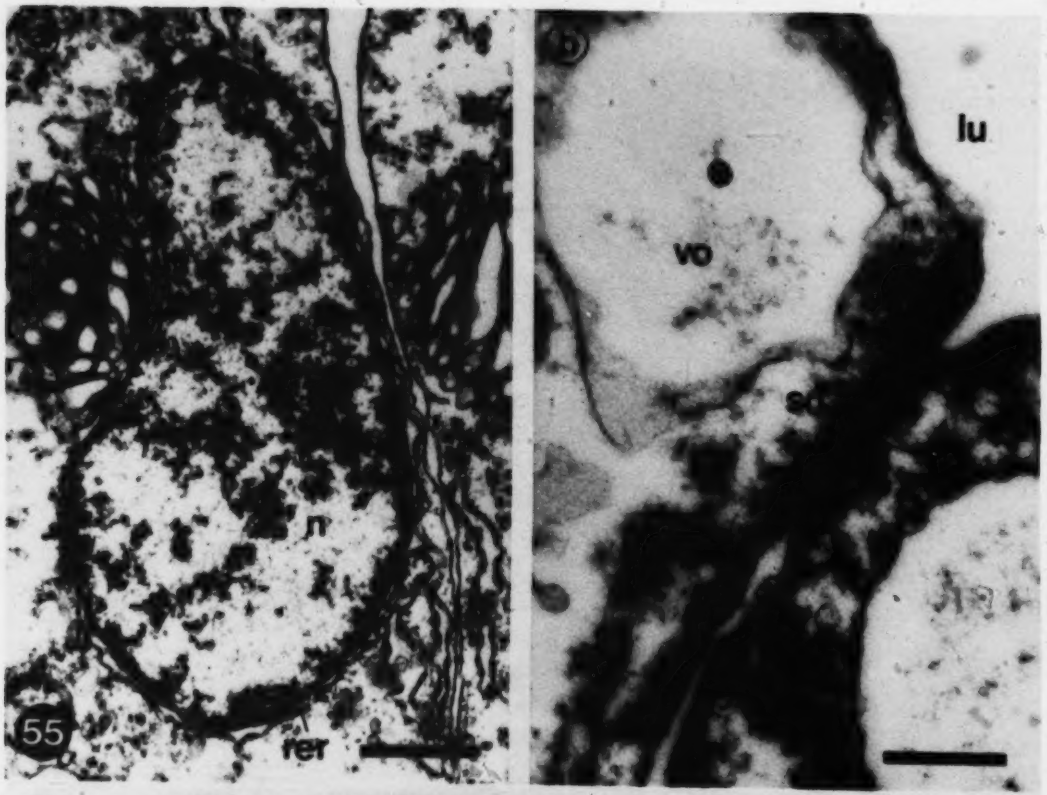
a
n
rer
55
b
lu
vo
sc

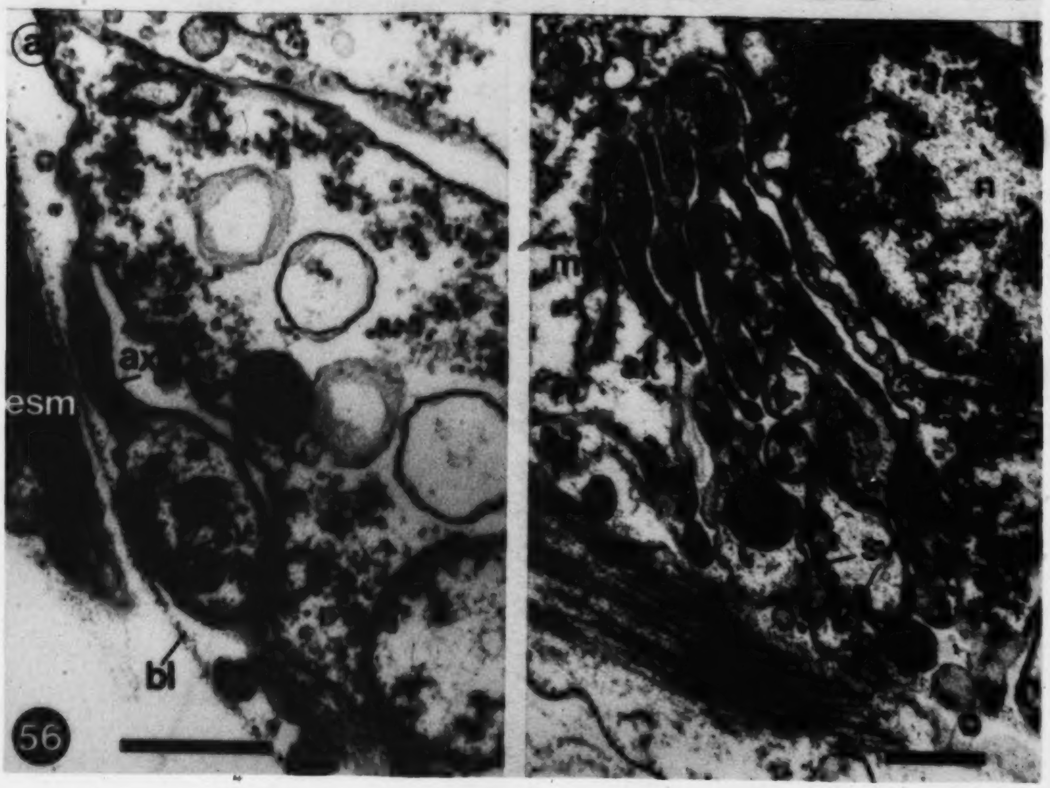
a
ax
esm
bl
56
b
m
n

Figure 57. a) TEM of the lower esophageal epithelium adjacent to the cardiac sphincter in an eight-armed pluteus of *D. excentricus*. b) Light micrograph of a cross-section through the cardiac sphincter of an eight-armed pluteus of *D. excentricus*. c) TEM of the myoepithelium that forms the cardiac sphincter in an eight-armed pluteus. bl - basal lamina; cs - cardiac sphincter; es - esophageal epithelium; esm - esophageal muscles; lu - lumen; mf - myofibrils; n - nucleus. Bars = 2 μm.

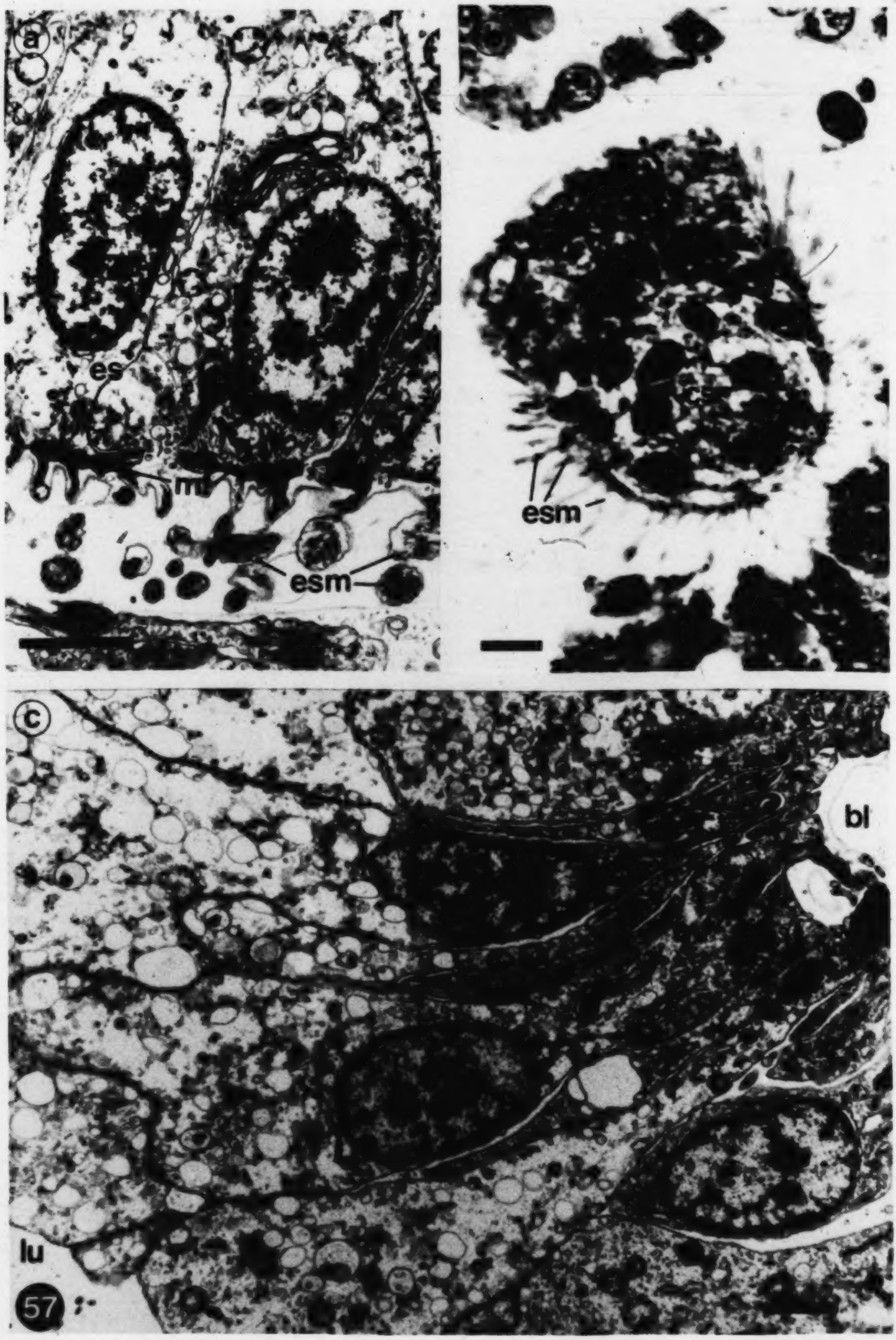
a
es
mi
esm
esm
c
bl
lu

57

Figure 58. a) TEM of the junction between two myoepithelial cells in the cardiac sphincter of an eight-armed *D. excentricus* pluteus. Bar = 0.5 μm.

b) A cross-section of a myofibril in the cardiac sphincter of an eight-armed pluteus. Bar = 0.5 μm.

c) and d) Myofibrils located in the basal regions of the myoepithelium of the cardiac sphincter in an eight-armed *D. excentricus* pluteus. In c), bar = 1 μm; in d), bar = 0.5 μm.

a - A-band; i - I-band; mf - myofibril; mi - mitochondria; mt - microtubules; ve - vesicle; z - Z-line; za - zonulae adhaerentes.

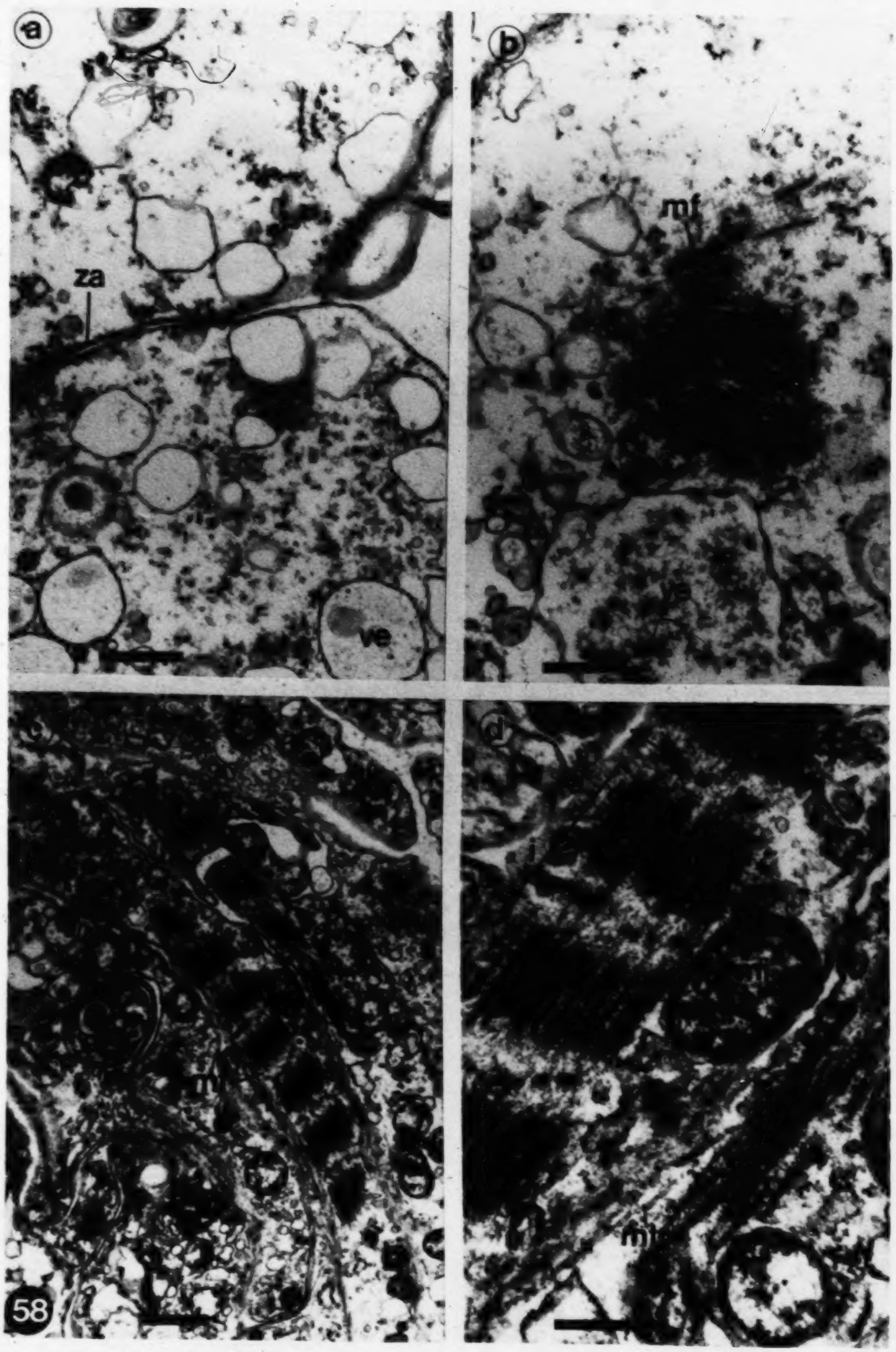
a
za
ve
b
mf
ve
58
m
d
mt

Figure 59. (a, b, c). Type I stomach cells of eight-armed *D. excentricus* plutei. bl - basal lamina; co - collagen; lu - lumen; mi - mitochondria; mv - microvilli; n - nucleus; rer - rough endoplasmic reticulum; ve_A - type A vesicles; ve_B - type B vesicles; ve_C - type C vesicles. In a), bar = 2 μm; in b) and c), bars = 1 μm.

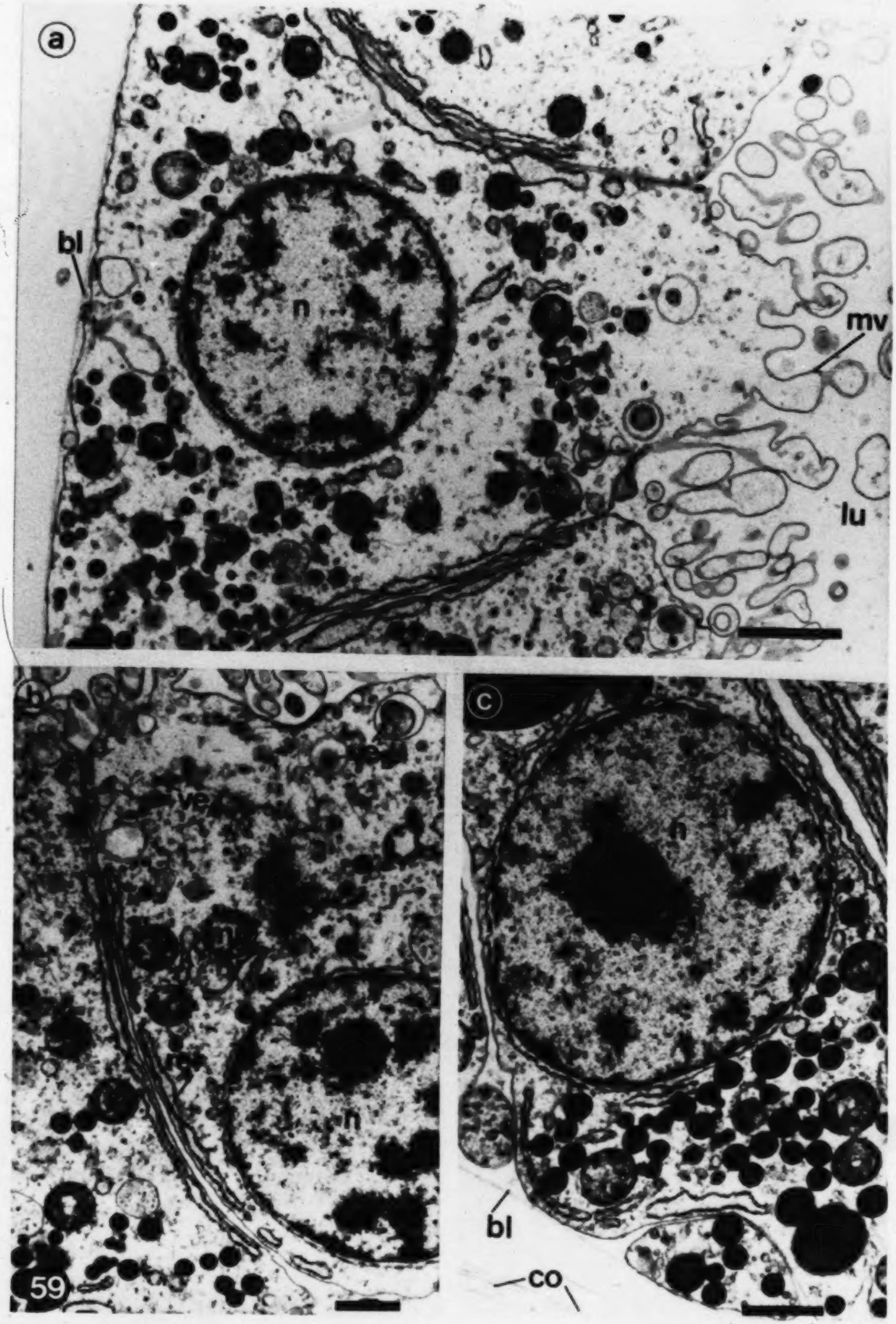
a
bl
n
mv
lu
b
ve
ve
n
59
c
n
bl
co

Figure 60. (a, b, c, d). Type I stomach cells of an eight-armed pluteus of *D. excentricus*. gb - Golgi body; mi - mitochondria; mt - microtubules; mv - microvilli; n - nucleus; rer - rough endoplasmic reticulum; ve_A - type A vesicles; ve_B - type B vesicles; ve_C - type C vesicles. Bars = 1 μm.

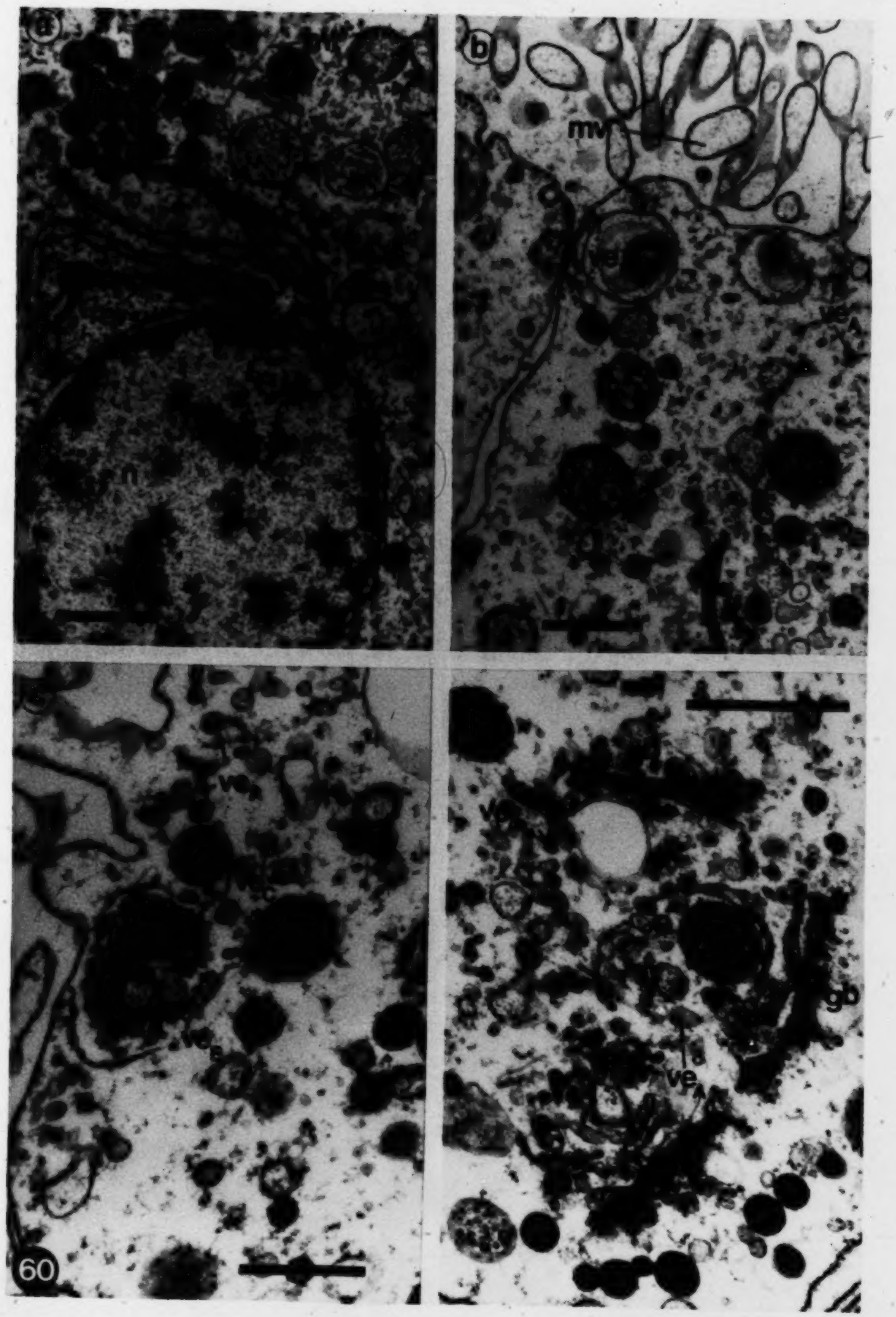
a
n
b
mv
ve
ve
ve
ve
gb
60

Figure 61. (a, b, c). Type II stomach cell of an eight-armed *D. excentricus* pluteus. ac - algal cell; an - algal cell nucleus; mi - mitochondria; mt - microtubules; n - nucleus; ne - nucleolus; rer - rough endoplasmic reticulum. In a), bar = 2 µm; in b) and c), bars = 1 µm.

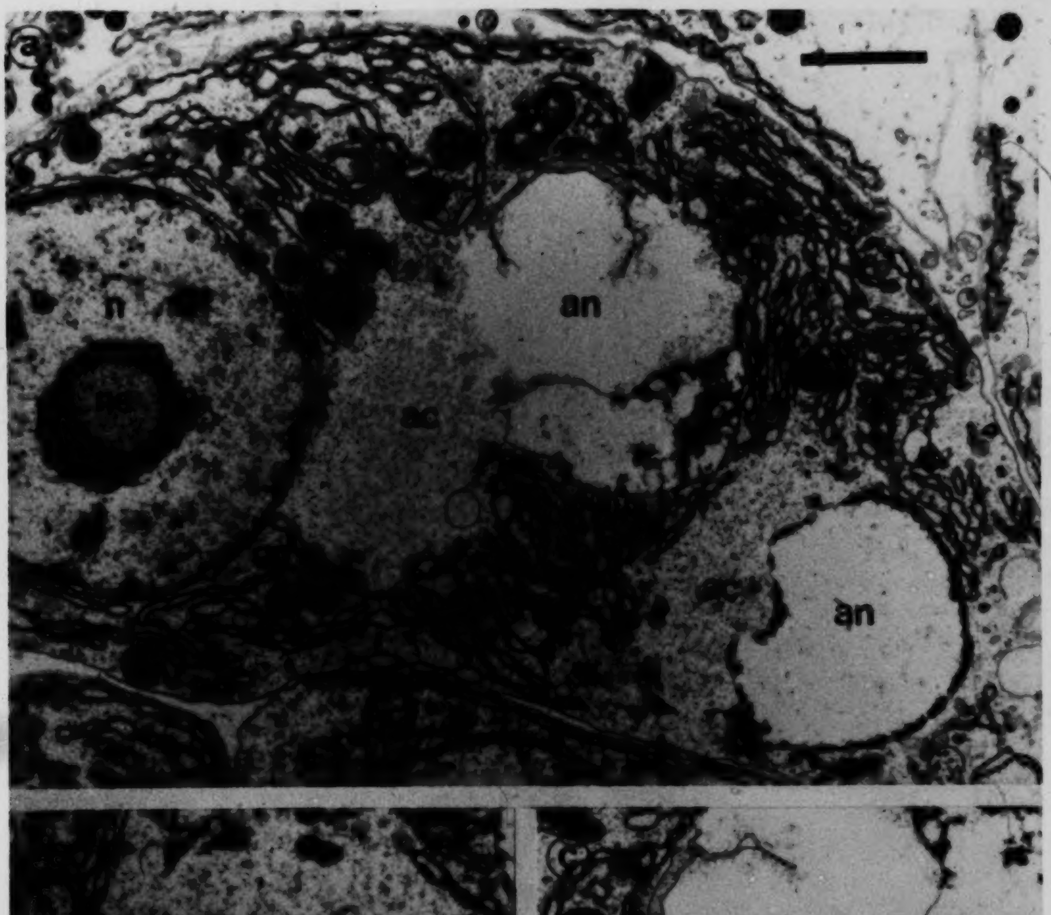
61
a
n
nc
an
ac
an
b
an
rec
c
ac
rer
mi
n
nc

Figure 62. (a, b, and d) Intestinal epithelium of an eight-armed *D. excentricus* pluteus; the myoepithelium of the pyloric sphincter is figured in c). bl - basal lamina; c - cilium; lu - lumen; mf - myofibril; mi - mitochondria; n - nucleus; ve - vesicle. In a), c) and d), bars = 1 µm; in b), bar = 0.5 µm.

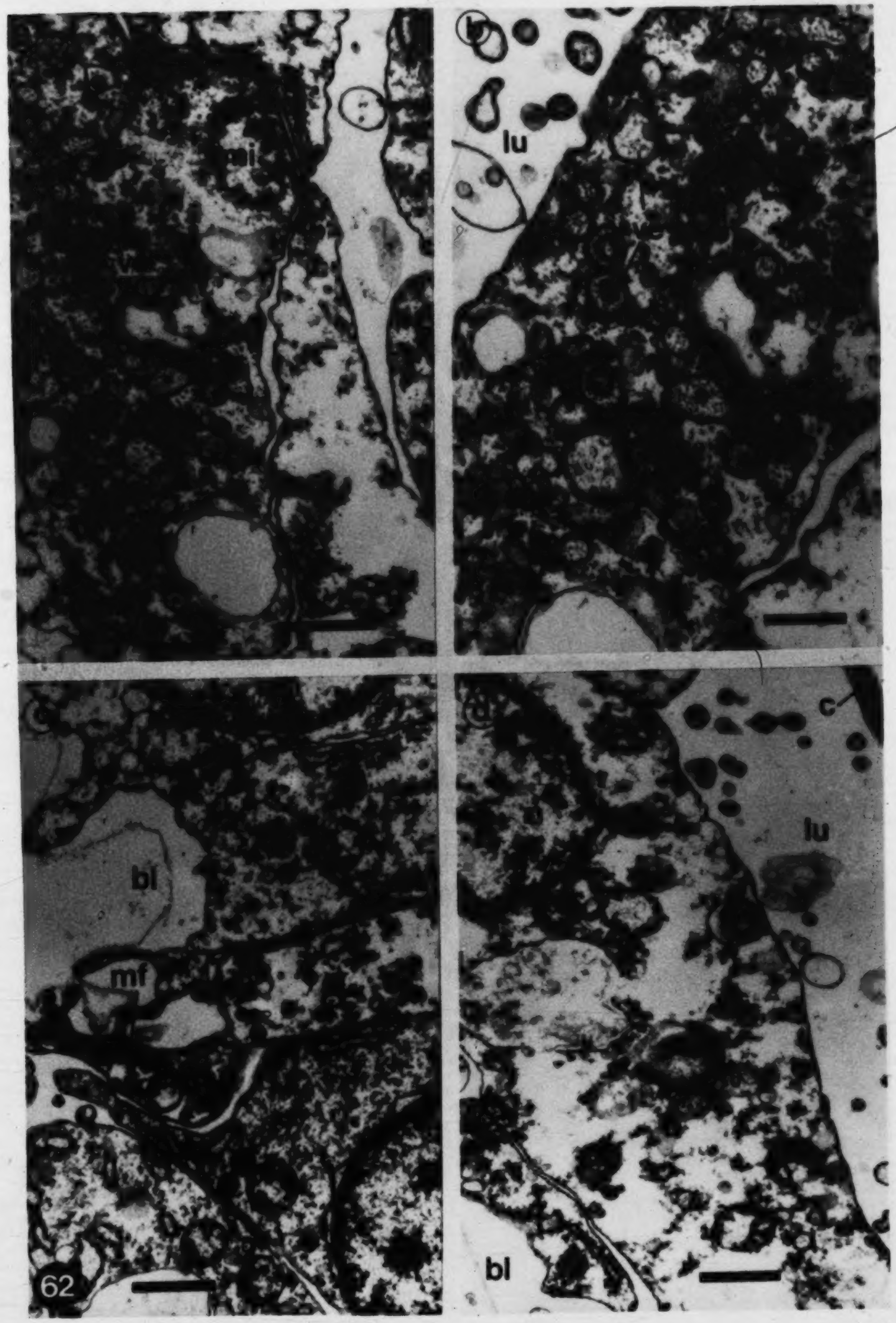
mi
v
b
lu
c
bl
mf
62
d
c
lu
bl

Figure 63. A graphical representation of peristalsis in the esophagus of pluteus larvae of *D. excentricus*. The sequential contractions of the circular bands of muscle, which surround the upper esophagus, produces a wave of peristalsis that transports food particles to the lower esophagus (a, b, and c). While the lower end of the upper esophagus is occluded, contraction of the longitudinally-directed muscles of the lower esophagus opens the cardiac sphincter and forces the bolus of food into the stomach (d). Contraction of the myoepithelium of the cardiac sphincter and relaxation of the esophageal muscles completes the sequence (e). Frequently peristalsis of the upper esophagus is repeated without contraction of the lower esophageal muscles.

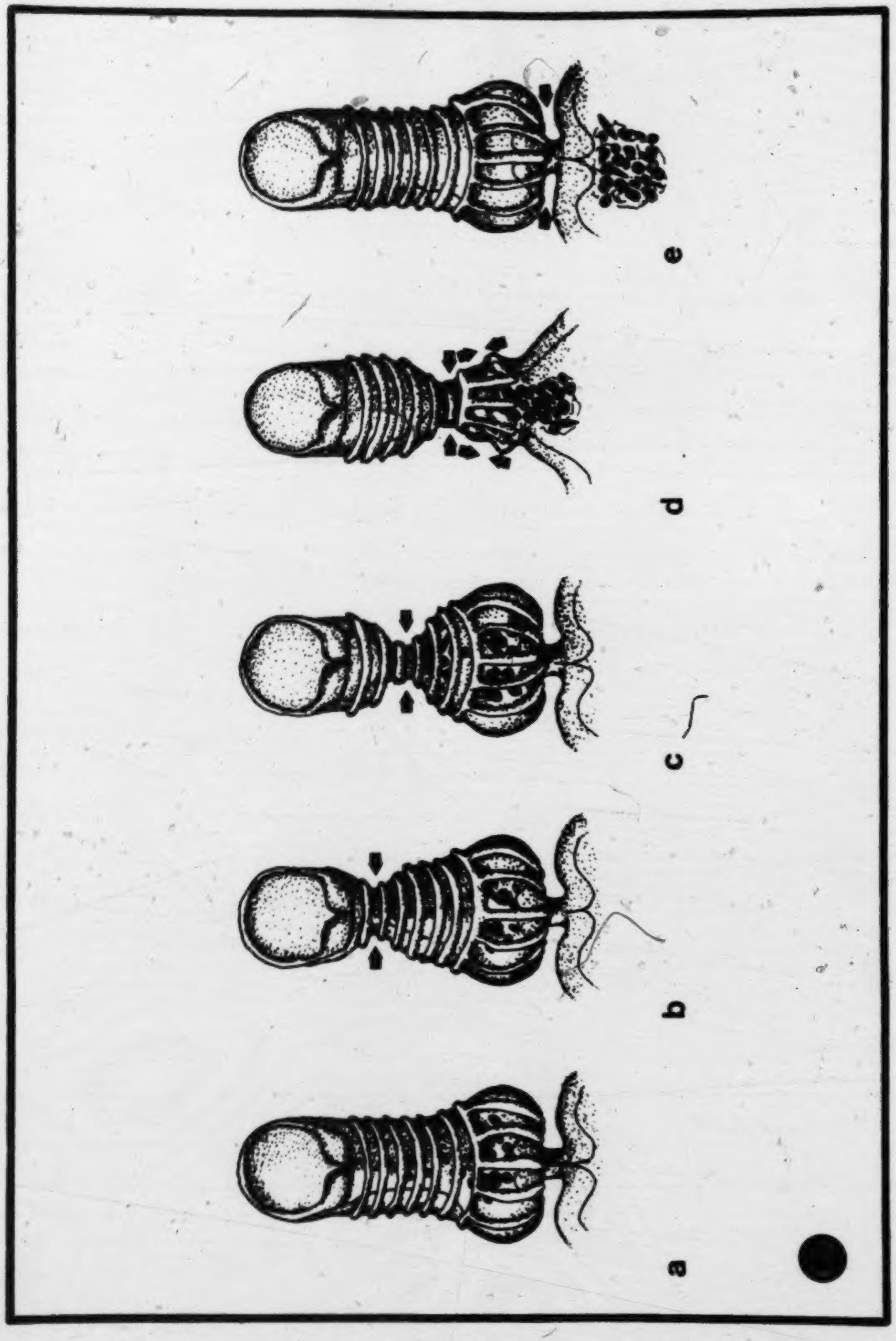
a
b
c
d
e

Figure 64. (a, b, c, d). Competent *D. excentricus* larvae. ad - adult rudiment; as - adult spines; lpo - left post-oral arm; lpd - left posterodorsal arm; m - mouth; ov - opening of the vestibule; pra - pre-oral arm; rpo - right post-oral arm; rpd - right posterodorsal arm; st - stomach; tf - tube feet. Bar = 100 µm.

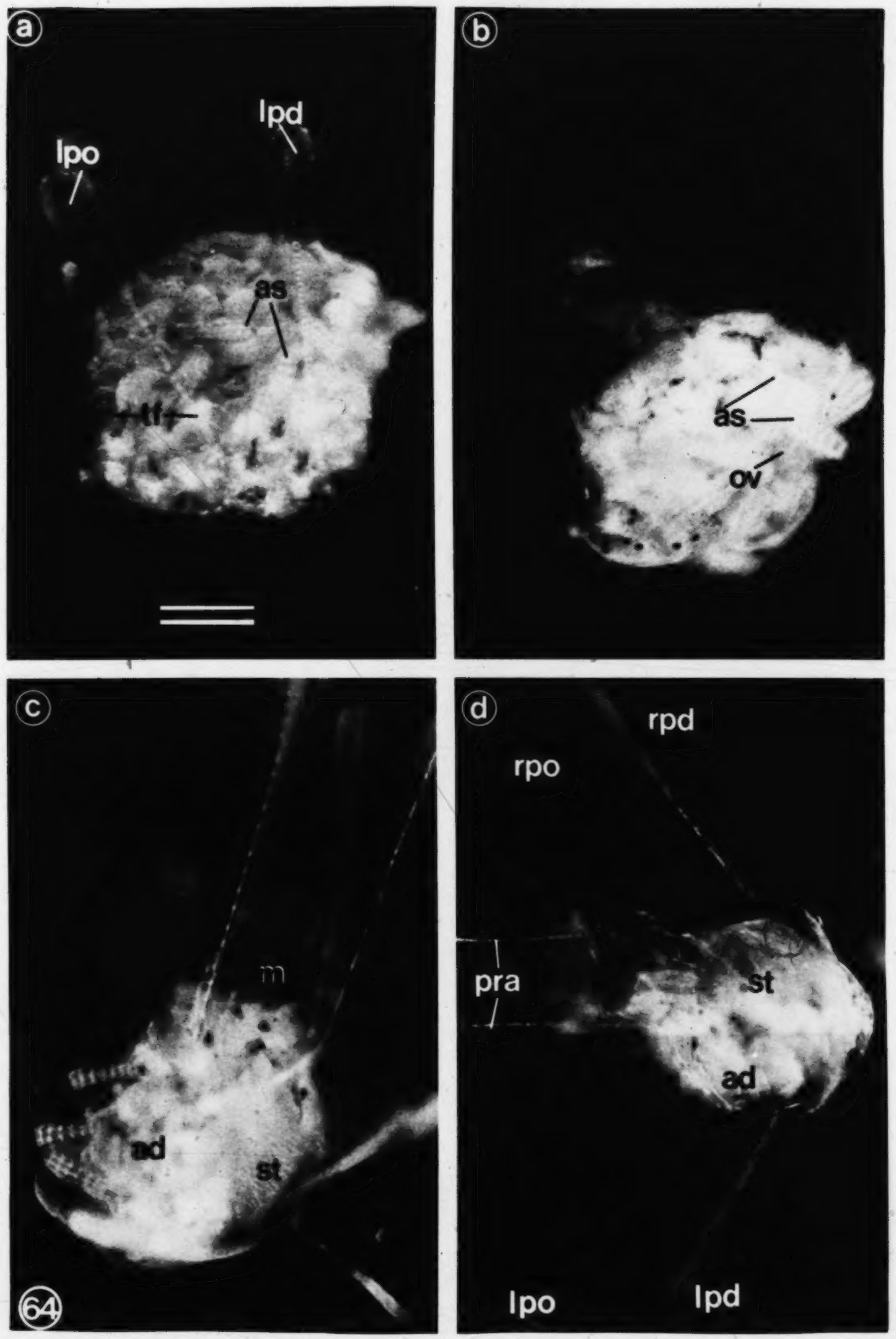
a
lpd
lpo
as
tf
b
as
ov
c
m
ad
st
64
d
rpd
rpo
pra
st
ad
lpo
lpd

Figure 65. The sequence of metamorphosis of *D. excentricus*.

a) Competent larva; b) eversion of the rudiment, 3 to 5 minutes; c) collapse of the larval form, 15 to 30 minutes; d) newly metamorphosed juvenile.

ad - adult rudiment; ala - anterolateral arms; as - adult spines; ep - larval epidermis; lpd - left posterodorsal arm; lpo - left post-oral arm; m - mouth; pra - pre-oral arms; rpd - right posterodorsal arm; rpo - right post-oral arm; sk - larval skeleton; tf - tube foot. Bar = 100 μm.

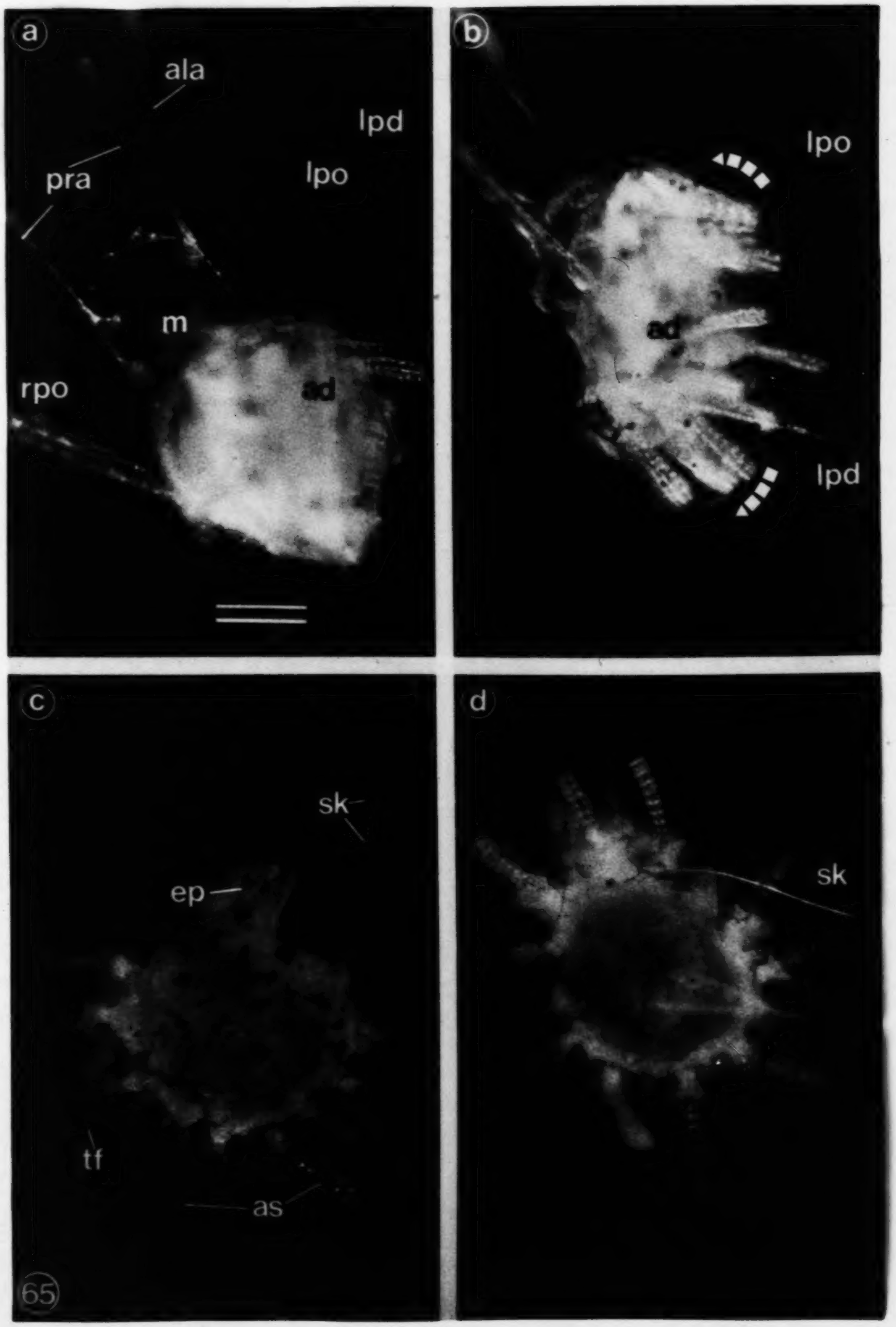
a
ala
lpd
pra
lpo
m
rpo
ad
b
lpo
ad
lpd
c
sk
ep
tf
as
65
d
sk

Figure 66. The sequence of metamorphosis of *D. excentricus*. a) competent larva; b) aboral view of juvenile immediately after eversion of rudiment; c) collapse of the larval form; d) newly metamorphosed juvenile. Arrows indicate membranous material which is to be discarded with the larval skeleton. ad - adult rudiment; ala - anterolateral arms; ep - larval epidermis; la - larval arms; m - mouth; pra - pre-oral arms; sk - larval skeleton; tf - tube foot. Bar = 100 μm.

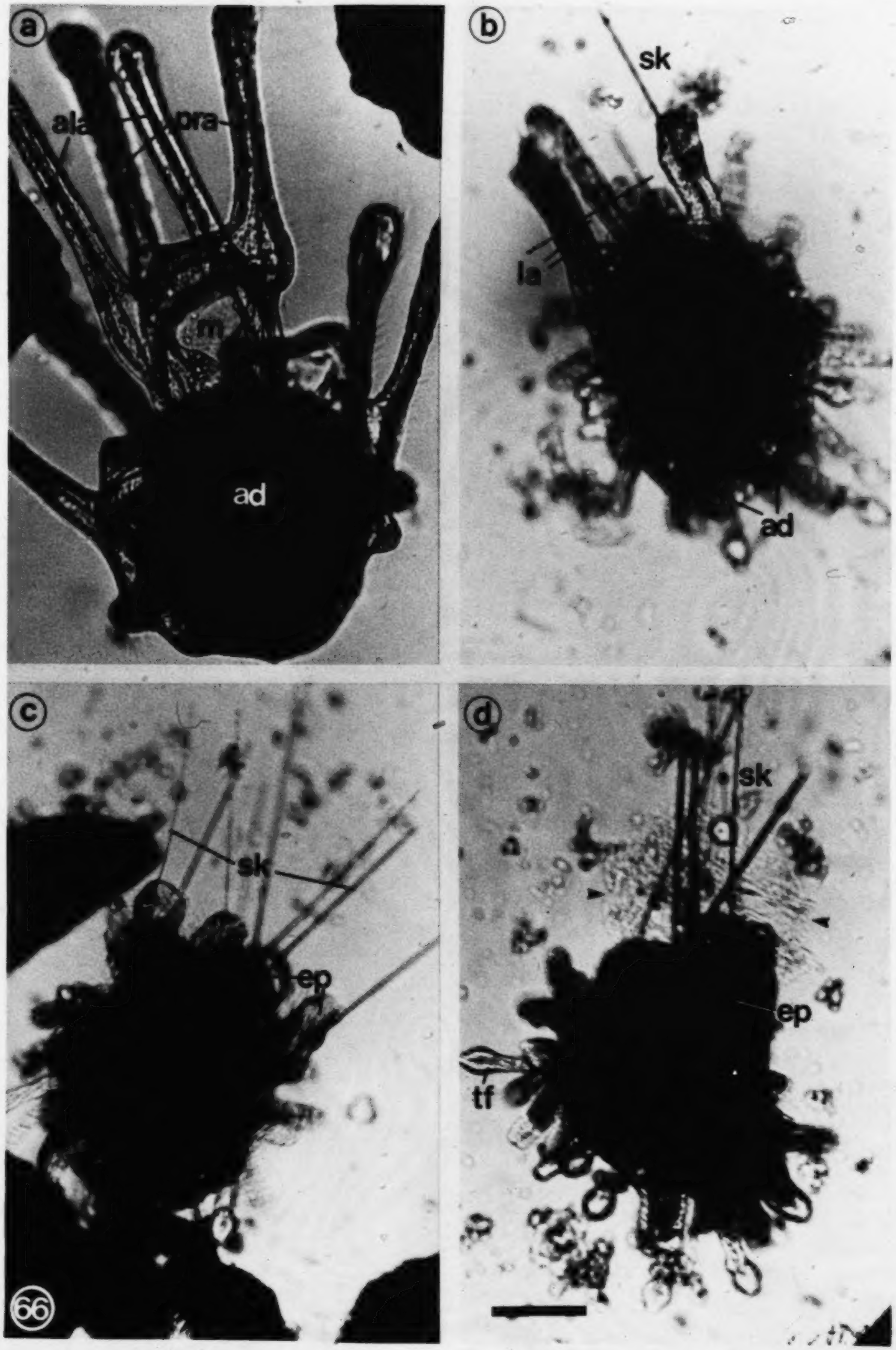
a
ala
pra
m
ad
b
sk
la
ad
c
sk
ep
66
d
sk
ep
tf

Figure 67. Juvenile *D. excentricus*, six days after metamorphosis: a) aboral view, b) oral view. as - spines; m - mouth; t - teeth; tf - tube feet. Bar = 100 µm.

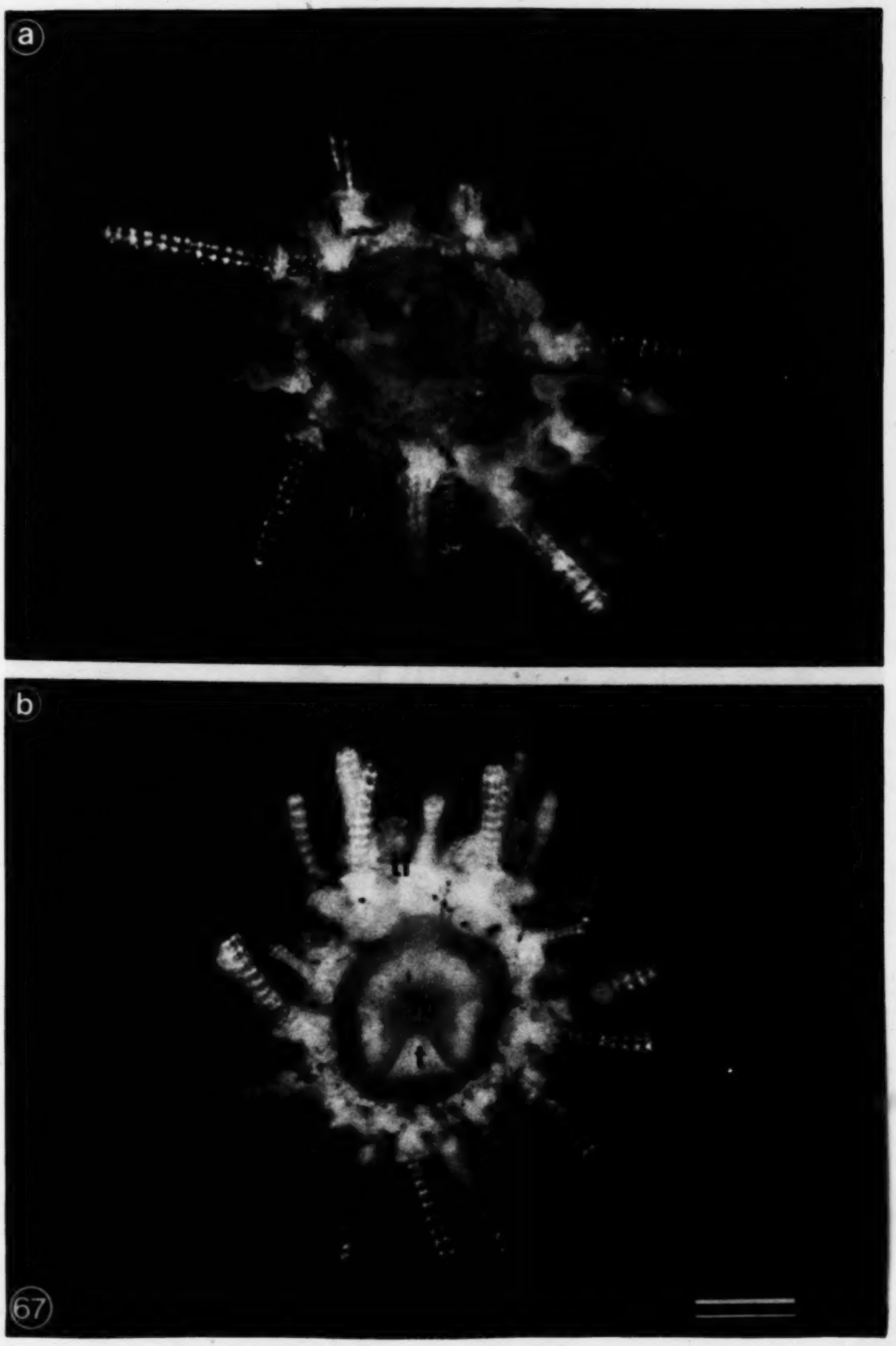
a
b
67

Figure 68. Juvenile *S. purpuratus*, six days after metamorphosis: a) aboral view, b) oral view. as - spines; m - mouth; pc - pedicellariae; t - teeth; tf - tube feet. Bar = 100 µm.

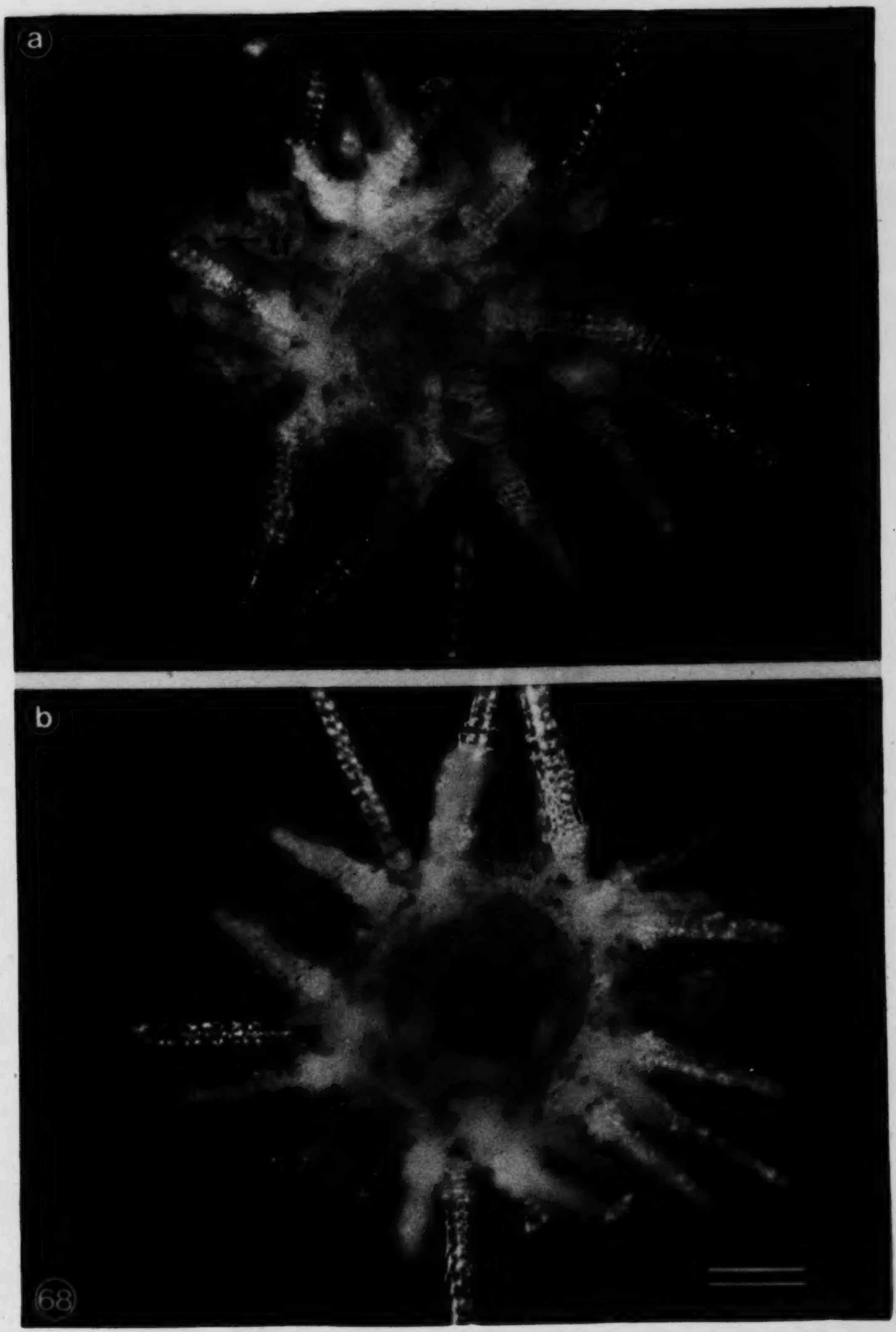
a
b
68

Figure 69. Light micrographs of a *D. excentricus* larva fixed during metamorphosis.

a) A section cut parallel to the oral-aboral axis of the adult rudiment. The larval form is collapsing into the aboral surface of the rudiment. Bar = 20 μm.

b) The dissociated larval epidermis. The arrows indicate a fragmented nucleus in an epidermal cell. Bar = 10 μm.

c and d) Dissociated larval epidermal and stomach cells. Bars = 10 μm.

as - spines; ds - dental sac; ep - larval epidermis; n - nucleus; rc - radial canal; sc - somatocoel; st - stomach; vep - epidermis of the vestibule.

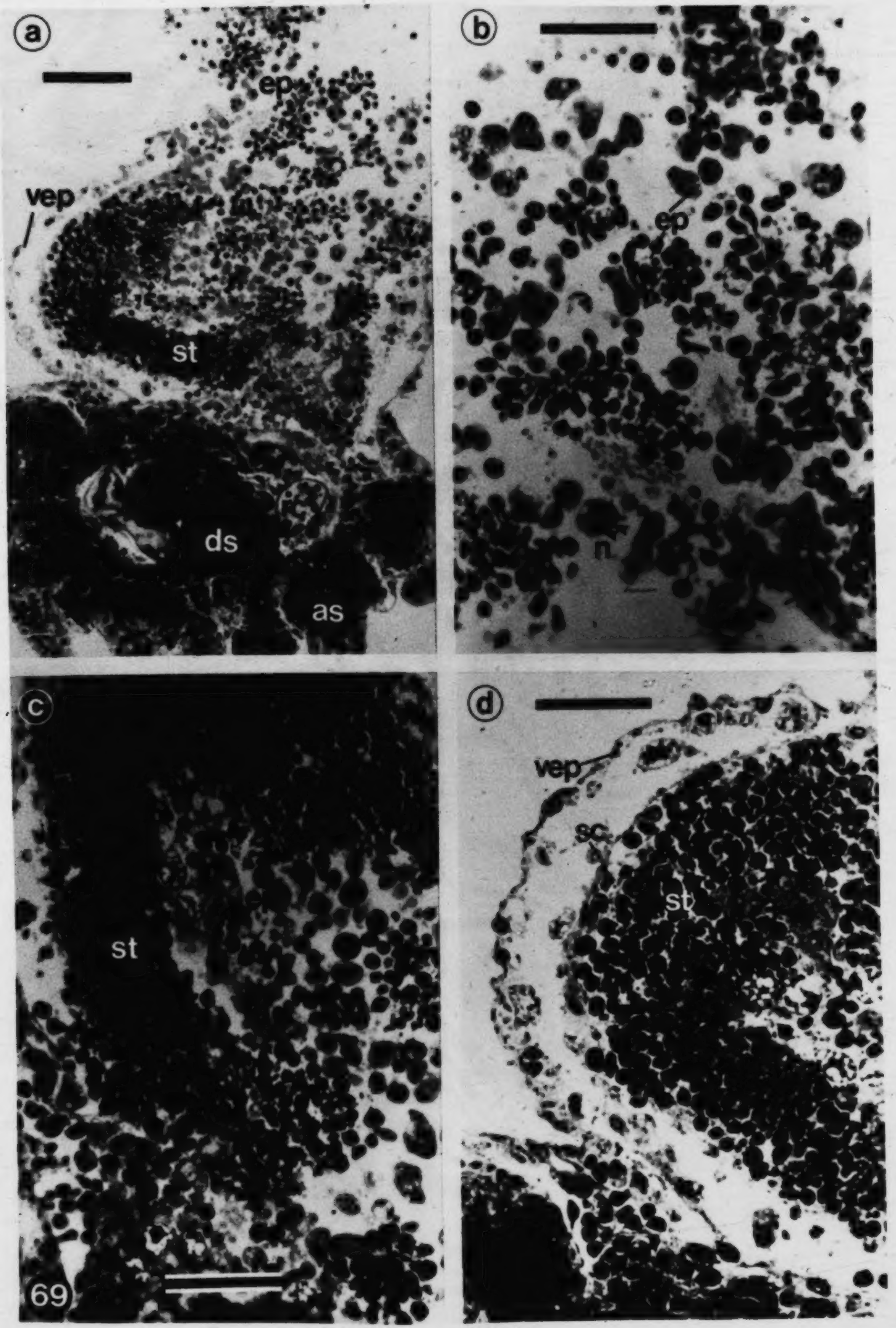
a
ep
vep
st
ds
as
b
ep
n
c
st
69
d
vep
sc
st

Figure 70. TEM of a *D. excentricus* larva fixed during metamorphosis (same specimen as in Figure 69). (a and b) Epidermal cells during the phase of metamorphosis in which the larval epidermis is drawn into the aboral surface of the juvenile. Bars = 1 µm. (c and d) Oblique section through the stomach epithelium. In c), bar = 2 µm; in d), bar = 1 µm. c - cilium; n - nucleus; mi - mitochondria; v_C - lipid vesicle.

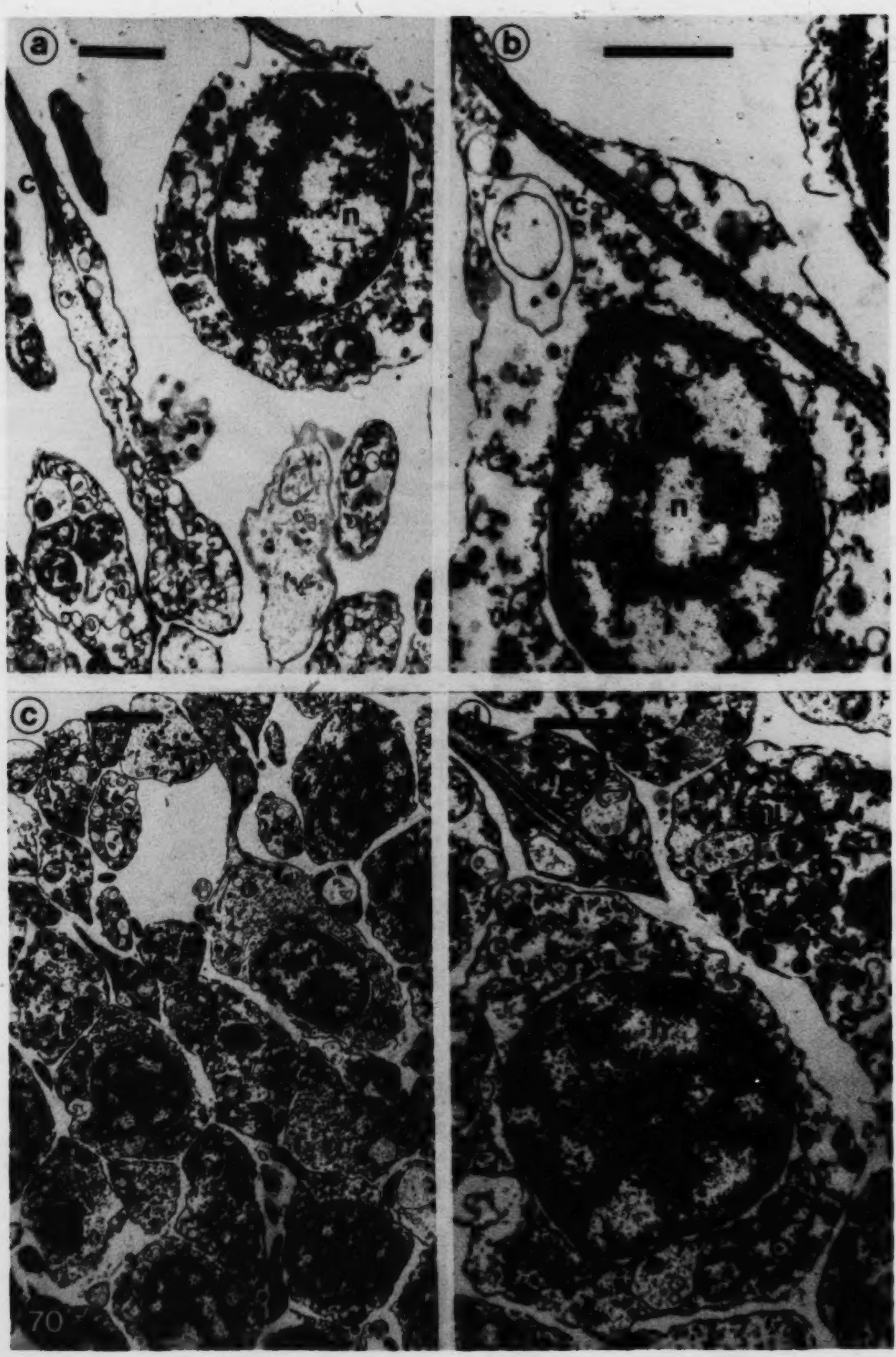
a
c
n
b
c
n
c
d
n
70

Figure 71. (a, b, c). Light micrographs of a juvenile *D. excentricus* which was fixed 48 hours after metamorphosis. The sections were cut at right angles to the oral-aboral axis. In a), bar = 20 µm; in b) and c), bars = 10 µm.

Figure 72. A juvenile *D. excentricus* which was fixed 7 days after metamorphosis. The section was cut at right angles to the oral-aboral axis. Bar = 20 µm.

a - anus; as - spine; bw - body wall; pl - primary loop of the gut; rl - recurrent loop; sc - somatocoel; st - larval stomach cells; te - adult test; vc - lipid vesicles.

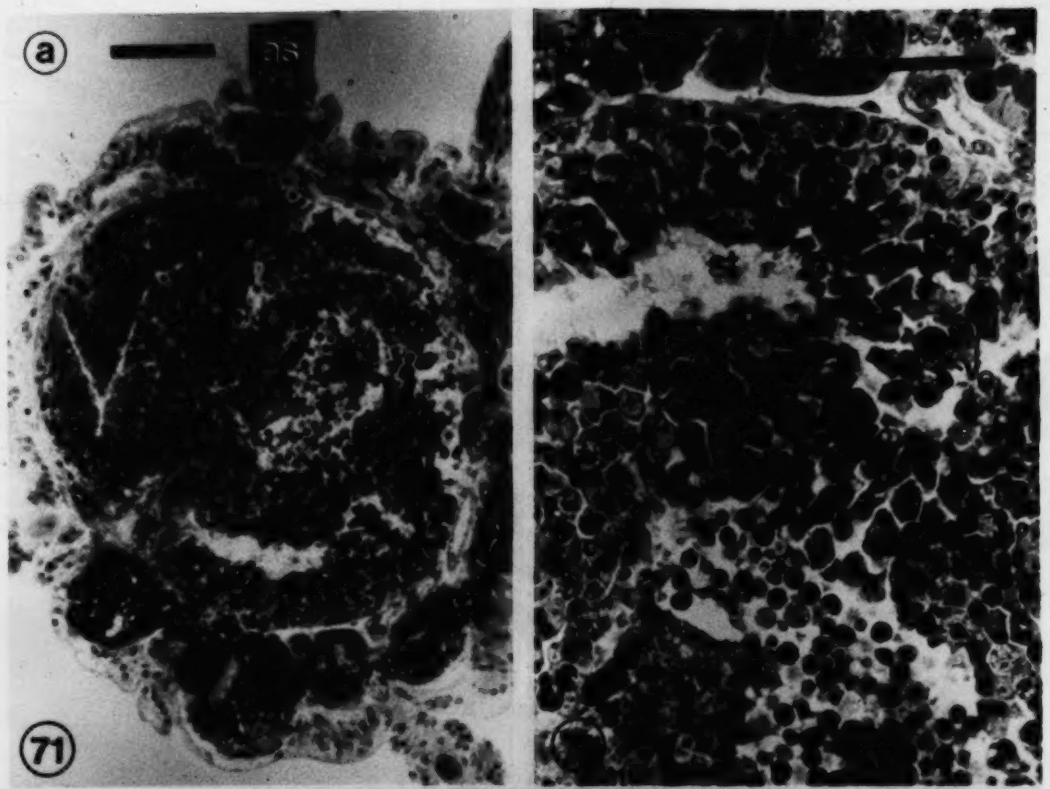
a
as
71

c
71

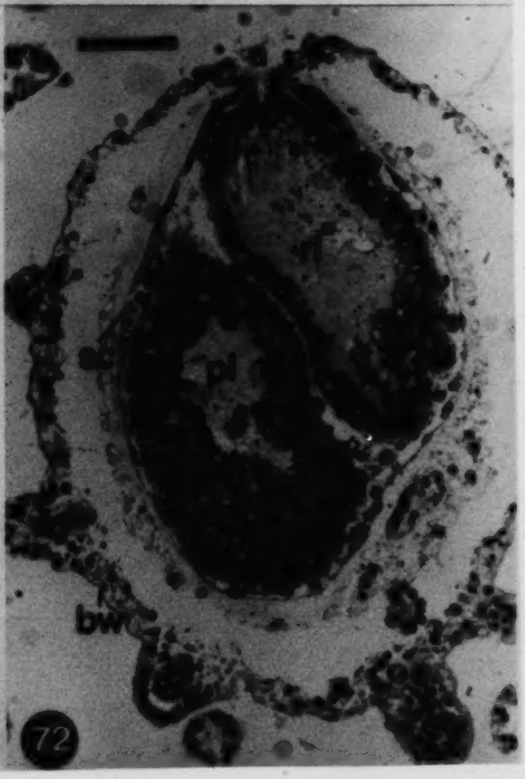
pl
bw
72

Figure 73. (a, b, c, d). TEM of stomach cells from a juvenile *D. excentricus* which was fixed 48 hours after metamorphosis. Note the phagosomes containing necrotic epidermal cells. ly - lysosome; n_s - stomach cell nucleus; n_d - epidermal cell nucleus. In a), bar = 2 μm; in b), bar = 1 μm; in c) and d), bar = 0.5 μm.

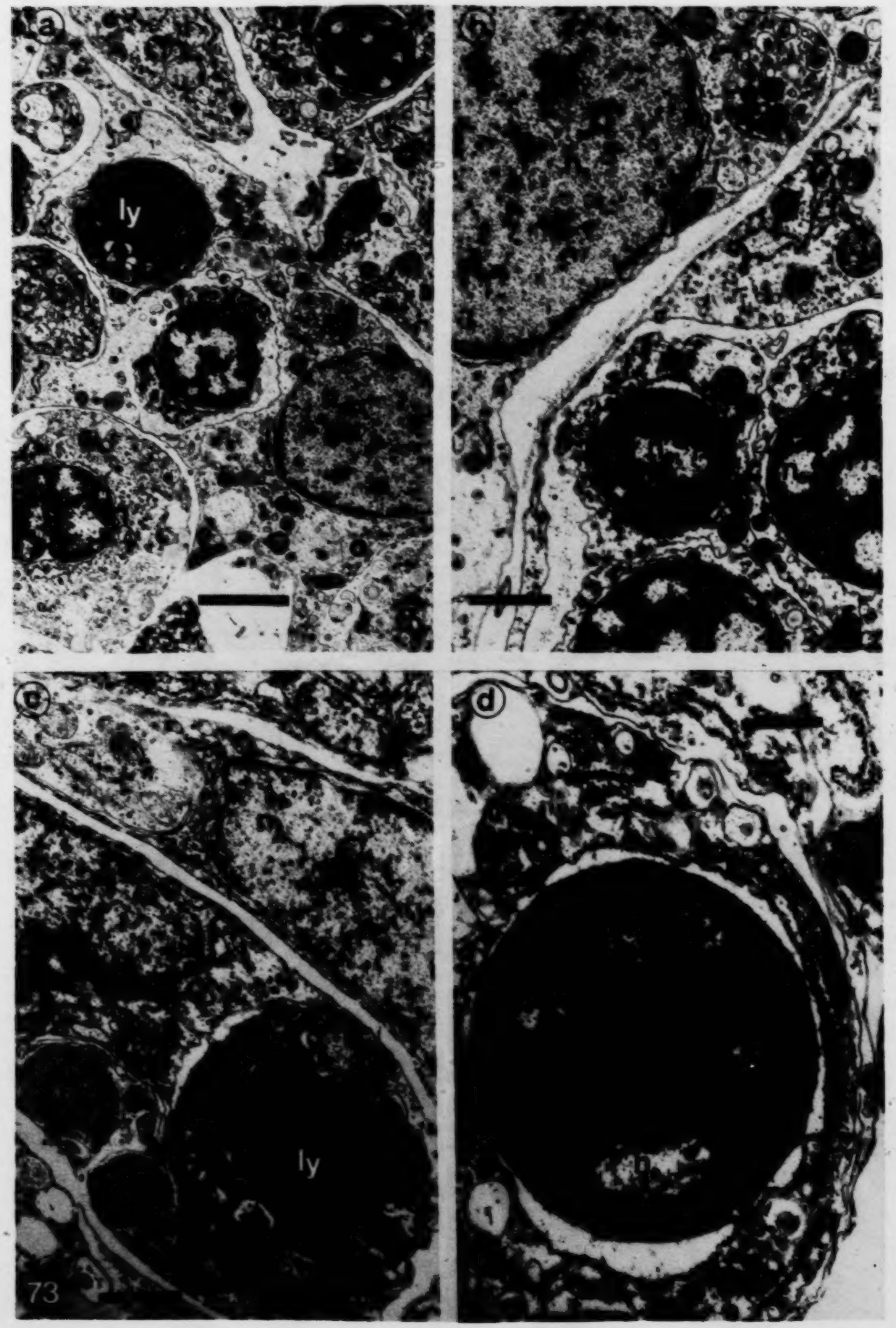
a
b
ly
c
d
ly
73

Figure 74. a) TEM of the primary loop of the gut of a juvenile *D. excentricus* which was fixed 7 days after metamorphosis. (b and c) TEM of the recurrent loop. bl - basal lamina; lu - lumen; ly - lysosome; n - nucleus; sc - somatocoel; v_c - lipid vesicle. Bars = 1 μm.

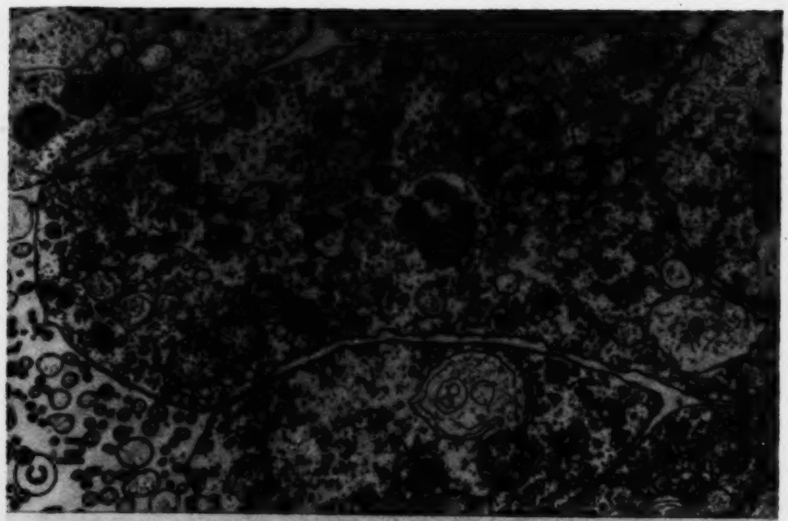
C

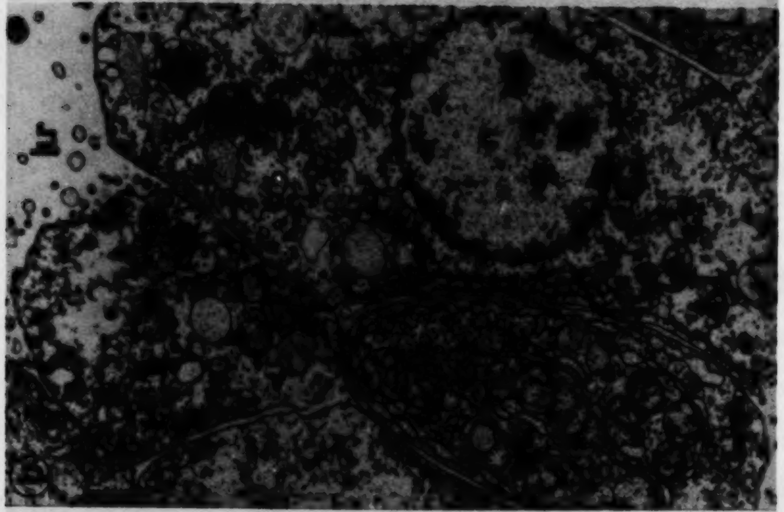

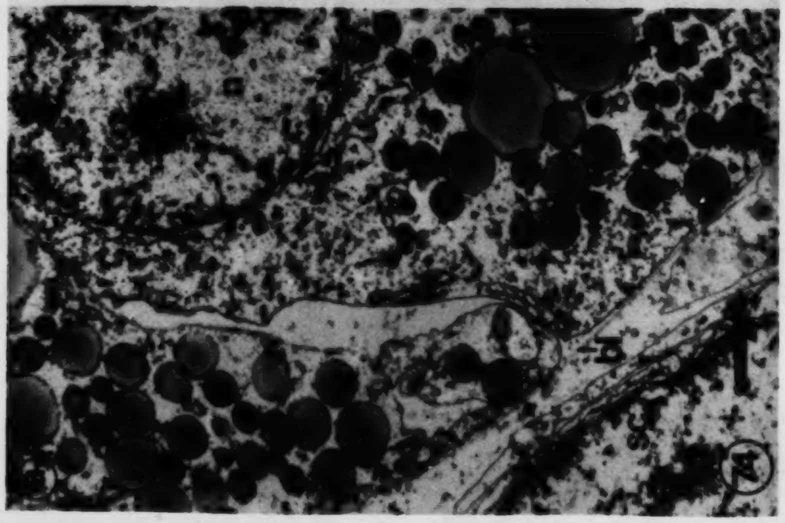
A

LITERATURE CITED

Agassiz, A. 1872. Revision of the *Echini* I and II. Cat. Mus. C. Z. vii: 1-378.

Agassiz, A. 1874. Revision of the *Echini* IV, Structure and Embryology of the *Echini*. Cat. Mus. C. Z. vii: 630-672.

Allen, R. D., David, G. B., Nomarski, G. 1969. The Zeiss-Nomarski interference equipment for transmitted light microscopy. Ztschr. fur Wiss. Mikros. und mikros. Tech. *69*: 192-221.

Bacon, R. L., Julier, S. 1963. Observations on the fine structure of echinoderm larvae. Anat. Rec. *145*: 203.

Baker, P. C., Schroeder, T. E. 1967. Cytoplasmic filaments and morphogenetic movement in the amphibian neural tube. Dev. Biol. *15*: 432-450.

Balinsky, B. I. 1950. On the developmental processes in mammary glands and other epidermal structures. Trans. R. Soc. Edinb. *62*: 1-31.

Balinsky, B. I. 1959. An electron microscope investigation of the mechanisms of adhesion of the cells in the sea urchin blastula and gastrula. Exp. Cell Res. *16*: 429-433.

Balinsky, B. I. 1975. An Introduction to Embryology. Fourth Edition. W. B. Saunder Company, Philadelphia.

Barros, C., Hand, G. S., Monroy, A. 1966. Control of gastrulation in the starfish *Asteria forbesii*. Exp. Cell Res. *43*: 167-183.

Berrill, N. J. 1961. Growth, Development, and Pattern. W.H. Freeman and Company, San Francisco.

Bull, A. L., Chester, C. G. C. 1966. The biochemistry of laminarin and the nature of laminarase. Advan. Enzymol. *28*: 325-364.

Burke, R. D. 1978. The structure of the nervous system of the pluteus larva of *Strongylocentrotus purpuratus*. Cell Tiss. Res. (in press).

Bury, H. 1896. The metamorphosis of echinoderms. Quart. J. Microscop. Sci. *38*: 45-135.

Bütschli, O. 1915. Bemerkungen zur mechanischen Erklarung der Gastrula-Invagination. Sitzber. Akad. Wiss. Heidelberg *6B*: 1-13 (Translation).

Byers, B., Porter, K. R. 1964. Oriented microtubules in elongating cells of the developing lens rudiment after induction. Proc. Nat. Acad. Sci. U.S. *52*: 1091-1099.

Cameron, R. A., Hinegardner, R. T. 1974. Initiation of metamorphosis in laboratory cultured sea urchins. Biol. Bull. *146*: 335-342.

Cameron, R. A. 1975. The initiation and early events of metamorphosis of sea urchins. Ph.D. Dissertation, U. of Calif., Santa Cruz.

Chia, F. S., Burke, R. D. 1978. Echinoderm metamorphosis: fate of larval structures. *In* Chia F. S., Rice M. E. (eds.) Settlement and Metamorphosis of Marine Invertebrate Larvae. Elsevier-North Holland, New York: 219-234.

Chia, F. S., Rice, M. E. 1978 (eds.) Settlement and Metamorphosis of Marine Invertebrate Larvae. Elsevier-North Holland, New York.

Cloney, R. A. 1966. Cytoplasmic filaments and cell movements. Epidermal cells during ascidian metamorphosis. J. Ultrastruc. Res. *14*: 300-328.

Cloney, R. A., Florey, E. 1968. Ultrastructure of cephalopod chromatophore organs. Z. Zellforsch. *89*: 250-280.

Cobb, J. L. S. 1968. The fine structure of the pedicellariae of *Echinus esculentus* (L) I. The innervation of the muscles. J. Roy. Microsc. Soc. *88*: 211-221.

Cobb, J. L. S., Laverack, M. S. 1966. The lantern of *Echinus esculentus* (L.) III. The fine structure of the lantern retractor muscle and its innervation. Proc. Roy. Soc. B *164*: 651-658.

Cobb, J. L. S., Pentreath, V. W. 1977. Anatomical studies of simple invertebrate synapses utilizing stage rotation electron microscopy and densitometry. Tissue and Cell *9*: 125-135.

Coleman, R. 1969. Ultrastructure of the tube foot wall of a regular echinoid, *Diadema antillarium* Philippi. Z. Zellforsch. *96*: 162-172.

Crawford, B. C., Chia, F. S. 1978. Coelomic pouch formation in the starfish *Pisaster ochraceus* (Echinodermata, Asteroidea). J. Morph. *157*: 99-120.

Czihak, G. 1971. Echinoids. *In* Reverberi G. (ed.) Experimental Embryology of Marine and Fresh-Water Invertebrates. North-Holland, Amsterdam: 363-506.

Czihak, G. 1975. (ed.) The Sea Urchin Embryo. Biochemistry and Morphogenesis. Springer-Verlag Press, Heidelberg.

Dan, K. 1960. Cytoembryology of echinoderms and amphibia. Int. Rev. Cytol. *9*: 321-367.

Dan, K., Okazaki, K. 1956. Cytoembryological studies of the sea urchin III. Role of the secondary mesenchyme cells in the formation of the primitive gut in sea urchin larvae. Biol. Bull. *110*: 29-42.

Davidson, E. H. 1968. Gene Activity in Early Development. Academic Press, New York.

Davidson, E. H., Allfrey, V. G., Mirsky, A. E. 1963. Gene expression in differentiated cells. Proc. Nat. Acad. Sci. U.S. *49*: 53-60.

DeVincentiis, M., Lancieri, M. 1970. Observations on the development of the sea urchin embryo in the presence of actinomycin D. Exp. Cell Res. *59*: 479-481.

Dure, L., Watters, L. 1965. Long-lived messenger RNA: evidence from cotton seed germination. Science *147*: 410-412.

Endo, Y., Uno, N. 1960. Intercellular bridges in sea urchin blastula. Zool. Mag. (Tokyo) *69*: 8-16.

Epel, D. 1967. Protein synthesis in sea urchin eggs: a "late" response to fertilization. Proc. Nat. Acad. Sci. U.S. *57*: 899-906.

Fankboner, P. V. 1978. Suspension-feeding mechanisms of the armoured sea cucumber *Psolus chitonoides* Clark. J. exp. mar. Biol. Ecol. *31*: 11-25.

Florey, E., Cahill, M. A. 1977. Ultrastructure of sea urchin tube feet. Evidence for connective tissue involvement in motor control. Cell Tiss. Res. *177*: 195-214.

Fristrom, D. 1976. The mechanism of evagination of imaginal discs of *Drosophila melanogaster* III. Evidence for cell rearrangement. Dev. Biol. *54*: 163-171.

Fristrom, D., Fristrom, J. W. 1975. The mechanism of evagination of imaginal discs of *Drosophila melanogaster* I. General considerations. Dev. Biol. *43*: 1-23.

Gemmill, J. F. 1914. The development and certain points in the adult structure of the starfish *Asterias rubens* (L.). Phil. Trans. Roy. Soc. London B *205*: 213-294.

Gemmill, J. F. 1916. The larva of the starfish *Porania pulvillus*. Quart. J. Microsc. Sci. *61*: 27-50.

Gibbins, J. R., Tilney, L. G., Porter, K. R. 1969. Microtubules in the formation and development of the primary mesenchyme in *Arbacia punctulata* I; distribution of microtubules. J. Cell Biol. *41*: 201-226.

Gillette, R. 1944. Cell number and cell size in the ectoderm during neurulation (*Amblystoma maculatum*). J. Exptl. Zool. *96*: 201-222.

Gilula, N. B. 1972. Septate junction development in sea urchin embryos. J. Cell Biol. *55*: 86a.

Gilula, N. B. 1973. Development of cell junctions. Amer. Zool. *13*: 1109-1117.

Giudice, G. 1973. Developmental Biology of the Sea Urchin. Academic Press, London.

Giudice, G., Mutolo, V., Donatuti, G. 1968. Gene expression in sea urchin development. Wm. Roux Entwicklsmech. org. *161*: 118-128.

Glaser, O. C. 1914. On the mechanism of morphological differentiation in the nervous system. Anat. Rec. *8*: 525-551.

Goldman, R., Pollard, T., Rosenbaum, J. 1976 (eds.) Cell Motility: Book A. Motility, Muscle and Non-muscle Cells. Academic Press, New York.

Granholm, N. H., Baker, J. R. 1970. Cytoplasmic microtubules and the mechanism of avian gastrulation. Dev. Biol. *23*: 563-584.

Greenhouse, G. A., Hynes, R. D., Gross, P. R. 1971. Sea urchin embryos are permeable to actinomycin D. Science *171*: 686-689.

Gross, P. R., Malkin, L. I., Moyer, M. A. 1964. Templates for the first proteins of embryonic development. Proc. Nat. Acad. Sci. U.S. *51*: 407-414.

Gustafson, T., Kinnander, H. 1956. Microaquaria for time-lapse cinematographic studies of morphogenesis in swimming larvae and observations on sea urchin gastrulation. Exp. Cell Res. *11*: 36-51.

Gustafson, T., Wolpert, L. 1961. Studies on the cellular basis of morphogenesis in the sea urchin embryo. Directed movement of primary mesenchyme cells in normal and vegetalized larvae. Exp. Cell Res. *24*: 64-79.

Gustafson, T., Wolpert, L. 1963a. The cellular basis of morphogenesis and sea urchin development. Int. Rev. Cytol. *15*: 139-214.

Gustafson, T., Wolpert, L. 1963b. Studies on the cellular basis of morphogenesis in the sea urchin embryo. Formation of the coelom, the mouth, and the primary pore-canal. Exp. Cell Res. *29*: 561-582.

Gustafson, T., Wolpert, L. 1967. Cellular movement and contact in sea urchin morphogenesis. Biol. Rev. *42*: 442-498.

Gustafson, T., Lundgren, B., Treufeldt, R. 1972a. Serotonin and contractile activity in the echinopluteus. A study of the cellular basis of larval behavior. Exp. Cell Res. *72*: 115-139.

Gustafson, T., Ryberg, E., Treufeldt, R. 1972b. Acetylcholine and contractile activity in the echinopluteus. A study of the cellular basis of larval behavior. Acta embr. exp. *2*: 199-223.

Hay, E. D. 1962. Cytological studies of dedifferentiation and differentiation in regenerating amphibian limbs. *In* Rudnick, D. (ed.) Regeneration Symposium, Development and Growth. Ronald Press Co., New York: 177-210.

Highsmith, R. 1977. Larval substrate selection, metamorphosis and mortality in the sand dollar, *Dendraster excentricus*. Amer. Zool. *17*: 935.

Hinegardner, R. T. 1969. Growth and development of the laboratory cultured sea urchin. Biol. Bull. *137*: 465-475.

Hinegardner, R. T. 1975. Morphology and genetics of sea urchin development. Amer. Zool. *15*: 679-689.

Hiramoto, Y. 1975. Force exerted by the cleavage furrow of sea urchin eggs. Dev. Growth Diff. *17*: 27-38.

His, W. 1874. Unsere Korperform und das physiologische Problem ihrer Entstehung. F.C.W. Vogel, Leipzig. (Summary translated).

Hörstadius, S. 1973. Experimental Embryology of Echinoderms. Clarendon Press, Oxford.

Hultin, T. 1961. The effects of puromycin on protein metabolism and cell division in fertilized sea urchin eggs. Experimentia *17*: 410-411.

Huxley, J. S. 1928. Experimentally induced metamorphosis in *Echinus*. Amer. Natur. *62*: 363-376.

Hyman, L. H. 1955. The Invertebrates: Echinodermata., Volume VI. McGraw-Hill Company, New York.

Ishikawa, H., Buschoff, R., Holtzer, H. 1969. Formation of arrowhead complexes with heavy meromyosin in a variety of cell types. J. Cell Biol. *43*: 312-328.

Immers, J., Lundgren, B. 1972. Aspects of differentiation and function of cilia and adjacent structures of the sea urchin larva. Acta Embr. Exp. *2*: 177-197.

Inoué, S., Stephens, R. E. 1975. (eds.) Molecules and Cell Movement. Soc. of Gen. Physiol. Ser. Vol. 30. Raven Press, New York.

Kawaguti, S. 1964. Electron microscopic structure of the podial wall of an echinoid, with special references to the nerve plexus and the muscle. Biol. J. Okayama Univ. *10*: 1-12.

Kemp, R. B., Lloyd, C. W., Cook, G. M. W. 1973. Glycoproteins in cell adhesion. Prog. in Surf. and Membr. Sci. *7*: 271-318.

Kersten, W., Kersten, H., Rauen, H. M. 1960. Action of nucleic acids on the inhibition of growth by actinomycin of *Neurospora crassa*. Nature *187*: 60-61.

Kiefer, B. I., Entelis, C. F., Infane, A. A. 1969. Mitotic abnormalities in sea urchin embryos exposed to actinomycin D. Proc. Nat. Acad. Sci. U.S. *64*: 857-862.

Klein, N. W., Pierro, L. J. 1963. Actinomycin D: Specific inhibitory effects on the explanted chick embryo. Science *142*: 967-969.

Kletzien, B. F., Perdue, J. F., Springer, A. 1972. Cytochalasin A and B: inhibition of sugar uptake in cultured cells. J. Biol. Chem. *247*: 2964-2966.

Krohn, W. 1849. Beitrag zur Entwicklungsgeschichte der Seeigel larven. Heidelburg (cited by MacBride, E.W. 1903).

Kruh, J., Borsook, H. 1956. Hemoglobin synthesis in rabbit reticulocytes *in vitro*. J. Biol. Chem. *220*: 905-915.

Kumé, M., Dan, K. 1968. Invertebrate Embryology. NOLIT Publishing House. Belgrade, Yugoslavia.

Lang, F., Atwood, H. L. 1973. Crustacean neuromuscular mechanisms: functional morphology of nerve terminals and the mechanism of facilitation. Amer. Zool. *13*: 337-355.

Lawrence, J. M., Lawrence, A. L., Giese, A. C. 1966. Role of the gut as a nutrient storage organ in the purple sea urchin. Phys. Zool. *39*: 281-290.

Lewis, W. H. 1947. Mechanics of invagination. Anat. Rec. *97*: 139-156.

Luft, J. H. 1961. Improvement in epoxy resin embedding methods. J. Biochem. Biophys. Cytol. *9*: 409-414.

Lundgren, B. 1974a. A quantitative estimation of the association of mitochondria to septate desmosomes in the sea urchin larva. Exp. Cell Res. *85*: 429-436.

Lundgren, B. 1974b. Aspects of sea urchin development from blastula to pluteus, with special reference to contractile elements and cell contacts. Ph.D. Thesis, Wenner-Gren Institute for Experimental Biol., University of Stockholm, Stockholm, Sweden.

MacBride, E. W. 1903. The development of *Echinus esculentus* together with some points on the development of *E. miliaris* and *E. acutus*. Phil. Trans. Roy. Soc. London B *195*: 285-330.

MacBride, E. W. 1914. The development of *Echinocardium cordatum*, Part 1. The external features of the development. Quart. J. Microsc. Sci. *59*: 471-486.

MacBride, E. W. 1918. The development of *Echinocardium cordatum*, Part 2. The development of the internal organs. Quart. J. Microsc. Sci. *63*: 259-282.

Mackie, G. O., Spencer, A. N., Strathmann, R. R. 1969. Electrical activity associated with ciliary reversal in an echinoderm larva. Nature *223*: 1384-1385.

Marsland, D., Zimmerman, A. M. 1963. Cell division: differential effects of heavy water upon the mechanisms of cytokinesis and karyokinesis on the eggs of *Arbacia punctulata*. Exp. Cell Res. *30*: 23-35.

Marsland, D., Zimmerman, A. M. 1965. Structural stabilization of the mitotic apparatus by heavy water in the cleaving eggs of *Arbacia punctulata*. Exp. Cell Res. *38*: 306-313.

McClay, D. R., Chambers, A. F., Warren, R. H. 1977. Specificity of cell-cell interactions in sea urchin embryos. Appearance of new cell-surface determinants at gastrulation. Dev. Biol. *56*: 343-355.

Millonig, G. 1961. Advantages of a phosphate buffer for OsO_4 solutions in fixation. J. appl. Phys. *32*: 1637-1646.

Monné, L., Harde, S. 1951. On the formation of the blastocoel and similar embryonic activities. Arkiv. Zool. *1*: 463-469.

Moore, A. R. 1927. Self differentiation of the intestine in larvae of the sand dollar, *Dendraster excentricus*. Proc. Soc. Exp. Biol. Med. *25*: 40-41.

Moore, A. R. 1930. Cell membranes and cell bridges in the formation of blastula and gastrula. Contrib. Marine Biol. Stanford Univ.: 188-203.

Moore, A. R., Burt, A. S. 1939. On the locus and nature of forces causing gastrulation in embryos of *Dendraster excentricus*. J. exp. Zool. *82*: 159-171.

Morgan, T. H. 1927. Experimental Embryology. Columbia University Press, New York.

Mortensen, T. 1920. Notes on the development of the larval forms of some Scandinavian echinoderms. Vidensk. Medd. dansk. naturh. foren. *71*: 133-160.

Mortensen, T. 1921. Studies on the development and larval forms of echinoderms. Copenhagen GEC Gad. 1-266.

Mortensen, T. 1931. Contributions to the study of the development and larval forms of echinoderms I-II. D. Kgl. Danske Videnske. Selsk. Akrifter Naturvidensk. OG. Mathem Afd. *9 IV*: 1-39.

Mortensen, T. 1937. Contributions to the study of development and larval forms of echinoderms III. Memoires de l'academic Royale des Sciences et des lettres de Danemark, Copenhague, Section des Sciences 9^{me} serie, t *VII*: 1-65.

Mortensen, T. 1938. Contributions to the study of development and larval forms of echinoderms IV. Memoires de l'academic Royale des Sciences et des lettres de Danemark, Copenhague, Section des Sciences, 9^{me} serie, t *VII*: 1-59.

Müller, J. 1846-1854. Abhandlungen uber die larven und Metamorphosen der Echinodermen. Abh. der. Kgl. Akad. der Wiss. zu Berlin. (Translated, in part).

Okazaki, K., Niijima, L. 1964. Basement membrane in sea urchin larvae. Embryologia *8*: 89-100.

Okazaki, K. 1975. Spicule formation by isolated micromeres of the embryo. Amer. Zool. *15*: 567-581.

Perry, M. M., Waddington, C. H. 1966. Ultrastructure of the blastopore cells in the newt. J. Embryol. exp. Morphol. *15*: 317-330.

Pitelka, D. R. 1974. Basal bodies and root structures. *In* Sleigh, M. A. (ed.) Cilia and Flagella. Academic Press, New York: 437-470.

Pollard, T. D., Weihing, R. R. 1973. Actin and myosin and cell movement. CRC Critical Reviews in Biochemistry *2*: 1-65.

Rappaport, R. 1967. Cell division: direct measurements of maximum tension exerted by the furrow of echinoderm eggs. Science *156*: 1241-1243.

Reynolds, E. S. 1963. The use of lead citrate at high pH as an electron opaque stain in electron microscopy. J. Cell Biol. *17*: 208-212.

Rhumbler, L. 1902. Zur Mechanik des Gastrulationsvorganges. Wm. Roux Entwicklsmech. org. *14*: 401-438 (Summary translated).

Richards, A., Porter, R. P. 1935. The mitotic index in pre-neural tube stages of *Fundulus heteroclitus*. Am. J. Anat. *56*: 365-393.

Richardson, K. C., Jarret, L., Finke, E. H. 1960. Embedding in epoxy resins for ultrathin sectioning in electron microscopy. Stain Technol. *35*: 313-323.

Rogers, A. W. 1969. Techniques of Autoradiography. Second Edition, Elsevier Publishing Company, Amsterdam.

Rosenbluth, J. 1972. Obliquely striated muscle. *In* Bourne, G.H. (ed.) The Structure and Function of Muscle. Volume I. Academic Press, New York: 389-421.

Roux, W. 1895. Gesammelte Abhandlungen uber Entwicklungsmechanik der Organismen. Wm. Roux Entwicklsmech. org. *1*: 1-816 (Summary translated).

Runnstrom, J. 1918. Zur Biologie und Physiologie der Seeigellarve. Bergens Mus. Aarb. *1918*: 1-60 (Summary translated).

Ryberg, E., Lundgren, B. 1975. Secretory cells in the foregut of the echinopluteus. Wm. Roux Archiv. *177*: 255-262.

Ryberg, E. 1977. The nervous system of the early echinopluteus. Cell Tiss. Res. *179*: 157-167.

Saunders, J. W. 1966. Death in embryonic systems. Science *154*: 604-612.

Saunders, J. W., Gasseling, M. T., Saunders, L. C. 1962. Cellular death in morphogenesis of the avian wing. Dev. Biol. *5*: 147-178.

Saunders, J. W., Fallon, J. F. 1967. Cell death in morphogenesis. *In* Locke, M. (ed.) Major Problems in Developmental Biology. Academic Press, New York: 289-314.

Schroeder, T. E. 1969. The role of the contractile ring filaments in dividing *Arbacia* eggs. Biol. Bull. *131*: 413-414.

Schroeder, T. E. 1972. The contractile ring II; determining its brief existence, volumetric changes and its vital role in cleaving *Arbacia* eggs. J. Cell Biol. *53*: 419-434.

Schroeder, T. E. 1973. Cleavage in HeLa cells: contractile ring filaments bind heavy meromyosin. Proc. Nat. Acad. Sci. U.S. *70*: 1688-1692.

Schroeder, T. E. 1975. Dynamics of the contractile ring. *In* Inoué, S., Stephens, R.E. (eds.) Molecules and Cell Movement. Raven Press, New York: 334-352.

Schroeder, T.E. 1976. Actin in dividing cells: evidence for its role in cleavage but not mitosis. *In* Goldman, R., Pollar, T., Rosenbaum, J. (eds.) Cell Motility: Book A, Motility, Muscle and Non-muscle Cells. Academic Press, New York: 265-278.

Sears, F.W., Zamansky, M.W. 1960. College Physics. Mechanics, Heat and Sound. Third Edition. Addison-Wesley Publishing Co., Reading, Mass., U.S.A.

Seeliger, O. 1892. Studien zur Entwicklungsgeschichte der Crinoiden. Zool. Zahrb. Abt. Anat. *6*: 481-483 (Summary translated).

Smith, D. S. 1972. Muscle. Academic Press, New York.

Spiegel, M., Ozaki, H., Tyler, A. 1965. Electrophoretic examination of soluble proteins synthesized in early sea urchin development. Biochem. Biophys. Res. Commun. *21*: 135-140.

Staehelin, L. A. 1974. Structure and function of intercellular junctions. Int. Rev. Cytol. *39*: 191-283.

Stearns, L. W. 1974. Sea Urchin Development: Cellular and Molecular Aspects. Dowden, Hutshinson, and Ross Inc., Stroudsburg, Pa., U.S.A.

Steele, D.H. 1977. Correlation between egg size and developmental period. Amer. Natur. *111*: 371-372.

Stell, W. K., Lightfoot, D. O. 1975. Color specific inter-connection of cones and horizontal cells in the retina of goldfish. J. comp. Neurol. *159*: 473-502.

Strathmann, M. 1968. Methods in Developmental Series. I. General Procedures and Echinodermata-Echinoidea. Friday Harbor Laboratories, Friday Harbor, Wash., U.S.A.

Strathmann, R. R. 1971. The behavior of planktotrophic echinoderm larvae: mechanisms, regulation, and rates of suspension feeding. J. exp. mar. Biol. Ecol. *6*: 109-160.

Strathmann, R. R. 1974. Introduction to function and adaptation in echinoderm larvae. Thal. Jugos. *10*: 321-339.

Strathmann, R. R. 1975. Larval feeding in echinoderms. Amer. Zool. *15*: 717-731.

Strathmann, R. R. 1977. Egg size, larval development, and juvenile size in benthic marine invertebrates. Amer. Natur. *111*: 373-376.

Strathmann, R. R., Jahn, T. L., Fonseca, J. R. 1972. Suspension feeding by marine invertebrate larvae: clearance of particles by ciliated bands of a rotifer, pluteus, and trochophore. Biol. Bull. *142*: 505-519.

Summers, E. G. 1970. The effects of actinomycin D on de-membranated *Lytechinus variegatus* embryos. Exp. Cell Res. *59*: 170-171.

Tannenbaum, J., Tannenbaum, S. W., Godman, G. C. 1977. The binding sites of cytochalasin D II. Their relationship to hexose transport and to cytochalasin B. J. Cell. Phys. *91*: 239-248.

Tattersall, W. M., Sheppard, E. M. 1934. Observations on the bipinnaria of the asteroid genus *Luidia*. James Johnstone Memorial Volume, University of Liverpool Press, Liverpool, England: 35-61.

Thaler, M. M., Cox, M. C., Villee, C. A. 1969. Actinomycin D: uptake by sea urchin embryos. Science *164*: 832-834.

Thorson, G. 1946. Reproductive and larval development of Danish marine bottom invertebrates with special reference to planktonic larvae in the sound (Øresund). Meddelser Komm. Danmarks fiskeri havundersøgelser, Ser. Plankton *4*: 1-523.

Tilney, L. G., Gibbins, J. R. 1969a. Microtubules in the formation and development of the primary mesenchyme in *Arbacia punctulata* II. An experimental analysis of their role in development and maintenance of cell shape. J. Cell Biol. *41*: 227-250.

Tilney, L. G., Gibbins, J. R. 1969b. Microtubules and filaments in the filopodia of secondary mesenchyme cells of *Arbacia punctulata* and *Echinorachnius parma*. J. Cell Sci. *5*: 195-210.

Tilney, L. G., Marsland, D. 1969. A fine structure analysis of cleavage induction and furrowing in the eggs of *Arbacia punctulata*. J. Cell Biol. *42*: 170-184.

Trinkaus, J. P. 1965. Mechanisms of morphogenetic movements. *In* DeHaan, R.L., Upsprung, H. (eds.) Organogenesis. Holt, Rinehart & Winston, New York: 55-104.

Trinkaus, J. P. 1967. Morphogenetic cell movements. *In* Locke, M. (ed.) Major Problems in Developmental Biology. Academic Press, New York: 125-176.

Trinkhaus, J. P. 1973. Modes of cell locomotion *in vivo*. *In* Locomotion of Tissue Cells. Excerpta Medica, Ciba Foundation 14 (New Series): 233-249.

Tschudy, D. P., Marver, H. S., Collins, A. 1965. A model for calculating messenger RNA half-life: short lived messenger RNA in the induction of mammalian α-aminolevulinic acid synthetase. Biochem. Biophys. Res. Commun. *21*: 480-487.

Ubisch, L. von 1913. Die Entwicklung von *Strongylocentrotus lividus*. Ztschr. Wiss. Zool. *106*: 409-448 (Summary translated).

Underwood, A. J. 1974. On models for reproductive strategy in marine invertebrates. Amer. Natur. *108*: 874-878.

Vacquier, V. D. 1971a. The appearance of β-1,3-glucanohydrase activity during the differentiation of the gut of the sand dollar pluteus. Dev. Biol. *26*: 1-10.

Vacquier, V. D. 1971b. The effects of glucose and lithium chloride on the appearance of β-1,3-glucanohydrase activity in sand dollar plutei. Dev. Biol. *26*: 11-16.

Vacquier, V. D., Korn, L. J., Epel, D. 1971. The appearance of α-amylase activity during the differentiation in sand dollar plutei. Dev. Biol. *26*: 393-399.

Vance, R. R. 1973. On reproductive strategies in marine benthic invertebrates. Amer. Natur. *107*: 339-352.

Watson, M. L. 1958. Staining of tissue sections for electron microscopy with heavy metals II. Application of solutions containing lead and barium. J. Biophys. Biochem. Cytol. *4*: 475-479.

Weiss, P., Garber, B. 1952. Shape and movement of mesenchyme cells as functions of the physical structure of the medium. Contributions to a quantitative morphology. Proc. Nat. Acad. Sci. U.S. *38*: 264-280.

Wessells, N. K., Roessner, K. D. 1965. Nonproliferation in dermal condensations of mouse vibrissae and pelage hairs. Dev. Biol. *12*: 419-433.

Wessells, N. K., Spooner, B. S., Bradley, N. D., Luduena, M. A., Wrenn, J. T., Yamada, K. M. 1971. Microfilaments in cellular and developmental processes. Science *171*: 135-143.

Wessells, N. L., Spooner, B. S., Luduena, M. A. 1973. Surface movements, microfilaments and cell locomotion. *In* Locomotion of Tissue Cells. Excerpta Medica, Ciba Foundation 14 (New Series): 53-77.

Wolpert, L., Mercer, E. H. 1963. An electron microscope study of the development of the blastula of the sea urchin embryo and its radial polarity. Exp. Cell Res. *30*: 280-300.

Wolsky, A., Wolsky, M. I. 1961. The effects of actinomycin D on the development of *Arbacia* eggs. Biol. Bull. *121*: 414.

Zimmerman, A. M., Marsland, D. 1964. Cell division: effects of pressure on the mitotic mechanisms of marine eggs (*Arbacia punctulata*). Exp. Cell Res. *35*: 293-302.